

Ministry of Higher Education and Science of the Republic of Kazakhstan
Al-Farabi Kazakh National University

578.832.1:043.5

As a manuscript

KHAIDAROV SAKEN ZHARKYNOVICH

Study of the antiviral activity of drugs against the *SARS-COV-2 virus in vitro*

8D05110 Virology

Dissertation for the degree
of Doctor of Philosophy (PhD)

Scientific consultants:

Burashev Yerbol Dosanovich

PhD, Head of the Laboratory "Monitoring of Infectious Diseases" of
Research Institute of Biological Safety Problems, Gvardeivsk, Zhambyl region,
Kazakhstan

Foreign scientific consultant

Edan Robert Tulman

PhD, Associate Professor,
College of Agriculture, Health and Natural Resources, Departments of Pathobiology
and Veterinary Science, University of Connecticut, USA

Republic of Kazakhstan

Almaty 2025

CONTENT

Notations and abbreviations	4
INTRODUCTION	5
1 LITERATURE REVIEW	
1.1 Coronaviruses	9
1.2 Antiviral drugs against SARS-COV2	20
1.3 Lethal mutagenesis as a purpose	27
1.4 Influenza virus and antivirals against it	30
1.5 Cell viability and antiviral assay – MTT and CCK8 methods	39
2 METHODS AND MATERIALS	
2.1 The Biological Samples	47
2.2 Equipment	48
2.3 Materials, reagents, and solutions	49
2.4 Molecular Biology Procedures	51
2.5 Comparative and phylogeny analysis of the nucleotide sequence of genes	55
2.6 Cell - cytotoxicity assay	57
2.7 The preclinical test of cytotoxic safe TAF and its antiviral properties in vivo on regular lab WT-Mice	60
3 RESULTS AND DISCUSSION	
3.1 Vero E6 cell infection and 72-hour incubation, titter production from Bronchoalveolar lavage fluid (BALF) and murine upper airways	64
3.2 Detection and isolation of the SARS-CoV-2/KAZ/B1.1/2021 variant, also known as the Alpha virus strain, using real-time PCR; Study morphological properties of the SARS-COV-2 virus	67
3.3 Phylogeny analysis of the SARS-CoV-2 strain/human/KAZ/Britain/2021, Alpha variant	71
3.4 Phylogeny analysis of the SARS-CoV-2 strain/human/KAZ/Britain/2021, Alpha variant	76
3.5 Antiviral drug cytotoxicity assays	
3.5.1 Determination of cytotoxicity of drugs for cell culture (CCK8)	82

3.5.2 CCK8 test for cell viability in four drugs at varying concentrations against SARS-CoV-2 Titters	88
3.5.3 MTT assay for cell viability in response to four drugs at varying concentrations against the SARS-CoV-2 Titters-Wuhan strain	91
3.6 Antiviral activity count after four drugs adding	92
3.7 The preclinical test of cytotoxic safe TAF and its antiviral properties in vivo on regular lab WT-Mice	93
3.8 Antivirals recommendation against SARS-COV2 according to provided results on RdRP-inhibition activity in vitro	102
CONCLUSION	103
REFERENCE	111
APPENDIX A - Parameters of sequencing primers; the entire SARS-CoV-2 / human / KAZ / B1.1/2021, Alpha variant strain genome ORF1ab and structure proteins (S, M, E, and N-Proteins)	121
APPENDIX B - The taxonomy of the SARS-CoV-2 strain human/KAZ/B 1.1/2021 the early SARS-COV2 lineage	126
APPENDIX C - The primary data of PCR-tests (runs)	130
APPENDIX D - Mutations of SARS-COV2 -Kazakhstan's strains to Wuhan's original strain	133
APPENDIX E - MONOGRAPH «VIRUSES (SARS-COV2, INFLUENZA A, D) MODERN SCIENTIFIC ASPECTS OF DIAGNOSIS AND TREATMENT»	136
APPENDIX F - DRUG BROCHURES	137

NOTATIONS AND ABBREVIATIONS

ACE2 - Angiotensin Converting Enzyme 2 (human)

BAL - Bronchoalveolar Lavage

BP-Base Pairs

CC- Cytopathic Capacity

COVID-19 – Coronavirus Disease (December 2019, Wuhan, China)

CPE – Cytopathic Effect

CE – Cytopathic Effect Inhibition

cDNA – Complementary Deoxyribonucleic Acid

HIV- Human immunodeficiency viruses

IC – Inhibition Concentration

vRNA - viral ribonucleic acid

NSP /SP - Non-Structural Proteins/Structural Proteins

MERS – Middle East Respiratory Syndrome (coronavirus)

MOI - Multiplicity Of Infection

MTT-(4,5-Dimethylthiazol-2-Yl)-2,5-Diphenyltetrazolium Bromide

ORF – Open Reading Frame

RBD-Receptor Binding Domain

RdRP- RNA-dependent RNA-Polymerase

RT- Reverse Transcriptase

PCR-Polymerase Chain Reaction

PFU - Plaque-Forming Unit

PP- Primers Pairs

SARS-COV 2- Severe Acute Respiratory Syndrome-Corona Virus 2

TAF – Tenofovir Alafenamide

TCID₅₀ (Tissue Culture Infectious Dose 50%)

TDF – Tenofovir Disoproxil

Vero – the subline of green monkey kidney tissue

WT – Wildtype.

INTRODUCTION

General description of the research: The dissertation focuses on the study of the biological and molecular genetic properties of current SARS-CoV-2 strains isolated within the territory of the Republic of Kazakhstan. It utilises RT-PCR, cell viability, viral titer production, and COVID-19 express test techniques, along with appropriate primers, to detect the NSP12 gene product. An in vitro study of the antiviral activity of drugs against the SARS-CoV-2 virus was conducted using the Vero E6 cell culture derived from *green monkey kidney tissue*.

Relevance of the research thesis

The COVID-19 pandemic in 2020 highlighted the extreme vulnerability of healthcare systems worldwide. First and foremost, the speed and intensity of spreading viral infection were a profound issue due to high viral load rates that most of the population could not withstand. Secondly, hospitalisation issues and insufficient bed and drug capacities were insufficient for effective containment. Thirdly, the severe cases of immune response caused significant health damage, predominantly to the lungs, and due to this feature, it was called a severe acute respiratory syndrome. One of the most critical issues with SARS-CoV-2 infection is its relatively rapid mutation rate and the human host's adaptation mechanisms, which occur through variations in the spike protein.

The research aims to study. This dissertation investigates the antiviral activity and cytotoxic safe drug concentrations of modern drugs against the SARS-CoV-2 virus in vitro by conducting a molecular analysis of circulating strains isolated during the pandemic.

The main tasks of the research to accomplish the purpose are as follows:

1. Sequencing genome Kazakhstan variant of the SARS-CoV-2 virus and characterising significant virus genes. Comparative and phylogenetic analysis of the nucleotide sequence of viral genes;
2. To identify the mutation of two SARS-CoV2 strains, the Alpha variant, which was to be isolated in Kazakhstan by comparing it with the original Wuhan strain;
3. To find the cytotoxicity - safe concentration of four antiviral drugs;
4. To identify the most effective and potent antiviral drug among three candidates: Ribavirin, Favipiravir (Fabiflu), and Tenofovir (Tenvir), as well as a corticosteroid with a safe concentration that minimises cell toxicity while maintaining high cell viability.
5. To determine the inhibition coefficient $IC_{10} \rightarrow IC_{50} \rightarrow IC_{100}$ - Range antiviral drug-Tenofovir (TAF) with acceptable SI (selectivity index);
6. To perform and confirm the preclinical test on wild-type (WT) mice to determine the antiviral efficacy of the potent drug at a safe concentration.

Research methods: The study employed biomolecular, genetic, cellular-based biotechnological, microbiological, and pharmaceutical processes.

The scientific novelty of the research: A three-stage dissertation study examining the effectiveness of the antiviral activity of the tableted drug against Kazakhstan's SARS-CoV-2/human/KAZ/B1.1/2021, the Alpha variant strain isolated and characterised, and an MTT assay on the Wuhan strain using original Tenvir (TAF) stock from China. Antiviral drug cytotoxicity and cell viability assays – Determining the optimal antiviral drug concentration (CC_{50}) using two colorimetric methods, CCK8 and MTT, *in vitro* in Kazakhstan. Three tableted forms of drugs demonstrated further inhibitory activities: Tenofovir (TDF and TAF), with $IC_{10} = 0.174 \mu M$, $IC_{50} = 1.74 \mu M$, and $IC_{100} = 174 \mu M$ at a concentration of $50 \mu g/ml$. Ribavirin: $IC_{10} = 2 \mu M$, $IC_{50} = 7 \mu M$, and $IC_{80-90} = 205 \mu M$ of $50 \mu g/ml$., Favipiravir: with $IC_{10} = 1.65 \mu M$, $IC_{37} = 318 \mu M$, of $50 \mu g/ml$. Dexamethasone showed no inhibitory properties at any concentration or volume. Comparison of the efficacy and cytotoxicity (CC_{50}/IC_{50}) of three tableted antiviral drugs, identifying an antiviral drug with a positive selectivity index (SI value), and analysis of the CCK8 assay test. Antiviral activity of three tableted prodrugs (active agents): Ribavirin, Tenofovir, and Favipiravir on Vero E6 cells line that is both susceptible and permissive for SARS-CoV2 virus – RdRP-inhibition, causing the lethal mutagenesis for viral replication with a significantly higher viral load $MOI:2$ or $TID_{50}=10$, whereas MOI of 0.01 is enough to cause cytopathic effect within 24 hours (200 times increase virus load decrease potential). The molecular and genetic characterisation of the RdRP (RNA dependent RNA polymerase) gene (NSP12- none structural proteins) and its 'genetical conservatism' of SARS-CoV-2/human/KAZ/B1.1/2021, Alpha variant strain in comparison with the original Wuhan strain; The assumption of antiviral activity was confirmed using Tenvir TAF (pure Aldrich stock concentration) with $10 \mu g/ml$ solution from original concentration $25 mg/ml$). All three antiviral drugs target the RdRP activity, making viral replication more challenging.

Subject of study

They are investigating the antiviral activity of medicines against the SARS-CoV-2 virus, focusing on its genetic and molecular characteristics and evaluating their efficacy. In addition to identifying the cytotoxic concentrations of the three antivirals, Tenofovir, Fabiflu, and Ribavirin, and the steroid drug Dexamethasone, the concentrations of these compounds were also determined.

The work's theoretical and practical significance is clearly understanding the effectiveness of three disputed antivirals and one hormonal (steroid) drug *in vitro*. To understand which drug demonstrates a sensible, i.e., pre-clinical, effect on wild-type mice in China and to establish a safe dosage for viral load, the author aims to enhance strategies for combating SARS-CoV-2 viral infection. During the pandemic, Kazakhstan faced multiple and numerous different cases of COVID-19 progressions and complication stages among infected patients with devastating post-corona effects and even lethal outcomes due to a poor understanding of the biological nature of

the SARS-CoV-2 virus. The primary objective of this dissertation work is to provide a deeper understanding not only of COVID-19 treatment but also of similar viral infection cases in the future. To evaluate the in vitro effectiveness of three antiviral agents and one hormonal (steroid) drug. To understand which of these drugs demonstrate not only practical, i.e., clinical, effects but also to establish the safe dosage in treatment strategies for COVID-19. The value of this work lies in several additional aspects: 1. Tenofovir, available in its two isoforms – TDF and TAF, has two origins: one is tableted (TDF), and the second is a laboratory standard stock (TAF). Both these forms showed similar effectiveness; furthermore, the last in vitro test on Tenofovir efficacy was performed in the 2000s. The antiviral effects were demonstrated on the Vero E6 cell model. Furthermore, the cytotoxic profiles of all four drugs were evaluated and confirmed. The non-structural protein sites on the viral genome were identified and quantified, and their biological ‘conservative’ nature was verified in the SARS-CoV-2/human/KAZ/B1.1/2021 Alpha variant strain.

The main provisions for the defence:

- 1) The SARS-CoV-2/human/KAZ/B1.1/2021, Alpha variant strain – is an object of antiviral study, aiming at the entire - ORF1ab, where ORF1a NSP1-11(Protease section) and ORF1b NSP12-16 (viral RNA replication site) with the strain-specific mutation that is responsible for the replication of viral genome RNA as well as for sub-genomic RNA that regulate the final assembly of virions.
- 2) The potent inhibition of the RdRP (RNA-dependent RNA Polymerase is detectable through an MOI count of 2 or lower (two viral particles for each host cell) in a 12 wells-sampling by Tenofovir (tableted TDF against The SARS-CoV-2/human/KAZ/B1.1/2021, Alpha variant) and TAF (lab stock) against original Wuhan strain) The tablet safe concentrations of Tenofovir, Favipiravir, Ribavirin, and Dexamethasone must support cell viability with a noncytotoxic viral load value of— MOI 2 (one host cell for two intact viral particle or plaque forming unit (PFU/ml)) with 200µl of virus volume) per 10.000 cells.
- 3) The cell counting techniques CCK8 and MTT demonstrate true cytotoxicity and antiviral assays on reliable Vero E6 cells with a high proliferation growth profile for four selected drugs: Tenofovir, Favipiravir, Ribavirin, and Dexamethasone.
- 4) Tenofovir (Tenofovir-TDF and TAF) is an effective antiviral drug among the four selected for inhibiting viral accumulation in infected Vero cells, achieving a maximum log₂ value of 100% with high cell viability rates at a relatively high viral load MOI of 2 or lower. In vivo, preclinical studies in China have shown a decrease in MOI₄ → MOI₂ viral load.

The relevance of the plan of based scientific works

This work was carried out as a PhD Thesis, ‘Studying the antiviral activity of drugs against the SARS-CoV-2 virus in vitro ’of Khaidarov Saken under the professional supervision of Burashev Yerbol who managed my research within the framework of the grant funding project on the topic: AP09058338 “Study of anti-viral

activity of drugs against SARS-CoV-2 virus in vitro and conducting molecular-epidemiological analysis of circulating Covid-19 strains“ under targeted funding for 2021–2023 with the support of the Science Committee of the Ministry of Science and Higher Education of the Republic of Kazakhstan. Special gratitude is extended to the Department of Pathobiology and Veterinary Science and the Center of Excellence for Vaccine Research at the University of Connecticut (UConn), Storrs, Connecticut, USA, which collaborated closely with the Research Institute for Biological Safety Problems (RIBSP), Gvardeyskiy, Kazakhstan. Additionally, thanks to the Health Science Center (School of Medicine) of Shenzhen University, located in Nanshan District, Shenzhen, during the 3-month PhD mobile program internship in 2024, experiments on TAF and mice were conducted, and the PhD study direction was continued.

The author's contribution to the results described in the dissertation: The author independently carried out the analysis of literature data on the researched problem, set research goals and objectives, conducted experimental research, analysed the obtained results, performed statistical processing, and wrote the dissertation.

Research approval: The research results and the main principles of the dissertation were presented and discussed at the following international scientific conferences and symposia: «Modern Scientific Technology» (February 9-10, 2023). Stockholm, Sweden, 2023: 3rd International Conference on Virology and Infectious Diseases, including COVID-19, held on October 24-25, 2022, in Dubai, UAE. Proceedings of the 1st International Scientific Conference, 26-27 January 2023, Warsaw, Poland II International Forum "Asfen Forum, new generation-2024" on June 6-7, 2024, in Almaty, Kazakhstan

Publications: The main result of the dissertation consists of 9 published works, including two articles in peer-reviewed international scientific journals indexed in the Web of Science or Scopus databases, two articles in the list of the Committee for Control in the Sphere of Education and Science of the Republic of Kazakhstan, and five theses published at international conferences.

Dissertation structure: The dissertation comprises 138 pages of computer-generated text, symbols, and abbreviations, as well as an introduction, a literature review, research materials and methods, research results and their discussion, a conclusion, and a list of used literature, totalling 115 entries. The work has seven tables, six mathematical formulas, 50 figures, five appendixes, and one monograph.

1 LITERATURE REVIEW

1.1 Coronaviruses

Coronaviruses (CoVs) are a large family of RNA viruses that have caused significant human outbreaks over the past five decades. While most cause mild respiratory illnesses, three novel coronaviruses have emerged since 2002, leading to severe disease, pandemics, and lasting global consequences. Here is a timeline and analysis of their impact:

Pre-2000s: Mostly Benign Human Coronaviruses. 1960s–1970s: The first human coronaviruses (HCoV-229E and HCoV-OC43) were identified, causing mild upper respiratory infections, commonly known as the common cold. 1980s–1990s: Two more seasonal coronaviruses (HCoV-NL63 and HCoV-HKU1) were discovered, also linked to cold-like symptoms. Impact: These viruses caused ~15–30% of annual common cold cases but were not considered significant threats.

2002–2003: SARS-CoV-1 (Severe Acute Respiratory Syndrome Coronavirus 1) Origin: Emerged in Guangdong, China, likely from bats via civet cats. Impact: Cases: ~8,098 confirmed cases, with 774 deaths (a 9.6% fatality rate). Spread: Rapid global transmission across 26 countries. Consequences: Highlighted the pandemic potential of zoonotic coronaviruses. SARS-CoV-1 was contained by 2003 through aggressive public health measures, including quarantines and contact tracing. Legacy: No cases have been reported since 2004, but this spurred research into coronavirus biology and pandemic preparedness.

2012–Present: MERS-CoV (Middle East Respiratory Syndrome). Origin: Emerged in Saudi Arabia, linked to dromedary camels (reservoir: bats). Impact: cases: ~2,605 cases, 936 deaths (34.4% fatality rate) as of 2023. Spread: Mostly limited to the Arabian Peninsula, with sporadic outbreaks from travel or hospital transmission. Challenges: High mortality but low human-to-human transmissibility limited its global spread [1-2]. Legacy: reinforced the need for surveillance of zoonotic viruses in animal reservoirs.

2019–Present: SARS-CoV-2 (COVID-19 Pandemic). Origin: Likely originated in bats, possibly via an intermediate host (e.g., pangolins), emerging in Wuhan, China. Impact: Global Spread: Over 700 million confirmed cases and ~7 million deaths worldwide (as of 2023). Health Burden: Severe respiratory illness, multisystem complications (e.g., Long COVID), and overwhelming strain on healthcare systems [1]. Socioeconomic Disruption: Lockdowns, travel restrictions, and economic recessions reshaped global societies. Evolution: Rapid antigenic drift led to concern variants (e.g., Alpha, Delta, Omicron), which evade immunity and require updated vaccines. Scientific Response: Unprecedented vaccine development utilising mRNA platforms and genomic surveillance.

Key Themes in Coronavirus Impact on Zoonotic Spillover: All novel coronaviruses (SARS, MERS, COVID-19) originated in animals, emphasising the risk of disruptions to the human-animal interface (e.g., wildlife trade, habitat encroachment) [1]. Pandemic Preparedness: SARS-CoV-1 and MERS-CoV exposed gaps in global health infrastructure, but SARS-CoV-2 revealed systemic vulnerabilities, such as vaccine inequity and misinformation. Long-term Health Effects: Post-viral syndromes, such as those associated with COVID-19, have become a significant focus of research and healthcare. Technological Advances: mRNA

vaccines, antiviral therapies (e.g., Paxlovid), and AI-driven surveillance emerged as critical tools [3]. Essential: Surveillance: Strengthen early detection of zoonotic viruses in wildlife and livestock. Equity: Ensure fair access to vaccines and treatments globally. Adaptability: Prepare for viral evolution (antigenic drift) and future spillover events. Public Trust: Combating Misinformation and Building Resilient Health Communication Systems. Coronaviruses have reshaped modern medicine, epidemiology, and society over the past 50 years. While SARS-CoV-2 is the most impactful to date, the history of CoVs underscores the need for vigilance against emerging pathogens in an interconnected world [4]. SARS-CoV-2 (Severe Acute Respiratory Syndrome Coronavirus 2) is responsible for COVID-19, a global pandemic that began in late 2019. Here are some key points about the virus: Classification and Structure. SARS-CoV-2 is a coronavirus, part of the *Coronaviridae* family. It is an enveloped, single-stranded RNA virus. The virus has spike (S) proteins on its surface that allow it to bind to and enter human cells via the ACE2 receptor. Transmission primarily occurs through respiratory droplets and aerosols, such as those released during coughing, sneezing, and talking. It can also spread via contaminated surfaces (fomites), though less commonly. Airborne transmission is possible in enclosed or poorly ventilated spaces. Virulence refers to the degree of pathogenicity or the ability of a virus to cause disease [5]. SARS-CoV-2 has demonstrated varying levels of virulence depending on the viral strain, host factors, and immune response. Here are key aspects of its virulence: factors Contributing to virulence include the spike (S) protein and ACE2 Receptor Binding. SARS-CoV-2 enters human cells via the ACE2 receptor, which is highly expressed in the lungs, heart, kidneys, and intestines. The spike (S) protein has a high binding affinity to ACE2, enhancing infectivity. Mutations in the S protein (e.g., in Delta and Omicron variants) have increased transmissibility and immune evasion. Viral Replication & Immune Evasion. SARS-CoV-2 has mechanisms that suppress early immune responses, primarily by inhibiting interferon production, which allows it to replicate efficiently before the immune system detects it [6]. Some variants (e.g., Delta) replicate more rapidly, resulting in higher viral loads and more severe disease, including an inflammatory response and a cytokine storm. In severe cases, an overactive immune response, known as a cytokine storm, leads to widespread inflammation, tissue damage, and organ failure. This excessive inflammation is responsible for severe complications like acute respiratory distress syndrome (ARDS) and multi-organ failure. CPE (Cytopathic Effect): Visible morphological changes in host cells caused by viral infection. These changes can include cell rounding, detachment, syncytia formation, or lysis and are used to diagnose the presence of viruses in cell cultures [7].

The virulence is more clearly evident in Table 1. Four variants were isolated from the beginning of the pandemic outbreak in Kazakhstan, and all four variants are shown in Table 1.

Table 1 - Different SARS-CoV-2 variants and their varying levels of virulence

Variant	Virulence Characteristics
Alpha (B.1.1.7, 2020)	Increased transmissibility, slightly higher virulence.
Delta (B.1.617.2, 2021)	High viral load, more severe disease, increased hospitalisation rates.
Omicron (B.1.1.529, 2021-Present)	High transmission, lower virulence, milder disease but immune evasion.

Delta variant had a higher virulence, leading to severe lung damage and higher hospitalization rates. Omicron and its subvariants tend to replicate more in the upper respiratory tract, which reduces lung involvement and severity but increases transmissibility [8]. Host Factors Affecting Virulence: Age - Older individuals are at a higher risk of developing severe disease. Comorbidities, including diabetes, hypertension, obesity, and immunosuppression, increase the severity of the condition. Vaccination Status: Vaccinated individuals generally have reduced disease severity. Genetics and Immune Response: Some individuals may have genetic predispositions that affect ACE2 expression or immune response [9]. Clinical Outcomes & Severity: mild cases (80%): Fever, cough, fatigue, sore throat, anosmia. moderate cases (15%): Pneumonia, difficulty breathing, mild hypoxia. severe cases (5%): ARDS, cytokine storm, organ failure, death [10]. The overall case fatality rate (CFR) varies by variant and healthcare availability but is lower than that of SARS-CoV-2 (2003) and MERS-CoV (2012), which had significantly higher mortality rates [11]. SARS-CoV-2 has demonstrated moderate virulence compared to other coronaviruses, with some variants, such as Delta, being more severe. In contrast, Omicron exhibits lower virulence but higher transmission rates. The virus's ability to evade immunity and mutate rapidly influences its pathogenicity and clinical impact [12]. The strain we worked with is the Omicron strain; nevertheless, it has a relatively high virulence due to a fast cytopathic effect (CPE) with a relatively low viral load (MOI of 2 in Kazakhstan and MOI of 0,1 in China). Viruses are endo-parasites that strongly depend on their host cell and its replication, transcription, and translation machinery. Viruses can infect both domains: the eucaryotic as well as procaryotic organisms (phages). It is challenging to classify them as true parasites or pseudoparasites. Viruses have compact genomes enveloped mostly by capsid proteins and can be comprised of either DNA as a genetic material or RNAs, as viruses can encode various types of transcriptase. Coronaviruses are named for their corona-shaped appearance when viewed under the electron microscope. Viruses, are they alive? According to the latest characteristics of life biology, viruses barely satisfy even half of their criteria, such as growth and development - viruses do not grow and do not develop in the classical meaning of these words. Only numbers

increase – the viral load in a host cell, which ultimately leads to its fatal bursting of the membrane and cytosol. Viruses possess neither *order* because they cannot be characterized as cellular organisms nor energy processing. However, many virions are highly ordered; instead, they use the ‘victim’ replication machinery to reproduce, expressing various enzymes on the eucaryotic ribosomes [12]. Viruses are so heavily dependent on host metabolism that they can survive only inside penetrated host cells. The size also plays a crucial role; most living organisms, even unicellular like bacteria or protists, require space – the biosphere to habitat it; viruses, in sharp contrast, mainly depend on particular hosts and their interactions in the biosphere. The only thing that relates viruses to living is heredity and adaptation capacities according to their features to regulate their gene expression independently. Are they DNA or RNA-type viruses? The viral genome can defend its critical regions of gene expression; these regions are called ORFs, i.e., open reading frames that react as enzyme–bioactive catalysis. The tiny size of viruses allows them not only to infect most organisms effectively but also to develop a profound number of strategies to regulate the populations of bacteria, fungi, plants, and other organisms. Viruses also could not be considered true parasites because, even though they cannot survive on their own, they usually kill their host relatively fast, like Ebola or Marburg virus, and they kill their hosts within several days [11]. This false parasite behaviour is their true weakness – low virulence and the ability to spread. The ideal pandemic viral pandemic scale is when a virus spreads not only fast but also allows a host to spread contamination fluids into the air as long as possible and keeps the so-called patient zero unaware of spreading until it is not too late. The virus is one of the most primitive life forms biology knows (apart from viroids, they are more primitive): it has only membrane proteins that enable them to penetrate the host cell membrane, nucleocapsid inside which the genetic material appears in either DNA or RNA-form. When the genetic material of a virus is inserted into the cytosol of the victim cell, the viral RNA, for instance, starts to dock on ribosomes and begin to produce immediately so-called reverse-orientated complicated enzymes like RNA driven RNA polymerase-enzyme that interacts with host DNA replication-machinery and starts to reproduce first the genetic material in positive sense direction, the reason why COVID-19 virus, for instance, has a definition as single-stranded RNA positive sense virus (ssRNA⁺). About two-thirds of the SARS-CoV type two virus genome is fully dedicated to enabling, protecting and sustaining the work of RdRP to ensure the viral survival through not only replicating the genetical material but also producing main components of virions like spike protein – the host membrane ‘opener,’ membrane protein -even viruses must have information about host membrane barrier in a cooperative form as Receptor binding domain - Angiotensin-converting enzyme 2 (RBD-ACE 2) [13-14]. The region that occupies 70% of about 30K base pairs (bp) is called ORF1ab (open reading frame), which expresses 16 non-structural proteins, paramount among them is NSP3, NSP5, and NSP12. The NSP5 is located in the ORF1a region, which facilitates its adaptation and docking on host ribosomes. The NSP12 is the most significant gene product of the COVID-19 virus and is responsible for RdRP expression. The rest, for instance, NSP-1-4 and NSP6-11, are responsible for enzymatic activity that promotes the work of NSP5 during primary replication

processes. The NSP13-16 also exhibits significant catalytic features that replicate the classical DNA replication process; instead of DNA, it uses RNA, and there is no need for leading or lagging strands, as seen during classical eukaryotic DNA replication [15]. Above all, NSP12 is the most significant gene product of the viral genome, specifically NSP12. They encode the most essential enzyme in the primary infection period – the RNA-driven RNA polymerase enzyme. NSP12 is so crucial that NSP13 and NSP11 are fulfilling the catalyst functions to enable NSP12's efficient functioning. Some antiviral drugs, like Remdesivir, disable RdRP from docking on RNA subunits and, therefore, stop the viral genome from replicating. Other antiviral drugs cause a phenomenon known as lethal mutagenesis in RNA metabolism, resulting in impaired viral survival or reduced viral load, which ultimately affects their functions and numbers. RNA-dependent RNA polymerase provides the viral genome with genetic variations through favourable point mutations. The viral survival entirely depends on RdRP, and its importance is paramount. In multiple investigations conducted in the early 2000s and in 2020, in China and the USA, it was confirmed that despite the high mutation potential of the SARS-CoV virus, few mutations appear from strain to strain, independently of its geographical origin and genome region of ORF1ab [16]. Severe acute respiratory syndrome-associated coronavirus 2 (SARS-CoV-2) is a life-threatening respiratory infectious condition caused by the SARS-CoV-2 virus, which belongs to the coronavirus family and genus Betacoronavirus—specifically, a single-stranded positive-sense RNA virus (ssRNA⁺). Variants of the SARS-CoV-2 coronavirus continue to emerge due to the virus's ongoing transmission and evolution worldwide. Since the pandemic was first declared by the World Health Organization (WHO) in March 2020 [1], the following variants have been identified: B.1.17 (alpha), B.1.351 (beta), P.1 (gamma), B.1.617.2 (delta), and B.1.1.529 (omicron) [18]. Kazakhstan reported the first human infection with COVID-19 coronavirus in March 2020 [17]. According to the Johns Hopkins University database, as of January. In October 2022, the Republic of Kazakhstan reported 1,484,400 confirmed cases, with 19,052 deaths [17]. The coronavirus, or SARS-CoV-2, belongs to the Coronaviridae family, which are enveloped, positive-sense, single-stranded RNA viruses [8]. The SARS-CoV-2 consists of a viral genome comprising fourteen open reading frames (ORFs), two-thirds of which encode sixteen nonstructural proteins (nsp 1–16) that make up the replicase complex [9,10]. The rest encodes the nine accessory proteins (ORFs) and four structural proteins: spike (S), envelope (E), membrane (M), and nucleocapsid (N), of which Spike enables SARS-CoV entry into the cytosol of the target cell [9]. As with any virus of this type, the Spike protein is the most variable, and due to this capacity, the SARS-Covs can penetrate the various cell membrane types of mammals [10]. There are approximately 30,000 nucleotides in RNA, encoding 11 proteins. Retroviruses have caused much harm over the years, and they're now a significant threat to human well-being. These types of viruses, belonging to the family Retroviridae, typically carry their genetic material as RNA. Thanks to an enzyme called reverse transcriptase (RT), they could use the host DNA. RT is responsible for copying genetic information from one virus particle to another. The most well-known viruses of that family are Lentivirus (human immunodeficiency virus (HIV)) and SARS-CoV-

2 (COVID-19) [11]. It is essential to mention that virus infections aim to replicate the viral genome and assemble new viral units to invade surrounding cells and tissues; these processes are often carried out lethally, potentially harming a cell or even an entire tissue system, such as the lungs. Thus, it is challenging to classify any viral 'organism' as a parasite whose long-term survival correlates with the host's well-being. 'The side effect' of viral infections as inflammatory or less obvious clinically distinguishable signs is the integration into the cell genome due to enzymatic activity of viral RNA of various tissue types; this, in the term, causes multiple types of critical mutations in renewable tissues having a sometimes the devastating disease like pneumonia, renal failure or other chronic, irreversible diseases. The negative impact of the global COVID-19 pandemic on the population is widespread and is only just beginning to be experienced. Therefore, the harm potential of this type of virus is never completely neutralised, and underestimating its pandemic capacities is the highest priority to avoid by any authority [12-16]. SARS – stays for severe acute respiratory syndrome. Most of those diagnosed with SARS were healthy adults between the ages of 25 and 70. Children under the age of 15 have been the victims of a few alleged SARS cases. SARS typically has an incubation period of 2 to 7 days but can last as long as 10. People who have an illness that meets the current WHO case definition for probable and suspected cases of SARS have a case fatality rate of around 3%. Since the COVID-19 pandemic emerged in 2020, the United Nations has considered this virus and related diseases a global challenge for healthcare systems worldwide. The consequence of SARS-CoV-2 infection could lead to chronic illnesses, long-term health issues, and sometimes, to some extent, medical and mental impairment, which is why some scientific journals' scope is fully dedicated to this problem. In many countries, the hospitalisation rates reached critical levels, so many infected ones were forced to stay at home and get treated far from inpatient wards. Pneumonia is a direct and widely spread clinical consequence among COVID-19-positive patients and needs to be separated according to the severity of the illness progress and lung damage surface. The more damage occurred, the less oxygenation gained via lung breath, so many patients with acute lung damage were heavily dependent on artificial lung ventilation apparatus in intensive care. It was crucial to monitor whether the pneumonia patients with COVID-19 infection were regularly assessed for bacterial infection and try to detect bacterial co-infection. The antibiotic treatment strategy would have been implemented if a need arose to prevent pulmonary collapse [16]. SARS-COV2 and its molecular feature mainly rely strongly on the viral Spike has an S1/S2 polybasic cleavage site that is proteolytically cleaved by cellular cathepsin L and the transmembrane protease serine 2 (TMPRSS2), and a receptor-binding domain (RBD) that mediates direct contact with a cellular receptor, angiotensin-converting enzyme 2 (ACE2) [18,19,20]. ORF1a and ORF1b are translated into viral replicase proteins as soon as the viral genome is inserted into the host cell's cytoplasm and cleaved into individual nascent proteins by both host and viral proteases. The RNA-dependent RNA polymerase (nsp12, which is derived from ORF1b) is formed by these [21]. The components of the replicase move the endoplasmic reticulum (ER) into double-membrane vesicles (DMVs) at this location, which makes it easier for the virus to

replicate genomic and subgenomic RNAs (sgRNA). The latter is turned into accessory or auxiliary proteins and viral structural proteins, making it easier for the virus to form particles [22,23]. In conclusion, the secondary part of the genome encodes the nine accessory proteins (ORFs) that ensure the viral mRNA genome is translated. It is worth mentioning that the replicase for accessory protein production is significantly more significant than the primary one. In addition, the four structural proteins are spike (S), envelope (E), membrane (M), and nucleocapsid (N), of which the spike protein enables SARS-CoV entry into the cytosol of the target cell [19]. ORF1a and ORF1b are translated into viral replicase proteins as soon as the viral genome is inserted into the cytoplasm of the host and cleaved into individual proteins (via the host and viral proteases, including PL^{pro}). These form the RNA-dependent RNA polymerase (nsp12 derived from ORF1b) [19]. The latter is turned into an accessory or auxiliary protein and viral structural proteins, making it easier for the virus to form particles [20-23], unlike HIV, which has a complicated capsid structure with sophisticated (negatively charged dNTPs⁻ permeable) pores that are permeable for negatively charged dNTPs, which serve as building blocks for the formation of RNA-host-DNA-hybrid. The SARS-COVs do not possess such protection from hostile enzymes inside the host cells [24]. The secondary part of the genome encodes the nine accessory proteins (ORFs), making it possible for the viral mRNA genome to be translated step by step. Furthermore, the replicase for accessory protein production must be integrated into the host genome to enable a virus to reproduce itself [21,24]. The structure of the genome and proteins of the SARS-CoV-2 virus resembles the typical structure of retroviruses, has a shell shape ranging from spherical to pleomorphic, and has a diameter of 80-100 nm. Different genera of retroviral virions exhibit distinct morphologies, yet they share the same core components, including an outer shell, two copies of the genetic material, and viral proteins. The envelope consists of lipids, which are formed from the plasma membrane of the host during budding, and glycoproteins, such as gp120 and gp41 in the case of HIV [25]. The outer lipid bilayer of the retroviral envelope protects it from the extracellular environment, promotes the penetration and exit of host cells through the endosomal membrane, and facilitates the entry of the virus into host cells and its easy fusion with their membranes - these are three distinct functions of the retroviral envelope. The retrovirus has a single-component, linear, dimeric ss-RNA (+) genome, measuring 8 to 10 kilobases in length, with a 5' envelope and a 3' poly-A tail. There are flanks for group-specific genes (gag), pol, pro, and envelope genes (env) between the R sites. The primers U3, R (PBS), and U5 binding sites form 5' long terminal repeats (LTRs). In the polypurine tract (PPT), the sections U3 and R form the 3' end. Reverse transcription uses a short repeating sequence at each genome end to ensure proper end-to-end transfer in the growing chain. On the other hand, U5 is a short exception sequence between PBS and R [26]. The 18 bases in PBS correspond to the 3' end of the tRNA primer. An untranslated leader region, the L region, indicates how genomic RNA is packaged. The proteins gag, protease, pol, and env form the core of the retroviral protein. Gag is the main structural protein of the retrovirus, which controls most of the virus assembly processes. Interactions with three Gag subdomains - the matrix (MA), the capsid (CA), and the nucleocapsid (NC) — influence many of

these assembly steps. Although gag subdomains are structurally different, their functions overlap during virus assembly [27,28]. To sum up, Tenofovir as a prodrug forms TAF and TDF effectively suppresses the protease activity of retroviruses and inhibits the primary protein synthesis, making the DNA or RNA fitness of this virus type unsustainable. According to the WHO dashboard, more than 6.4 million people worldwide died from COVID-19 by August 18, 2022. The omicron strain has been diagnosed in over 590 000 000 people worldwide. A brand-new variant that appeared toward the end of November 2021 is now the most common strain worldwide and has contributed to the ongoing rise in several nations. In several high-income nations, vaccination is significantly reducing the number of cases and hospitalizations, but a lack of universal access to vaccines leaves many populations vulnerable. Even in vaccinated people, there are still questions about how effective and for how long the current vaccines against Omicron and other new SARS-CoV-2 variants are. There is still a need for more efficient COVID-19 treatments as a whole. The CoVID-19 global spreading, as well as the avalanche of research and false information, has shown how important it is to have reliable, easily accessible, and frequently updated living guidelines so that new findings can be understood and clear recommendations for clinical practice can be provided [29]. Apart from the severe acute respiratory syndrome and acute respiratory distress syndrome (ARDS) causing severe health impairment, COVID-19 is also capable of causing post-COVID-19 health conditions like cognitive impairment states. Other neurological and non-neurological deficits, such as fatigue and mental health symptoms, may overlap or cluster with cognitive deficits. In conditions following COVID-19, fatigue or exhaustion manifests as severely depleted systemic energy levels unrelated to activities or exertion and unaffected by usual rest or sleep. The quality of one's life, physical and cognitive function, social participation, and employment are all negatively impacted by fatigue. The core symptoms of depression following COVID-19 include a persistent low mood and sadness for at least two weeks and a markedly diminished interest in enjoyable activities. Depression can also cause problems sleeping, changes in appetite, fatigue, thoughts of self-harm or suicide, and feelings of worthlessness. Anxiety symptoms can include restlessness, racing or uncontrollable thoughts, difficulty concentrating, a sense of dread, difficulty sleeping, a lack of appetite, and irritability [29-30]. The SARS-COVID2 consists of a viral genome: fourteen open reading frames (ORFs), two-thirds of which encode sixteen non-structural proteins (nsps 1–16) that make up the replicase complex [30,31]. The rest encodes the nine accessory proteins (ORFs) and four structural proteins: spike (S), envelope (E), membrane (M), and nucleocapsid (N), of which Spike enables SARS-CoV entry into the cytosol of the target cell [22]. As with any virus of this type, the Spike protein is the most variable, and due to this capacity, the SARS-COVs can penetrate the various cell membrane types of mammals [33-34]. ORF1ab in SARS-CoV-2 is a critical open reading frame (ORF) that plays a central role in the virus's replication and transcription machinery. Here is a structured overview. Genomic Context: SARS-CoV-2 Genome - A single-stranded, positive-sense RNA virus with a genome of approximately 29,903 nucleotides. The 5' two-thirds genome contains ORF1a and ORF1ab, which encode large polyproteins. Key

Features of ORF1ab. Ribosomal Frameshift Mechanism: ORF1ab is expressed via a -1 ribosomal frameshift during translation of ORF1a. This occurs at a "slippery sequence" followed by an RNA pseudoknot structure, causing the ribosome to shift reading frames and continue translation into ORF1b. Result: A longer polyprotein (pp1ab) is produced, combining ORF1a and ORF1b regions, whereas ORF1a alone produces a shorter polyprotein (pp1a). Polyprotein Processing: The pp1ab polyprotein is cleaved by viral proteases (3CLpro/Mpro and PLpro) into 16 non-structural proteins (NSP1–NSP16). These NSPs form the replication-transcription complex (RTC), which is essential for viral RNA synthesis. Key Non-Structural Proteins (NSPs): NSP12 (RdRP): RNA-dependent RNA polymerase, a target for antivirals (e.g., Remdesivir). NSP13 (Helicase): Unwinds RNA during replication. NSP14: Proofreading exonuclease, reducing mutation rates. NSP15 (EndoRNase) and NSP16 (2'-O-MTase): Modify RNA to evade host immune detection. Viral Replication: ORF1ab-derived proteins are indispensable for replicating the viral genome and subverting host defences. Antiviral Targets: Enzymes like RdRP and proteases (3CLpro) are prime targets for drug development (e.g., Paxlovid inhibits 3CLpro). Conservation: ORF1ab is highly conserved among coronaviruses, making it useful for diagnostics (e.g., PCR primers) and broad-spectrum therapeutics. Mutations in ORF1ab (e.g., P323L in NSP12) may influence viral fitness or drug resistance but are less common than those in structural proteins, such as Spike. Surveillance of ORF1ab helps track viral evolution and inform the development of countermeasures. Protease activity in SARS-CoV-2 is crucial for viral replication and pathogenesis. The virus encodes two key proteases that process its polyproteins into functional components. The first is the main Protease (Mpro or 3CLpro). It cleaves the large polyproteins (pp1a and pp1ab) translated from the viral RNA into non-structural proteins (nsps) required for replication and transcription. Specifically, it cleaves at 11 conserved sites, generating mature proteins like the RNA-dependent RNA polymerase (RdRP) and helicase. Structure: A cysteine protease characterized by a catalytic dyad comprising Cys145 and His41. Functions as a homodimer, with each monomer containing three domains (I-III). The second protease, Papain-Like Protease (PLpro), plays a role in cleaving the polyprotein at three sites to release nsps 1-3. Immune Evasion: Removes ubiquitin and interferon-stimulated gene 15 (ISG15) from host proteins, thereby dampening antiviral immune responses, including NF- κ B and interferon signalling. Structure: A cysteine protease featuring a catalytic triad comprising Cys111, His272, and Asp286. Contains a ubiquitin-like domain for substrate recognition. Therapeutic Target: Less advanced than Mpro inhibitors, but investigational compounds (e.g., GRL-0617) aim to block PLpro's dual role in viral processing and immune suppression. Understanding the structure-function relationships of ORF1ab facilitates the design of inhibitors to disrupt viral replication [20-21].

Studies on frameshifting mechanisms could lead to novel antiviral strategies targeting this process. In summary, ORF1ab is a cornerstone of SARS-CoV-2 biology, driving viral replication and serving as a key focus for therapeutic and diagnostic innovation [19-20,33, 37, 49].

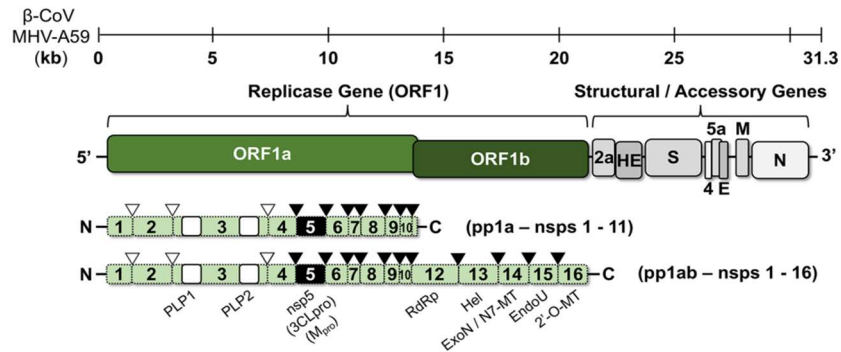


Figure 1 - The schematized viral genome of a beta strain, containing approximately 31.3 kb. The polyprotein regions (pp) or so-called open reading frames (ORFs) are primarily represented in the viral genome for replicase genes, serving as fragments of which are defined as non-structural proteins or NSPs. The most promising regions to target are nsp5 and nsp12, which are essential for viral replication.

The structural genes encode proteins for further purposes: spike (S), envelope (E), membrane (M), and nucleocapsid (N), as well as auxiliary or accessory proteins [22,35]. Receptor binding protein (RBD): viral spike protein, glycolysis, S1-Domain, ACE-2 Recognition, Furin, S2-Domain, TMPRSS2, cell and viral membrane fusion. The viral infection caused by SARS-CoV-2 begins with the RBD and consists of two subunits, S1 and S2, respectively. They are non-covalently associated subunits. The S1 Subunit binds to ACE-2, and the S2 subunit anchors the S2-protein to the membrane. The S2-subunit contains the fusion peptide and other molecular machinery required to mediate membrane fusion upon invasion of a new host cell, enabling the viral genome to enter the cytosol [37]. After contact with the spike protein, Furin accurately cleaves the outer part of the spike protein, known as the S1 domain, thereby releasing the inner core of the spike protein. This S2 domain is also cleaved by transmembrane serine protease 2 (TMPRSS2) [31]. After these, spike protein unfolds and anchors into the host cell membrane. Thus, the membrane of the virus and the host cell begin to fuse, allowing the viral genome to penetrate the cytosol of the host cell. A ribosome binds to the viral RNA and initiates the translation of its genetic code. It results in a long protein chain containing non-structural proteins (NSPs). NSPs are capable of cutting the neighbouring chains. First, they release short naps capable of binding to a ribosome and occupying it, allowing the bound ribosome to read only the viral RNA and not the host cell's messenger RNA (mRNA). From this very beginning phase, we can say that the infected host cell becomes a virus-building factory, thanks to the virus's control over the cell's translation machinery [35,48,63]. The primary spike protein structure is the key aspect of understanding viral pathogenesis, and its primary structure is depicted in Figure 2.

The viral entry activation of respiratory cells, such as lung cells, is mediated by the transmembrane protease serine 2 (TMPRSS2), which is not present in Vero kidney cells, even though the SARS-CoV-2 virus can be readily grown in them. The COVID-19 pandemic presented enormous global challenges to national healthcare (NHC). The initial response to the spread of such an epidemic was how to treat infected patients to achieve a clinical effect [35-39].

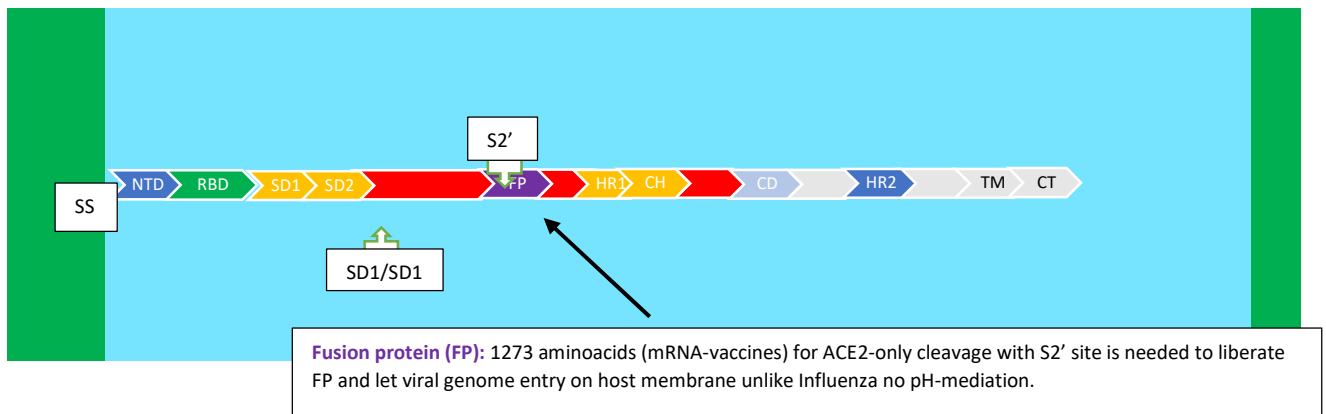


Figure 2 – The COVID-19 virus is composed of the primary structure of the spike protein. Different domains are displayed in different colours. SS, single sequence; NTD, N-terminal domain; RBD, receptor binding domain; SD1, subdomain 1; SD2, subdomain 2; S1 / S2, protease cleavage site S1 / S2; S2', protease cleavage site S2'; FP, fusion peptide; HR1, heptad repeat 1; CH central helix; CD connection domain; HR2 - heptad repeat 2; TM - Transmembrane domain; CT - cytoplasmic tail. Arrows indicate the place of cleavage by protease.

People around the globe stormed pharmacies to obtain paracetamol, which is effective against fever; others claimed anti-flu drugs, hoping to experience their therapeutic effects, and some even bought out antibiotics, considering that they would also be beneficial. COVID-19 is a single-stranded positive-sense RNA (+) (ssRNA) coronavirus that attaches to the host cell receptor, ACE2, via the spike glycoprotein in combination with surface protease TMPRSS2. This virus relies heavily on replicase targets, including RNA-dependent [56]. RNA polymerase (RdRP), Helicase, Exonuclease, and Endoribonuclease. None of those mentioned above claimed drugs could handle the fast-increasing viral load and could bring neither therapeutic nor prophylactic (preventive) effects. Since then, scientists worldwide have launched a global effort to identify the most effective drugs against viral infections with replication-inhibiting properties that can alleviate patients' symptoms. Virus infections are complicated to fight without harming the host cells because the viral genome utilises the host cell's machinery to replicate and assemble into new copies. The viral load is entirely dependent on the assembly rates. For example, in the case of COVID-19, a single infected host cell can produce over 10,000 new coronaviruses before the cell bursts. To sum up, understanding how effectively to fight and treat viral infections requires grasping the viral life cycle, which involves several stages, including attachment to the host cell receptor. Most animal-specific viruses have an additional lipid membrane, known as an envelope, with protein spikes that facilitate attachment to a target cell. In the case of SARS-CoV-2, these spikes are part of the structural protein's composition [32].

1.2 Antiviral drugs

In the last 60 years of development, most antiviral drugs were designed for long-term infection; only 43 antiviral drugs are against HIV alone, which has not satisfied the trend for the last several decades. Additionally, 75 antiviral drugs target the viral molecular machinery, specifically proteins, while 13 target host proteins. It would probably make more sense if antiviral drugs targeted host proteins, as it is harder to develop resistance due to the host DNA, which generates lower mutation rates. We are witnessing a shortage of effective antiviral drugs for several reasons. Host factors could be another angle. Some antivirals, such as interferons, enhance the immune response. But many are direct-acting [43-44, 46]. The challenge is to ensure that the drug affects only the virus. For instance, nucleoside analogues get incorporated into viral DNA, causing chain termination. However, they might also affect host DNA if not selective enough, leading to side effects. In terms of unique characteristics, key points may include their targeted mechanisms, the challenge of resistance, the narrow spectrum, the need for timely administration, and the complexity of development due to virus-host interactions [40]. Additionally, combination therapies are used to overcome resistance and their role in managing chronic infections (such as HIV) versus acute infections (like influenza). Additionally, the fact that viruses are intracellular parasites makes targeting them without harming host cells a challenging task. Antibiotics can target cell walls or ribosomes, which are different in bacteria. Viruses lack ribosomes, so antivirals must target alternative sites, such as viral polymerases or proteases. Mechanism of action (specific stages), specificity and selectivity, issues with resistance, narrow spectrum, timing of use, combination therapies, and challenges in development. Maybe also mention examples like acyclovir, Tamiflu, HIV drugs, and HCV DAAs. IC_{50} (Half-Maximal Inhibitory Concentration) is the concentration of a drug required to inhibit 50% of viral replication or enzymatic activity in vitro. It measures a drug's potency in directly blocking viral components (e.g., viral enzymes like RdRP or 3CL protease). Remdesivir (RdRP inhibitor): IC_{50} values are determined by its ability to inhibit viral RNA polymerase activity [45-46,49]. Paxlovid (nirmatrelvir/ritonavir): IC_{50} reflects inhibition of the SARS-CoV-2 3CL protease. CE (Cytopathic Effect Inhibition) - CE assays measure a drug's ability to protect host cells from virus-induced damage (cytopathic effect, CPE) in cell cultures. It evaluates both antiviral activity and cell viability (toxicity). Drugs like molnupiravir are tested for their ability to reduce SARS-CoV-2-induced CPE in cultured cells. EC_{50} (Half-Maximal Effective Concentration) is often reported, representing the concentration of the drug required to achieve 50% protection from CPE. IC_{50} : Prioritizes drugs that directly target viral machinery, such as RdRP inhibitors like remdesivir. CE (EC_{50}): Identifies drugs that are non-toxic and effective in cellular models, bridging in vitro results to in vivo outcomes. A drug with a low IC_{50} (potent) but high EC_{50} (ineffective in cells) may fail due to poor cellular uptake or toxicity. Successful antivirals (e.g., Paxlovid) combine a low IC_{50} (potent viral inhibition) with a low EC_{50} (adequate cell protection). Both metrics are critical in antiviral development, with IC guiding mechanistic studies and CE ensuring translational potential [48].

Antiviral therapy has been one of the most complex and expensive fields of pharmaceuticals for many decades, and only a few new antivirals have been developed in the last 60 years. This sad tendency can be seen in Figure 3, which shows time lags.

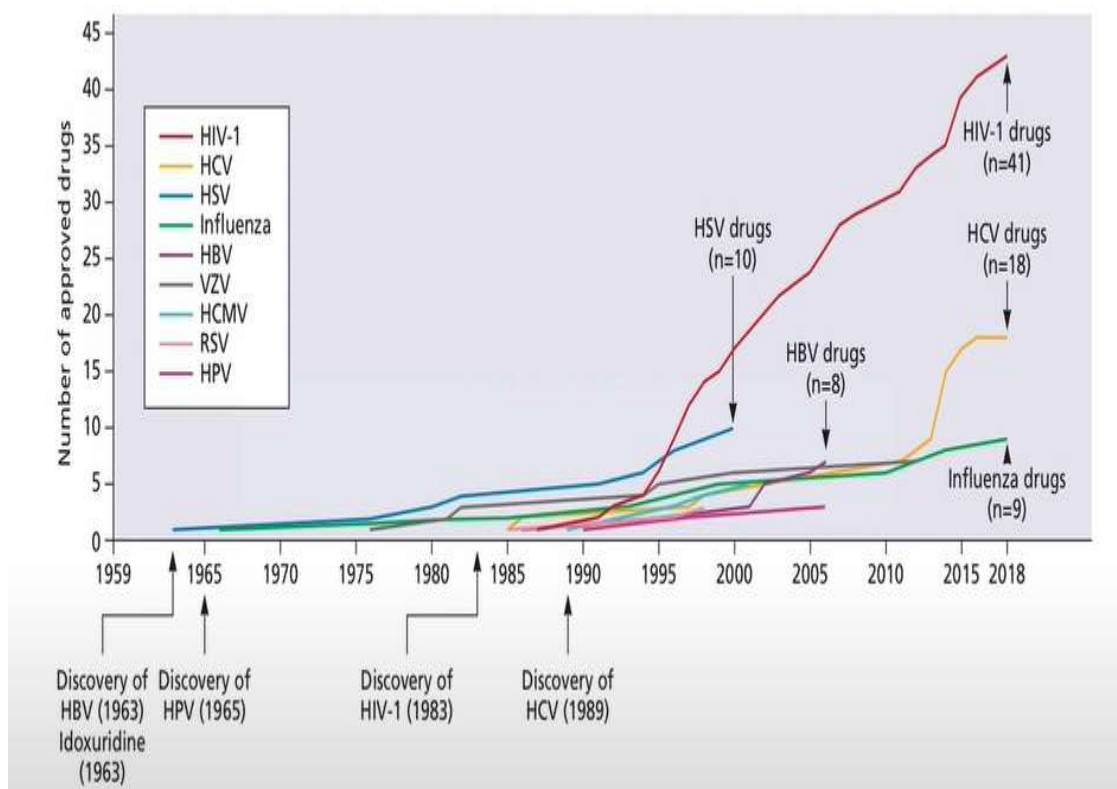


Figure 3 - 60 years of antiviral drug development in the USA since the early 1960s in the 20th century; unfortunately, research on antiviral medications began only after the discovery of viruses. This allowed the viral infection to spread or adapt to human immunity and the human genome, causing the pharmaceutical industry many problems in establishing strategies to fight the viral invasion [28-29].

Thus, only a few drugs were approved to combat them effectively. To make matters worse, pharmacology and science were primarily focused on persistent viral diseases that require lengthy and expensive therapy to reduce the viral load in host cells. Furthermore, viruses are difficult to treat without serious side effects. In addition to the scarcity of antiviral drugs, it has another fatal flaw: its viral targets were primarily designed against chronic and slowly developing viral pathogens. To make matters worse, only 37% were intended to inhibit polymerase activity. Figure 4 shows this grim allocation of antivirals. So, putting it all together, the unique aspects are their targeted approach to specific viral mechanisms, the need for precision to avoid host toxicity, dealing with rapid viral mutation and resistance, often narrow spectrum, critical timing in administration, use in combinations, and the complexity in developing drugs that can effectively interrupt viral processes without harming the host [51,53-54].

Since viruses can hide in specific cells or reservoirs (such as latent herpes), antivirals must be able to penetrate those areas. For chronic infections, long-term use is needed, which requires drugs with reasonable safety profiles [54].

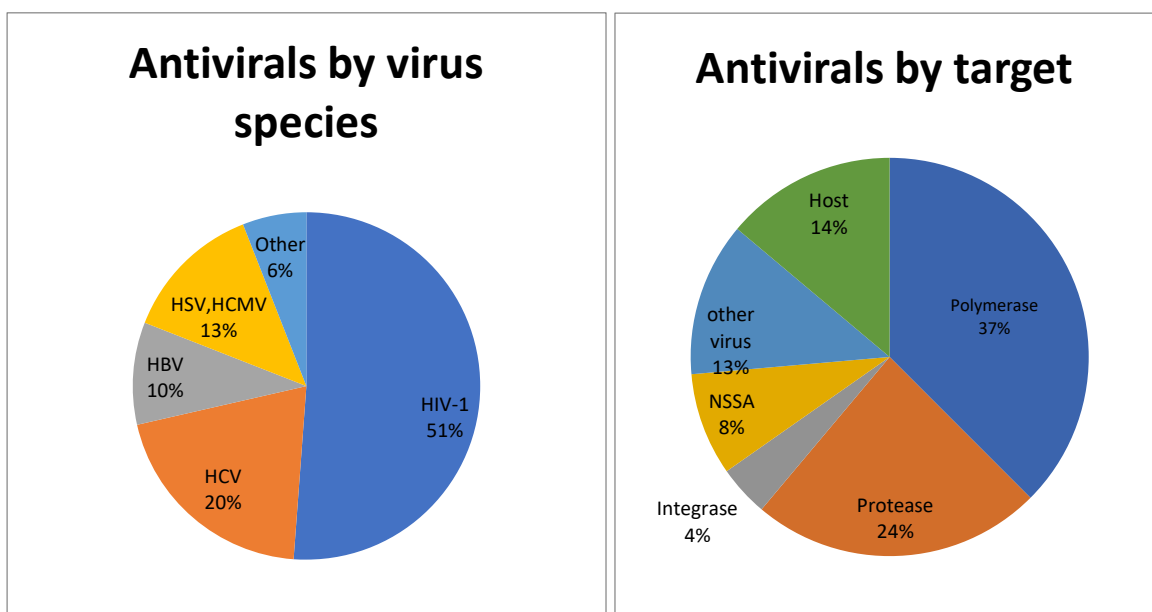


Figure 4 — Antivirals by virus species and target.

First and foremost, compounds that interfere with virus growth can have adverse effects on the host cell. This means side effects are common and, in most cases, unacceptable. Additionally, every step in the viral replication cycle engages host functions [30-31]. Secondly, some medically and clinically important viruses cannot be propagated, as there is no suitable animal model, and they are too hazardous to work with. These viruses include HBV, HPV, smallpox, Ebola virus, Lassa virus, and Marburg virus [53-54]. Thirdly, a compound must completely block virus replication. It must be potent. Antiviral potent drugs cannot afford to block enzyme activity only partially as many standard pharmaceuticals can. Otherwise, we develop antiviral drug resistance due to mutated strains. And, of course, we should not forget the financial aspect – it is costly. For many decades, antiviral medicine production has created four main groups. They are 1) Anti-influenza, 2) anti-HIV drugs, 3) Anti-hepatitis, and 4) Anti-herpes. Figure 4 illustrates the allocation of antiviral drugs by virus species and their specific targets. Overall, the majority of antiviral medications focus on HIV, while polymerase activity is the least targeted mechanism. The first pie chart shows that 46% of antiviral drugs are developed to combat HIV, making it the most researched virus. Other viruses, such as Hepatitis B and C (HBV/HCV), account for 21%, while herpes viruses represent 17%. Influenza and other viruses comprise more petite proportions, at 11% and 5%, respectively. The second chart highlights the targets of these antiviral drugs—the most significant proportion (37%) targets polymerase activity, essential for viral replication. Proteins involved in viral molecular mechanisms are targeted by 31% of drugs, while integrase inhibitors account for 4%. Approximately 28% of antivirals are directed at host DNA or proteins, indirectly affecting virus survival [54-56]. In

summary, most antiviral drugs are aimed at treating HIV and focus on polymerase activity or viral proteins. However, a considerable portion also targets host cellular mechanisms, reflecting efforts to develop broader treatments for persistent viral infections. This data underscores the challenges in Favipiravir (nucleoside analogue) is pyrazine analogue T-705 and a capable inhibitor of influenza viral RNA polymerase [33]. Favipiravir's metabolite (Favipiravir RTP (ribofuranosyl 5'-triphosphate) interacts with viral RNA-dependent polymerase (RdRP). It is assumed that the antiviral effect can be downgraded in the appearance of purine nucleotides ATP and GTP. In addition, this metabolite can be identified as a 'false' purine by the viral RdRP [34]. Previous in vitro studies have shown that SARS-CoV-2 Vero E6-infected cells exhibit a tolerable cytotoxic response, with a half-cytotoxic concentration (CC50) of 400 μ M and above [35]. Thus, it became clear that Favipiravir could be used at high concentrations as a safe and effective medicine against COVID-19 infection. Ribavirin (a nucleoside analogue) is a well-known antiviral drug that interferes with RNA and DNA replication by acting as a guanosine analogue (Guanine triphosphate (GTP)). The RNA-polymerase is no single target. However, its structure prevents RNA capping during the maturation of the RNA strand, which is heavily dependent on natural guanosine, thereby keeping RNA from degradation [36]. Some studies have shown no significant cytotoxicity in the Vero cell model at 31.3 μ g/mL ribavirin concentrations [37]. The clinical experience during the pandemic revealed that patients with worsening cases were administered 400mg every 8 hours, in addition to methylprednisolone, to decrease the progressive viral load activity [38]. The high specialization of the ribavirin drug led doctors to pair it with either IFN- α 2a or IFN- α 2b (interferon) to cover the therapeutic threshold and stop viral replication [38]. In 2003, in Canada, ribavirin therapy with a dose of 500mg every 8 hours for 4-6 days long was also combined with a corticosteroid in 40% of SARS patients [39]. Ribavirin is a universal antiviral agent that can be taken alone or in combination with antiviral compounds, such as interferon or immunosuppressants like corticosteroids, in a worsening clinical condition.

Tenofovir (nucleotide analogue) belongs to both anti-HIV drugs and Antihepatitic drugs, according to the producer's manual. Tenofovir represents the reverse transcriptase inhibitors, or nucleoside reverse transcriptase inhibitors (NRTIs), which are structural analogues of nucleic acids, adenosine monophosphate, which competitively inhibit the reverse transcription by causing the chain termination after they get involved in viral DNA. This viral DNA incorporation causes so-called 'lethal mutagenesis.' Tenofovir is also an antiviral drug against chronic hepatitis B as a nucleotide analogue. Tenofovir inhibits the HBV (hepatitis B virus) polymerase by competing with natural substrate in cooperation with growing viral DNA-strand causing, as in HIV (human immune deficit virus) chain termination, subsequently stalls the reverse transcription and synthesis of viral DNA. Tenofovir is another nucleotide analogue initially designed to inhibit the HIV (human immunogenicity virus) reverse transcriptase by interfering with the ATP-Polymerization in the growing nucleic acid chain [44]. Tenofovir was also assumed to be effective against COVID-19 as it showed the tendency to dock the RNA-dependent RNA-polymerase (RdRP) and silence its activity in replication as well as in transcription and translation of structural and

accessory proteins, making virions assembly almost impossible [50]. Tenofovir, which is used in our study for oral administration medicine in the form of disoproxil fumarate (TDF), has many side effects if it is used in high dosages, such as renal toxicity, bone density degradation, etc. [44-45]. *In-vitro* studies suggest that at concentrations under 100 μ M, tenofovir does not inhibit the viral replication in VeroE6 cells at multiple infections in a so-called preventive way when tenofovir was administered one hour before infection and up to 48 hours post-infection. In the discussion of results, researchers came to the idea that tenofovir in ATP-forms requires the activation by host kinase, and any cell type probably has the proper kinase activity to launch the tenofovir antiviral features. Try a study on human airway epithelial cells [42,43]. According to the medicine producer's manual, dexamethasone is a synthetic glucocorticoid (GCS), a methylated derivative of fluor prednisolone. Provision of anti-inflammatory, anti-allergic, immunosuppressive action, increased sensitivity of beta-adrenergic receptors to endogenous catecholamines. The anti-inflammatory effect is linked to decreased capillary permeability, stabilization of cell membranes (especially lysosomal) and organelle membranes, inhibition of eosinophil and mast cell release of inflammatory mediators, induction of lipocortin formation, and reduction in the number of mast cells that produce hyaluronic acid. It acts on all stages of the inflammatory process: it inhibits the synthesis of prostaglandins (Pg) at the level of arachidonic acid (lipocortin inhibits phospholipase A2, inhibits the liberation of arachidonic acid and inhibits the biosynthesis of endoperoxides, leukotrienes, which contribute to inflammation, allergies, etc.), the synthesis of "pro-inflammatory cytokines" (interleukin 1, tumour necrosis factor-alpha, etc.); increases the resistance of the cell membrane to the action of various damaging factors. The immunosuppressive effect is brought on by lymphoid tissue involution, inhibition of lymphocyte proliferation (especially T-lymphocyte proliferation), suppression of B-cell migration and interaction between T- and B-lymphocytes, inhibition of cytokine release from lymphocytes and macrophages (interleukin-1, 2; interferon gamma) [94]. And decreased antibody production. The antiallergic effect develops as a result of a decrease in the synthesis and secretion of allergy mediators, inhibition of the release of histamine and other biologically active substances from sensitized mast cells and basophils, a decline in the number of circulating basophils, T- and B-lymphocytes, mast cells; suppression of the development of lymphoid and connective tissue, reducing the sensitivity of effector cells to allergy mediators, inhibition of antibody formation, changes in the body's immune response. It is worth mentioning that 0.5 mg of dexamethasone is equivalent to roughly 3.5 mg of prednisone (or prednisolone), 15 mg of hydrocortisone, or 17.5 mg of cortisone, depending on the degree of glucocorticoid action. According to WHO data, dexamethasone should be used in severe cases of COVID-19, especially if a patient is dependent on live-supporting systems [42-49]. Since the author's antiviral study mainly rests on tableted forms, there are some recommendations that consumers must follow to reduce the side effects. In Figure 5, the maximum daily doses prescribed by the manufacturer's recommendations are the effective doses of antiviral effect of Favipiravir, Ribavirin, and Tenofovir for humans (in vivo) for Vero E6 cells (in vitro). Toxicity is defined as the amount or degree of a substance required to be poisonous. It

depends on the amount and concentration involved, frequency of use, interactions of the person receiving the substance of interest, and individual reaction of the person [44,50]. Any drug improvement begins with the revision of its efficacy and pre-clinic or clinical trials. In severe cases, doctors combine drugs to achieve a better therapeutical effect, which cannot be performed in vitro due to the high cytotoxicity potential of antiviral drugs

The drug dose reflects both efficacy and the rising chance of unwanted side effects. Antivirals are severe cell poisonous agents that destroy infected cells. SARS-CoV-2 proteases are pivotal for its lifecycle and are significant targets for antivirals. Mpro inhibitors already play a clinical role, while PLpro remains an emerging target with dual antiviral/immunomodulatory potential. Structural and mechanistic insights continue to drive therapeutic innovation.

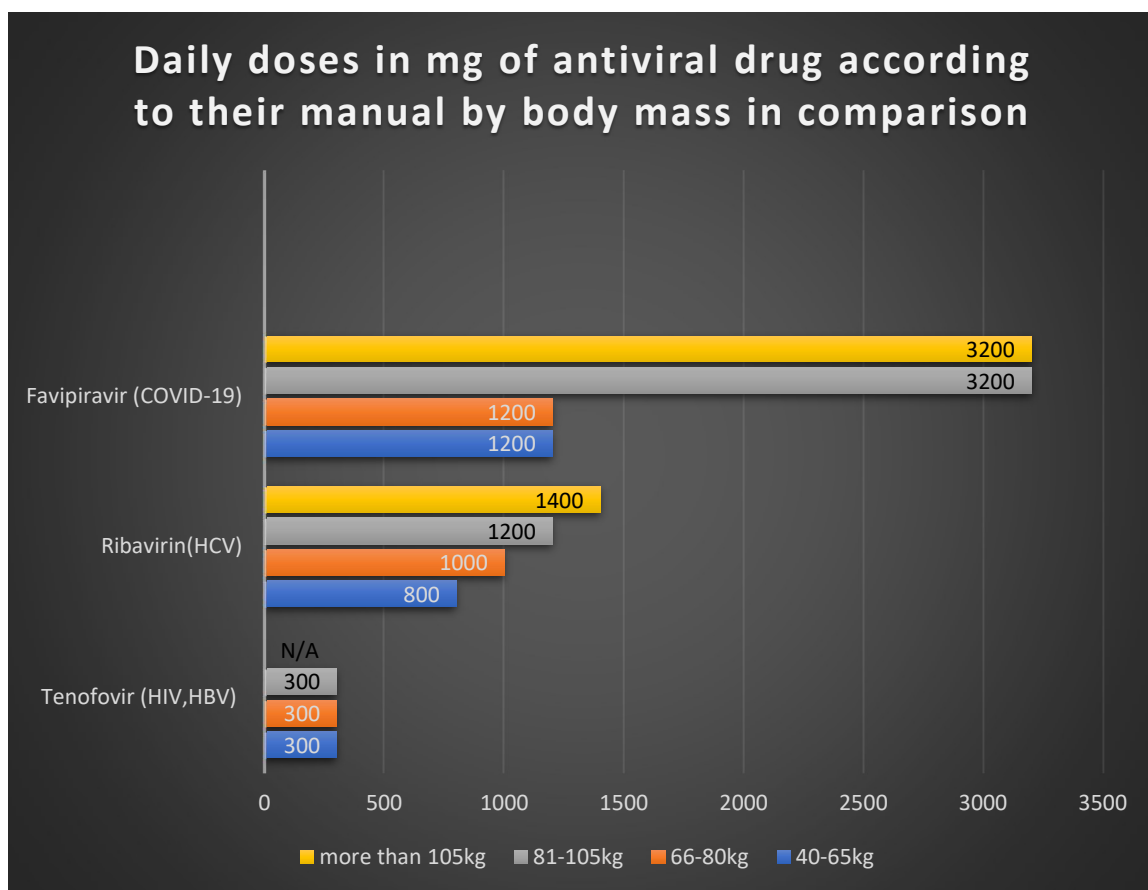


Figure 5 - Daily doses in mg of antiviral drug according to their manual by body mass compared to humans [drug brochures → Appendix F].

It is known in the market as *Fabiflu*, a specialized medicine for treating SARS-CoV-2 infection, and its dose is very high. It is designed to be administered within ten days for minor or moderate stages of COVID-19 infection. Unlike Fabiflu, Ribavirin, for instance, was designed to slow down hepatitis C replication for up to 72 weeks, requiring a daily dose of the medication. Tenofovir is recommended to be taken orally

once daily, with one tablet containing 300 mg of tenofovir, for an extended period under strict physician supervision and control, as per the manufacturer’s manual and relevant publications [34-49]. Effective doses of antiviral effects of Favipiravir, Ribavirin, and Tenofovir on humans (in vitro) in Vero E6 cells. After the first SARS-CoV-1 pandemic in 2003. The dose recommendations for tenofovir and favipiravir were prescribed after in vitro studies; see Figure 6.

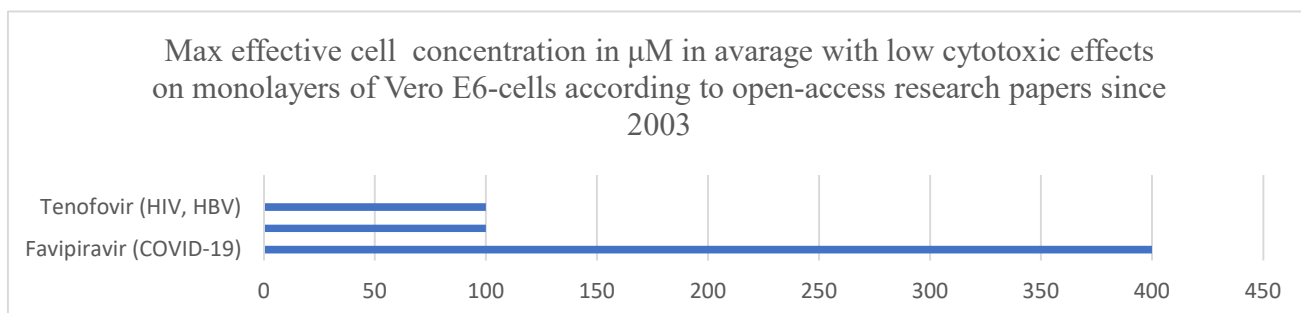


Figure 6 – Maximum effective cell concentration in μM , on average, with minimal cytotoxic effects on monolayers of Vero E6 Cells, as reported in open-access research papers published since 2003.

The Vero E6 model also demonstrates the toxicity edge for monolayer cells, where tenofovir and ribavirin could be effective, and dose control plays a significant role not only in achieving absolute viral RNA/DNA replication silencing but also in minimizing the negative side effect impact on contacting cells and tissues. Effective concentration and potency (EC_{50} , EC_{90}), concertation efficacy of three drugs (Inhibition activity): half maximal viable concentration (EC_{50}) may be a degree of the concentration of a medicate, counter-acting agent (*e.g.*, antibodies), or toxicant that actuates a reaction *midway* (halfway) between the pattern and *the* most outstanding value after an indicated introduction time, saying it differently, EC_{50} can be specified as the concentration needed to obtain a 50% drug-effect. In our case, all three antiviral drugs are expected to have them because we are planning to achieve EC_{90} or even EC_{99} , or in some cases, it is referred to as IC_{99} , which represents the maximum inhibition potential.

$$\text{pEC}_{50} = -\log_{10}(\text{EC}_{50}) \quad (1)$$

There is a comprehensive range of EC_{50} values in formula (1) for drugs, which are regularly found to vary from *nM* to *mM*. Thus, it is often more sensible to refer to the logarithmically transformed pEC_{50} values rather than the EC_{50} . The term "potency" refers to the EC_{50} value. The lower the EC_{50} value, the lower the drug concentration required to achieve 50% of the maximal effect, and the higher the potency. The EC_{10}

and EC_{90} concentrations induce 10% and 90% maximal responses, respectively. However, viral replication must be stopped completely; even 90% silencing or ‘breaking’ of replication is not enough to achieve the therapeutic effect of antiviral medication. Thus, so-called old drugs, such as ribavirin and tenofovir, are designed to be administered for an extended period and in relatively moderate concentrations to inhibit viral replication activity in host cells. Ribavirin and Tenofovir are the antivirals for long-run drug therapy for primary purposes. Still, the increased concentration for ten days of prescribed therapy like favipiravir can be either a reasonable risk for a cheap and effective alternative or a ‘side-effect disaster’ for a chance to fight COVID-19, for instance, or influenzas. To make matters worse, the effective concentration (EC_{10} , EC_{50} , EC_{90}) measure was heavily criticized in 2003 due to its ‘vagueness’ [34-38, 51]. To support the idea of the vagueness of this measure methodology, a study on the effectiveness of antivirals as individual agents and as a drug combination was conducted in Japan to demonstrate how E_{50} values vary across *in vitro* studies. The difference between minimum and maximum values is, on average, 40 times [39-50]. Thus, the values of EC_{10} and EC_{90} also demonstrated a wide range of ‘runaway’ values, with data integrity issues. To sum up, to fight the viral replicase of fast-developing SARS-COV2 (i.e., its intercellular spread), almost 100% silencing is required, and to gain this, physicians prescribe either high drug doses within ten days on average with a particular drug like T-705 (favipiravir) or a combination of medications like ribavirin with corticosteroids (such as dexamethasone), or even 300mg tenofovir daily up to one week period, yet not at critical phase of COVID-19 infection.

1.3 Lethal mutagenesis as a purpose

Almost all Nucleoside analogues increase the mutation rates so high that viral replication machinery synthesized in ORF1ab gets disturbed so critically that either the RNA subunits do not attach to RdRP-like Remdesivir does [44,56,95] or the direct inhibition of RdRP through coping false RNA strands is blocked, just like our discussed purine analogues: Favipiravir, Ribavirin, and Tenofovir [50-51]. A clear and distinct correlation is evident in Figure 7.

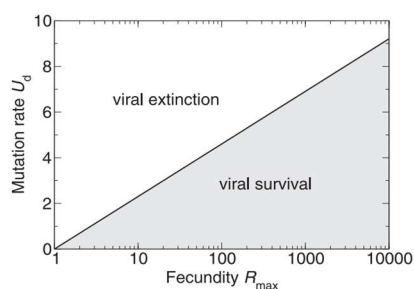


Figure 7 — The lethal mutagenesis characterization for virus existence.

Since any virus, after entering the host cytosol, consists of genetic information (mRNA), the high error rates in replicating itself play a critical role. Thus, the threshold line between extinction and survival is thin. As proofreading is crucial for viral survival, it is also important for pharmacology to target the viral replicating machinery in a host cell. To ensure viral extinction, we must have 100% inhibition [94-98]. As

an mRNA virus, COVID-19 has two ways to fight against it: vaccination and drug intervention. The drug intervention of these antivirals is mostly bound with RdRP-inhibition to reach lethal mutagenesis of viral infection. When the viral genomic RNA (gRNA) ingests itself in the host cell, it has relatively unstable single-stranded positive genomic RNA that requires replicated as soon as possible to be able to replicate new genomic RNA for structural protein synthesis and assembly; furthermore, after replicating itself the 'original' genomic RNA craves to build the sub-genomic RNAs (sgRNA) via transcription, these sg-RNAs (with capped mRNA, as in eucaryotic cells) are essential for translation in expressing the structural proteins that go to viral assembly as well as newly replicated RNA. As a result, inhibiting or interfering with the viral replicase represents a serious arsenal in antiviral therapy that allows us to insert mutated gRNA or damaged gRNA into the assembly process, providing so-called extinction by a fatal error in the viral genome during and after replication [48,50,55]. As mentioned, ribavirin was invented roughly 40 years ago and showed antiviral efficacy in human and animal lines. As a guanosine analogue, it goes to host kinase as ribavirin triphosphate and pairs with cytidine or uridine-triphosphate. It mimics the purine nucleobase, causing severe mutations during replicase and causing lethal mutagenesis as anti-viral therapy, reducing the viral load rates [49-51, 88]. In 2019, a new drug against influenzas had the same RdRP-inhibiting properties as ribavirin, and it showed promising results during the COVID-19 pandemic. Both drugs are nucleoside inhibitors. Unlike ribavirin, molnupiravir is a pyrimidine analogue. It is worth mentioning that ribavirin is a more cost-effective and closely monitored drug than molnupiravir, demonstrating similar effectiveness. Nevertheless, during the pandemic crisis in 2003 and 2019, the treatment was combined either with other medications or so-called adjuvants like interferons and corticosteroids to achieve maximum outcomes from treatment, and ribavirin was a classic example of these combination lines with acceptable survival as well as recovery rates among mild and moderate patients with SARS and SARS-COV2 infection. [37-38,50-51].

Favipiravir is another effective nucleoside and nucleotide inhibitor with a proven wide-spectrum activity against viruses that strongly rely on RdRP. In countries such as India and Japan, favipiravir demonstrated high rates of clinical effectiveness and relatively low cytotoxicity, as well as a low side-effect potential. Along with ribavirin, it was primarily prescribed for mild to moderate patients with a 9-to 14-day inpatient background. [34-35]. *Favipiravir* also shows a good response against host RNA-dependent replicase kinase, enabling it to act as an effective lethal mutagenesis agent not only in SARS-CoV-2 populations but also against deadly diseases such as Ebola, influenza, and rabies, which makes it an asset as an antiviral medicine. Additionally, it is an effective drug against Influenza A and B, particularly for prophylaxis and mild infections [34, 49, 92].

Tenofovir is the most cytotoxic drug on our antiviral drug list (only 300mg oral administration is allowed daily). It also belongs to the nucleoside inhibitor class, incorporating RdRP, which renders viral DNA synthesis unviable and slows down the virulence potential. Initially, it was designed against HIV and Hepatitis B viral invasion [44,91,93-94]. As it was already mentioned, the immune system in humans is

responsible for the ‘overdefensive’ response to the viral invasion, causing massive tissue damage depending on age group, causing severe pneumonia as the ‘final act’ of immunity – the so-called ‘*cytokinetic storm*’ which probably was the main reason of lethal outcomes during Spanish influenza pandemic after WWI. All three antiviral drugs are clinically prescribed for patients with mild to moderate viral infections, reducing the viral load through lethal mutagenesis and enabling the achievement of viral extinction. In severe cases, doctors mostly take steroids to calm the overreacted immune response that could be lethal if it is not stopped, and here comes corticosteroids in combination with antiviral therapies like with ribavirin already in 2003. The antiviral effect was so highly effective that the WHO (World Health Organization) recommends dexamethasone as an additional and safe medication for treating COVID-19 infections in patients with mild to moderate symptoms [57, 76]. The bone infarct is mainly caused by the chronic appearance of immune passivation as well as during other health-destructive patterns like alcohol misuse and chronic smoking. The dose risk primarily begins with 500mg of corticosteroids administered daily for 1-3 months [57]. The dexamethasone has a 4mg/ml interveinal administration protocol during the COVID-19 treatment, and only a physician decides on the effective dose. The WHO recommends using 15-20 mg a day in mild stages of infection as an auxiliary therapy option. But what happens with severe cases is still not clear, and everything is highly individual, and intense steroid therapy was inevitable to fight progressing pneumonia and other signs of acute COVID-19 complications [57].

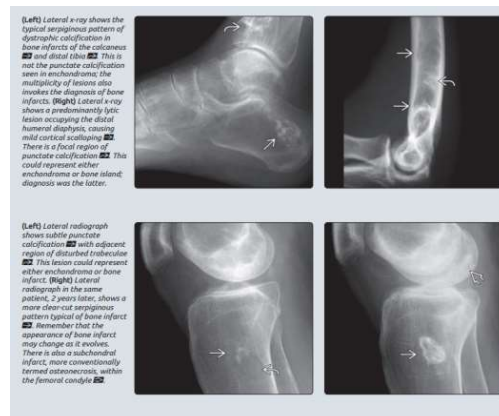


Figure 8 - The bone infarct x-ray image taken from a patient with an immune-mediated medical background.

Figure 8 shows the severe side effects of extensive corticosteroid use. To conclude, lethal mutagenesis must occur within the NSP12 machinery, responsible for synthesizing the viral genome and the subgenomic viral RNA, thereby completing the viral life cycle within the host cell.

1.4 Influenza virus and antivirals against it

Influenza virus-like SARS-CoV-2 is a low viral load-driven infection pathogen that requires relatively low PFU/mL to initiate disease, commonly referred to as a viral ‘cold’. The strain naming of SARS-CoV-2 depends on the occurrence of spike-protein mutations, just as with the Influenza A virus [59]. No matter how fast SARS-CoV-2 and Influenza A viruses can mutate and adapt, they strongly rely on surface proteins in their life-cycle or pathogenesis. Thus, making vaccines against them is a feasible task. There are four types of influenza viruses: influenza A, B, C, and D, all of which differ in nucleoproteins and matrix proteins depending on their antigenic differences [59-61]. Influenza A virus A (IAV) is responsible for respiratory ailments. These unpredictable pathogens threaten human health and animals through continuous evolution, antigenic drift, and shifts. The natural reservoir of IAV is aquatic wild birds, from which they can move to another terrestrial host, including terrestrial birds and mammals [61-63]. Influenza A, B, and C belong to the family Orthomyxoviridae, which comprises small viruses. Coronavirus, the virus family, has a negative RNA segmented genome with continuous and step-by-step activation during the infection period, which lasts up to 72 hours. Still, antiviral management is only effective within the first 48 hours, as it suppresses viral replication and reduces viral load intensity, thereby enhancing innate and adaptive immunity. Their primary characterization is based on the classification of main surface glycoproteins, specifically HA (hemagglutinin) and NA (neuraminidase). [61-63]. Influenza viruses have a standard terminology, like any other widespread virus, which includes the virus type (A and B, respectively). The species from which it was isolated (if it does not belong to humans, for example, pigs or birds); the place where it was isolated (express PCR is required for identification - diagnosis of influenza infection); isolate number; year of isolation; and only for influenza A virus subtypes HA and NA. It is worth mentioning that by now, only 16 for HA and 9 for NA subtypes (variations) in every season circulating influenza A were found, among which only 3 HA (H1, H2, and H3) and only 2NA (N1 and N2) subtypes (mutated variations) have caused human epidemics, as confirmed by sustained, widespread, human-to-human transmission [63]. Thus, *A/Kazakhstan, Almaty/2125/2024 (H3N2) - an example of a viral strain isolated this year in Kazakhstan – is profoundly concerned*. The same pattern can be observed in SARS-CoV-2 virus strains, which exhibit multiple and varied mutations of the so-called ‘sugar coat’ on the Spike protein, facilitated by mutated Spike protein strains such as Gamma, Delta, Lambda, Mu, and Omicron. Since spike proteins enable the SARS-CoV-2 virus, or rather a virion produced from infected host cells like those in the respiratory tract, to evade the innate immune system, spike protein mutations provide various features, including higher virulence, more effective and robust vital enzymes, and their supporting segments, such as NSP9 in RNA-dependent RNA polymerase. Still, one glycoprotein segment remains unchanged in all variants of concern – the D416G mutation [58]. Overall, the Influenza A virus and SARS-CoV-2 Virus, as companions, represent a severe threat to immune-compromised individuals and pose continuous challenges for physicians and pharmacies to find optimal, effective treatment strategies, thereby minimizing the post-COVID-19/influenza effect or period on patients and relatively healthy people. To

make things worse, the influenza A virus diagnostics is not as rapid and seriously taken as the SARS-COV2 diagnostics in a cohort of treating doctors or among infected patients. Regarding Influenza A treatment, an infected person must take an anti-influenza drug, such as oseltamivir, as soon as possible, ideally within 48 hours after the first signs of illness appear, to ensure effective and further antibiotic treatment. The same applies to COVID-19. Last but not least, the influenza A virus has a significantly smaller viral genome compared to SARS-CoV-2; still, SARS-CoV-2 is capable of reproducing itself relatively quickly and effectively in terms of evading and silencing the antiviral mechanisms common to all viral replication machinery. Most viruses do not change if environmental, mental, and immunity factors do not stress them. Therefore, it is relatively easy for our immune system to recognize them from one year to the next. However, Influenza virus A or B is different. The keys or glycoproteins (HA and NA) on its surface change with each generation, making previously matured Antibodies, mostly IgGs, useless. Each year, the influenza virus undergoes mutations, which ensure genetic variability within its viral RNA or genome. This process occurs gradually, causing the glycoproteins on the viral surface to change, resulting in a gradual antigenic shift within the influenza genome—a phenomenon known as step-ahead mutations in antigen-antibody interactions [58, 59]. Nevertheless, these changes are primarily seasonal effects that rely on weakened population immunity, and only relatively minor changes or alterations in glycoproteins are required to infect or reinfect the target host cell. The more deadly changes appear when inter-species sustained – antigenic shift takes place. Viruses are highly selective invaders; some attach birds' lung cells only and ignore human lung cells; however, if a bird population is located among other species like mammals and birds- the virus adapts to, for instance, the pigs' lungs and is capable of invading humans thanks to surface proteins matching or rather multiple matching properties of two glycoproteins (HA and NA). The hybrid set of surface proteins of the avian influenza virus, capable of penetrating both target cells of birds and target cells of pigs, poses a much more severe threat to humans than the "native" influenza virus because of antigenic drift that gets all complete changes or mutation variations of keys (HA and NA) at ones without gradual adaptation period, resulting a rapid and an unhindered spreading of new influenza virus in the host cells experiencing only innate and an unspecified immunity reaction that can lead to severe damage or life-threatening conditions, such as 'cytokinetic shock' or overwhelming uncontrolled viral load that also could cause 'septic shock' within few days after the incubation period. Moreover, most infected patients died from secondary bacterial infections. The deadliest registered pandemic was caused by this virus in 1918, killing over 400.000 people worldwide. Since antibiotics were not yet invented, most patients died from secondary bacterial infections that spread when the Influenza virus weakened the innate immune system [64-66]. It is also known that Coronaviruses came into contact with humans, similar to influenza, through wild birds; however, SARS-CoV-2 originated from wild bats, which likely underwent antigenic shift interactions with the human immune system. To summarize, influenza viruses rely heavily on two glycosylated membrane proteins, just as SARS-CoV-2 does.

The COVID-19 outbreak revitalized research interest in antiviral drug studies and the treatment of seasonal viral infections, such as influenza A, B, and SARS (severe acute respiratory syndrome). This is not a single disease, but a group of diseases caused by different viruses yet sharing similar symptoms and courses. SARS is often referred to as a simple cold and is generally considered harmless, especially in adults. However, the virus can cause serious complications, so there is no need to self-medicate. The cause of SARS can be any virus from a large group that includes more than 200 pathogens. These include adenoviruses, rhinoviruses, coronaviruses (of varying degrees of danger), parainfluenza viruses, and other microorganisms. Influenza's antivirals are the newest antiviral drugs and possess not only protease inhibitory properties but also generally inhibit the viral replication machinery through direct RNA-chain termination, with comparative nucleotide substitution that directly correlates with drug concentration (CE) and drug cytotoxicity (CC), respectively. Favipiravir, as Fabiflu tablets, enables scientists worldwide to gain insight into COVID-19 treatment, despite Favipiravir (T-705) being primarily designed in Japan to combat Influenza A and B viral infections [64]. In addition, anti-flu drugs are among the most recent developments in antiviral medicine production, research, and development, closely related to SARS-CoV-2 infection. Thus, it makes sense to discuss so-called Influenza Antiviral drugs. *M2-ion channel inhibitors block the M2 channel, thereby restricting the passage of protons (H⁺) that are necessary to trigger the release of viral genes (vRNA) into the host cell.* Amantadine and Rimantadine are also prescribed by doctors worldwide, even for people with COVID-19 manifestations [67-73]. Another class of anti-influenza drugs is *endonuclease inhibitors* [65]. The best-known drug of this kind is Baloxavir, whose primary purpose is to selectively inhibit the cap-dependent endonuclease, a highly significant enzyme involved in initiating influenza virus mRNA synthesis. The intervention caused by Baloxavir prevents viral gene transcription and, therefore, viral replication within the host nucleus and cytoplasm. As we can see, unlike SARS-COV2 -replication, influenza is strongly dependent on cell nucleus-ribosome interactions. The last class of ant-influenza drugs is the *neuraminidase inhibitors*. The active agents of this drug class exert their antiviral activity by inhibiting the viral neuraminidase enzyme, which is found on the surface of the viral particle. In the absence of intact neuraminidase, the virus loses its ability to cleave sialic acid and ability to escape the cell. Almost the same process has SARS-COV2-virus, which heavily relies on Spike-glycoprotein that also cleaves on surface membrane, but to ACE2-protein, to enter the host cytoplasm and thanks to complicated NSPs interactions and forming DMVs (double membrane vesicle) a safe place to assemble the viral components like newly synthesized genome packed with nucleocapsid protein viral RNA. Thus, unlike the Influenza virus, the SARS-CoV-2 virus can quickly leave a host cell in a 'safe' embedded vesicle form with all the necessary components to initiate a viral infection. The drugs that belong to *the neuraminidase inhibitor class are* Oseltamivir, Peramivir, and Zanamivir. To sum up, the Anti-Influenza drugs have three classes of antiviral activity: a) M2-ion channel inhibitors, b) endonuclease inhibitors, and c) neuraminidase inhibitors.

The antiviral drugs amantadine and rimantadine are M2-ion channel inhibitors; however, new strains of seasonal Influenza A virus have started developing drug resistance against these widely used antivirals [70-72].

Amantadine (adamantane-1-amine) is primarily designed to combat Influenza A virus infection due to its ability to interfere with the viral M2 protein, the ion pore channel, thereby hindering viral replication in both mRNA synthesis and vRNA [71-73]. Rimantadine (α -methyl-1-adamantane methylamine hydrochloride) is as effective as amantadine and relatively safe, serving as an M2 inhibitor. It was primarily designed in the 1980s to combat the spread of influenza A virus infection [70]. Figure 9 illustrates the entire interfering mechanism of the M2-ion channel on the viral membrane. In addition, amantadine has anti-inflammatory features that are already being used against virus infections like Hepatitis C in a combination of Ribavirin and synthesized interferon [74], even though seasonal occurring Influenza A and B virus in western countries like USA started to develop resistance towards M2-Protein inhibition, mainly, against amantadine as well as rimantadine [75]. In Kazakhstan and other post-Soviet countries, neither studies nor data are conducted or collected on any tendencies of anti-viral resistance. Still, amantadine and rimantadine are cheap and effective antivirals against flu clinal manifestations (symptoms). They can also be used in conjunction with effective and inexpensive medication strategies against other viral infections whose replication machinery relies on acidification processes. The author may claim that these M2-ion inhibitors would show high efficacy in Kazakh populations due to lower antiviral drug pressure for at least a decade [76]. When SARS-CoV-2 gained pandemic scale, physicians and researchers worldwide began to utilize and study the so-called ‘time-proven’ antiviral drug arsenal, among which amantadine and rimantadine were explored as a strategy to stop viral spread both within individuals and populations as a therapeutic approach. Since the M2-or Matrix 2 protein is a surface protein, the SARS-CoV-2 Spike protein could be inhibited by administering the M2-surface protein with the help of amantadine. Firstly, amantadine is expected to have an antiviral effect on SARS-CoV-2 Replication by blocking a 5- α -helix channel, also known as the “viroporin channel,” in the hydrophobic region of the intramembrane space of COVID-19 [94,98]. Secondly, some assumptions (hypotheses) suggest that amantadine can downregulate and inhibit the dysfunctional state of *cathepsin L (CTSL)* and other *lysosomal enzymes*. These two mechanisms have been proposed as potentially significant in interfering with and hindering the ability of the SARS-CoV-2 virus to enter target cells and facilitate virus replication [77]. Amantadine and rimantadine were studied in vitro on veroe6 cells and showed remarkable results. Both the use of amantadine and rimantadine, as well as the combinations of redeliver + amantadine, redeliver + rimantadine, and rimantadine alone, inhibited SARS-CoV-2 infection, primarily at the viral level following in vitro infection [78]. To sum up, M2-Ion inhibitors were in active use in Western countries to combat not only seasonal outbreaks of Influenza type A and B viruses but also as an additional treatment against

other viral infections, such as Hepatitis C. Furthermore, since the emergence of COVID-19, they have also been used against the SARS-CoV-2 virus. The viral interior of Influenza A and B and SARS-COV2 are relatively similar; the RNP machinery of replication activation resembles, to some extent, the nucleocapsid protein functions of SARS-COV2-virus that hold together the 30K nucleotides long RNA genome. According to some studies, the M2-ion channel inhibitors are primarily potent against the Influenza A-type and show only partial antiviral effects on the Influenza B-type. Thus, the primary purpose of antivirals remains ineffective; viral replication does tolerate even 90% of damage caused by antivirals, which has often been confirmed since the 1980s [71-77]. Ribavirin inhibits Influenza A through multiple mechanisms: Inhibits Viral RNA Synthesis. Ribavirin mimics guanosine, disrupting viral RNA polymerase function. Causes Lethal Mutagenesis. Introduces mutations in viral RNA, reducing virus viability. Inhibits Host IMPDH Enzyme. Lowers GTP levels, impairing viral replication. Efficacy against Influenza A: In Vitro & Animal Studies: Show inhibition of Influenza A replication. Clinical Studies: Some early studies suggested modest benefits in severe cases. Not as effective as neuraminidase inhibitors (e.g., oseltamivir, zanamivir). Resistance & Limitations: high doses required → Increased risk of hemolytic anaemia. Narrow therapeutic index (toxic at high doses). Not widely recommended for standard Influenza A treatment. Current Role in Influenza Treatment. Not first-line therapy for Influenza A due to better alternatives (oseltamivir, peramivir, Baloxavir). Toxicity concerns. Possible use in severe cases or resistant strains, but limited clinical evidence. While Ribavirin has in vitro activity against Influenza A, its clinical use is limited due to toxicity, lower efficacy compared to standard treatments, and availability of safer alternatives. Neuraminidase inhibitors (oseltamivir, zanamivir) and cap-dependent endonuclease inhibitors (Baloxavir) remain the preferred treatments for Influenza A. In Figure 9, we can see the precise mechanisms of Influenza A replication inhibition pathways. While possessing broad-spectrum antiviral activity, Ribavirin faces several significant challenges as an anti-influenza drug, limiting its clinical utility. Like other influenza antivirals, Ribavirin must be administered early in infection. However, its pharmacokinetics and practical administration challenges often delay treatment, reducing efficacy. Teratogenicity: Ribavirin is contraindicated in pregnancy due to risks of birth defects, restricting its use in a high-risk population (pregnant individuals) [41-42]. Broad-Spectrum Mechanism: As a nucleoside analogue, it interferes with host RNA synthesis, resulting in cytotoxicity and side effects such as fatigue, nausea, and liver toxicity. Ribavirin's toxicity profile, uncertain clinical efficacy, complex administration, and the availability of safer, more effective alternatives render it a suboptimal choice for influenza treatment. Its use is generally reserved for severe cases where benefits outweigh risks, often in combination therapies or research settings. Ribavirin could inhibit the SARS-CoV2 replication. Most SARS-CoV-2 variants, including Alpha, evolved due to natural selection pressures, not ribavirin-induced mutagenesis.

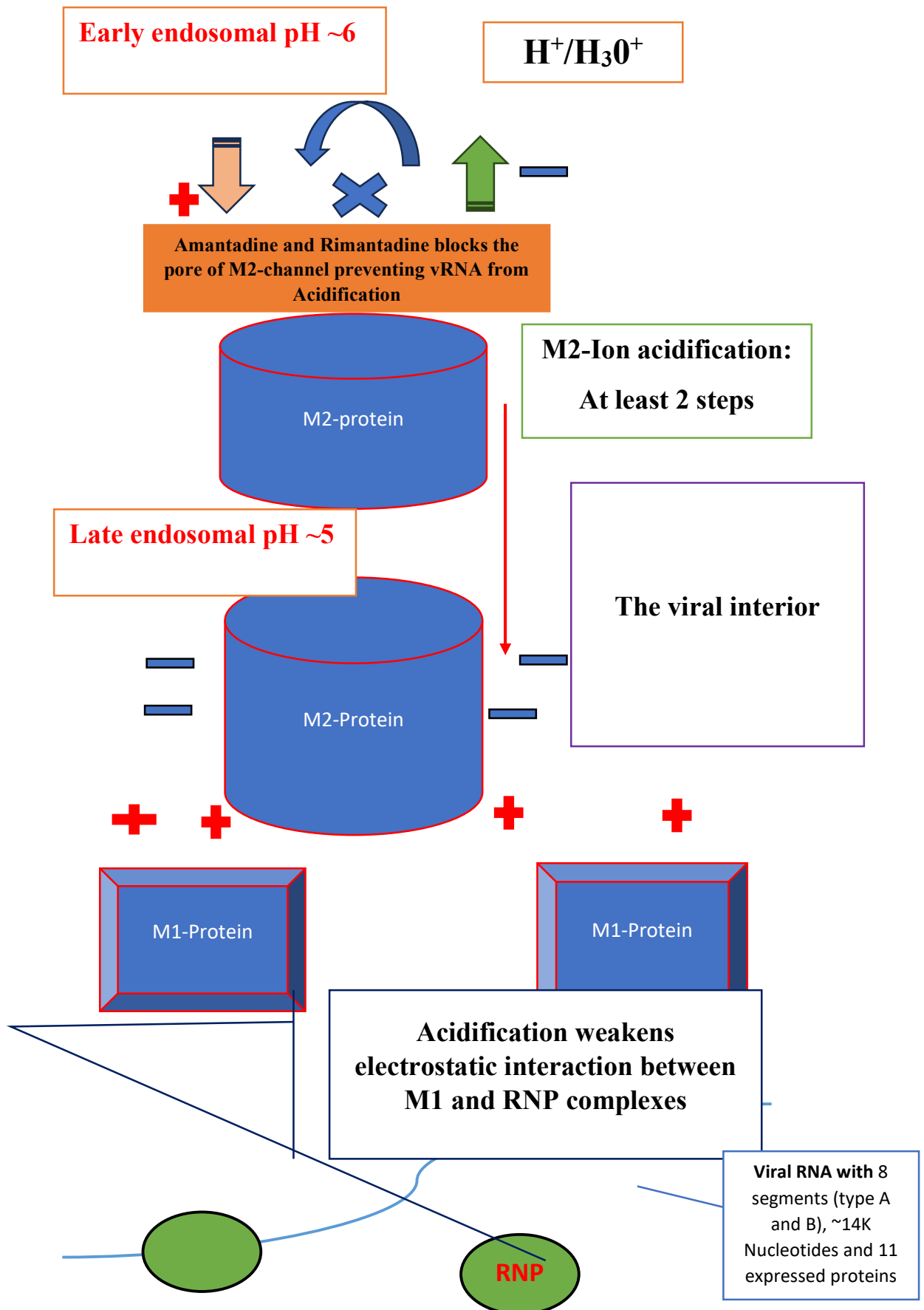


Figure 9 – The general scheme of the typical anti-influenza drug.

The M2-M1 Proteins' activity enables viral RNA to be sent into the cell cytosol. The importance of acidification by M2 protein is paramount. The highly viral genome replication begins with M2-acidic activation, without which neither infection nor further viral genome replication is possible. Thus, for many decades M2-inhibitor like amantadine and rimantadine, which block/bind directly to the pores of the M2 protein channel and prevent the replication of the viral genome - while RNP is transported to the target nucleus (lung cells), viral RNA and mRNA-mRNA are produced [79], and then the main proteins of the viral membrane: HA, NA, and M2 are translated from the replicated viral mRNA and carefully inserted into the endoplasmic reticulum (ER). Then, the Golgi trans network (TGN) is transported to the cell surface, and the virus's life cycle is completed. Endonuclease inhibitors would significantly inhibit SARS-CoV-2 Ribosome cleavage and docking in the primary stages of nucleotide production processes. Additionally, it can hinder the docking of subgenomic RNA on host ribosomes that are capable of producing the structural protein of the SARS-CoV-2 virus. Baloxavir is a prodrug of Baloxavir marboxil, a source of bioactive Baloxavir acid that inhibits the cap-dependent endonuclease, which is crucial for the synthesis of viral mRNA and, subsequently, for viral replication [80-84]. The RNA-dependent RNA polymerase in influenza A and B is called the viral ribonucleoprotein complex [84-85]. These complexes replicate both viral mRNA to produce the necessary proteins and to create a viral genome for virions. The RNA-dependent RNA polymerase of influenza A and B consists of three unique functional subunits: the acid polymerase protein (PA), the main protein of polymerase 1 (PB1), and the main protein of polymerase 2 (PB2) [86]. The protease activity must be triggered quickly and accurately to bind to the 5'-mRNA capsule, initiating the replication of viral mRNA and facilitating the translation of viral nucleoproteins. Interestingly, the host mRNA mechanism is actively involved; viral RNA has only primers to initiate the replication of viral mRNA, which, in turn, is converted into proteins for further structural purposes.

Thus, nucleoside analogues can also have a significantly negative impact on viral genome fitness, causing fatal errors that disable Influenza A and B from replicating the mature RNA, and their combination with Baloxavir represents pharmacokinetic and bioactive (di-phosphate as well as tri-phosphate) inhibitory activity. Baloxavir is a potent drug against Influenza A and B viruses, showing low levels of cytotoxicity and drug resistance by 2024 [85]. In addition, it is typically prescribed for infants before the age of 12 and exhibits minimal side effects, making it a potential preventive measure against seasonal influenza A and B strains. The prevention makes sense because, generally, antiviral drugs are effective within the first 48 hours as potent agents to stop the initial viral spread of influenza A and B viruses, and Baloxavir is no exception. Furthermore, the administration of antiviral drugs must be closely monitored to prevent the development of persistent drug resistance among circulating viral infection variants annually [87-89]. Baloxavir and Favipiravir are novel antiviral drugs and the safest ones in invitro and clinical studies. Favipiravir can also inhibit the polymerase essential protein 1 in the influenza RdRP complex [88,90]. Unlike the flu infection, SARS-CoV-2 has a duration of about 7-10 days before antiviral drugs can

be effective. The new Fabiflu 400mg tablets, along with Baloxavir 40 mg and 80mg, subsequently represent an effective combination against seasonal Influenza A and B, as well as the SARS-CoV-2 virus variant of concern, especially for children and individuals with compromised immunity. Finally, the last group of Influenza antiviral drugs targets the most fundamental enzyme of Influenza A and B – the neuraminidase, located on the surface of viral particles [91]. The inhibition of this enzyme represents paramount importance in combating the spread of the flu virus, regardless of whether it is of the influenza A or B type. In sharp contrast to M2-Ion channel inhibitors, the neuraminidase inhibitor oseltamivir is potent in stopping the spread of viral infections in Influenza types A and B. The type B virus does not have an M2 Protein, and drugs like amantadine or rimantadine show no clinical effect in patients with an Influenza B virus infection [91-92]. The neuraminidase inhibition mechanism occurs during the terminal stage of virion assembly within the host cell; without the active neuraminidase enzyme, the newly produced virus cannot cleave sialic acid and, therefore, is unable to escape from the infected host cell in the respiratory tract [92-94]. The oseltamivir is antiviral agent. It is a prodrug whose active metabolite, oseltamivir carboxylate, selectively inhibits the neuraminidase of influenza virus types A and B. Neuraminidase is a glycoprotein that catalyses the cleavage of the bond between the terminal sialic acid and sugar, thereby facilitating the spread of the virus in the respiratory tract. This process involves the release of virions from an infected cell and their penetration into epithelial cells of the respiratory tract, which prevents the inactivation of the virus by epithelial mucus. Oseltamivir carboxylate acts outside cells and competitively inhibits viral neuraminidase. It suppresses the growth of the influenza virus in vitro and inhibits the replication of the virus, as well as its pathogenicity, in vivo. Reduces the release of influenza A and B viruses from the body [90]. According to recent studies, oseltamivir shows its maximum clinical effect within 36 hours during the 48-hour infection period and significantly reduces symptomatic signs during on-time treatment [59-89]. To sum up, oseltamivir 75mg can be used as a prevention medication as much as Baloxavir 40mg during the seasonal influenza outbreak. Both drugs are safe and effective against Influenza A and B types and can be used among vaccinated and immunocompromised individuals during the so-called flu season. Baloxavir exhibits relatively low antiviral resistance, with a resistance rate of only 1%, and oseltamivir has a resistance rate of 2%, respectively. The combination treatment with Oseltamivir, an Antiviral drug, as an additional (complementary) agent, along with Ribavirin (1200 mg daily), showed a relatively high therapeutic effect in clinical trials involving COVID-19-positive patients in mild and severe stages of disease progression, significantly increasing recovery and survival rates among patients [92]. Numerous studies in China during the pandemic showed that three antiviral drugs, remdesivir (nucleoside analogue), oseltamivir, and zanamivir (neuraminidase inhibitor too), have high higher molecular binding energies with ACE2-receptor after molecular coupling procedures. Thus, the sialic acid enzyme inactivation activities interfere with the SARS-CoV2 entry by silencing the ACE2-receptor on the host cell membrane [92-93]. It is also worth mentioning that oseltamivir has the property to regulate the neutrophil immune cell migration and their activation seriously decreasing the chance of developing sepsis and

other overreaction -neutrophil-related cell damage during COVID-19 progression both in humans and mice respiratory tract via ROS-production in target cell [95]. Overall, the neuraminidase enzyme inhibitor – oseltamivir shows a broad spectrum of antiviral activity, especially during seasonal Influenza A and B outbreaks as prevention therapy and a cellular immune response during mild and severe stages of COVID-19. The oseltamivir carboxylate outside the cell acts as immunoglobulin that seriously jeopardizes the further spreading of the virus without additional immune response and does not mitigate the secondary or active immunity functions. In addition, the antiviral drug – oseltamivir has a relatively low viral resistance percentage, about 2%, and in Kazakhstan, maybe even lower. Generally speaking, all Influenza antivirals make great medication backup strategies for clinicians because the discussed drug types, in most cases, are safe and primarily treat Influenza A and B, whose incubation period or efficacy threshold or anti-viral effective window is potent first 48 hours, whereas SARS-CoV2 has 7-10days to be treated effectively by anti-viral active drugs with various combination options. The SARS-CoV-2 treatment combination with oseltamivir can, in some cases, replace the Dexamethasone adjustment in severe COVID-19 patients in ICU (intensive care unit) departments. 10/22/2020 The U.S. Food and Drug Administration (FDA) has approved the antiviral drug Remdesivir for use in adults and children 12 years of age and older and weighing at least 40 kg (about 88 pounds) to treat COVID-19 that requires hospitalization. According to the FDA, Remdesivir should only be administered in a hospital or health care setting that can provide emergency care comparable to inpatient hospital care. Remdesivir is the first COVID-19 treatment to receive FDA approval [94]. Remdesivir can be efficiently metabolized to active nucleoside triphosphate in several human cell lines [96]. In vitro studies have demonstrated that the nucleoside triphosphate functions as an incorporation competitor for adenosine triphosphate, confusing viral RdRP, acting as a delayed RNA chain terminator against the Ebola virus [97,98], evading viral exoribonuclease testing, and causing a decrease in viral RNA synthesis. Recently, remdesivir has been shown to exhibit antiviral activity following viral entry in Vero E6 cells, supporting its antiviral mechanism as a nucleotide analogue [99]. The relevance of antigenic shift between Influenza A and SARS-CoV-2 lies in understanding their distinct evolutionary mechanisms, pandemic potential, and implications for public health strategies. To sum up, Influenza antivirals tend to act on SARS-CoV-2 in the same way as they do against Influenza A or B. This drug category is of higher interest because it can act quickly and cause less cytotoxic damage. Furthermore, their antiviral effects are better understood, and their drug concentration increase is less hazardous than that of Ribavirin or Tenvir. So, putting it all together, the special aspects are their targeted approach to specific viral mechanisms, the need for precision to avoid host toxicity, dealing with rapid viral mutation and resistance, often narrow spectrum, critical timing in administration, use in combinations, and the complexity in developing drugs that can effectively interrupt viral processes without harming the host. Antivirals are specialized tools requiring precise targeting, strategic use to combat resistance, and tailored development for each virus, reflecting their complex interplay with host biology.

1.5 Cell viability and antiviral assay – MTT and CCK8 methods

The MTT assay protocol is based on the conversion of water-soluble MTT (3-(4,5-dimethylthiazol-2-yl)-2,5-diphenyltetrazolium bromide) compound to an insoluble formazan product. NB: MTT is also a free molecule as *abl46345* (Thiazolyl blue tetrazolium bromide). Viable cells with active metabolism convert MTT into formazan. Dead cells lose this ability and, therefore, show no signal. Thus, colour formation is a valuable and convenient marker of only viable cells. The absorbance at OD 590 nm is proportional to the number of viable cells. The MTT assay measures the metabolic activity of the cells being analysed; the more significant the metabolic activity in the sample, the higher the signal. This should be taken into account when interpreting the assay's results. Reagent Preparation: Briefly centrifuges small vials at low speed before opening [104].

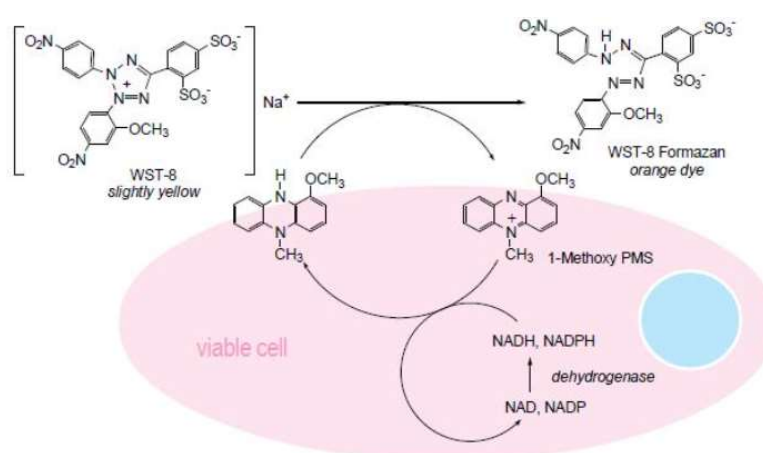


Figure 10 - The CCK8 kit cell viability count. Cell Counting Kit-8 (CCK-8) enables sensitive colorimetric assays to determine cell viability in cell proliferation and cytotoxicity studies.

Dojindo's highly water-soluble tetrazolium salt, WST-8, is reduced by cell dehydrogenase activities to form a yellow-coloured formazan dye soluble in tissue culture media. The amount of the formazan dye generated by the activities of dehydrogenases in cells is directly proportional to the number of living cells.

Cell Counting Kit-8 (CCK-8) enables sensitive colorimetric assays to determine cell viability in cell proliferation and cytotoxicity studies. Dojindo's highly water-soluble tetrazolium salt, WST-8, is reduced by cell dehydrogenase activities to form a yellow-coloured formazan dye soluble in tissue culture media. The amount of the formazan dye generated by the activities of dehydrogenases in cells is directly proportional to the number of living cells. The detection sensitivity of CCK-8 is higher than that of other tetrazolium salts, such as MTT, XTT, MTS, or WST-1 [100].

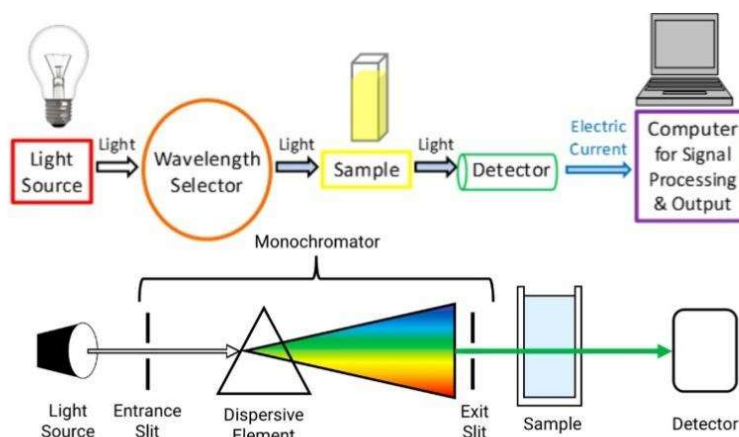


Figure 11- The 96wells compact UV-spectrometer. It is suitable both for CCK8 and MTT-assay cytotoxicity and cell viability assays. Such methods were employed in China using the MTT and CCK-8 assays, as well as in Kazakhstan.

It was advantageous because the cell viability results could be delivered on the same day. The main principles of the CCK8 -assay are depicted in Figures 10 and 11). In addition, the UV-spectrometer enabled the team to take numerous vital measurements in support of the thesis aim, allowing them to determine CE and Cell viability more quickly, especially with CCK8 Kits in BSL4 labs, where the SARS-CoV-2 virus had to be kept intact.

Cytotoxicity (antiviral drugs)

The cell-killing property of an RNA-dependent – RNA polymerase inhibitor (Nucleotide or Nucleoside), independent of the mechanism of cell death, is referred to as cytotoxicity. Establishing that the activity of an inhibitor occurs at concentrations that do not cause cytotoxicity is a critical component of demonstrating that the measured antiviral effect is virus-specific. It forms the cornerstone in selecting a potential drug candidate for further development. The cytotoxic effect of an inhibitor can be determined by calculating the median 50% cytotoxic concentration (CC₅₀), defined as the concentration of the test inhibitor that results in a 50% reduction in cell viability. Inhibitors that act in the middle of the cycle may affect one or more of the many processes involved in viral replication. For example, the polymerase inhibitor T-705 inhibits virus replication when added to viral cultures within six hours of viral infection [93]. When cell viability is ensured, we can use various drug concentrations, considering the viral load (counted in MOI) and, as Figure 12 shows, Favipiravir's EC₅₀, which depends on intact viral particles.

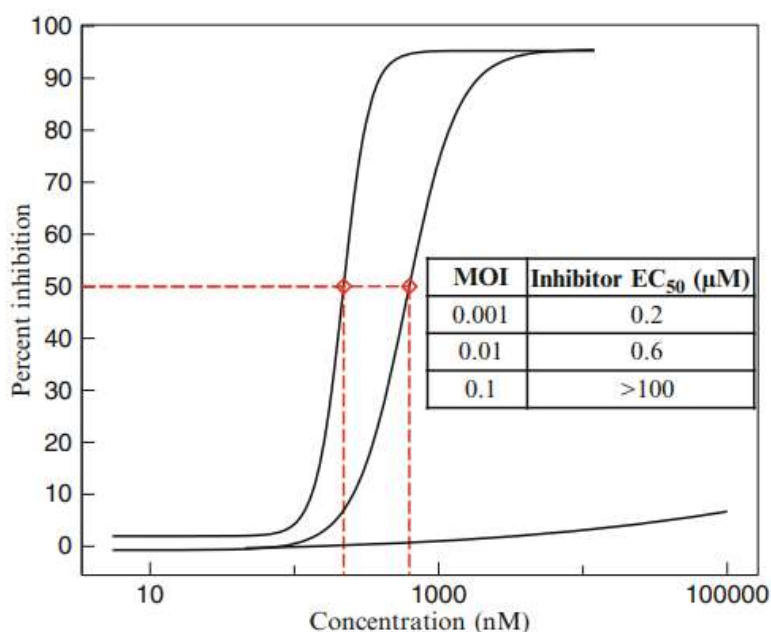


Figure 12—Example of the Effect of MOI 0.001, 0.01, and 0.1 on the EC₅₀ of T-705 or Favipiravir [92-93].

In Figure 12, it is evident that the explicit dependence of MOI on EC₅₀ increases. The percentage of inhibition reaches 50% at MOI 0.001 and MOI 0.01, respectively, within relatively comparable value ranges, namely 0.2 and 0.6 μM. Still, when MOI achieves 0.1, the drug concentration reaches almost 100 μM, representing a more than 100-fold increase in EC₅₀ concentration. IC₉₉ is the inhibitor concentration required to stop viral replication; it is typically 100 times more than the EC₅₀. The relationship between inhibitor concentration (nM) and the percentage of inhibition at

three multiplicities of infection (MOI): 0.001, 0.01, and 0.1. It also includes a table summarizing each MOI's EC₅₀ values (effective concentration required to achieve 50% inhibition). At MOI = 0.001, the curve rises steeply, reaching 50% inhibition at a low concentration of 200 nM (EC₅₀ = 0.2 μM). This indicates high sensitivity to the inhibitor at this level of infection. For MOI = 0.01, the curve shifts to the right, requiring higher concentrations to reach the same effect. The EC₅₀ value is 600 nM (0.6 μM), showing reduced sensitivity compared to MOI = 0.001. At MOI = 0.1, the curve flattens significantly, and even at high concentrations (>100 μM), it does not reach 50% inhibition. The table lists EC₅₀ for this MOI as ">100 μM," indicating minimal effectiveness. In summary, the effectiveness of the inhibitor decreases as the MOI increases, requiring higher concentrations for inhibition. The inhibitor is highly potent at low MOI levels, while at higher MOI levels, its impact diminishes significantly [101-104].

MOI (Multiplicity of Infection), TCID₅₀, PFU/mL, or IU/mL is related to EC₅₀ (the concentration of a drug that causes a semi-maximal response). Using a four-parameter regression method (a statistical technique for fitting a curve), mathematics enables us to conduct experiments and translate their results into something understandable, comparable, and meaningful. When converting TCID₅₀/ml (tissue culture infectious dose, the amount of virus required to kill 50% of the cells in the culture) to PFU/ml (plaque-forming units, the number of viable virus particles), we multiply by 0.7. Typically, we terminate the PCR (polymerase chain reaction) after approximately 40 cycles (Figure 13).

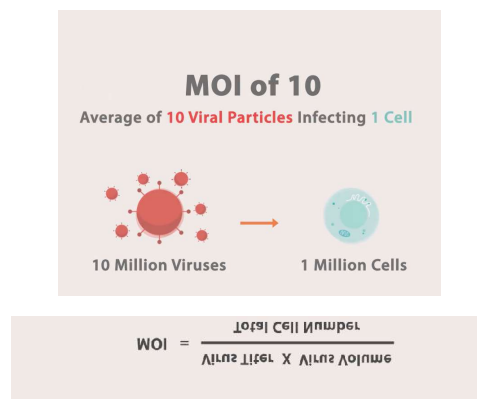


Figure 13 — MOI count, in our case, 0.2 mL or 200 μL of intact virus volume, corresponding to an MOI of 2. The lower the MOI, the more sensitive the test for viral activity. If we have a high MOI value, the CC₅₀ cannot be detected because CPE can destroy all available cells, and a higher antiviral concentration would be needed. For our purposes, it is not necessary to concern ourselves with the number of viruses in a single cell.

What we need to understand – and what the Poisson distribution helps us with – is two key points: If some cells get more than one virus, others will not. For any given

MOI (the average number of viruses per cell), we can calculate the percentage of cells that will not be infected with any virus, which we denote as $P(0)$. $P(0)$ is simplified and presented in formula (2). Logically, if the proportion of cells that will not be infected is known, subtract this value from 100%. What proportion of cells will be infected, regardless of the number of viruses each infected cell receives?

$$P(0) = e^{-\text{MOI}} \quad (2)$$

Viral stock of MOI of 2

At an MOI of 2, without any experiment, we expect 86% of cells to become infected.

Using the formula (2), we gain:

$$P(0) = e^{-\text{MOI}} = e^{-2} = 1 / e^2 = 1 / 2.71828^2 = 1 / 7.389 = 0.1353$$

(~14% of cells not infected)

By subtraction: 100% – 14% = 86% infected

Subsequently, if we examine MOIs lower than 1, we observe that, for instance, at an MOI of 0.5, we achieve a 40% infection rate, and at an MOI of 0.1, we achieve a 10% infection rate.

Converting from TCID50 to IU

Since the MOI can ultimately be described in terms of infectious units, our $P(0) = e^{-\text{MOI}}$ can also be written as:

$$P(0) = e^{-\text{IU/ml}} \quad (3)$$

Re-arrange this equation from TCID50 to infectious units to determine the number of IU when we know $P(0)$. Remember that $P(0)$ is the probability of not being infected by formula 3 and we get:

$$P(0) = e^{-\text{IU/ml}} \text{ becomes } \text{IU/ml} = -\ln_e P(0) \quad (4)$$

Now consider our TCID50: the virus concentration at which there is a 50% chance of infection. At the limiting dilution of our TCID50 assay, we have a 50% chance of disease, which means a 50% chance of non-infection; therefore, $P(0) = 0.5$. Now, substituting $P(0) = 0.5$ into the rearranged equation:

$$\text{IU/ml} = -\ln_e (0.5)$$

$$\ln_e(0.5) = -0.693$$

$$So, IU/ml = -(-0.693) = 0.693 \text{ (5)}$$

This is often rounded to 0.7 for simplicity. Therefore, at a 50% infection rate, we have approximately 0.7 IU per cell. Or we can say that 1 TCID50 corresponds to 0.7 IU.

Hence, whenever we need to convert TCID50/ml values into IU/ml values, we multiply by 0.7. Therefore, it is always important to report the unit of measure (TCID50 or IU), as this provides information on the amount of infectious virus and the assay used to determine it.

The cell culture monolayer was infected with SARS-CoV-2 at a multiplicity of infection (MOI) of 2, using the SARS-CoV-2/human/KAZ/B1.1/2021 and SARS-CoV-2/human/KAZ/Britain/2021 strains, respectively, with an infectious titer of 7 logs TCID50/ml. After one hour of virus contact with the cells at 37°C, the cell monolayer was washed three times with phosphate-buffered saline (pH 7.2). The studied drugs were applied to the infected cells at different concentrations (experiment) or in the maintenance medium (control), and the plastic panels were then placed in a CO2 incubator for 5 days. The antiviral effect of the drugs was calculated by the ratio of the infectious activity of the virus in the experimental and control samples. All experiments were performed in triplicate. The main criteria for assessing the effectiveness of the drugs in vitro were the following indicators [100]: a decrease in the infectious titer of the virus under the influence of the drug (D, lg), the inhibition coefficient (Ci, %) and the chemotherapeutic index (CTI). The decrease in the level of virus accumulation under the influence of the drug (D, lg) was determined by the formula:

$$D = A_k - A_o \text{ (6)}$$

where A_k is the level of virus accumulation during cultivation without the addition of the studied drug to the nutrient medium (in lg TCID50/ml); A_o is the level of virus accumulation during cultivation with the addition of the studied drug to the nutrient medium (in lg TCID50/ml). The formula calculated K_i :

$$K_i = (A_k - A_o)/A_k \cdot 100\% \text{ (7)}$$

The MIC/IEC ratio was taken as the drug's CTI value, where IEC is the minimum effective virus-inhibiting concentration that reduces the virus titer by at least two lg TCID50 [99].

A continuous culture of Vero cells, highly sensitive to the SARS-CoV2 virus, was used to analyse the preparations' antiviral activity in vitro. The cells were cultured in 24-well plastic plates using RPMI 199 medium and supplemented with 10% fetal bovine serum and 100 U/ml gentamicin. The maintenance medium contained the same mixture but with the addition of 1% fetal serum.

The MTT assay in China is used to measure cell viability. Viral accumulation with a viable drug concentration can result in either a significant decrease or no effect, as depicted in Figure 14.

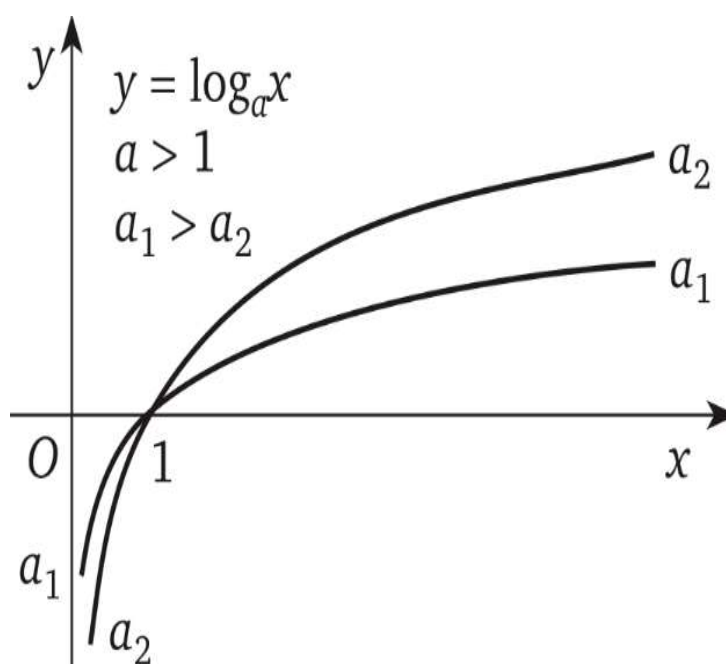


Figure 14 - Functions with different bases: with bases $a > 1$ and with bases in the range $0 < a < 1$. The a_2 -value is expected to be the highest achievable viral load while a_1 will be the highest inhibition rate of antiviral drugs or decreased the viral load exponential growth

Cytotoxicity Assays (CC_{50} , SI - SI-evaluate drug toxicity in host cells) were performed using this assay. CC_{50} (Cytotoxic Concentration 50%): The concentration of the drug that causes 50% cell death. Selectivity Index (SI) = CC_{50} / IC_{50} (higher SI indicates a better antiviral effect with lower toxicity). This evaluation was conducted using two methods: in Kazakhstan, the CCK-8 method was employed, and in China, the MTT assay was performed. Our antiviral drug assays were based on potent antivirals characterised by low IC_{50} values, high selectivity indices (SI), rapid viral clearance, and improved patient survival. Toxic Drugs: low SI (high cytotoxicity).

Ineffective Drugs: No significant reduction in viral load or clinical improvement was observed in the results [103–104].

To determine the MOI (Multiplicity of Infection), you need both the number of plaque-forming units (PFU) and the number of target cells. MOI is calculated as:

$$\text{MOI} = \text{PFU} / \text{number of cells}$$

Thus, if you have 4×10^5 PFU and 1×10^5 cells, the MOI would be 4

MOI (Multiplicity of Infection) from TCID₅₀/ml, you need two additional pieces of information:

1. The number of target cells (e.g., cells per well or flask).
2. The volume of virus inoculum used (e.g., in millilitres).

MOI is calculated as:

$$\text{MOI} = \text{total infectious units} / \text{number of cells}$$

Conversion Factor:

TCID₅₀ is a statistical measure of viral titer.

1 TCID₅₀ \approx 0.69 infectious units (derived from the Poisson distribution).

Suppose you have:

- 1.2×10^5 TCID₅₀/ml viral stock,
- 1×10^5 cells,
- 1 ml of virus added.

1. Convert TCID₅₀ to infectious units:

$$1.2 \times 10^5 \text{ TCID}_{50}/\text{ml} \times 0.69 = 8.28 \times 10^4 \text{ infectious units/ml}$$
$$1.2 \times 10^5 \text{ TCID}_{50}/\text{ml} \times 0.69 = 8.28 \times 10^4 \text{ infectious units/ml}$$

2. Total infectious units used:

$$8.28 \times 10^4 \text{ infectious units/ml} \times 1 \text{ ml} = 8.28 \times 10^4 \text{ infectious units}$$
$$8.28 \times 10^4 \text{ infectious units/ml} \times 1 \text{ ml} = 8.28 \times 10^4 \text{ infectious units}$$

3. Calculate MOI:

$$\text{MOI} = 8.28 \times 10^4 / 1 \times 10^5 = 0.828$$

Therefore 1.2×10^5 TCID₅₀/ml is MOI of 1 [101-108]

2 METHODS AND MATERIALS

2.1 The biological Samples (bronchial fluids from mid and heavy patients)

They are taken from sick patients (cotton swabs: nasotracheal swabs) during the COVID-19 pandemic, with their consent in favour of scientific research, as authorised by the Scientific and Practical Center for Sanitary and Epidemiological Expertise and Monitoring, Almaty. Strain: *SARS-CoV-2/human/KAZ/B1.1/2021 Alpha variant* and kept in freezers at -96°C^0 . Viral titer Preparation for SARS-CoV-2 from a Human Specimen: A viral stock was prepared from a human specimen (e.g., nasopharyngeal swab, BALF), and the virus had to be isolated, propagated, and quantified under biosafety level 3 (BSL-3) conditions. Bronchoalveolar lavage fluid (BALF): The sample was centrifuged at $3,000 \times g$ for 10 min to remove debris. Then, it was filtered, and the supernatant was filtered through a $0.45 \mu\text{m}$ filter to remove bacteria. The aliquots were stored at -80°C if not used immediately [102]. Infection Procedure: Cells were seeded in T25/T75 flasks or 6-well plates at 80% confluency. The cells were washed with PBS, and DMEM containing 2% FBS was added. The specimen broth was inoculated with human specimen filtrate at an MOI of 2. It was incubated at 37°C with 5% CO_2 for 1–2 hours, with gentle rocking every 15 minutes. Remove the inoculum and replace it with fresh DMEM + 2% FBS. Incubate for 48–72 hours, monitoring for cytopathic effect (CPE) and viral cytotoxicity. Harvest the supernatant when ~80% cytopathic effect (CPE) is observed [101]. Viral Stock Preparation: Collect supernatant into sterile tubes. Centrifuge at $3,000 \times g$ for 10 min to remove cell debris. Filter using a $0.22 \mu\text{m}$ filter (to remove cellular contaminants). Aliquot into cryovials and store at -80°C [102]. Viral titer quantification: One of the following methods was used to determine the viral titer: a plaque assay, considered the gold standard. Vero E6 cells were seeded in 6-well plates until they reached 100% confluency. Serial dilutions of the viral stock ranged from 10^{-1} to 10^{-7} . A volume of 0.2 mL was inoculated per well, and the plates were incubated for 1 hour at 37°C . The wells were overlaid with DMEM containing 2% FBS and 1% agarose. The plates were incubated for 3–5 days, then fixed with formaldehyde and stained with crystal violet. The plaques were counted, and the Plaque-Forming Units per mL (PFU/mL) were calculated [17, 102, 115].

The murine tissue extraction procedures

Mice were killed by breaking their spine (tearing the connection between the spinal cord and the rest of the body) fast and humanely. Surface and mice body sterilisation was conducted with 70% ethanol. Dissection: Upper Airway - The skin was removed from the head and neck. Nasal Turbinates: Forceps excise the nasal cavity, cutting behind the incisors and along the zygomatic arch. Trachea: The larynx was cut below and above the bronchi, avoiding lung contamination. Decontaminate tools with 10% bleach or 70% ethanol. The waste was either autoclaved or chemically inactivated [110].

2.2 Equipment

- oligonucleotide synthesizer H-16, K&Laborgeraete, Germany;
- thermal cycler GeneAmp PCR System 9600, Applied Biosystems;
- thermal cycler TC-512, Techne;
- thermal boards DryBlockHeater, Techne;
- shakers, vortexes Vortex-Genie 2 Shaker, Cole-Parmer;
- automatic micropipettes, Eppendorf;
- apparatus for electrophoresis of nucleic acids G100, Pharmacia;
- gel documenting system “BioRad,” USA;
- microcentrifuge “MiniSpin”, Eppendorf;
- refrigerator – 20 °C;
- a package of application programs for analysing DNA sequences: DNASYM MAX 1.0, Sequencer, Vector NTI, BioEdit, GENEDOC, and Staden package.
- Microplate reader (OD, optical density) Plate Verification instrument for Hipo MPP-96, BioSAN [101-103].

Equipment and disposals for MTT-kit:

- Microplate reader capable of measuring absorbance at OD 590 nm
- Pipettes and pipette tips, including multichannel pipette
- Tubes for the preparation of reagents and buffer solutions
- 96-well plates with a clear, flat bottom for antiviral assays with safe drug cytotoxicity [107].

Equipment and disposals for Cell counting kit 8 (CCK8) - Microplate reader capable of measuring absorbance at OD 450 nm

- Pipettes and pipette tips, including multichannel pipette
- Tubes for the preparation of reagents and buffer solutions
- 12 well-plates with a clear flat bottom for drug cytotoxicity assay
- 96 well-plates with a clear flat bottom for antiviral assay with safe drug cytotoxicity
- Multi-channel pipette (8 or 12 channel: 10-100 Pl)
- CO₂ incubator
- Clean bench
- Haematocytometer or cell counter
- Centrifuge and rotor for a 15 ml centrifuge tube [106].

2.3 Reagents and solutions

The murine tissue extraction materials

- Sterile surgical tools (forceps, scissors), 10% neutral buffered formalin, or freezing media.
- Personal protective equipment (PPE): respirator, gloves, gown.

The Vero cells E6

Vero C1008 [Vero 76, clone E6, Vero E6], derived from an African green monkey kidney obtained from Sigma Aldrich. These are anchorage-dependent cells that have applications in molecular and cell biology research.[106] Vero E6 cells enable high titers of the severe acute respiratory syndrome coronavirus (SARS-CoV-2 virus) [107]. Split sub-confluent cultures (70-80%) 1:3 to 1:10, i.e., seeding at $1-3 \times 10^6$ cells/cm² using 0.25% trypsin or trypsin/EDTA; 5% CO₂; 37 °C. The Vero cells are *50% susceptible to SARS-CoV-2 virus infection and 100% permissive, meaning they can support viral replication within them*. Thus, this type of cell culture is justified for use as an in vitro model in our thesis work.

The pre-clinical test of cytotoxic safe TAF in vivo test on 30-week-old WT-Mice

- SARS-COV2 4×10^5 plaque-forming units (PFU) or MOI of 4
- Sterile syringe 5ml
- small sterile scissors
- PBS-buffer 3%
- TBST-buffer -5%
- 50µg/ml of TAF
- Sterile PBS, DMEM, tissue homogeniser
- Centrifuge
- 0.22 µm filters.
- Vero E6 cells (for plaque assays).

Plaque assay reagents/material

- Overlay medium: 2× MEM + 1.5% agarose (or 0.8% methylcellulose).
- Neutral red or crystal violet stain.

The culture medium

Dulbecco's Modified Eagle's Medium (DMEM) - high glucose, with 4500 mg/L glucose, sodium pyruvate, and sodium bicarbonate, without L-glutamine, liquid, sterile-filtered, suitable for cell culture. Vero E6 cells (confluent in 96-well plates). BALF sample (processed to remove debris/mucus). Cell culture medium (e.g., DMEM supplemented with 2% fetal bovine serum [FBS] and antibiotics). Sterile pipettes, 96-well plates, biosafety cabinet. Inverted microscope.

PCR

- Recombinant Taq DNA Polymerase, 5000 units/mL, Sigma.
- T4 DNA Ligase;
- ProtoScript® II First Strand cDNA Synthesis Kit;
- RNAZap decontamination solution;
- Super Script IV One-Step RT-PCR System with Platinum Taq DNA Polymerase (Invitrogen, USA) (100 reactions);
- 310 and 31xx Running Buffer, 10X;
- BigDye™ Terminator v3.1 Cycle Sequencing Kit, 100 reactions;
- Reagent for safe staining of agarose gel SYBR Safe DNA gel stain;
- UltraPure™ nuclease-free distilled water;
- Microcentrifuge tubes, 1.5 ml, 500 pcs. pack; Eppendorf;
- Microtubes 0.2 ml with flat cap 1000 pcs/pack Tubes, 0.2 mL, flat cap 1000/pc Eppendorf;
- Microtubes, 0.5 mL, flat cap, 1000 tubes per pack, Eppendorf.

MTT Assay Kit

(Cell Proliferation)—MTT Assay Kit *ab211091* is an easy-to-use, non-radioactive, high-throughput assay for measuring cell proliferation, viability, and cytotoxicity.

MTT Reagent (50 mL):

- Ready to use as supplied.
- Equilibrate to room temperature before use and open the vial under sterile conditions.
- The reagent was Aliquoted to ensure a sufficient volume for the desired number of assays.
- Store at -20°C, protected from light

MTT Solvent (150 mL):

- Ready to use as supplied.
- Equilibrate to room temperature before use.
- Store at -20°C.
- Once opened, use within 2 months
- -199 Media: a mixture of Hanks salts, glutamine, inorganic salts, amino acids, vitamins, glucose, and phenol red, dissolved in purified water and sterilised by membrane filtration. This medium is designed for cell cultivation outside the incubator, as it is prepared using Hanks' salts with a low sodium bicarbonate content (1.0 g/l). Cat. No.: C230p [102].

The virus preparation and safety procedures

An isolate of the SARS-CoV-2/human/KAZ/B1.1/2021, Alpha variant strain, was passaged in Vero E6 cells to establish a high-titer stock for all our experiments. Since SARS-CoV-2 is classified as a high-risk pathogen in Kazakhstan, all virus procedures, including infecting cell lines and subsequent monitoring, are conducted in a BSL-2 (Biosafety Level 2) laboratory. All direct manipulation with either viral titers or growth-active virus strains in biological tissues is performed using human biomaterials under BSL-3/4 bio-lab conditions.

2.4 Molecular Biology Procedures

Bronchoalveolar Lavage Fluid -supernatant collection

The BALF was centrifuged at $2,000 \times g$ for 10 minutes at 4°C to pellet cells and debris. The supernatant was transferred to a sterile tube. Filtered through a $0.22 \mu\text{m}$ syringe filter to remove residual particles. The specimen was then aliquoted and stored at -80°C unless used immediately. Not all BALF specimens were intact, and the viral load of the SARS-CoV-2 virus was sufficient only in a fraction of the 117 BALF tubes provided.

Murine Upper Airways (Nasal tissue)-supernatant collection

The homogenised tissue was centrifuged at $2,000 \times g$ for 10 min at 4°C . The supernatant was collected through a $0.22 \mu\text{m}$ filter. It was stored at -80°C if needed.

Viral Cultivation on VeroE6 Cells

The VeroE6 cells were grown in DMEM supplemented with 10% fetal bovine serum (FBS) and antibiotics (penicillin/streptomycin) at 37°C and 5% CO_2 until they reached 80–90% confluence.

Vero E6 Cells - Infection

Supernatants were thawed quickly. BALF/murine supernatants were thawed at 37°C . The cell culture medium was aspirated. Adding the supernatant (e.g., 100–500 μL per well of a 6-well plate). And its dilution in maintenance medium (DMEM + 2% FBS) if needed. The Incubation lasted 1–2 hours at 37°C with gentle rocking every 15 min. Post-inoculation: Replacement of inoculum with fresh maintenance medium containing antibiotics. CPE Observation: Under a microscope, the culture was checked daily for cytopathic effects (cell rounding, syncytia, and detachment). The efficient extraction of SARS-CoV-2 from bronchoalveolar lavage fluid (BALF) and murine airways, followed by successful cultivation in VeroE6 cells, is crucial for virological studies.

Viral RNA isolation

mRNA was extracted for downstream processes, including RNA sequencing, qPCR, and reverse transcription for cDNA synthesis. Because it enables researchers to examine gene expression under specified conditions at a given moment (Figure 15) [17,102,115].

Total RNA is isolated using various techniques. Phenol-chloroform extraction is a traditional method that has been replaced by Trizol, which separates RNA from DNA and proteins based on their solubility. The RNA remains in the aqueous phase and was precipitated using isopropanol. Silica-Based Column Purification: Kits were available for rapid RNA isolation (e.g., Qiagen RNeasy) using silica membranes that selectively bind RNA under specific buffer conditions. Since total RNA includes other forms, such as rRNA and tRNA, mRNA typically accounts for only 1–5% of total RNA. Two main methods enriched mRNA: Oligo-dT Beads. These beads were coated with oligo(dT) sequences that bind to the poly-A tail of eukaryotic mRNAs. Non-polyadenylated RNAs (rRNA, tRNA) were washed away, leaving enriched mRNA. Ribosomal RNA Depletion: In cases where poly-A tails were absent (in prokaryotes), specific kits or methods were used to remove rRNAs, enriching the mRNA fraction. According to the manufacturer’s instructions, viral RNA was isolated from virus-containing material (nasotracheal swabs) using the QIAamp Viral RNA Mini Kit (Qiagen). For 50 RNA preps, the following reagents were required: 50 QIAamp Mini Spin Columns, carrier RNA, 2 mL Collection Tubes, and RNase-free buffers [17, 102, 115].

Confirmation of viral load via RT-qPCR (genomic copies)

The qRT-PCR targeted the N, E, S, and M genes and the ORF1ab gene. A standard curve was used to estimate genome copies, final storage, and biosafety. The viral stock was stored at -80°C in small aliquots to prevent freeze-thaw cycles. The SARS-CoV-2 was handled under BSL-3 conditions with personal protective equipment (PPE), including N95 respirators, face shields, gowns, and gloves. The work surfaces with 10% bleach or 70% ethanol were washed. SARS-CoV-2 was isolated from a nasopharyngeal swab by authorized specialists, and these bio-samples were isolated from a nasopharyngeal swab by a biosafety institute in Gvardevskiyi. They were propagated in Vero E6 cells cultured in MEM containing 2% FBS. Seventy-two hours after the infection, supernatants containing the released viral particles were collected and centrifuged at 600 g for 5 minutes. Virus stocks were stored at -80°C until use [17, 102, 115].

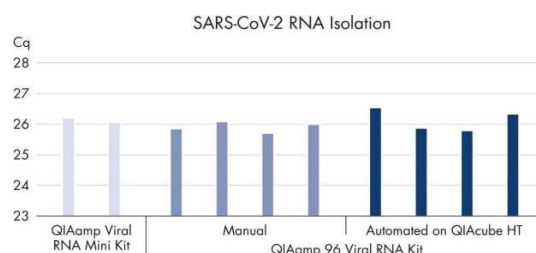


Figure 15 - Manufacturers ensure the efficacy of the viral RNA Mini Kit in quantity.

No phenol-chloroform extraction was required. Viral RNA binds specifically to the QIAamp silica membrane while contaminants pass through. PCR inhibitors, such as divalent cations and proteins, were completely removed in two efficient wash steps, leaving pure viral RNA to be eluted in either water or a buffer provided with the kit. QIAamp RNA technology enabled the isolation of viral RNA from cell-free body fluids,

making it ready for RT-PCR and blotting procedures. QIAamp sample preparation technology is fully licensed [102,104].

Selection and synthesis of primers

The primers were designed in the institute lab using various computer programs, mainly Oligo 6 and Vector NTI Suite 10. The reaction composition and temperature-time regimes were selected based on the annotation attached to the enzyme and the properties of the primers. The designed primers were synthesized on the H-16 oligonucleotide synthesizer (manufactured in Germany) according to the instructions attached to the device. The elution of synthesized primers from the columns was performed using a concentrated ammonia solution. The primers were then dried on a rotary evaporator and purified by alcohol precipitation [17,102,115].

Conducting PCR

A set of superscribed III One-Step RT-PCR with platinum Taq, Invitrogen, was used to perform the PCR. The reaction composition and temperature-time regimes were selected based on the annotation attached to the enzyme and the properties of the primers. Techne produced specific DNA sites using a GeneAmp PCR 9600 thermal cycler (Applied Biosystems) and TC512. Further detection of amplification products was performed using the Pharmacia “G-100” horizontal electrophoresis device. For electrophoresis, a 1% solution of agarose in TA was used. The results were visualised and recorded with the “Quantity One” program. “DNA Ladder 1 kb” from Invitrogen was used as a comparative marker for molecular weights. The SuperScript III One-Step RT-PCR System with Platinum Taq High Fidelity is designed for convenient end-point detection and analysis of RNA molecules by one-step RT-PCR. This one-step formulation enabled cDNA synthesis and PCR amplification in a single tube, utilising gene-specific primers and target RNAs derived from either total RNA or mRNA. It also allows detecting a wide range of RNA targets, up to 10 kb in length, at variable concentrations (1 pg to 1 µg of total RNA). This system had two major components: SuperScript III RT/Platinum Taq High Fidelity enzyme mix and 2X reaction mix [102].

Gene sequencing

The AMPure XP bead-based reagent is used for DNA cleanup in various genomic applications, including sequencing, qPCR, ddPCR, PCR, microarrays, and other enzymatic reactions. This reagent was utilised in an optimised buffer to bind selectively DNA fragments of 100 bp and larger to paramagnetic beads. Excess primers, nucleotides, salts, and enzymes were removed by simply washing [102-105]. Viral RNA and DNA are isolated using a set of QIAamp virus RNA and triazole reagents according to the manufacturer’s instructions. The RNA was eluted with water, two times 40 µl each. Given that the entire genome of the SARS-CoV-2 virus consisted of approximately 30,000 nucleotides at the time, a set of primers was used to amplify the whole genome for sequencing. PCR was performed using single-stage RT-PCR systems (III) [102,115]. Cleaning of PCR products was carried out using the AMPure kit according to the manufacturer’s instructions. The quality of PCR products is

checked by electrophoretic analysis. PCR sequencing products were obtained using the BigDye Terminator v3.1 Cycle Sequencing Kit. The purification of the sequencing reaction was performed using the Clean Seq Kit. The sequencing was performed on 16 capillary sequencers of the Genetic Analyzer 3130xl (Applied Biosystems/Hitachi). Genomic assembly, genome annotation, comparative genomics, and phylogenetic analysis were performed using the CLC Genomic Workbench 11.0.1 program. Genome-wide sequencing of ILT strains using the next-generation sequencing method, the Ion GeneStudio sequencer. The S5 system was bundled with the Ion Chef SmartStart system [102-103].

Production of virus fragments by PCR

For two-thirds (~ 70%) of the genome sequencing of SARS-CoV-2 virus variants, the total RNA was successfully isolated from virus-containing material, followed by reverse transcription (cDNA) according to the manufacturer's protocol. Amplicons of the ORF1ab gene from variants of the SARS-CoV-2 virus, obtained through classical PCR, were then loaded into a 1.0% agarose gel and documented using the Gel Capture program on a MiniBIS Pro transilluminator device. The PCR report presented the results using 46 pairs of primers designed explicitly for the ORF1ab gene of SARS-CoV-2 virus variants [103-104]. COVID-19 Antigen Count of GenSure Kit from a Specimen Swab: TID50. While antigen tests were fast and convenient, they were generally less sensitive than RT-PCR tests but also less expensive. This means they missed some cases, especially if the viral load was low (e.g., early or late in the infection). They are more effective when used in individuals with a high viral load who are symptomatic. A follow-up PCR test is often recommended in cases of negative results with a high clinical suspicion of COVID-19. Their rapid turnaround makes them useful for mass screening and for situations where immediate decisions are needed, such as in emergency departments or before gatherings. In summary, while antigen tests offer speed and ease of use, understanding their limitations is crucial. They are a valuable tool in the overall strategy to control COVID-19, mainly when used with more sensitive tests, such as PCR, as needed. Figure 16 illustrates the express test, which confirms the viral load and ensures that the viral inhibition assay is conducted correctly. In conclusion, working with SARS-COV2 is hazardous research, so optimising time and effort is favourable. That is why we used the Kazakhstan CCK8 cell viability assay kit. Furthermore, RNA isolation kits are also time-efficient and do not require phenol. In lab experience, we must pay attention to every step because access to the BSL3/4 lab is limited, and working there is subject to numerous restrictions and safety rules. The Research Institute for Biological Safety Problems is home to the country's first Biosafety Level 3 (BSL-3) laboratory, which was designed by international standards. PCR remains the gold standard for SARS-CoV-2 diagnostics, but addressing these challenges requires harmonising technical precision, logistical agility, and adaptive public health strategies. Still, it is expensive, so using the antigenic express test is a better and less costly option, as shown in Figure 16 [17,115].

2.5 Comparative and phylogeny analysis of the nucleotide sequence of genes

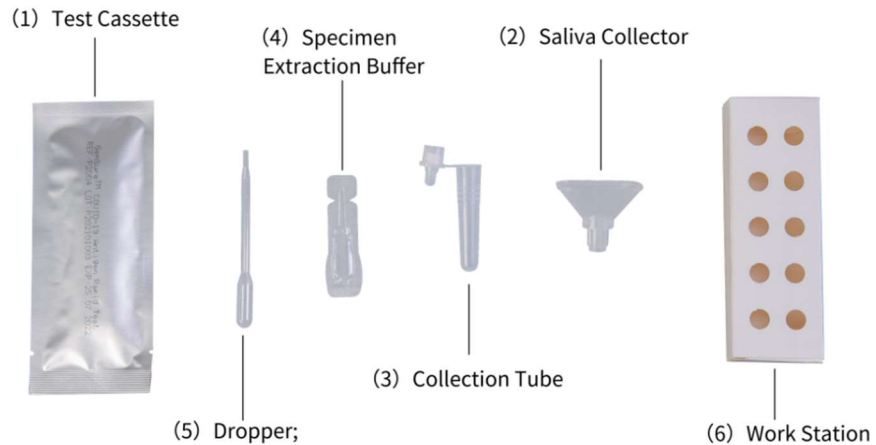
The complete genomes of the SARS-CoV-2 virus, downloaded from GenBank, are used for the full analysis. Phylogenetic trees were created using the maximum similarity method on the CLC Genomics Server 12.0, employing the "Neighbour Joining" method and the Jukes-Cantor model with a gamma distribution of 1.0 and 100 replications to assign confidence levels to branches. The MEGA 7.0 application is also used for phylogenetic analysis.

Lineage Classification and Interpretation: Variant Designation - Ambiguous criteria for variants of concern (VOCs) result in inconsistent classifications. Convergent Evolution: Independent mutations (e.g., Spike protein's N501Y) mimic shared ancestry, inflating false lineage relationships. Data Quality and Heterogeneity. Incomplete Sequences: Many genomic sequences are partial, leading to analysis gaps. Sequencing Errors: Artifacts from RNA extraction, reverse transcription, or sequencing platforms introduce false mutations. Contamination: Cross-contamination between samples or host RNA can skew results. Metadata Issues: Inconsistent or missing metadata (e.g., collection date, location) hampers contextual interpretation. Sampling Biases: Geographic and Temporal Bias - Overrepresentation of sequences from specific regions or time points skews the tree structure and lineage spread interpretation. Missing Lineages: Gaps in sampling (e.g., undetected intermediates) fragment evolutionary continuity. These challenges underscore the need for rigorous methodologies, interdisciplinary collaboration, and scalable computational frameworks to accurately reconstruct the evolution of SARS-CoV-2 and inform public health responses.

When applying ANOVA (Analysis of Variance) to comparative and phylogenetic analyses of nucleotide sequences, the goal is typically to assess whether there are statistically significant differences in genetic variation, substitution rates, or sequence-derived metrics across groups or clades. While ANOVA is not directly applied to raw nucleotide sequences, it is a powerful tool for analysing sequence-derived metrics (e.g., genetic distances and substitution rates) in comparative and phylogenetic studies. Key considerations include Using phylogenetic ANOVA to correct for evolutionary non-independence and validating assumptions (normality and homogeneity of variance). Additionally, pairing ANOVA with post-hoc tests and visualization is crucial for interpreting differences between clades, populations, or functional groups. Always integrate phylogenetic context for evolutionary questions to avoid spurious correlations and ensure biological validity.

Antigen-based SARS-CoV2 identification

Antigen-based identification of SARS-CoV-2 is a rapid diagnostic method that detects viral proteins, or antigens, in respiratory samples, such as nasal or throat swabs. These tests are widely used for screening and diagnosis due to their speed, cost-effectiveness, and ease of use [115].



Microorganism	Concentration	Cross-Reactivity (Yes/No)
Influenza A (H1N1, H3N2)	1.0×10^5 TCID ₅₀ /mL	No
Avian influenza (H5N1, H7N9)	1.7×10^5 TCID ₅₀ /mL	No
Influenza B (Victoria, Yamagata)	2.5×10^5 TCID ₅₀ /mL	No
Parainfluenza virus	1.0×10^5 TCID ₅₀ /mL	No
Respiratory Syncytial Virus	3.8×10^5 TCID ₅₀ /mL	No
Rhinovirus	1.4×10^5 TCID ₅₀ /mL	No
Adenovirus	1.1×10^5 TCID ₅₀ /mL	No
Measles virus	1.0×10^6 TCID ₅₀ /mL	No
Human coronavirus (OC43, 229E, NL63)	1.0×10^5 TCID ₅₀ /mL	No
MERS coronavirus	1.2×10^5 TCID ₅₀ /mL	No
Mycoplasma pneumoniae	1.0×10^6 CFU/mL	No
Chlamydia pneumoniae	1.0×10^6 CFU/mL	No
Legionella pneumophila	1.1×10^6 CFU/mL	No

Figure 16—Overview of the GenSure™ COVID-19 Antigen Rapid Test Kit [115].

It utilises polymer immunochromatographic technology and a double-antibody sandwich principle to qualitatively detect the N (Nucleocapsid) protein antigen from SARS-CoV-2 in human nasal swab specimens. Testing is limited to laboratories and medical institutions. This express test is efficient in terms of instant testing. The antigen test is high-speed and reliable. It involves pouring the swab into viral inoculated titer and testing it on viral load.

2.6 Cell- cytotoxicity assay

Dose escalation *in vitro*.

The drug tableted forms were dissolved in DMEM medium, thoroughly mixed at room temperature for 30 minutes, and then diluted to the doses specified in Table 2.

Table 2 – The CC-test (cytotoxic test) of four drugs in increasing stock concentrations and exposure time, with a control for each drug, on E6-vero cells (24-well assay). The manufacturer or local distributors deliver the medications in stock concentrations in water-soluble agents.

1X (4МГ/МЛ) DEX. 1ml 10 µM	2X в 10 ml 20 µM	3X10 ml 30 µM	4X10 ml 40 µM	5X10 ml 50 µM	Control
1X 1300 µM (200МГ/МЛ) FAV 1ml	2X10ml 2600µM	3X10 ml 3900µM	4X10 ml 5200 µM	5X10 ml 6500 µM	Control
1X 820 µM (200МГ/ml) Ribo. 1ml	2X10 ml 820µM	3X10 ml 1640µM	4X10 ml 2460µM	5X10 ml 3280µM	Control
1X (300/МЛ) Teno. 1ml 1045µM	2X 10 ml 2090µM	3X10 ml 3135µM	4X10 ml 0	5X10 ml 0	Control
1day	1day	1day	1day	1day	1day

The medium was prepared using DMEM (D6546) supplemented with two mM L-glutamine (G7513) and 10% FBS/FCS (F2442, Fetal Bovine Serum). This medium consisted of DMEM with 2% bovine serum and 0.01% (100 U/ml) antibiotics (Penicillin-Streptomycin).

Dose-de-escalation *in vitro*

The 24 wells with Vero E6 cells were filled with further drug concentration patterns: Favipiravir concentrations were: 1270µM, 318 µM, 127µM, 12,7µM, 1,27µM, 0,127µM and control Ribavirin concentrations were: 820µM, 205 µM, 82µM, 8,2µM, 0,82µM, 0,082µM and control Tenofovir concentrations were: 1050µM, 174µM, 10,5µM, 1,5µM, 0.105µM and control. Dexamethasone concentrations were 10 µM, 20 µM, 30 µM, and control. The samples were transferred to a 5% CO₂ incubator at 37 °C for 72 hours. According to the manufacturer's instructions, viral RNA was

isolated from virus-containing material using the QIAamp Viral RNA Mini Kit (Qiagen). An isolate of coronavirus infection was used as an object of research.

CCK8 test for cell-viability in four drugs of concentration

The CD8-Kit-8 (KK-8) enables sensitive colourimetric analyses to determine the viability of cells in the study of cell proliferation and cytotoxicity. The doxo-tetrazole salt, WST-8, which is soluble in water, is restored in cells by dehydrogenase activity, forming a yellow formazan dye soluble in tissue culture medium. The amount of the dye formazan, formed due to the activity of dehydrogenases in cells, is directly proportional to the number of living cells. Step 1: Add 10 μ l of Cell Counting Kit-8 to each well in a 96-well microplate. Step 2: Place in a CO₂ incubator for 1-4 hours to react. Step 3: Measure the absorbance at 450 nm with a microplate reader [106, 115].

2.7 Determination of cytotoxicity of drugs for cell culture

Dexamethasone, Ribavirin, Tenofovir, and Favipiravir were selected for study to evaluate their antiviral activity against the SARS-CoV-2 virus. Before determining the antiviral activity, a working dose was established that did not cause toxicity in cell culture. Dexamethasone was used in ampoules containing 4 mg/ml in 5 dosages (20, 16, 12, 8, and 4 mg/ml).

Measuring the Efficacy of Antivirals Against SARS-CoV-2

Researchers evaluate the effectiveness of antiviral drugs against SARS-CoV-2 using in vitro (cell-based) and in vivo (animal models) studies, as well as clinical trials (human studies). The most common efficacy metrics include viral load reduction, cytotoxicity, and clinical outcomes.

In Vitro (Cell Culture) Studies

These assays measure the extent to which a drug inhibits viral replication in infected cells. Plaque Reduction Assay (PRA): Measures the ability of a drug to reduce the formation of virus-induced plaques in a cell monolayer. – This approach was performed in China, yielding results identical to cytotoxicity assay results. Output: Plaque reduction (%) or IC₅₀ (half-maximal inhibitory concentration). TCID₅₀ (Tissue Culture Infectious Dose 50%): Measures the drug's effect on reducing the number of infectious viral particles. The reduction in TCID₅₀ titer was determined by quantitative reverse transcription polymerase chain reaction (qRT-PCR), which measures SARS-CoV-2 RNA levels in the culture supernatant after treatment. Output: Viral RNA copies/ml (Ct values).

The main steps of the pre-clinical test of cytotoxic safe TAF in vivo test on 30-week-old WT-Mice

Thirty 30-week-old mice were intranasally infected with 4×10^5 Plaque-forming units (PFU) of SARS-CoV-2 and three wild-type (WT) C57BL/6 mice that received the same dose of the viral challenge were set as the control without TAF

treatment and were left for 24 hours in an isolated vivarium box. After 24 hours of infection, 50 µg/ml of TAF was injected into 30 WT 30-week-old mice and left for 24 hours in an isolated vivarium box [108-109]. If a person is infected at a MOI of 4, that would result in a high infection rate; however, how does this translate to the plaque assay? It may be necessary to determine the titer of the virus stock after infecting at an MOI of 4. Perhaps the intention is to test antiviral agents by first infecting at a multiplicity of infection (MOI) of 4 and then observing the effect on plaque formation. In this case, the antiviral assay was the primary purpose and serves, first and foremost, to enhance the diversity of the methodology.

The tissue Homogenate

Weigh tissue and homogenize in cold DMEM (10% w/v, e.g., 100 mg tissue in 1 mL DMEM). Centrifuge at $10,000 \times g$ for 10 min at 4°C to pellet debris. Supernatant through a 0.22 µm filter. The filter removes bacteria and particles. Aliquoted and stored at -80°C, avoiding repeated freeze-thaw cycles [108-109].

Plaque Assay on Vero E6 Cells

Seed Vero E6 cells in 6- or 12-well plates (at 90–100% confluency). Serially dilute tissue homogenate (e.g., 10^{-1} to 10^{-6}) in serum-free MEM. Infect cells: Add 100–200 µL of diluted homogenate per well to the aspirate media. Incubate for one hour at 37°C (gently rock every 15 min). Overlay with agarose/methylcellulose: Add 2 mL overlay medium (2× MEM + 1.5% agarose + 2% FBS). Incubate for 3–4 days at 37°C with 5% CO₂, then stain the plaques with crystal violet or neutral red [108-109].

Plaque assay with the Wuhan strain of SARS-CoV-2 at an MOI of 4 on Vero E6 cells

Cell Preparation: Vero E6 cells were seeded at 2×10^6 cells/well in 6-well plates and incubated overnight at 37°C and 5% CO₂. Virus Infection (BSL-3): The virus stock was diluted in serum-free MEM to achieve MOI 4 (e.g., 4 PFU/cell). Calculation: If cell density = 2×10^6 cells/well, total PFU needed = $4 \times 2 \times 10^6 = 8 \times 10^6$ PFU/well. The cell media was aspirated, and the virus inoculum (1 mL per well) was incubated for 1 hour at 37°C with gentle rocking. Overlay Application: The equal parts were mixed of 2× MEM (with 4% FBS and 2× antibiotics) and 3% low-melt agarose (pre-cooled to 42°C). The 2 mL/well-added overlay was used to immobilise virions. It was let to solidify at room temperature (RT), then it was incubated at 37°C with 5% CO₂. Plaque Development: Monitor daily for CPE. The Wuhan strain typically forms plaques in 3–4 days. Fix and Stain: Add 10% formalin for two hours (the virus was inactivated in BSL-3). Remove the agarose and stain it with 0.1% crystal violet for 10 minutes to visualise the plaques. Plaque Counting: Confluent lysis was expected at an MOI of 4, resulting in individual plaques becoming indistinguishable. If plaques overlap, report results as a percentage of cell lysis rather than PFU/ml.

2.7 The preclinical test of cytotoxic safe TAF and its antiviral properties in vivo on regular lab WT-Mice

Regular lab mice are not always susceptible to human viruses because the virus may not bind well to the receptors in their cells. For SARS-CoV-2, the virus enters via the ACE2 receptor. Therefore, mice with human ACE2 may be more suitable. It is thought that there are transgenic mice, such as hACE2 mice. However, the dissertation thesis satisfied with the WT-mice pre-clinical study.



Figure 17 – The isolation box for wild-type (WT) mice (five regular lab mice, 30 weeks old, in each box) in BSL2 lab conditions. These 30 mice were intranasal infected with SARS-COV2 (MOI of 4) and left for 24 hours in an isolated box.

Are there other models? Maybe mice adapted to the virus through serial passage? Or maybe using adenovirus to express hACE2 in regular mice? The BALB/c and C57BL/6 strains are being used; however, they may not become infected unless the virus is adapted. Therefore, the best option is likely to use hACE2 transgenic mice. The strains are close to K18-hACE2. They express ACE2 under a promoter that might target epithelial cells, which could make them more susceptible [108-109].

Performing statistical data analysis with ANOVA (Analysis of Variance) involves comparing group means to determine if there are statistically significant differences. Below is a step-by-step guide to conducting ANOVA, including software. Step-by-Step Workflow. The *in vitro* study of TAF at 50 µg/ml showed a cytosine concentration. TAF was provided by the Aldrich manufacturer in pure diluted lab stock, unlike TDF, which was diluted from the tablet form.

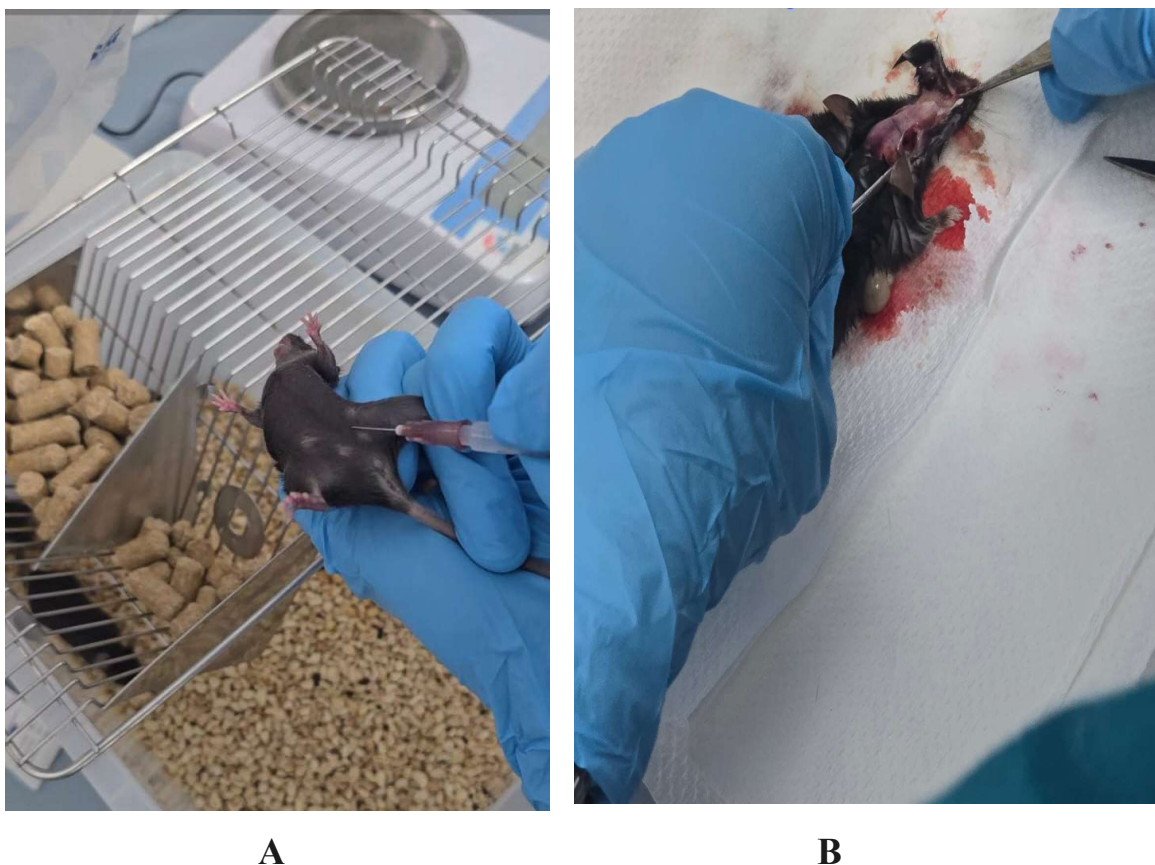


Figure 18 – A. 50µg/ml dose of TAF was injected into 30 mice, and three were used as controls without any treatment and were left for 24 hours. B. Upper airway tissue extraction from 33 mice, 24 hours after drug injection.

For tissue extraction, the upper airway includes nasal turbinates and trachea. The timing post-infection is crucial. Viral load peaks around 2-3 days in the upper airways. They should collect tissues at the right time point. Storage conditions after extraction depend on the downstream applications: - 80 °C for RNA and formalin for histology. However, our experiment was not designed to gather detailed information, such as viral RNA isolation, and our experiments did not address concerns related to transmission research and ACE2 humanisation. The primary objective of the *in vivo* study is to test the antiviral properties of 50µg/ml TAF in WT mice. Since the experiments did not cover the specified SARS-CoV-2 strain nor ACE2h-transfected cells, the time for cytotoxicity was 24 hours, and the viral infection period at MOI 4 was also 24 hours. None of the mice died from TAF injection or intranasal virus infection, as regular wild-type mice are not susceptible to regular human SARS-CoV-2 viral infection [108-109].



Figure 19 – Three steps of mouse tissue purification and homogenisation for antigen expression testing confined from MOI 1 to MOI 4. Starting from cutting→ sieve grinding →centrifugation with was buffers (PBS step 1 and 2, PBST-step 3)

It should be highlighted first that regular mice cannot be infected with the original Wuhan strain without adaptation. Maybe they are unaware and need to check their model. If they proceed without adapting the virus or using transgenic mice, they might not get any infection. So, the initial step is crucial. The experiment was designed to confirm the cytotoxic tolerance of TAF in a mouse model, and virus compatibility was also considered, which is why upper airway tissue was extracted rather than ACE2-rich receptor–lungs. Performing a plaque assay on Vero E6 cells using the Wuhan strain of SARS-CoV-2 at a multiplicity of infection (MOI) of 4. A plaque assay is a method used to measure the number of infectious virus particles in a sample. Vero E6 cells are commonly used for SARS-CoV-2 because they express ACE2 receptors, which the virus uses to enter cells. The mouse tissue was used as the titter material, and since the original viral load was high, the snout tissue served as a viral titter source for the Plaque assay via the VeroE6-cell line, which was stained after 72 hours of incubation. WT mice + Wuhan strain (no adaptation): Likely no plaques due to lack of replication; however, according to this dissertational work, mice snout tissue delivered viral load MOI of 2 from the original MOI of 4; therefore, TAF in the concentration of 50µg/ml inhibited viral replication potently in 30 WT mice with not adapted Wuhan strain of SARS-CoV2 virus. In vivo TAF injection → in vivo SARS-CoV-2 intranasal infection. Snout tissue extraction. In vitro plaque assay: viral load count and antiviral efficacy count. Virus viability is confirmed via TCID₅₀ – count. The pH and temperature (improper solidification inhibits plaque formation) were checked, as were the count and overlay pH and temperature. In Figure 19, the homogenisation step involved homogenising tissue in cold PBS (1 mL per 100 mg tissue) using a bead homogeniser. To achieve clarification, the samples were centrifuged at 3,000 × g and 4°C for 10 min. The supernatant was collected (filter through a 0.22 µm filter if necessary). The Vero cells were seeded in 6-well plates at a density of 80–90%

confluency. Inoculation was performed by diluting the clarified supernatant 1:10 in the infection medium (DMEM supplemented with 2% fetal bovine serum, FBS). Adsorb for 1 hour at 37°C. The fresh medium was replaced every 24 hours during incubation at 37°C with 5% CO₂. Serial dilution was performed on the supernatant, and Vero E6 monolayers were infected, overlaid with agarose, and stained with crystal violet after 48 to 72 hours. Calculate PFU/ml.

In conclusion, this procedure enabled the author to evaluate SARS-CoV-2 replication in a murine model and subsequently propagate it in vitro, a critical step for pathogenesis and therapeutic studies. Furthermore, the Spearman-Kärber method can provide a robust, assumption-free estimate of effective doses, making it ideal for preliminary analyses or when parametric models are inappropriate. Proper handling of dose extrapolation and monotonicity is critical for accuracy; still, the plaque assay was informative enough. The use of supernatant extraction from bronchoalveolar lavage fluid (BALF) and murine upper airways for SARS-CoV-2 cultivation on VeroE6 cells is favoured due to a combination of biological, technical, and practical factors. VeroE6 cells express the ACE2 receptor and TMPRSS2 protease, which SARS-CoV-2 requires for entry into cells. However, these cells lack robust innate immune responses (e.g., interferon production), making them permissive to viral replication. Supernatants from BALF/airways provide pre-cleared, cell-free virus that can directly bind to VeroE6 cells without interference from host immune mediators or debris. Supernatants contain cell-free virions that are already primed for infection. In contrast, tissue homogenates require additional steps (e.g., freeze-thaw cycles, mechanical disruption) to release the virus, which may damage the virions or reduce their infectivity. Swab samples often have low viral titers compared to BALF/airway lavage. Viral viability: Supernatants contain replication-competent virus, confirmed by cytopathic effect (CPE) in VeroE6 cells. Supernatant extraction from BALF and murine upper airways is optimized to Maximize recovery of cell-free, infectious viruses. Minimize host-derived inhibitors. Ensure compatibility with VeroE6 cells' susceptibility and culture conditions. This method strikes a balance between biological relevance, technical feasibility, and biosafety, making it the gold standard for isolating and propagating SARS-CoV-2 in vitro. Other approaches require additional optimization and are less consistent for primary viral cultivation. When analysing data from experiments involving supernatant extraction from BALF and murine upper airways for SARS-CoV-2 cultivation on VeroE6 cells, Analysis of Variance (ANOVA, updated version 3) was a powerful statistical tool for comparing differences in viral titers, cytopathic effects (CPE), or other quantitative outcomes across multiple experimental groups.

3 RESULTS AND DISCUSSION

3.1 Vero E6 cell infection and 72-hour incubation, titter production from Bronchoalveolar lavage fluid (BALF) and murine upper airways.

Vero cells are an ideal model for SARS-CoV-2 infection because they can host and sustain the viral infection and do not require procedures such as trypsinization, as demonstrated by both MTT and CCK8 methods. ACE2 Receptor Expression: Vero E6 cells express the angiotensin-converting enzyme 2 (ACE2) receptor, which SARS-CoV-2 uses for cellular entry. This makes them highly susceptible to infection and replication of the virus. So, the extensive cytopathic effect can be detected on the first day of incubation. After 72 hours, over 80% of cells are severely damaged, while the cell prefiltration of Vero cells remains intact even after 5 days. Thanks to Vero cells, 12 selected intact BALF samples demonstrated a target viral load MOI of 2, as antiviral studies were conducted using tableted drugs. Such viral load enabled the author to detect antiviral activity. The viral titter from Vero E6 cells with an MOI of 2 could be used in antiviral assays. In contrast, the BALF supernatants from 12 samples were prioritised for molecular biology purposes, such as sequencing and qPCR/real-time PCR procedures. MOI of 1 corresponds to one virion for a target cell, as determined by the express antigen COVID-19 test, GenSure. In China, Shenzhen University had in stock Tenvir (TAF) tablets 25mg. Since the cytotoxic-safe concentration needed to observe antiviral activity was already known. Impaired Interferon Response: These cells have a defective interferon signalling pathway, reducing innate antiviral defences and allowing unchecked viral replication, leading to higher titers. Limitations Considered: The non-human origin may introduce viral genetic changes not observed in human cells; however, antigenic properties remain relevant for vaccine purposes. Alternatives, such as human cell lines (Calu-3, Caco-2), may better model human infection but are less practical for high-titer production. Cytotoxicity Assessment: Before evaluating antiviral activity, it is crucial to ensure that the tested drug does not harm healthy cells. The CCK-8 assay helps determine the cytotoxic concentration (CC50) of a drug. The Cell Counting Kit-8 (CCK-8) assay is a widely used colourimetric assay for measuring cell viability and cytotoxicity. It is based on the reduction of WST-8, a water-soluble tetrazolium salt, to a formazan dye by cellular dehydrogenases in metabolically active cells. Drug Efficacy Measurement: When testing antiviral drugs, the CCK-8 assay indirectly reflects viral replication. A high viability in infected and treated cells suggests the drug effectively inhibits viral replication, whereas a low viability indicates poor antiviral action or cytotoxic effects. Calculation of Selectivity Index (SI): The SI value (CC50/EC50) is essential for evaluating a drug's therapeutic potential. A higher SI indicates a better antiviral effect with minimal toxicity.

Scalability and Practical Use: Ease of Culture: As a continuous cell line, Vero E6 cells are easy to maintain and scale, making them ideal for industrial vaccine production (e.g., inactivated virus vaccines). Regulatory Acceptance: Their established use in vaccine manufacturing (e.g., for polio, rabies) provides a regulatory advantage for SARS-CoV-2 vaccine production.

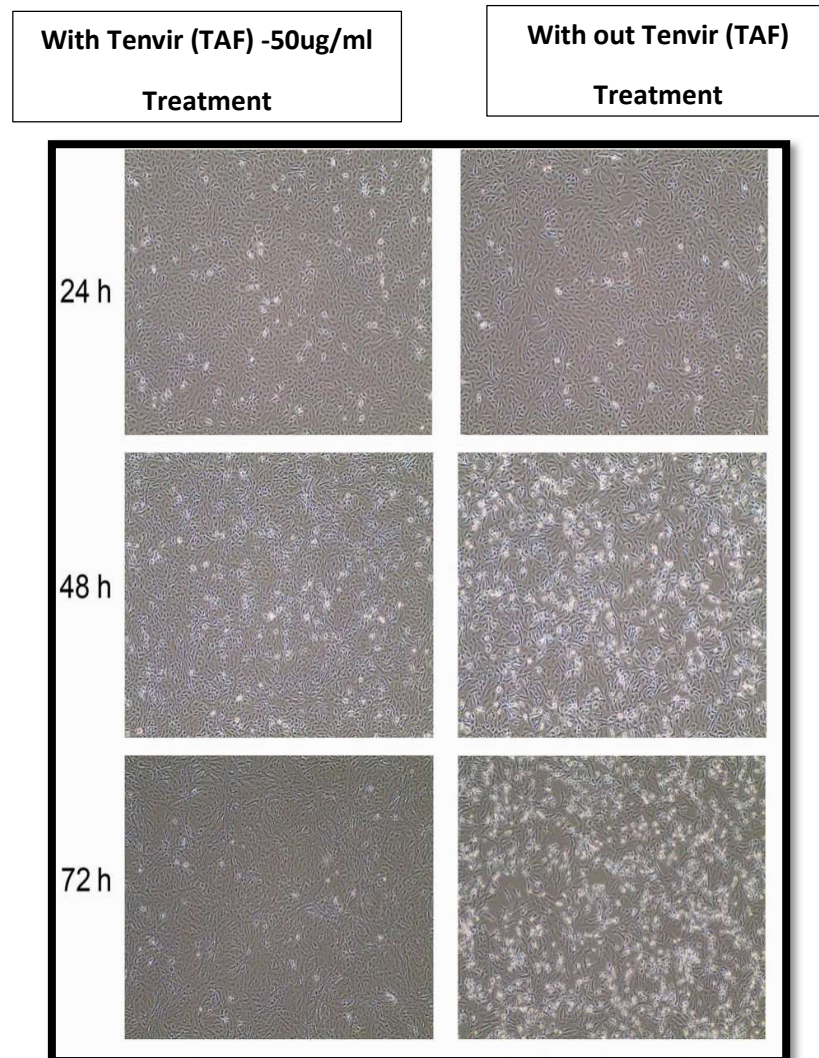


Figure 20 - The SARS-CoV-2 Wuhan strain, kindly provided by the Wuhan Institute of Virology, causes cytopathic effects on monolayers of Vero E6 cells. Vero-E6 cells were inoculated with SARS-CoV-2 at a 10 TCID₅₀ viral titer, or MOI of 1 (20,000 virions per 1×10^5 cells). GenSure sensitivity for SARS-CoV2: MOI of 0.0001-20. n=3.

The efficient replication of SARS-CoV-2 in Vero E6 cells enables the production of high viral concentrations, or titers, which are essential for applications such as vaccine development, antiviral testing, and neutralisation assays. Vero E6 cells are a cornerstone for SARS-CoV-2 titer production due to their biological compatibility, scalability, and established role in virology and vaccine development.

Reproducibility: Consistent viral growth in Vero E6 ensures reliable results in research, diagnostics, and drug screening. Adaptation Studies: While serial passage in Vero E6 may select for viral mutations (e.g., deletions of furin cleavage sites), these adaptations can aid in studying viral evolution and attenuation.

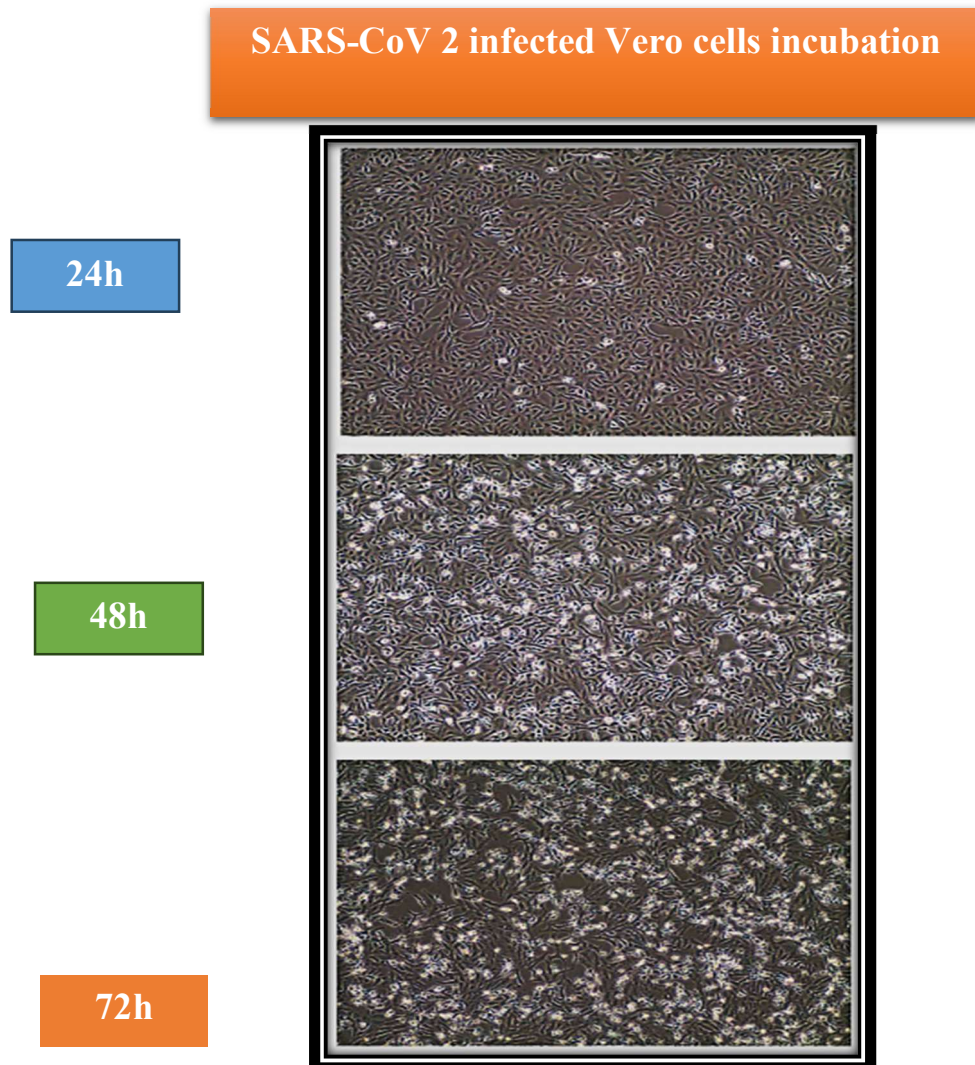


Figure 21 - SARS-CoV-2 causes cytopathic effects on monolayers of Vero E6 cells. Vero-E6 cells were inoculated with SARS-CoV-2 at a 10 TCID₅₀ viral titer, or MOI of 2 (200,000 virions per 1×10^5 cells), which corresponds to an MOI of 1, where one virion is present for every target cell – as determined by the Express Antigen COVID-19 test, GenSure. GenSure sensitivity for SARS-CoV2: MOI of 0.0001-20.

To conclude, BSL-3/4 authorised lab personnel were instructed to run the antiviral assay at least three times using a 50 µg/ml TAF prodrug salt against SARS-CoV-2 (2 µl of viral stock) with a control. Results can also be seen in Table 6, using the Antigen count of the GenSure kit from a specimen swab, as well as on the CCK8 platform after 24 hours of exposure.

3.2 Detection and isolation of the SARS-CoV-2/KAZ/B1.1/2021 variant, also known as the Alphavirus strain, using real-time PCR; Study morphological properties of the SARS-COV-2 virus

The strain SARS-CoV-2/human/KAZ/Britain/2021 consists of 29,815 nucleotides and belongs to the lineage B.1.1.7, according to the Pangolin COVID-19 database [18]. The SARS-CoV-2/human/KAZ/B1.1/2021 strain was obtained from the Scientific and Practical Center for Sanitary and Epidemiological Expertise and Monitoring, a branch of the Republican state enterprise with the right of economic use, the National Center for Public Health, Ministry of Health, Republic of Kazakhstan. According to the manufacturer's protocol, nucleic acids were extracted from the test sample using a QIAamp Viral RNA Mini Kit (Qiagen, Germany). Reverse transcription was performed using the SuperScript VILO cDNA synthesis kit (Invitrogen, USA). To amplify the entire genome of the virus, 65 primer pairs were designed using the online Primer-BLAST program (<http://www.ncbi.nlm.nih.gov/tools/primer-blast>) to generate amplicons ranging in size from 600 to 750 bp, with a tile overlap of approximately 100 bp. These amplicons were generated by PCR and visualized by 1.2% agarose gel electrophoresis (Sigma, USA). PCR amplicons were purified using the Pure Link PCR purification kit (Thermo Fisher Scientific, USA). Purified amplicons were sequenced using the Sanger dideoxy method using an AB3130xl (Hitachi Applied Biosystems) 16-capillary genetic analyzer autosequencer with the Big Dye Terminator 3.1 cycle sequencing kit (ABI, Foster City, CA, USA). Raw chromatograms were collected using Sequencer version 5 (Gene Codes Corp.) [18]. Over Ct 25 is not informative, and Ct 20 is too low, indicating a viral load that is too high (see Table 3). Additionally, it illustrates the stages of the subsequent RT-PCR analysis, serving as an example of sample recognition by Ct peaks. A typical RT-PCR analysis typically comprises a maximum of 40 thermal cycles. The lower the Ct value, the higher the amount of viral genetic material in the sample, serving as an approximate indicator of viral load. The Ct values obtained in this manner are semi-quantitative, allowing for the distinction between high and low viral loads. An increase in the Ct value by 3 points approximately corresponds to a 10-fold decrease in viral genetic material. There is no difference between the Ct and Cq values. These values are all the same, but they are with different names. Ct means threshold cycle, and Cq means quantification cycle. The MIQE (Minimum Information for Publication of Quantitative Real-Time PCR Experiments) guidelines recommend using the more generic quantification cycle (Cq) term to standardize qPCR nomenclature. Table 3 presents the results of eight PCR test/confirmation samples; for further details, see Appendix C. The standard deviation is $p=0.5$. In conclusion, the supernatant's isolated viral genetic material (vRNA/cDNA) was preserved as a primary viral titer with strain-specific fixation. In cases of secondary low viral load, it is possible that the virus could have been reused, and Vero cells reinfected to obtain a human SARS-CoV-2 specimen.

Table 3 - Ct-values of Bronchoalveolar lavage fluid- 12 samples in 8 runs

№	Type	R1Ct	R2Ct	R3Ct	R4Ct	R5Ct	R6Ct	R7Ct	R8Ct
1	Sample Bronchoalveolar lavage fluid	24,13	24	23,89	24	24,2	24,14	24,3	24,3
2	Sample Bronchoalveolar lavage fluid	18,43	18,23	19	20	21	18,49	18,28	18,28
3	Sample Bronchoalveolar lavage fluid	17,23	16,87	17,11	18,2	18	17,28	16,88	16,88
4	Sample Bronchoalveolar lavage fluid	23,20	22,8	23,29	22,83	18,5	23,23	22,8	22,8
5	Sample Bronchoalveolar lavage fluid	22,64	22,51	22,69	23	22,9	22,66	22,51	22,51
6	Sample Bronchoalveolar lavage fluid	17,48	17,52	17,99	18	17,69	17,38	17,52	17,52
7	Sample Bronchoalveolar lavage fluid	30,76	30	30,6	31	31	30,71	30	30
8	Sample Bronchoalveolar lavage fluid	27,62	28	27,5	28	27,89	27,68	28	28
9	Sample Bronchoalveolar lavage fluid	28,13	28,33	28,33	29	28,34	28,18	28,33	28,33
10	Sample Bronchoalveolar lavage fluid	26,47	26,89	26,9	27,1	27,25	26,44	26,89	26,89
11	Sample Bronchoalveolar lavage fluid	30,51	30,08	30,1	30	30,1	30,54	30,08	30,08
12	Sample Bronchoalveolar lavage fluid	31,26	31,26	33	32	30,2	31,27	31,26	31,26
13	Negative control	0,00	0,00	0,00	0,00	0,00	0,00	0,00	0,00
14	Positive control	30,26	30,26	30,26	30,26	30,26	30,26	30,26	30,26

This method provides a standardized approach for quantifying infectious SARS-CoV-2 in BALF, which is crucial for understanding pathogenesis and evaluating antiviral therapies. Report results as TCID₅₀/mL or convert to PFU/mL (1 TCID₅₀ ≈ 0.7

PFU). To standardise the nomenclature of PCR analysis, the MIQE manual (Minimal Information on Publication of Quantitative Real-Time PCR Experiments) recommends using the more general term "quantitative evaluation cycle" (Cq). Real-time PCR typically determines the target sequence's absolute number or compares the target sequence's relative amounts in the samples. Although fluorescent dyes and real-time PCR probes must be used sequentially, significant background fluorescence often occurs in most real-time PCR experiments. Therefore, it is essential to bypass this background signal to get meaningful information about your goal. Two values solve this problem in real-time PCR: the threshold line and the Cq value. A threshold line is a point or detection stage at which the fluorescence intensity in a reaction exceeds the background level. Before performing the PCR, the software will set a threshold value in your cycler. A line in your graph represents a level more significant than the background fluorescence, which also intersects your reaction curve at the beginning of the exponential phase. The Cq value is the cycle number of the PCR at which the reaction curve of your sample exceeds this threshold line. This value indicates the number of cycles required to detect a fundamental signal in your samples. If the PCR is performed in real-time, a reaction curve will be generated, and thus, multiple Cq values will be obtained for each sample. Your cycler's software calculates and displays the Cq value for each of your samples in a graph. The Cq values are inversely proportional to the amount of nucleic acid contained in your sample and correlate with the number of target copies in your sample. Lower Cq values (typically less than 28 cycles) indicate the presence of multiple target sequences. Higher Cq values (more than 38 cycles) mean less of your target nucleic acid. However, high Cq values may also indicate problems with the target or PCR setting.

Bronchoalveolar lavage (BAL) fluid is often used to evaluate patients with suspected or confirmed SARS-CoV-2 infection, especially in severe or atypical cases. Here are some key points regarding BAL fluid in SARS-CoV-2-positive patients:

Diagnostic utility - BAL fluid can provide a high diagnostic yield. In patients where upper respiratory samples (such as nasopharyngeal swabs) are negative or inconclusive—particularly in critically ill patients—the analysis of bronchoalveolar lavage (BAL) fluid may reveal the presence of the virus.

Viral Load: Studies have shown that BAL fluid from COVID-19 patients often contains a high viral load, sometimes even higher than what is detected in upper respiratory samples. This high viral load can be identified using RT-PCR, where low cycle threshold (Ct) values indicate higher amounts of viral RNA.

Disease Severity Correlation: A high viral load in BAL fluid is frequently associated with severe disease. In patients with significant lower respiratory tract involvement, the viral RNA concentration in BAL fluid tends to be high, correlating with the extent of lung injury.

Inflammatory Profile: BAL fluid analysis can provide insights into the local immune response beyond viral detection. It often reveals the presence of inflammatory cells, such as macrophages and neutrophils, as well as elevated levels of cytokines and chemokines. This information helps understand the pathogenesis of lung injury in COVID-19.

Procedural Considerations: While BAL can offer valuable diagnostic and research information, the procedure is invasive and poses a risk of aerosolising the virus, which requires strict infection control measures. As a result, BAL is typically

reserved for patients with severe disease or when less invasive samples have not yielded precise results. The following results of the test are shown in Figure 22.

The 117 samples were gained from Bronchoalveolar lavage fluid. However, only 12 were worth testing and titrating onto VeroE6 cells, which are permissive and susceptible to SARS-CoV-2 reproduction. The rest of the samples showed few traces of viral nucleotides or an entire absence of viral RNA in the BALF supernatants.

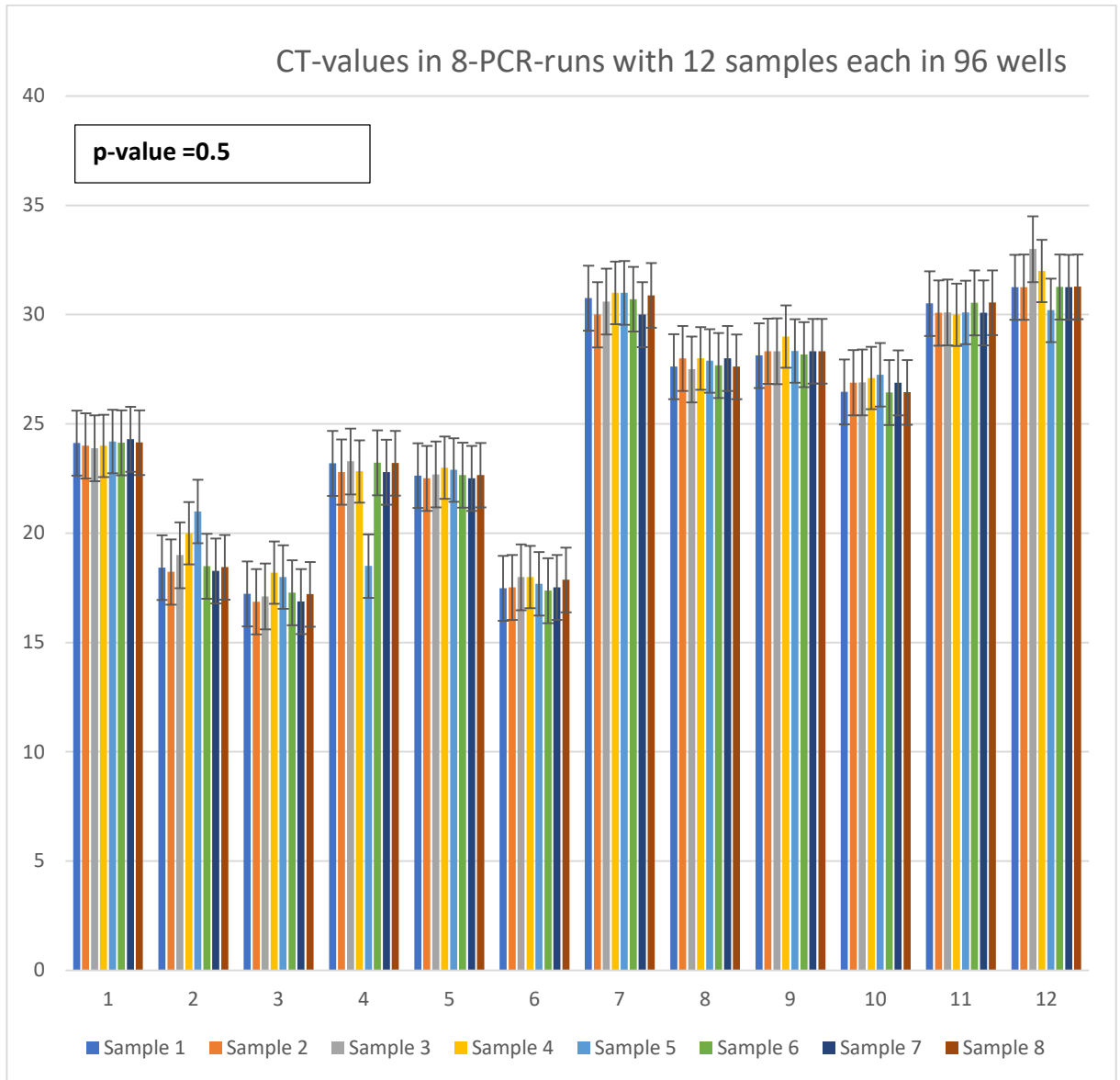


Figure 22 – Eight times repeated PCR runs with presumably 12 intact biological samples, the lowest CT/CQ value of 17, and the highest of 30. Based on the SEM, the following are the margins of error (or confidence intervals) at different confidence levels. Depending on the field of study, a confidence level of 95% (or statistical significance of 5%) is typically used for data representation. As can be seen, the first half has a significantly higher viral load than the second one. To achieve a sufficient number of pathogens, our stock allocation consisted of 200 μ L of the viral titer, corresponding to a multiplicity of infection (MOI) of 2.

The first six samples in Figure 21 showed an acceptable viral load and viral infection, while the remaining six demonstrated a lower viral load; nevertheless, this was sufficient to trigger the cytopathic effect (CPE) and initiate the inhibition assay. The total number of samples tested was 117, but only 12 were selected from the human samples as intact and proceedable.

Determination of Morphological Characteristics of SARS-CoV-2 Viral Strains

To determine and compare morphological characteristics, viral preparations related to various variants of the SARS-COV-2 virus were taken: Wuhan, British, Delta, and Omicron. As a result, it was found that virions are spherical, measuring 115-125 nanometers in diameter, with spikes (surface glycoproteins) approximately 10 nanometers in length. Electron microscopy of the virus is presented below in Figure 22 on a 100nm scale.

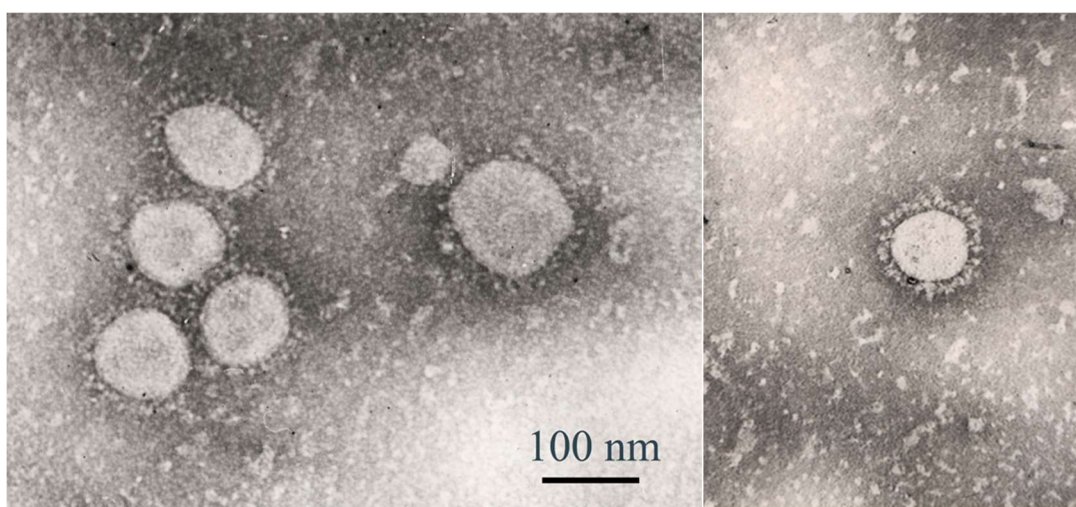


Figure 23 - Electron microscopy of the SARS-COV-2 virus. UV. 120,000, on a microscope (Jeol JEM-100 XC, provided by Kozhabergenov N.S.) [115].

As a result, it was found that virions are spherical, measuring 115-125 nanometers in diameter, with spikes (surface glycoproteins) approximately 10 nanometers in length. Electron microscopy of the virus is presented below in Figure 16 on a 100nm scale. Counting the intact viral load via Electron microscopy, the viral load is extrapolated as particles per milliliter (e.g., particles/mL) based on counted volume.

3.3 PCR production of fragments of SARS-COV-2 virus genes and sequencing of significant infection genes (whole viral genome)

In most cases, the leading indicators of PCR (sensitivity, specificity, product yield, and the feasibility of further manipulations with the final product) are determined by how well the specific structures of the primers are selected and optimised [45]. Currently, several information databases (RefSeq, GenBank) and numerous programs (Primer3, FastPCR, etc.) are available for designing primers, depending on the purpose. The search and development of nucleotide sequence primers were manually searched on the NCBI website using the GenBank database. The nucleotide sequence of specific

primers was selected based on the reference strain MN908947.3. The specificity of the primers was verified with the NCBI Primer-BLAST Service. The primers were chosen so that each pair overlapped, and their sequences were conservative among all variants of the SARS-CoV-2 virus. As a result, 65 pairs of sequencing primers were selected to develop the complete genome of SARS-CoV-2 virus variants with an overlap of about 100 nucleotide pairs (bp). The estimated amplitude length ranges from 604 to 772 bp.

NSP12 is an enzyme formed inside the DMV that enables SARS-CoV-2 to copy and produce not only genomic RNA but also subgenomic RNAs, which directly contribute to the synthesis of structural proteins and facilitate the host ribosome's reprogramming for its purposes.

Table 6 – Sequencing primer parameters for the main gene product of SARS-CoV-2/human/KAZ/B1.1/2021, the Alpha variant, on ORF1b, specifically NSP12, responsible for RNA-dependent RNA polymerase. The sequence is 2697 bp long, the same as the Wuhan-Hu-1 strain (GenBank MN908947.3), which is 2696 bp.

#	Primer orientation	Sequence (5'->3')	Start	Stop	T C ⁰ (primer heat temp)	GC %	Product size(bp)
PP 28	Forward	TGGAACCACCTTGTAGGTTT	12891	12910	56.57	45.00	652
	Reverse	AGCCCTGTATACGACATCAG	13542	13523	56.52	50.00	
PP 29	Forward	ACCCTGTGGGTTTTACTT	13341	13360	56.86	45.00	706
	Reverse	AACAATACCAGCATTTGCA	14046	14027	56.32	40.00	
PP 30	Forward	TACGCCAACTTAGGTGAACG	13963	13982	57.93	50.00	639
	Reverse	TAGATTACCAGAAGCAGCGT	14601	14582	56.36	45.00	
PP 31	Forward	CCACTTCAGAGAGCTAGGTG	14478	14497	57.04	55.00	713
	Reverse	CTCTAGTGGCGGCTATTGAT	15190	15171	56.88	50.00	
PP 32	Forward	CCAAGTCATCGTCAACAACC	14913	14932	57.03	50.00	644
	Reverse	CATTAACATTGGCCGTGACA	15556	15537	56.71	45.00	
PP 33	Forward	GTGTTGTAGCTTGTACACACC	15372	15391	56.96	50.00	659
PP 34	Forward	ATGTTGGACTGAGACTGACC	15834	15853	56.86	50.00	669
PP35	Forward	TCCGTATGTTTGCAATGCTC	16374	16393	56.80	45.00	712

That is why collecting data from NSP12 mutations, particularly about ORF1ab, is so important. The KAZ/B1.1/2021 strain is part of B. 1.1.7. Therefore, the Orf1b mutations would be the same as the Alpha variant. The KAZ/B1.1/2021 strain is part of the global B.1.1.7 lineage [115].

No unique ORF1b mutations specific to Kazakhstan have been widely reported; however, localised genomic surveillance may identify minor variations.

Mutation no.	Nucleotide position	Gene	Reference base (GenBank accession no. MN908947)	Nucleotide change
1	106	5' UTR	C	T
2	241	5' UTR	C	T
3	344	ORF1ab	C	T
4	2530	ORF1ab	A	G
5	3037	ORF1ab	C	T
6	4449	ORF1ab	C	A
7	4455	ORF1ab	C	T
8	4475	ORF1ab	C	T
9	5829	ORF1ab	A	C
10	9749	ORF1ab	A	G
11	9867	ORF1ab	T	G
12	10198	ORF1ab	C	T
13	11289	ORF1ab	C	
14	11290	ORF1ab	T	
15	11291	ORF1ab	G	
16	11292	ORF1ab	G	
17	11293	ORF1ab	T	
18	11294	ORF1ab	T	
19	11295	ORF1ab	T	
20	11296	ORF1ab	T	
21	11297	ORF1ab	A	
22	14408	ORF1ab	C	T
23	15017	ORF1ab	C	T
24	20759	ORF1ab	C	T
25	21080	ORF1ab	A	G
26	21446	ORF1ab	A	G
27	21646	S	C	T
28	21648	S	C	T
29	21784	S	T	A
30	21789	S	C	T
31	21846	S	C	T
32	23014	S	A	C
33	23403	S	A	G
34	23520	S	C	T
35	23751	S	C	T
36	23997	S	C	T
37	24000	S	G	T
38	24538	S	A	T
39	25688	ORF3a	C	T
40	26110	ORF3a	C	T
41	27015	M	G	T
42	27389	ORF6	C	T
43	27630	ORF7a	C	T
44	27667	ORF7a	G	A
45	27739	ORF7a	C	T
46	28881	N	G	C
47	28882	N	G	A
48	28883	N	G	A
49	29436	N	A	T
50		3' UTR		T
51		3' UTR		A
52		3' UTR		C
53		3' UTR		T

Figure 24 - RNA-dependent RNA polymerase nucleotide positioning of SARS-CoV-2/human/KAZ/B1.1/2021, the Alpha variant, on NSP12, with a nucleotide position almost identical to that of the Wuhan-Hu-1 strain (13442–16236) [Wuhan-Hu-1 - GenBank MN908947.3] [17].

The SARS-CoV-2/human/KAZ/B1.1/2021 strain was obtained from the Scientific and Practical Center for Sanitary and Epidemiological Expertise and Monitoring, a branch of the Republican state enterprise with the right of economic use, the National Center for Public Health, Ministry of Health, Republic of Kazakhstan. According to the manufacturer's protocol, nucleic acids were extracted from the test sample using a

QIAamp Viral RNA Mini Kit (Qiagen, Germany). Reverse transcription was performed using the SuperScript VILO cDNA synthesis kit (Invitrogen, USA). To amplify the entire genome of the virus, 65 primer pairs were designed using the online Primer-BLAST program (<http://www.ncbi.nlm.nih.gov/tools/primer-blast>) to generate amplicons ranging in size from 600 to 750 bp, with a tile overlap of approximately 100 bp. These amplicons were generated by PCR and visualized by 1.2% agarose gel electrophoresis (Sigma, USA). PCR amplicons were purified using the PureLink PCR purification kit (Thermo Fisher Scientific, USA). Purified amplicons were sequenced using the Sanger dideoxy method using an AB3130xl (Hitachi Applied Biosystems) 16-capillary genetic analyser autosequencer with the Big Dye Terminator 3.1 cycle sequencing kit (ABI, Foster City, CA, USA). Raw chromatograms were collected using Sequencer version 5 (Gene Codes Corp.).

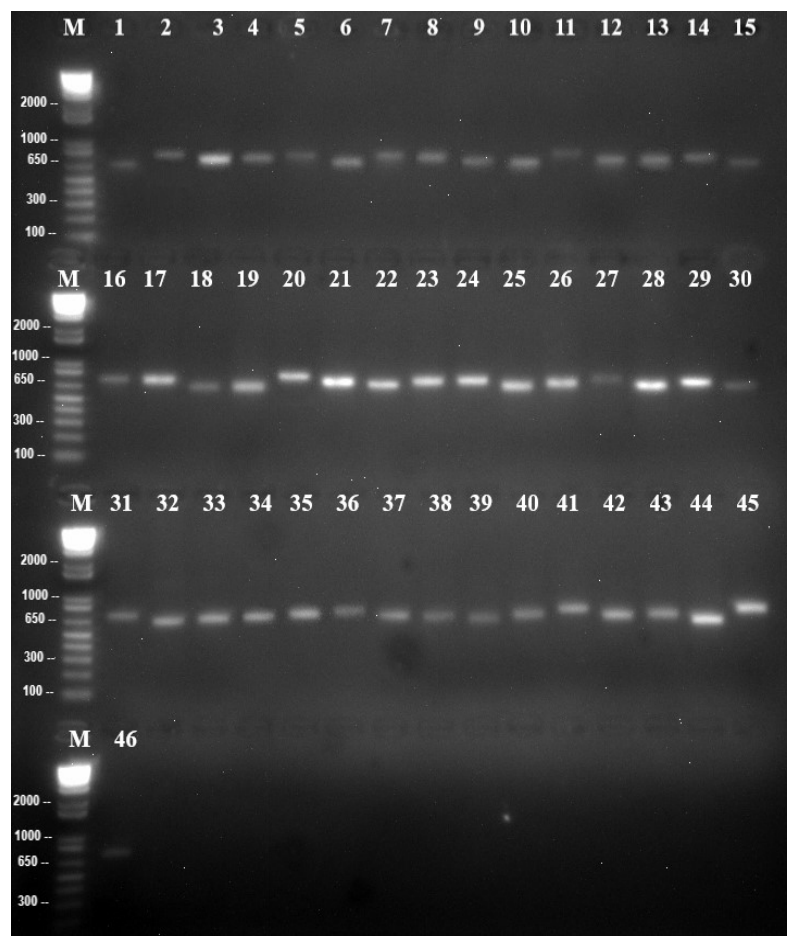


Figure 25 — Electropherogram of the RT-PCR results for the ORF1ab variant B or Alpha variant genes [115].

Electrophoretic analysis yielded products with molecular weights ranging from 604 to 772 bp from the ORF1ab gene. The length of the amplicon corresponds to the size of the synthesised primers.

The viral genome after ORF1ab

In addition to the 16 NSPs previously identified, 30-32% of the SARS-CoV-2 virus genome is composed of structural proteins, including spike, shell, membrane, and nucleocapsid proteins. These proteins enable the replicated genome to exit the host cell it has invaded and continue infecting surrounding cells. The auxiliary proteins ORF 3-10 are allocated between and among structural proteins closer to the 3'-UTR ends.

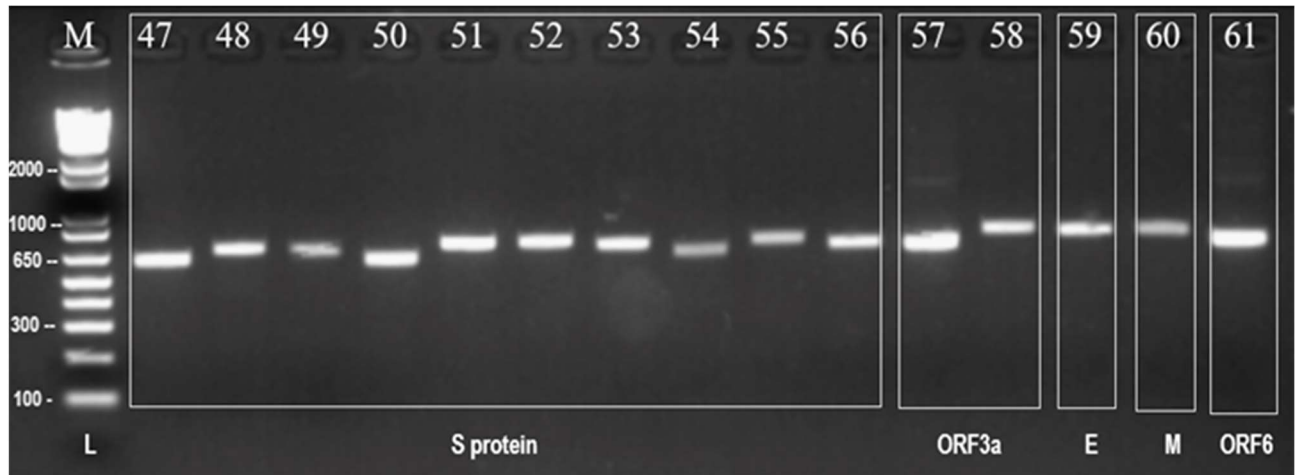


Figure 26 - Electropherogram of the RT-PCR results for the S, ORF3a, E, M, ORF6, and ORF7a variants of the SARS-CoV-2 virus.

The spike-protein product is produced directly after NSP13, which supports the theory that S-protein expression is essential for viral replication processes at the onset of RdRP activity.

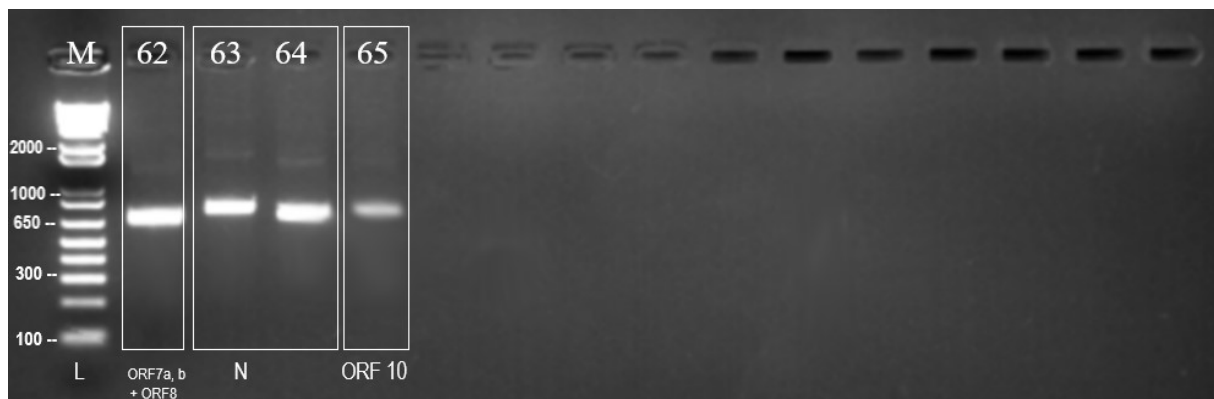


Figure 27 - Electropherogram of the results of RT-PCR genes ORF8, N, and ORF10 variants of the SARS-CoV-2 virus

As a result of the work, putative products of the SARS-CoV-2 virus were obtained using developed sequencing primers. The spike protein product consists of 1,273 bp, the most significant structural protein product, and its nucleotide sequence differs slightly from that of the original 2020 Wuhan strain. In general, spike proteins are the target of vaccine development issues, and their neutralization must be achieved

in the extracellular space before they can penetrate the host cell membrane. Figure 20 illustrates the genome structure and virion composition of the SARS-CoV-2 -Wuhan strain, the virus responsible for COVID-19. It provides an overview of the RNA genome, the non-structural and structural proteins, and the physical structure of the very first virus strain. The genome structure of SARS-CoV-2 consists of a single-stranded RNA sequence, with multiple regions encoding different proteins. The ORF1a and ORF1b sections contain non-structural proteins (NSPs) essential for viral replication and transcription. These include NSP3 (Papain-like protease), NSP5 (3CL-protease), NSP12 (RNA-dependent RNA polymerase), and NSP13 (Helicase). Additionally, structural proteins such as Spike (S), Envelope (E), Membrane (M), and Nucleocapsid (N) are encoded at the 3' end of the genome. The diagram also highlights accessory proteins, which play roles in immune evasion and pathogenesis. The SARS-CoV-2 virion structure, shown in the lower part of the diagram, is a spherical particle with a lipid envelope. The Spike (S) protein protrudes from the surface and is responsible for binding to human cells. Inside the virus, the Nucleocapsid (N) protein surrounds the viral RNA, while the Envelope (E) and Membrane (M) proteins help in virus assembly and release.

3.4 Phylogeny analysis of the SARS-CoV-2 strain/human/KAZ/Britain/2021, Alpha variant

Among the first strains that were isolated in the territory of Kazakhstan and were registered in B.1.1.7 lineage because primarily this strain came from Europe (Figure

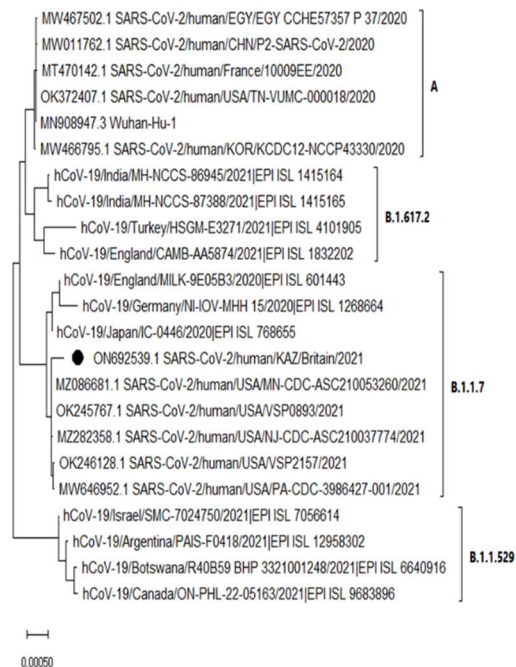


Figure 28 - Phylogenetic analysis of the SARS-CoV-2 strain/human/KAZ/Britain/2021, Alpha variant – near genomic sequencing with the B.1.1.7 lineage [17,115].

Phylogenetic analysis of isolate SARS-CoV-2/human/KAZ/Britain/2021, the Alpha variant, comprising 11 global strains belonging to lineages B.1.617.2, B. 1.1.7, and B.1.1.529, obtained from the GISAID database (<https://www.gisaid.org>), and 11 global strains belonging to lineages B and B. 1.1.7, obtained from the NCBI database (<https://www.ncbi.nlm.nih.gov/>).

Strain SARS-CoV-2/human/KAZ/Britain/2021 (black circle) shares a common ancestor with several U.S. isolates. Phylogenetic analysis was performed using MEGA X. Here, the x-axis represents the scale of the tree. For further information on B. 1.1.7, lineage, see Appendix A and B. Strain *SARS-CoV-2/human/KAZ/Britain/2021* was obtained from the Scientific and Practical Center for Sanitary and Epidemiological Expertise and Monitoring branch of the National Center for Public Health, a republican state enterprise on the right of economic use of the Ministry of Health of the Republic of Kazakhstan. According to the manufacturer's protocol, nucleic acids were extracted from the test sample using a QIAamp Viral RNA Mini Kit (Qiagen, Germany). Reverse transcription was performed using the SuperScript VILO cDNA synthesis kit (Invitrogen, USA). For amplification to cover the entire genome of the virus, 65 primer pairs were designed using the online program Primer-BLAST (<http://www.ncbi.nlm.nih.gov/tools/primer-blast>) to generate amplicons ranging in size from 610 to 770 bp; each of the designed primers overlaps with the others by approximately 100 bp. These primers were subjected to PCR and visualized using 1.5% agarose gel electrophoresis (Sigma, USA). The resulting whole PCR products were purified using the PureLink PCR purification kit (Thermo Fisher Scientific, USA). These purified amplicons were sequenced using the Sanger dideoxy method using an AB3130xl (Hitachi Applied Biosystems) 16-capillary genetic analyzer autosequencer with the BigDye Terminator 3.1 cycle sequencing kit (ABI, Foster City, CA, USA). Raw chromatograms were collected using Sequencer version 5 (Gene Codes Corp.). The sequences were aligned using BioEdit version 7.2.5 to assemble the genome. Phylogenetic analysis was performed using MEGA X (8). The assembled complete genome sequence of strain SARS-CoV-2/human/KAZ/Britain/ 2021 is 29,815 nucleotides long, with a GC content of 38%. The resulting sequence was analyzed using the Pangolin COVID-19 database (<https://pangolin.cog-uk.io>) and found to belong to lineage B.1.1.7. The amino acid mutations were compared with a reference sequence, and the results are presented in Table 1. Phylogenetic analysis showed that the studied viral genome and several U.S. isolates have a common ancestor. In Kazakhstan, four variants of concern (VOC) strains were isolated: the first, the Almaty strain, which is also known as the Wuhan strain of 2020. 2) SARS-CoV-2 variant/human/KAZ/B 1.1/2021, Alpha variant. -2021, 3) Delta -, and 4) Omicron—variant 2021/2022. For further details, refer to Appendices A and B. The SARS-CoV-2 Alpha variant (B.1.1.7), including the strain human/KAZ/Britain/2021, exhibits specific mutations in key genes, primarily driven by evolutionary selection rather than an altered mutation rate. Baseline Mutation Rate: SARS-CoV-2 typically accumulates ~1–2 mutations per genome per replication cycle, equivalent to $\sim 1-2 \times 10^{-3}$ substitutions per site per year. The Alpha variant does not possess mutations in the viral polymerase (e.g., nsp14) that alter its proofreading ability, so its mutation rate remains

consistent with that of other lineages. Mutations in ORF1ab, N, and ORF8 are less frequent but still significant, arising from random mutations that may confer subtle fitness advantages.

Phylogenetic analysis of the SARS-CoV-2 strain (human/KAZ/B 1.1/2021), *Alpha variant*.

Phylogeny analysis of the SARS-CoV-2/human/KAZ/B1.1/2021, Alpha variant isolate. The phylogeny was generated using the neighbour-joining method (9). The optimal tree is shown.

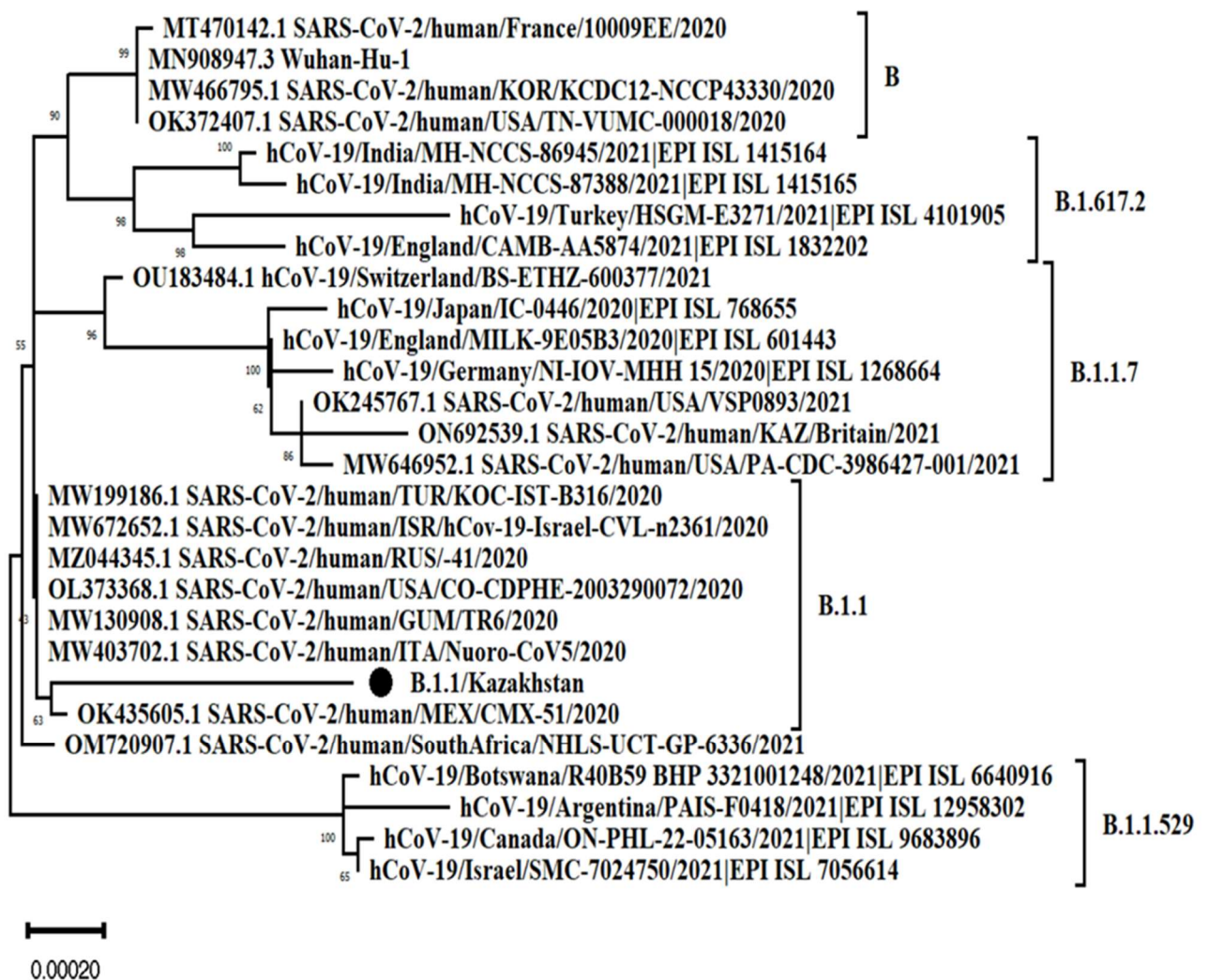


Figure 29 - Phylogeny analysis of the SARS-CoV-2 strain/human/KAZ/B 1.1/2021, Alpha variant [17,115].

The percentage of replicate trees in which the associated taxa clustered together in the bootstrap test (500 replicates) are shown next to the branches (10). The tree is drawn to scale, with branch lengths measured in the same units as the evolutionary distances used to infer the phylogenetic tree. The evolutionary distances were calculated using the Kimura 2-parameter method (11), representing the estimated

number of base substitutions per site. This analysis involved 28 nucleotide sequences. Codon positions included are 1st, 2nd, 3rd, and noncoding. All positions containing gaps and missing data were eliminated (complete deletion option). The final data set comprised a total of 25,145 positions. Evolutionary analyses were conducted in MEGA 11 (12). For further information on B. 1.1.7, lineage, see Appendix A and B.

Uploading a genome-wide nucleotide sequence to the GenBank database

The virus data were obtained using the Sequencer V.5.4 program. The isolated nucleotide sequence of the virus strain's genome was uploaded to the NCBI database under the registration numbers ON692539.1, dated June 7, 2022, and OP684305.1, dated October 20, 2022. The obtained sequences were analyzed using the Pangolin COVID-19 database (<https://pangolin.cog-uk.io>), establishing that they belong to lineages B.1.1.7 and 1.1 (A and B, respectively). The uploaded data can be seen in Figure 29.



Figure 30 - A. Identification of the SARS-CoV-2 strain variant/human/KAZ/Britain/2021 according to the Pangolin COVID-19 database. B. Determination of the SARS-CoV-2 strain variant (human/KAZ/B 1.1/2021) as the Alpha variant, based on the Pangolin COVID-19 database analysis of the nucleotide sequence of the entire genome of SARS-CoV-2 viruses isolated in the Almaty region of the Republic of Kazakhstan [115].

The analysis of the nucleotide sequence of the whole genome showed that the strains isolated in the Almaty region are 100% similar to SARS CoV-2/human/KAZ/Britain/2021, ISO alpha-3 code: KAZ and SARS-CoV-2/human/KAZ/B1.1/2021, ISO alpha-3 code: KAZ and have 99.80% and 99.82% of

the total similarity. Identity with the reference strain SARS-CoV-2, the Wuhan-Hu-1 isolates belonging to the B-line (Figure 30).

Comparison of the isolated strains of two variants: SARS-CoV-2 (human/KAZ/B.1.1/2021) and SARS-CoV-2 (human/KAZ/B. 1.1/2021). /Alpha variant.

Isolates were gained from the Scientific and Practical Center for Sanitary and Epidemiological Expertise and Monitoring samples. After studying the biological properties, these isolates were deposited in collections of microorganisms under the following names: *SARS-CoV-2 / human / KAZ / B1.1/2021* and *SARS-CoV-2 / human / KAZ / Britain / 2021. /Alpha variant.* Sequencing of significant viral genes. Comparative and phylogenetic analysis of the nucleotide sequence of viral genes. The analyzed strains exhibited a total of 97 nucleotide variations. Among these, 33 mutations were identified in the SARS-CoV-2/human/KAZ/B1.1/2021 strain, 35 mutations were found in the SARS-CoV-2/human/KAZ/Britain/2021 strain, and seven mutations were observed in both the OP684305.1 strain and the SARS-CoV-2/human/KAZ/Britain/2021 strain. Deletions were detected in two strains at three different positions, resulting in 18 single nucleotide deletions; of these, nine deletions were common to both strains, six were exclusive to the SARS-CoV-2/human/KAZ/Britain/2021 strain, and three were unique to the SARS-CoV-2/human/KAZ/B1.1/2021 strain. Additionally, four single nucleotide insertions were observed in the SARS-CoV-2/human/KAZ/B1.1/2021 strain, which was absent in the reference strain. As detailed, 39 mutations (41%) were located in the ORF1ab region, and 26 mutations (27.3%) were found in the Spike protein. Eight mutations (8.4%) were present in gene N.

Table 4 - Key Mutations in the Alpha Variant (B.1.1.7) vs. Wuhan Strain

Genomic Region	Mutations	Functional Significance
Spike Protein (S)	- Δ69-70 (deletion)	Linked to immune evasion and diagnostic S-gene target failure (SGTF) in PCR tests.
ORF1ab	- T1001I, A1708D, I2230T	Mutations in non-structural proteins (NSPs) linked to replication efficiency or fidelity.
Nucleocapsid (N)	- D3L, R203K, G204R, S235F	Enhances viral packaging/RNA binding associated with higher viral loads.

Mutations in the other areas of the virus were recorded as follows: 2 mutations (2.1%) in the 5UTR, three mutations (3.15%) in ORF3a, one mutation (1%) in the M gene, and four mutations (4.2%) each in ORF6, ORF7a, ORF8, and the 3UTR. The SARS-CoV-2 Alpha variant (B.1.1.7 lineage), including strains such as SARS-CoV-2/human/KAZ/B1.1/2021 (identified in Kazakhstan in 2021), carries multiple mutations compared to the original Wuhan-Hu-1 strain (NCBI reference:

NC_045512.2). Below is a breakdown of key mutations and their functional implications, as depicted in Table 4.

Additionally, four single nucleotide insertions were observed in the SARS-CoV-2/human/KAZ/B1.1/2021 strain, which was absent in the reference strain. As detailed, 39 mutations (41%) were located in the ORF1ab region, and 26 mutations (27.3%) were found in the Spike protein. Eight mutations (8.4%) were present in gene N. Mutations in the other areas of the virus were recorded as follows: 2 mutations (2.1%) in the 5UTR, three mutations (3.15%) in ORF3a, one mutation (1%) in the M gene, and four mutations (4.2%) each in ORF6, ORF7a, ORF8, and the 3UTR. The SARS-CoV-2 Alpha variant (B.1.1.7 lineage), including strains such as SARS-CoV-2/human/KAZ/B1.1/2021 (identified in Kazakhstan in 2021), carries multiple mutations compared to the original Wuhan-Hu-1 strain (NCBI reference: NC_045512.2). Below is a breakdown of key mutations and their functional implications. Kazakhstan-Specific Context: The KAZ/B1.1/2021 strain is part of the global B.1.1.7 (Alpha) lineage. No unique Kazakhstan-specific mutations have been widely reported; however, regional genomic surveillance may identify minor variations.

Table 5 - Comparison of Alpha vs. Wuhan Strain

Feature	Wuhan Strain	Alpha Variant (B.1.1.7)
Key Spike Mutations	None	N501Y, Δ69-70, P681H, D614G
Transmissibility	Baseline	~50–70% higher
S-gene PCR Target	Detected	Dropout (Δ69-70)
Dominant Period	2019–2020	Late 2020–2021 (pre-Delta)

Delta (B.1.617.2) and Omicron (B.1.1.529) eventually displaced the variant due to their higher transmissibility and ability to evade the immune system. Appendix D contains a detailed table listing mutations, including the specific mutation and corresponding nucleotide position. Epidemiological Context in Kazakhstan

In conclusion, the isolated strains SARS-CoV-2/human/KAZ/B.1.1/2021 (a local Kazakhstan lineage) and SARS-CoV-2/human/KAZ/B. 1.1.7 (Alpha variant) share 98% similarity. B.1.1 (KAZ): This variant likely circulated during the early phases of the pandemic, with a limited public health impact due to its lower transmissibility. Alpha (B.1.1.7): Introduced through international travel, it led to a surge in cases and a strain on healthcare systems before being displaced by Delta (B.1.617.2).

3.5. Antiviral drug cytotoxicity assays

3.5.1 Determination of cytotoxicity of drugs for cell culture (CCK8)

Dexamethasone (a hormone), Ribavirin (a purine analogue), Tenvir (a purine analogue), and Fabiflu (a purine analogue) were chosen to study their antiviral activity against the SARS-CoV-2 virus. Before determining the antiviral activity, a working dose that did not cause toxicity to the cell culture was established.

Dexamethasone - CCK8 Viability test

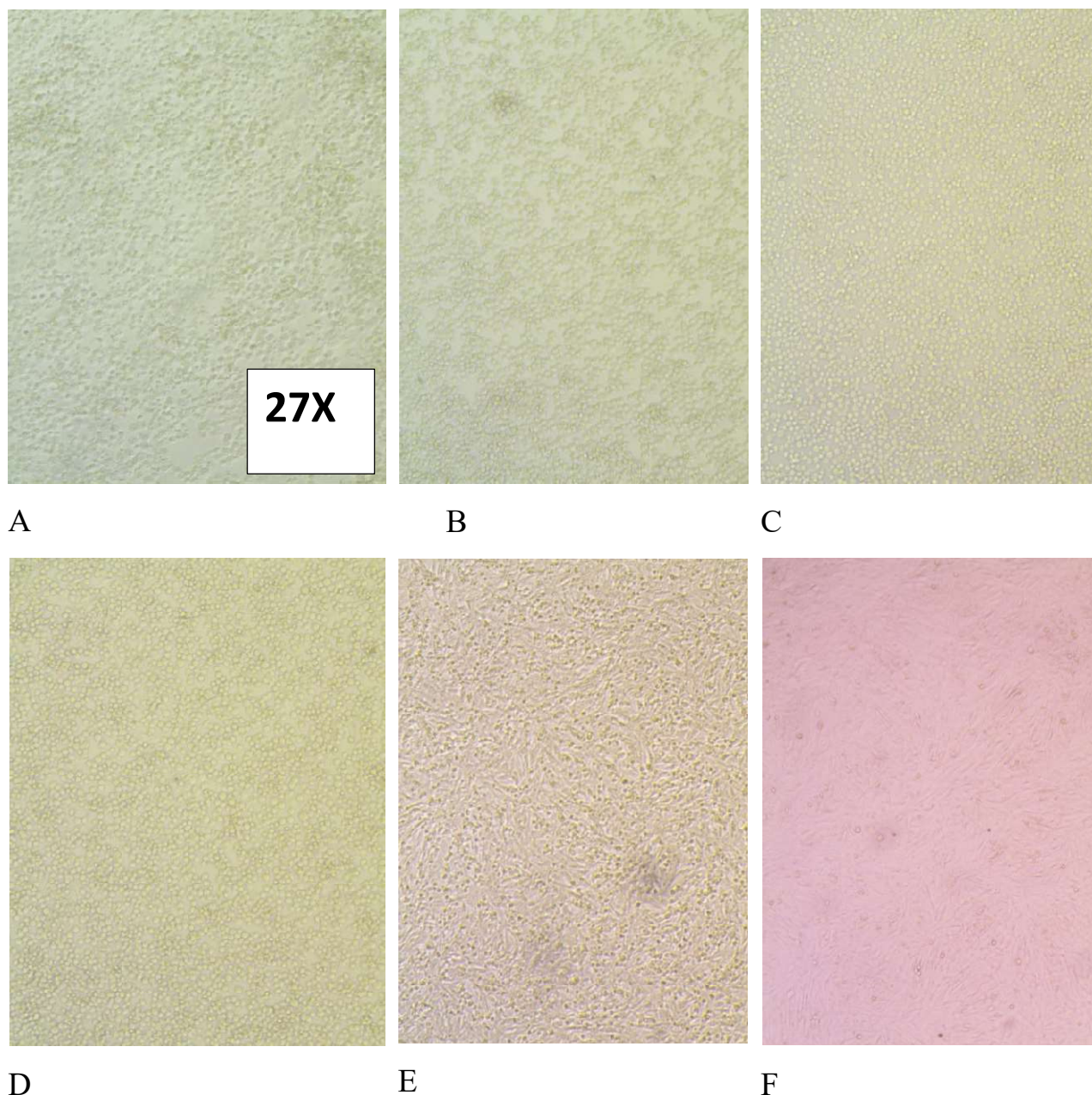


Figure 31 - Determination of cytotoxicity of Dexamethasone in Vero cell culture
A – 20 mg/mL, B – 16 mg/mL, C – 12 mg/mL, D – 8 mg/mL, E – 4 mg/mL, F – Vero control (untreated) - 72-hour exposure, n = 3. Main Absorbance Wavelength: 450 nm.

The higher the concentration, the denser the cell layers stimulated in incubation conditions, mostly indirectly, because dexamethasone only slightly stimulates cellular

growth over time. As shown in Figure 31, cell growth stimulation by Dexamethasone is evident: the mass multiplication of cell monolayers, even from a stock concentration of 4.37 ml (column A), and the mass multiplication of cell monolayers from double stock concentration (8.74 ml, column B). The start of bursting cells from monolayers is due to space limitations. Triple stock concentration 13,11 ml column C, the moderate bursting of cells from monolayers due to space limitations, from four times stock concentration 17,48 ml column D, the acute bursting of cells from monolayers due to space limitations visual evidence of second layer growth, five times stock concentration 21,85 ml column E, the complete rupture of tissue integrity of monolayers due to space limitations, the multiple layers formations. It was found that the drug Dexamethasone at a dosage of 4 mg/ml is not toxic to cell culture and will be used to study the inhibition of antiviral activity. Additionally, with increasing doses of the drug Dexamethasone, the dynamics of cell rounding and swelling are observed. Control refers to untreated Vero cells in this context. As shown in Figure 30, a 72-hour exposure to dexamethasone affected only the prefiltration rates of Vero E6 cells, without harming cell viability, as measured by CCK8, across all concentration ranges. Dexamethasone was used in ampoules containing 4 mg/ml in 5 dosages (20, 16, 12, 8, and 4 mg/ml). The results are presented in Figure 31. Control refers to untreated Vero cells in this context.

A drug viability concentration assay is an experimental procedure used to evaluate the effect of various drug concentrations on cells' viability (or survival). This type of assay is commonly used in drug development and pharmacological research to determine a compound's cytotoxicity or therapeutic efficacy. Here is an overview of what it involves: Cell Seeding: preparation: Cells are plated in multi-well plates (e.g., 96-well plates) at an appropriate density to ensure exponential growth during the assay. Objective: This setup allows consistent and reproducible results across multiple conditions. Drug Treatment: Concentration Gradient - Cells are treated with a range of drug concentrations, often in a serial dilution format, to capture the entire dose-response curve. Incubation: The cells are incubated for a set period (commonly 24–72 hours), which allows the drug to exert its effect. Viability Assessment: Assays Used: Several assays can be employed to measure cell viability, including MTT/MTS Assay, which measures metabolic activity by reducing tetrazolium salts to formazan. Measurement: The output is typically quantified by measuring absorbance, fluorescence, or luminescence, which correlates with the number of viable cells. Data Analysis: Dose-Response Curve: Viability data is plotted against drug concentration to generate a dose-response curve. IC_{50} Determination: The IC_{50} (the concentration at which the drug reduces cell viability by 50%) can be calculated from the curve. This is a key parameter for comparing the potency of different drugs. Statistical Analysis: Replicates and proper controls (such as untreated cells and vehicle controls) are crucial for obtaining reliable and interpretable results.

The drug viability concentration assay is a fundamental tool in biomedical research that provides quantitative insights into a drug's cytotoxic or cytoprotective effects. It helps researchers optimise dosing and identify promising therapeutic candidates.

Ribavirin -CCK8 Viability test

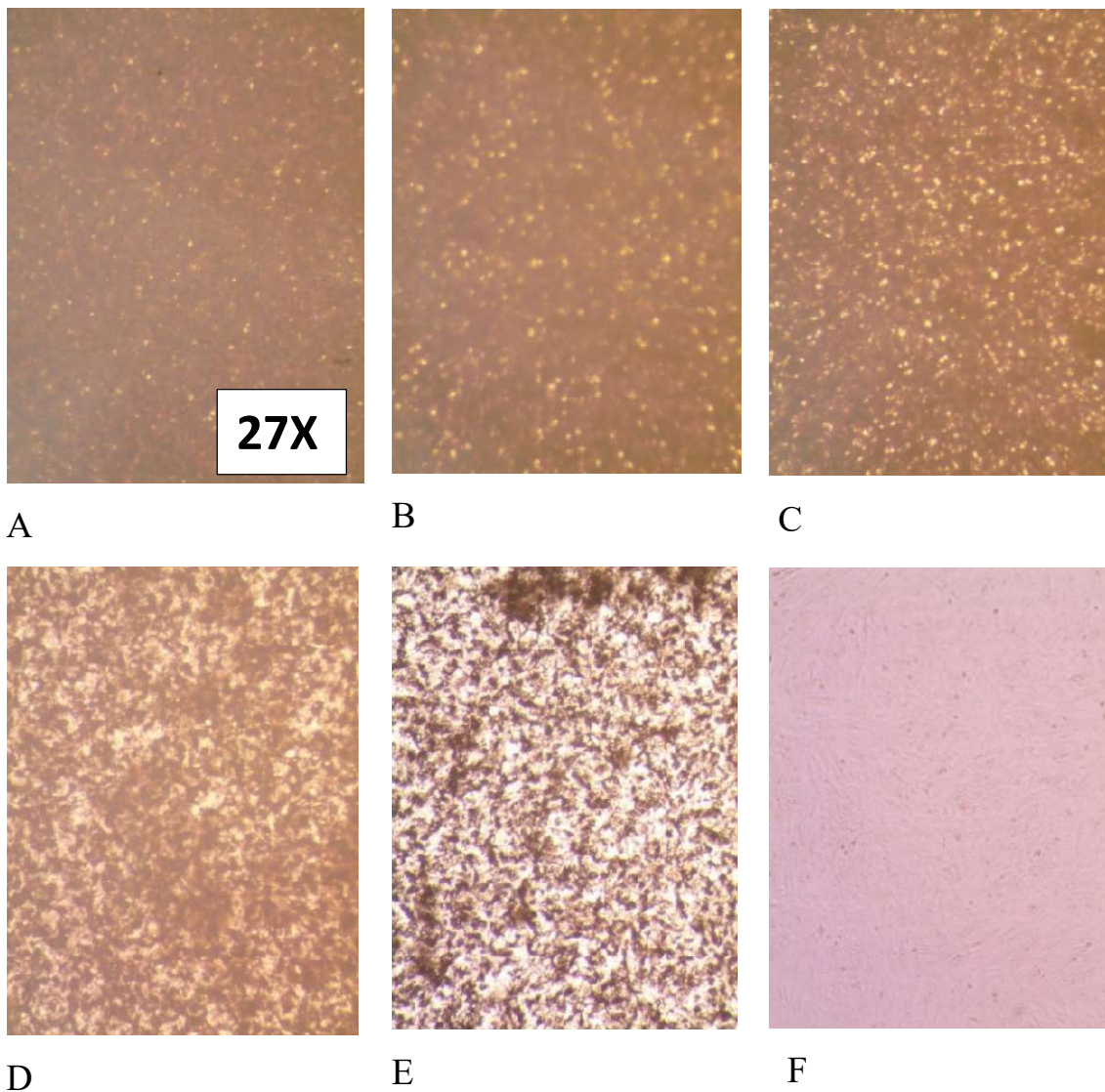


Figure 32 - Determination of the cytotoxicity of Ribavirin in Vero cell culture
A – 200 µg, B – 150 µg, C – 100 µg, D – 75 µg, E – 50 µg, F – Vero control (untreated).72 hours exposure, n=3. Main Absorbance Wavelength: 450 nm.

Ribavirin shows high toxicity rates (cell layers are torn even at minimum concentration) since only a few concentrations are recommended to achieve the therapeutic effect. Control refers to untreated Vero cells in this context. The mass destruction of cell monolayers, evident signs of a cellular necrosis process, occurred even at the stock concentration (200 mg) in column A and after five times the concentration (1000 mg) in column B. The CCs (cytotoxic concentrations) were too high for VeroE6 cells to survive during a 72-hour incubation. Therefore, starting from

a two-fold increase, the wells were practically cell-free and did not differ significantly from the 5-fold increase, as shown in Figure 32. Vero control means that no drug was added, and its growth had no cytotoxicity load; as a result, Vero cells successfully proliferated throughout the entire cell viability assay. The subsequent CCK8 cell viability measures were obtained: 50 μg : 75-80% \pm 0,03 75 μg : 55-65% \pm 0,03, 100 μg : 35-40% \pm 0,03, 150 μg : 20-25% \pm 0,03 and 200 μg : 10-15% \pm 0,03.

Tenvir (TDF) tableted Tenofovir - CCK8 Viability test

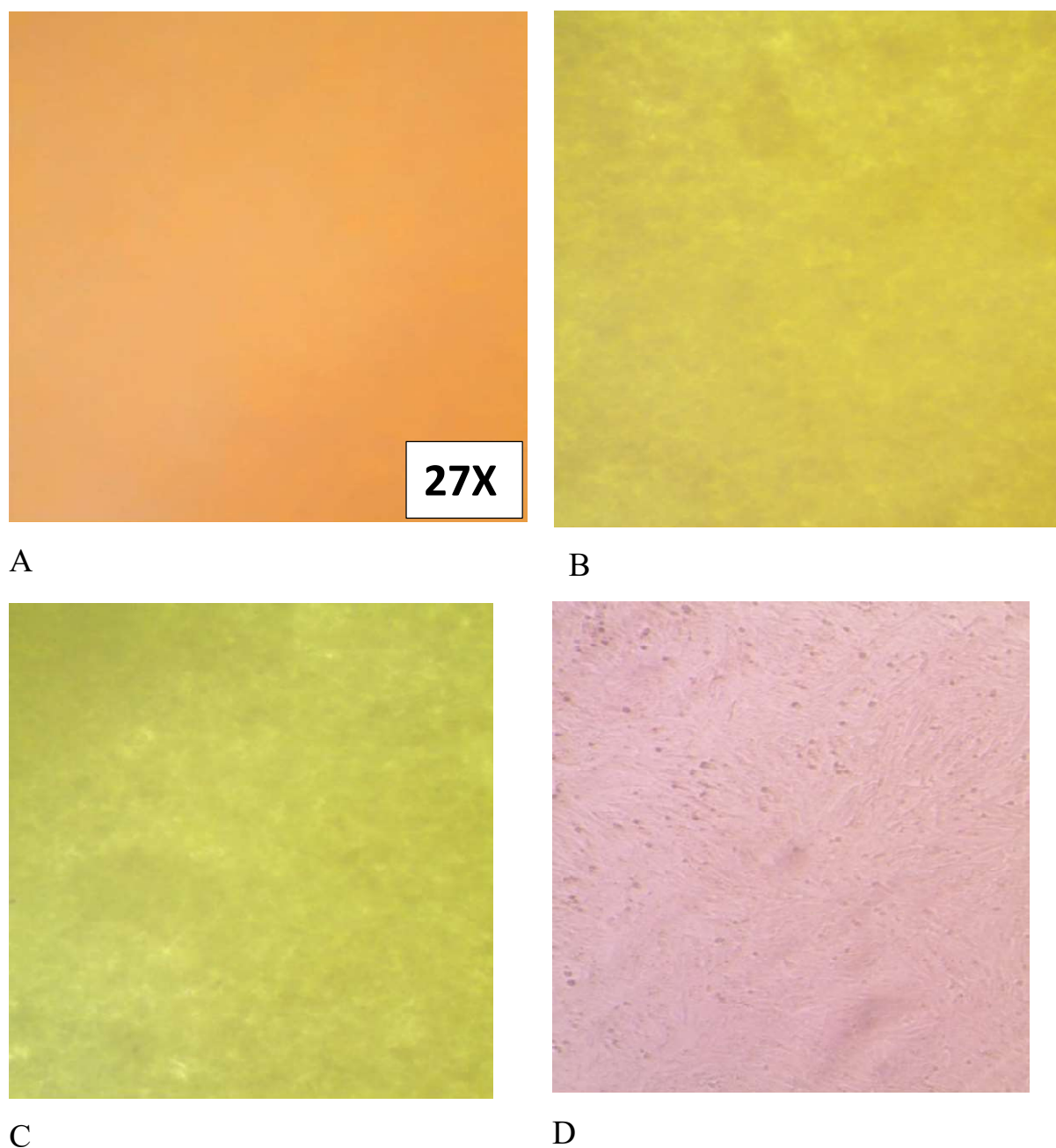


Figure 33 - Determination of Tenvir cytotoxicity in Vero cell culture. A – 300 μg , B – 150 μg , C – 100 μg , D – 50 μg . 72 hours exposure, n=3. Main Absorbance Wavelength: 450 nm. The 50 $\mu\text{g}/\text{ml}$ - dose reached a cell viability rate of 90% [115].

Tenvir also exhibits high toxicity rates, as cell layers are torn even at minimum concentrations because only a relatively few concentrations are recommended to achieve therapeutic effects. The subsequent CCK8 cell viability measures were obtained: 50 μg : 90-95% \pm 0,03 75 μg : 85-90% \pm 0,03, 100 μg : 75-80% \pm 0,03, 150 μg : 65-70% \pm 0,03 and 200 μg : 50-55% \pm 0,03. The destruction of cell monolayers, with apparent cellular necrosis, occurred even at the stock concentration (300 mg) of column A and after three times the concentration (900 mg) of column B. The CCs (cytotoxic concentrations) were too high for VeroE6 cells to survive during a 72-hour incubation. Therefore, starting from 300mg of tenofovir, the wells were practically cell-free, and a 2-fold increase (600mg) did not differ significantly from the 3-fold increase. The results showed that Tenvir at a dosage of 50 μg is non-toxic to cell culture and will be used to study its antiviral activity inhibition. Additionally, with an increase in the dosage of the Tenvir drug, alkalisation of the medium and cell detachment from the surface are observed (Figure 33) [115].

Fabiflu (tableted Favipiravir) - CCK8 Viability test

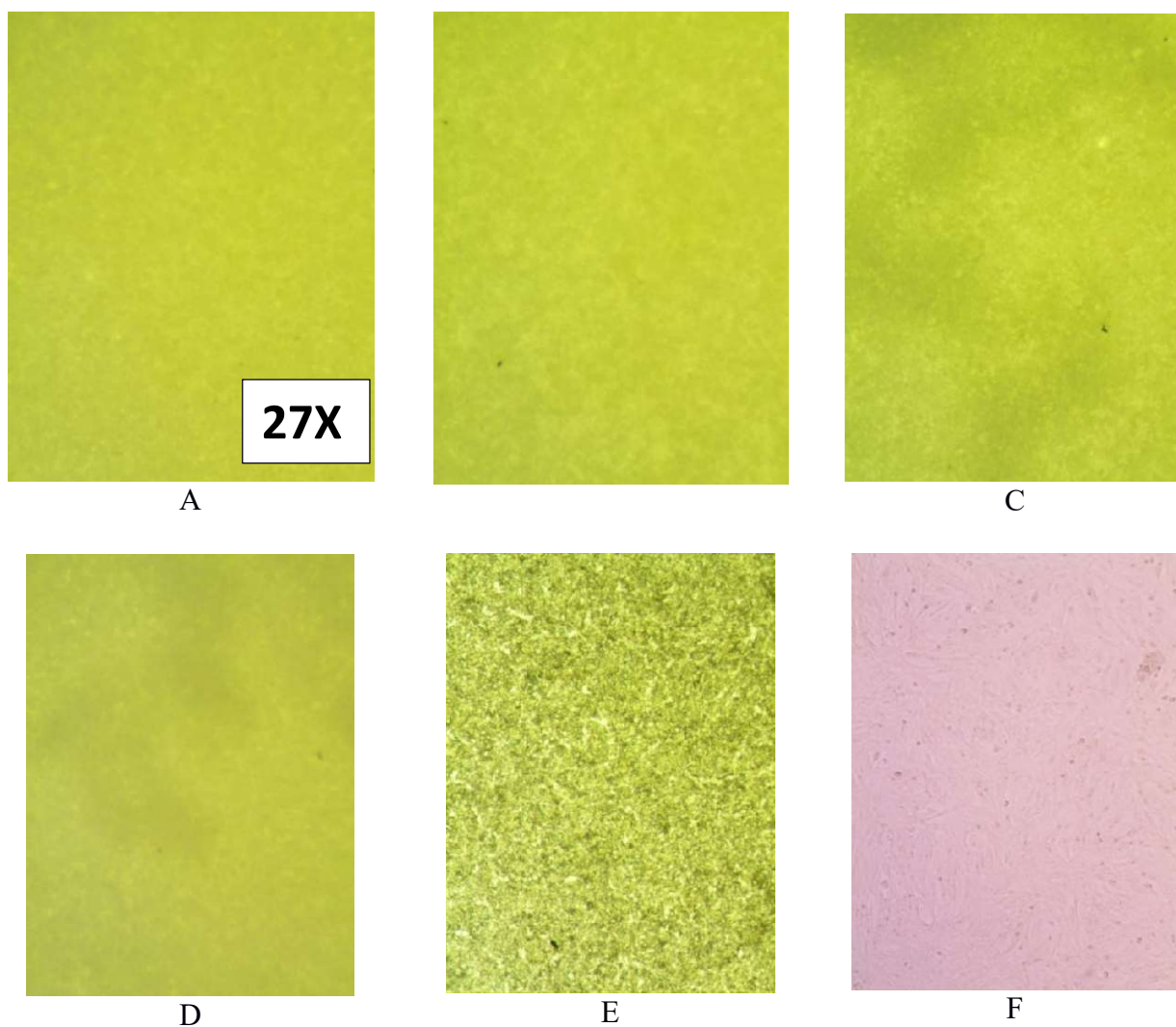


Figure 34 - Determination of cytotoxicity of Fabiflu (Favipiravir) in Vero cell culture. A – 200 μg , B – 150 μg , C – 100 μg , D – 75 μg , E – 50 μg , F – Control Vero (untreated). 72-hour exposure, n = 3. Main Absorbance Wavelength: 450 nm.

Next, studies were conducted to determine the cytotoxicity of the drug Fabiflu in five dilutions, each containing 200 mg, at dosages of 200, 150, 100, 75, and 50 mg. The CCK8 cell viability measures were obtained: 50 µg: 70-80%±0,03 75 µg: 65-70%±0,03, 100 µg: 35-40%±0,03, 150 µg: 25-30% ±0,03 and 200 µg: 20-25% ±0,03 (Figure 34).

The visual results are presented in Figure 33. The cytotoxic effect increases with the destruction of cell monolayers, even from the stock concentration (200mg) and after 2 (column B), 3 (column C), and 4 (column D) times, as the concentration rises from the stock concentration. The CCs (cytotoxic concentrations) were too high for VeroE6 cells to survive during a 72-hour incubation; therefore, starting from a two-fold increase, the wells were essentially cell-free. Fabiflu shows high toxicity rates (cell layers are torn at higher concentration); however, at the lowest concentration, the cells were only dyed, and some cellular layers were visually intact. As a result, it was found that the drug Fabiflu, at a dosage of 50 mg, is non-toxic to cell culture and will be used to study its antiviral activity inhibition. Additionally, with an increase in the dosage of the drug Fabiflu, alkalisation of the medium and cell detachment from the surface is observed. The general cytotoxic assay showed heavy Vero cell survival conditions. Apart from Dexamethasone, at the beginning of the stock concentration, all monolayered cells showed neither cell proliferation nor signs of visual cellular integrity until the concentration reached 50 µg/ml.

In conclusion, 72 hours of exposure to four drugs demonstrated the full viability potential of VeroE6 cells and their ability to sustain SARS-CoV-2 replication during viral titer production from supernatants obtained from biosamples. Dexamethasone's influence on Vero cell viability appears to be context-dependent, primarily varying with concentration and exposure duration. Here is a synthesised summary based on available data: Standard Concentrations (e.g., 100 nM to 1 µM): Studies indicate that dexamethasone, at concentrations commonly used in cell culture (e.g., 100 nM to 1 µM), does not significantly impair the viability of Vero cells. For example, experiments using MTT assays or similar viability tests showed no adverse effects after 48 hours of treatment. This aligns with its frequent use in virology and cell culture to modulate gene expression or enhance viral yield without harming cells. High Concentrations or Prolonged Exposure: At higher doses (e.g., 10 µM or greater), dexamethasone may exhibit cytotoxic effects, potentially reducing viability through mechanisms such as apoptosis. Such effects are consistent with glucocorticoid behaviour in some cell types, although epithelial cells, such as Vero, may be less sensitive compared to immune cells. Contextual Effects: Dexamethasone may enhance cell survival under stress (e.g., serum starvation) by mitigating stress responses. However, under normal conditions, its primary role in Vero cultures is often supportive rather than detrimental. Dexamethasone generally does not compromise Vero cell viability at standard experimental concentrations. However, researchers should optimize doses and monitor exposure times to avoid potential toxicity at higher levels.

3.5.2 CCK8 test for cell viability in four drugs at varying concentrations against SARS-CoV-2 Titters

The combined data in Figure 34 shows the antiviral drugs in the DMEM medium at a relatively safe concentration. The experiment was repeated five times in the colourimetric assay using the CCK8 tablet, where the WST-8 formazan product absorbs light. The absorbance at 450 nm is proportional to cell viability.

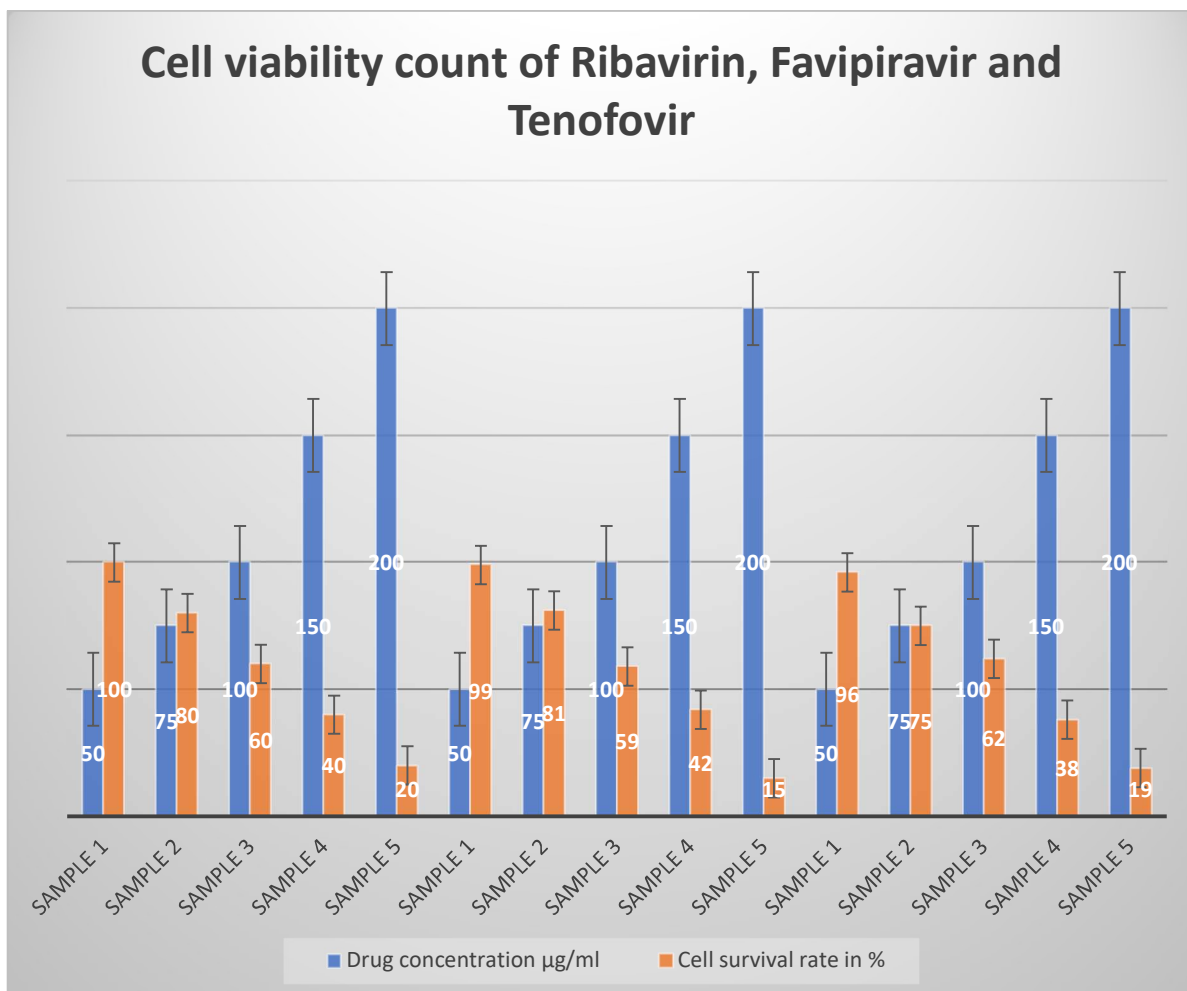


Figure 35 – Survival rates of VeroE6 cells in percentage in the presence of 5 drug concentrations of Ribavirin, Favipiravir, and Tenofovir, ranging from 50 µg/ml to 200 µg/ml viral load or MOI 2, after 24 hours of exposure [115].

These experiments were repeated three times, and each drug had five concentration samples to determine the correlation between IC and CC values at a 450 nm wavelength. The experiment was conducted within a single day. The results are shown in Table 7. Sample 1 has the highest survival rate. This experiment was repeated three times at 450nm wavelength.

The 96-well colour was brownish yellow, visually indicating that the cultured cells were viable starting from 50 µg/mL and becoming increasingly paler (beginning to fade) with increasing concentration.

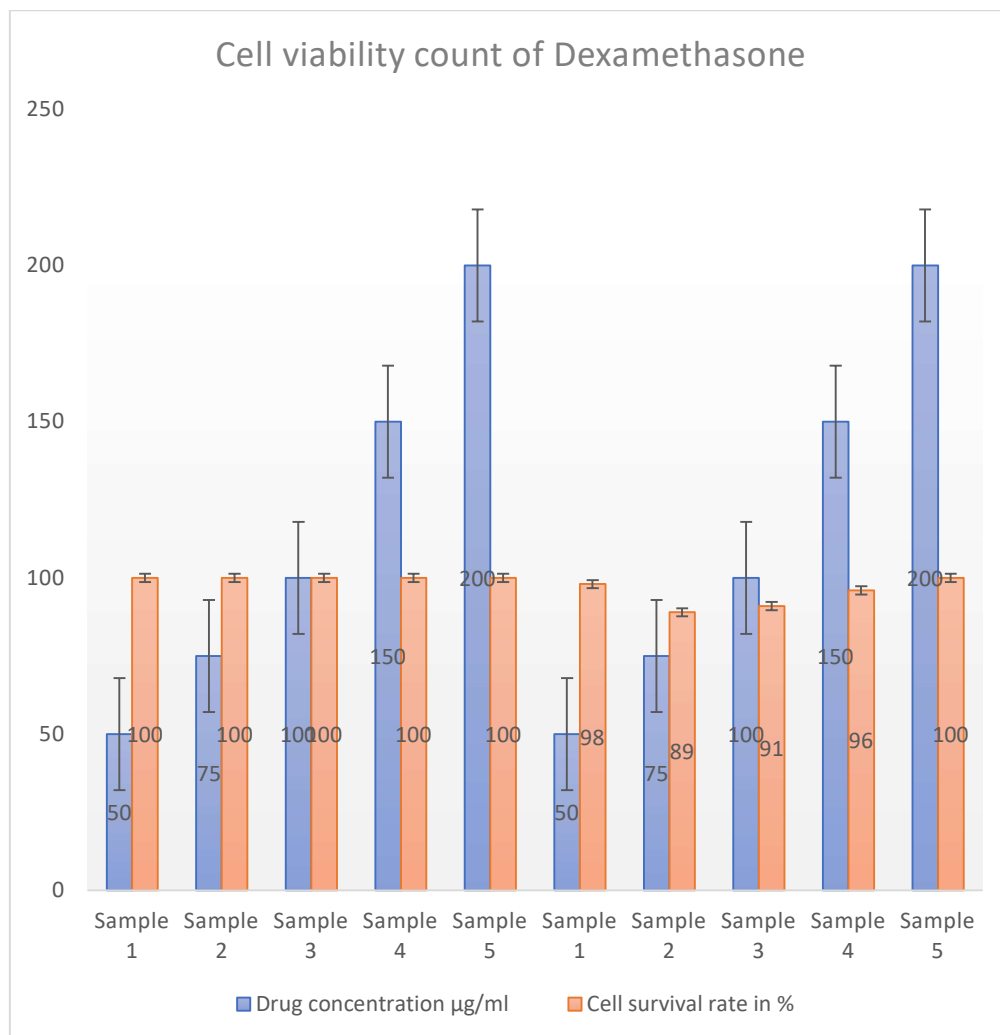


Figure 36 – VeroE6 cells survival rates in percentage in the presence of 5 Dexamethasone concentrations, starting from 20 mg/ml, 16 mg/ml, 12 mg/ml, 8 mg/ml, 4 mg/ml at viral load or MOI 2. n=3, and each drug had five concentration samples to see the correlation between IC and CC values at 450nm wavelength. The results are presented in Table 7, with n = 3.

To conclude, the survival rates are equal from samples 1-5. This experiment was repeated three times at a wavelength of 450 nm using a CCK-8 kit. The amount of the formazan dye generated by the activities of dehydrogenases in cells is directly proportional to the number of living cells. The blooming colour did not change with increased dexamethasone concentration, as this corticosteroid fosters cell growth. The viability could not be determined due to the growth of Vero cells during the increase in dexamethasone concentration, and subsequent light reflection was not possible, considering the cells to be mesoblastic inactive—Main Absorbance Wavelength: 450 nm.

3.5.3 MTT assay for cell viability in response to four drugs at varying concentrations against the SARS-CoV-2 Titters-Wuhan strain

Figure 33 also shows the MTT data, which illustrates the antiviral drugs in a DMEM medium at a relatively safe concentration. n = 5 using the colorimetric assay MTT tablet. Reference Wavelength (Optional): 600–650 nm. This can be used to correct for background absorbance due to media, plastic plates, or other factors.

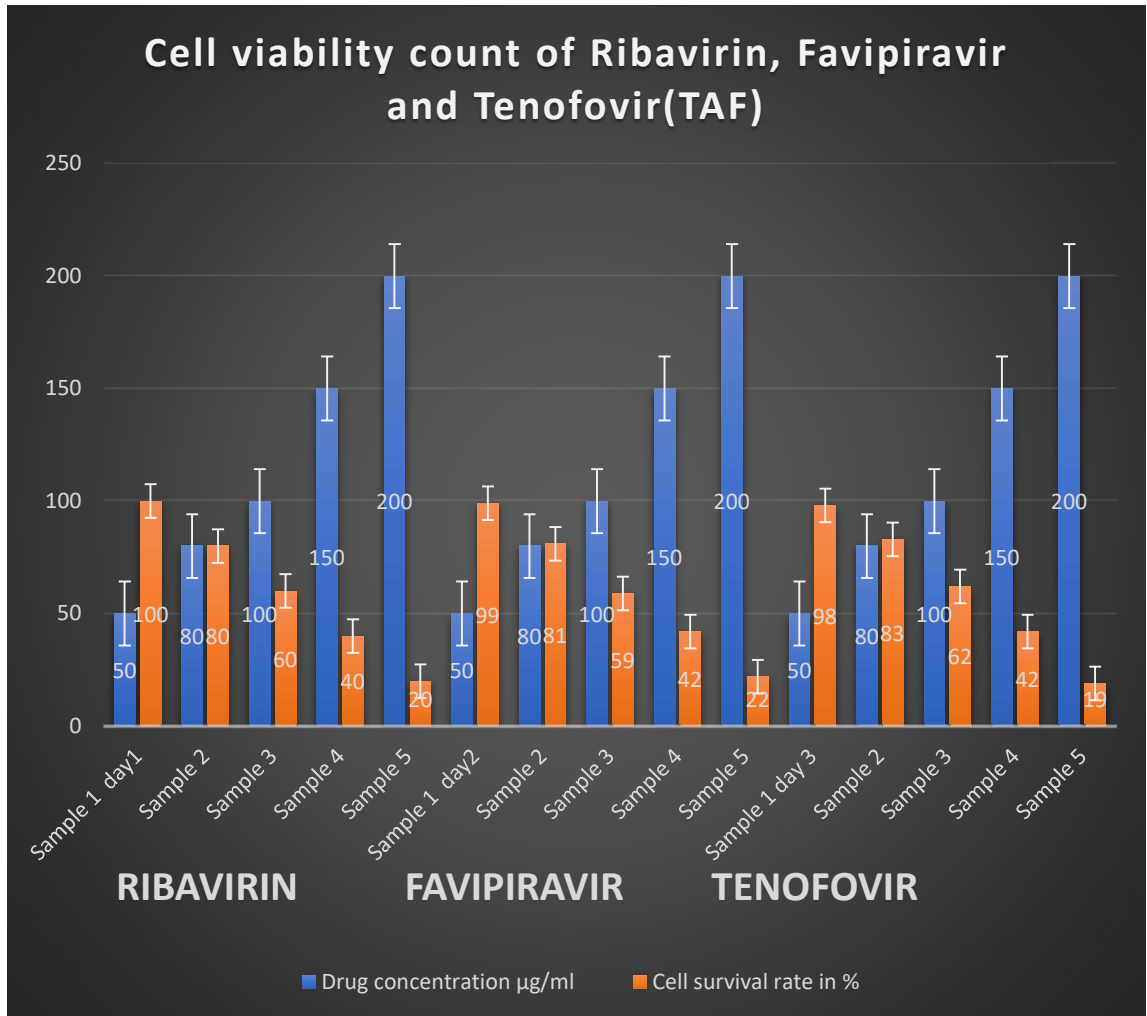


Figure 37 – VeroE6 cells survival rates in percentage in the presence of 5 drug concentrations of Ribavirin, Favipiravir, and Tenofovir (TAF) starting from The antiviral drug concentration is 50 µg/ml, and the viral titer is 200 µg/ml or MOI 2, with a 24-hour exposure.

These experiments were repeated three times, and each drug had five concentration samples to see the correlation between IC and CC values.

The results are shown in Table 6, and Vero cell viability is in Figure 37. The cell viability values were reliable on days 4 and 5, and the Margin of error was too high.

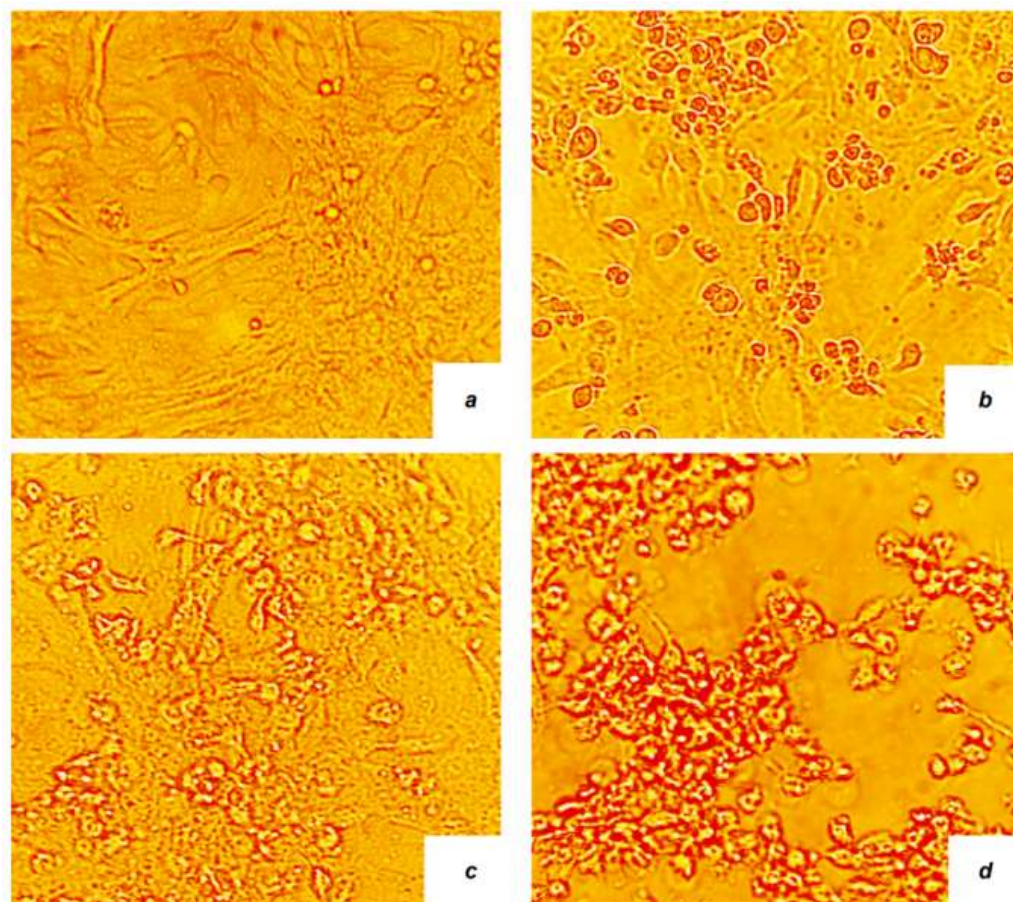


Figure 38 – The Vero cell passage antiviral screening on day 5 post-infection with the virus of different passage levels. a — uninfected cells/control; b — 1st passage; c — 2nd passage; d — 3rd passage at the drug concentration 50ug/ml and viral load of MOI 2.

The MTT kit was used to assess cell viability in a 5-day experiment conducted in the BSL4 lab. The longer the passages lasted, the fewer surviving cells could be detected. MTT absorbance measurements at 590 and 690 nm are commonly used in cell viability assays to assess metabolic activity.

590 nm (Main Absorbance Wavelength)

This is where the formazan product, produced by metabolically active cells reducing MTT, absorbs light. The absorbance at this wavelength is directly proportional to cell viability; higher absorbance indicates more viable cells.

690 nm (Reference Wavelength / Background Correction)

This range is used to correct for background noise from nonspecific absorbance. It accounts for debris, plate scratches, or other optical imperfections. Always include blank wells (media without cells) to adjust for baseline readings.

Before reading, calibrate the plate reader and ensure that MTT crystals fully dissolve in DMSO (or another suitable solubilizing agent). If 690 nm is unavailable, an alternative is to use a blank control well (with just media) for baseline correction.

The viability test was conducted in China using the MTT assay protocol and in Kazakhstan using the CCK-8 Kit protocol. The CCK8 ingredients are a water-soluble tetrazolium salt, WST-8, which is reduced by cell dehydrogenase activities to form a yellow-coloured formazan dye soluble in tissue culture media.

Table 6 - Virus accumulation (log) and plaque-forming units (PFU/mL) of Kazakhstan's strain and the Wuhan strain in China, along with viral load and positivity test results. The data differences are significant compared to the control ($p \leq 0.05$). The Wilcoxon test for related samples was used.

Drug sample	Passage 1	Passage 2	Passage 3	CoV2-test
Dexamethasone (5wells-1control)	7,20±0,04	7,18±0,04	7,23±0,04	+
Ribavirin 50ug/l (5wells-1control)	6,30±0,15	6,42±0,15	6,38±0,15	-
Favipiravir/T-705 50ug/l (5wells-1control)	6,99±0,05	6,93±0,05	6,97±0,05	+
Tenofovir (TDF) 50ug/l (5wells-1control)/TAF 50ug/l in China (Wuhan strain)	5,03±0,15/4.83±0,15	5,03±0,15/4.88±0,15	5,03±0,15/4.89±0,15	-/-

Vero E6 cells maintained >90% viability at tenofovir concentrations up to 50 μ M, as determined by MTT assays after 48-hour exposure. Higher concentrations showed increased cytotoxicity, though specific viability percentages above 50 μ M were not detailed in the provided studies [110]. The amount of the formazan dye generated by the activities of dehydrogenases in cells is directly proportional to the number of living cells. Since dexamethasone demonstrated almost no cytotoxic effect dynamics in Kazakhstan, there was no need to repeat the dexamethasone antiviral screening during my PhD internship in China. Figure 37 illustrates the advantages of the CCK8 kit over the MTT technique.

To conclude, the plaque-forming units (PFU/mL) quantify infectious viral particles in a sample, reflecting the concentration of replication-competent SARS-CoV-2 virions capable of forming plaques, or zones of cell death, in a cell monolayer. Unlike RNA-based methods (e.g., RT-qPCR) or electron microscopy (EM), PFU/mL directly measures viable viruses, making it crucial for studying infectivity, antiviral efficacy, and vaccine development. FU/mL remains the gold standard for quantifying infectious SARS-CoV-2 despite its labour-intensive nature. It is indispensable for research requiring functional viruses (e.g., neutralisation assays and pathogenesis studies). For clinical diagnostics, RT-qPCR dominates due to speed, but PFU/mL provides critical insights into viral infectivity and transmission dynamics.

3.6 Antiviral activity count after four drugs adding

The study of the antiviral activity of the drugs was conducted in a culture of Vero cells infected with the SARS-CoV-2 virus, variant B, based on the coefficient of inhibition of the cytopathic activity of the virus and its replication. After 24 hours of

incubation following cell infection at a dose of 10 TCID₅₀ (viral titer), when drugs were added at a concentration range of 50 µg/ml, the cytopathic effect of the virus was detected to varying degrees. As a result of a study on the antiviral activity of the drugs Dexamethasone, Ribavirin, Tenofovir, and Favipiravir, the inhibition rates were 0%, 80%, 99.31%, and 37.37%, respectively. Tenvir showed the highest degree of inhibition and is one of the most effective drugs for treating viral infections.

Table 7 – The CCK8 results of assessing the antiviral activity of drugs against the SARS-CoV-2 virus, variant (Alpha) B, in Vero cell culture to inhibit virus replication. The prodrug Tenvir-TAF (Tenofovir alafenamide), unlike Tenvir-TDF (tenofovir disoproxil fumarate), has a lower concentration in tablet form – only 25mg. However, both salts are necessary to promote the absorption of the active molecule, tenofovir, in the intestine. The drugs were added 1 hour prior to cell culture infection with the SARS-CoV-2 strain. The data differences are significant compared to the control ($p \leq 0.05$). The Wilcoxon test for related samples was used [115].

Drug	Concentration µg/ml	Virus accumulation lg, plaque- forming units (PFU/ml)	Suppression of reproduction virus, lg	Inhibition coefficient, Percentage %
Dexamethasone	4(392,464·mol ⁻¹)	7,20±0,04	0	0
Ribavirin	50244,206g·mol ⁻¹)	6,40±0,15	0,85. EC50=7µM	80,00. EC90/80(max)=205µM
Tenvir (TDF)	50(287.216 g·mol ⁻¹)	5,03±0,15	2,24.EC50=174µM	99,31.EC90/100(max)=over174µM
Tenvir (TAF)	50(287.216 g·mol ⁻¹)	4.83± 0,15	2,44.EC50=174µM	99,57.EC90/100(max)=over174µM
Fabiflu (T-705)	50(157.10 g·mol ⁻¹)	6,99±0,05	0,22.EC10=1,65µM	37,37.EC90/100(max)=must be 318 µM

After suction, the distribution of Tenofovir across the body is determined by the salt with which the drug is conjugated. In the case of TDF, most of the TFV is released from binding to the salt after suction, and the drug is widely distributed in various tissues. In contrast, in the case of TAF, it is the other way around since TFV remains mainly associated with its alaphenamide salt. Its distribution is limited to cells with high carboxylesterase and cathepsin A activity, such as hepatocytes and lymphocytes [90,93-99]. The detailed inhibition assays are shown in Figures 36-39, where the CE or IC% aligns with the CC%.

Ribavirin-inhibition assay

This indicates that IC₉₀ was achieved through pretreatment with Vero cells. Some cells started showing low survival rates for at least two reasons: Firstly, the viral load can cause a cytopathic effect. Secondly, even drug concentrations at the EC₅₀ can reduce the general host-cell fitness, especially for drugs administered orally [114].

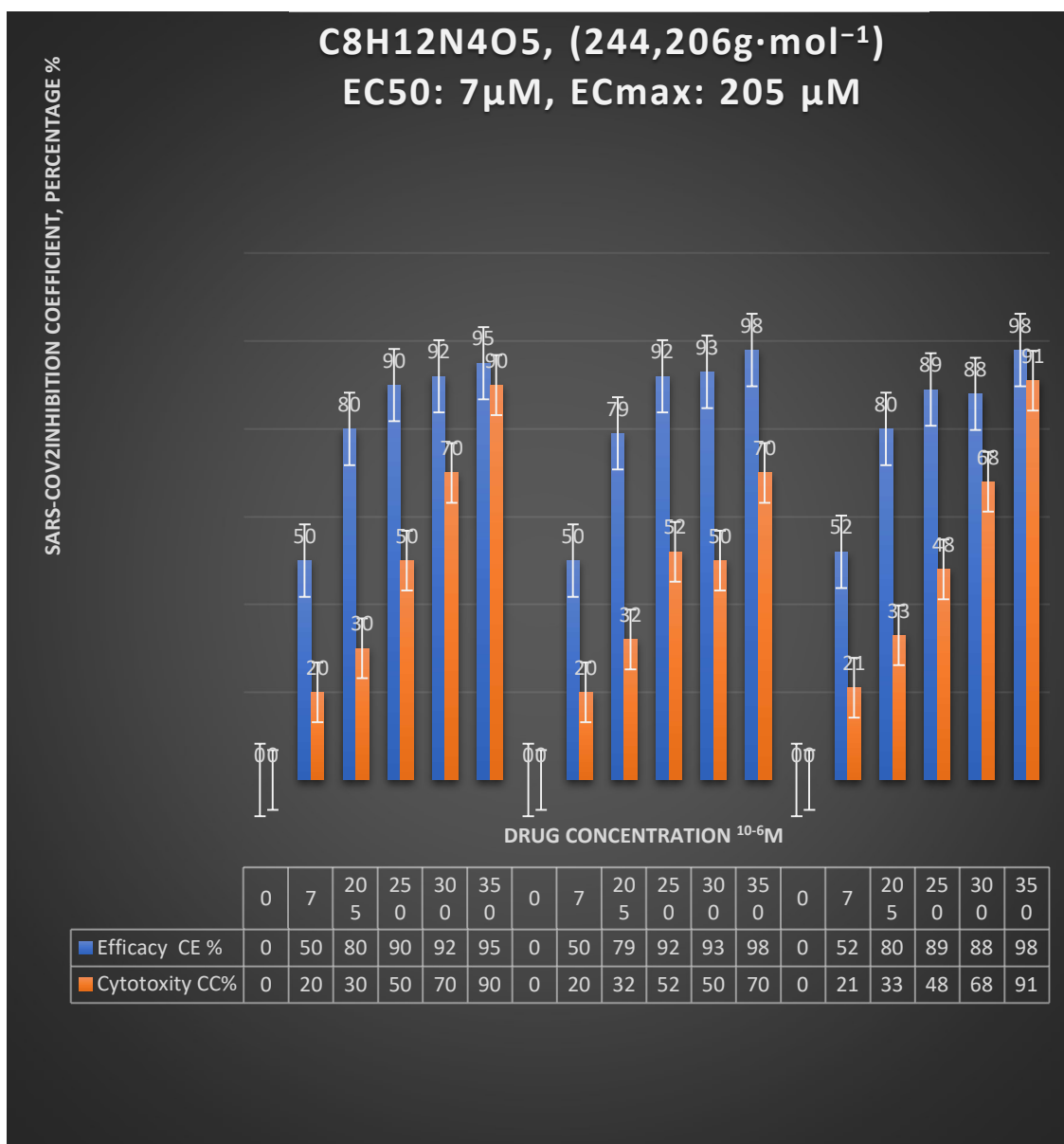


Figure 39 - The intact VeroE6 cells, seeded in 96-well plates, were inoculated with SARS-CoV-2 at a titer during a 24-hour infection phase, and then 205 μM ribavirin was added. The 205 μM concentration and below of Ribavirin is considered a cytotoxic safe concentration; therefore, the tested inhibitor concentration did not affect cell viability (CC-levels) and viral stock dilution MOI 2, n = 3.

Even a 350 μM concentration of Ribavirin led to 95% efficacy with less than 20% cell viability or 70% of the control cell (CC) value. Ribavirin is hepatotoxic and has the potential for mitochondrial cytotoxicity (see Figure 37). We were unable to detect the CC₅₀; however, we did measure the Cmax at 50 μg/ml. The EC max is about

90% inhibition and above, but cell viability decreases with higher drug concentration. Additionally, the high viral load contributed to the CC% in CPE (cytopathic effect).

Tenofovir - inhibition assay

This indicates that IC₉₉ was achieved through pretreatment with Vero cells. Some cells started showing low survival rates for at least two reasons: Firstly, the viral load can cause a cytopathic effect. Secondly, even drug concentrations at the EC₅₀ can reduce the general host-cell fitness, especially for drugs administered orally.

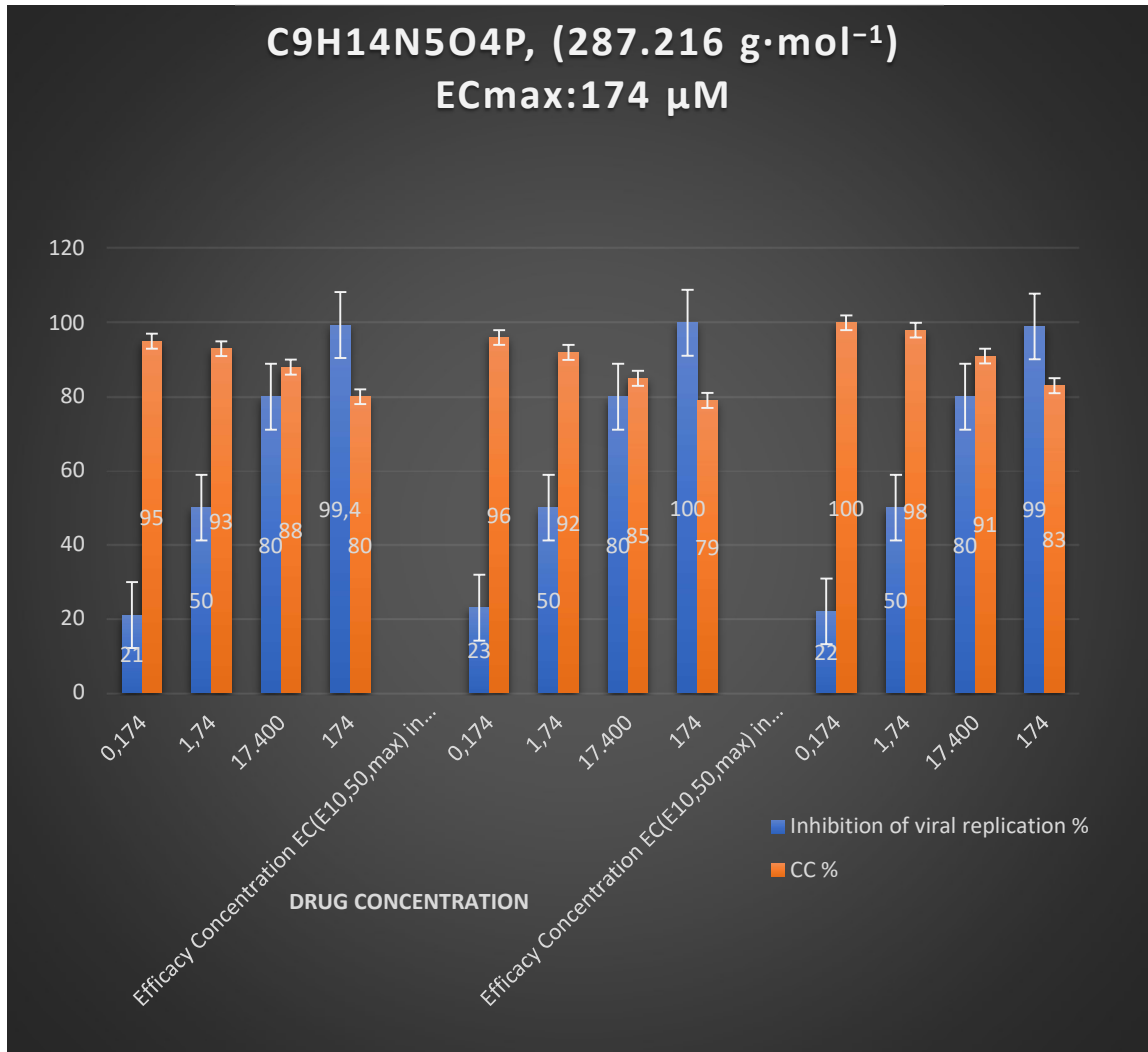


Figure 40 - The intact VeroE6 cells seeded in 96-well plates were inoculated with SARS-CoV-2 at a titer during a 24-hour infection phase, and then IC₁₀ (0.174 μM), IC₅₀ (1.74 μM), and IC₁₀₀ (17.4 μM) Tenvir (Tenofovir) were added. The viral load was cytotoxicity high – MOI 2 - and cell viability had decreased before the initiation of antiviral treatment. n=3 [115].

Tenofovir at 174 μM and below is considered a cytotoxicity safe concentration; therefore, the tested inhibitor concentration did not affect cell viability (CC levels). The presence of an IC₁₀ concentration in which cells survived indicates that Tenvir is not

a cytotoxic drug. It is also assumed that if we had 25µg/ml of TDF or TAF, the viral inhibition would have been the same as with a 50µg/ml prodrug concentration.

Favipiravir (T-705) - inhibition assay

This indicates that IC₃₇ was achieved through pretreatment with Vero cells. Some cells started showing low survival rates for at least two reasons: Firstly, the viral load can cause a cytopathic effect. Secondly, even drug concentrations at the EC10 level, in our case, can reduce the general host-cell fitness, especially for drugs with oral administration mechanisms.

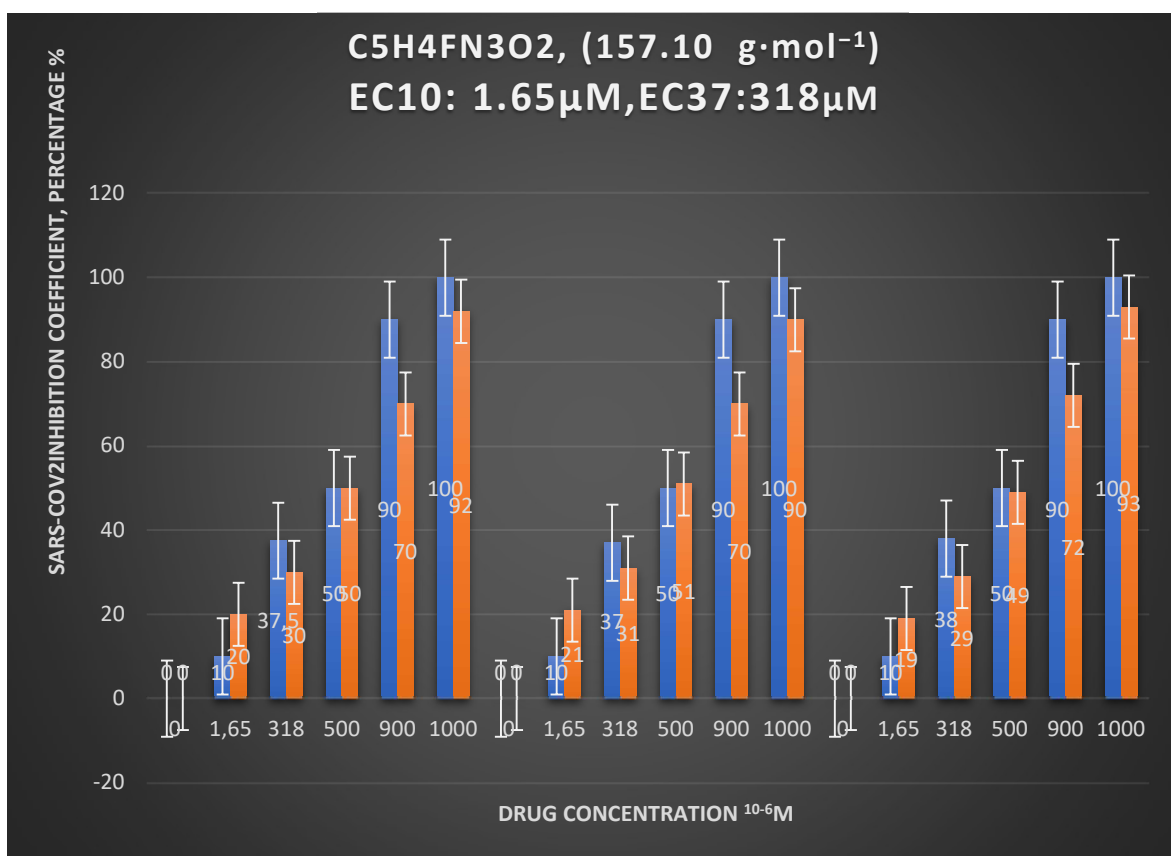


Figure 41 - The intact VeroE6 cells, seeded in 96-well plates, were inoculated with SARS-CoV-2 at a titer during a 24-hour infection phase, and then 318 µM Favipiravir was added. The viral load was cytotoxic in terms of CPE at an MOI of 2, as determined by three replicate experiments (n = 3).

Tenofovir is nephrotoxic in overdose and has kidney cytotoxicity potential. Cell viability decreased before the start of antiviral treatment at a concentration of 318 µM, which is below the cytotoxic safe concentration of Favipiravir; therefore, the tested inhibitor concentration did not affect cell viability (CC-levels) or viral stock dilution (10⁻⁷). A relatively high drug concentration reaches the EC_{37.37} at 318 µM. However, EC₁₀ is relatively low, at approximately 1.65 µM. EC max is predicted to be about 90% inhibition and above. Still, cell viability decreases dramatically as the cells die

with an EC50 at higher drug concentrations, up to 1000 μM . According to the data obtained, Favipiravir is not a practical purine analogue against the SARS-CoV-2 virus at a viral load of MOI 2. Figure 40 illustrates the toe-to-toe dynamics between CE% and CC% dynamics, where 90% of cells died with nearly 100% viral inhibition [115].

Dexamethasone- inhibition assay

Before beginning antiviral treatment, cell viability decreased at a concentration of 10 μM and below, which is a safe concentration for dexamethasone; therefore, the tested inhibitor concentration did not affect cell viability. The EC max is almost 0% inhibition; cell viability decreases with higher drug concentration with no antiviral effect. However, the cell prefoliation of Vero E6 cells was also stopped, as in the drug cytotoxicity assay [113].

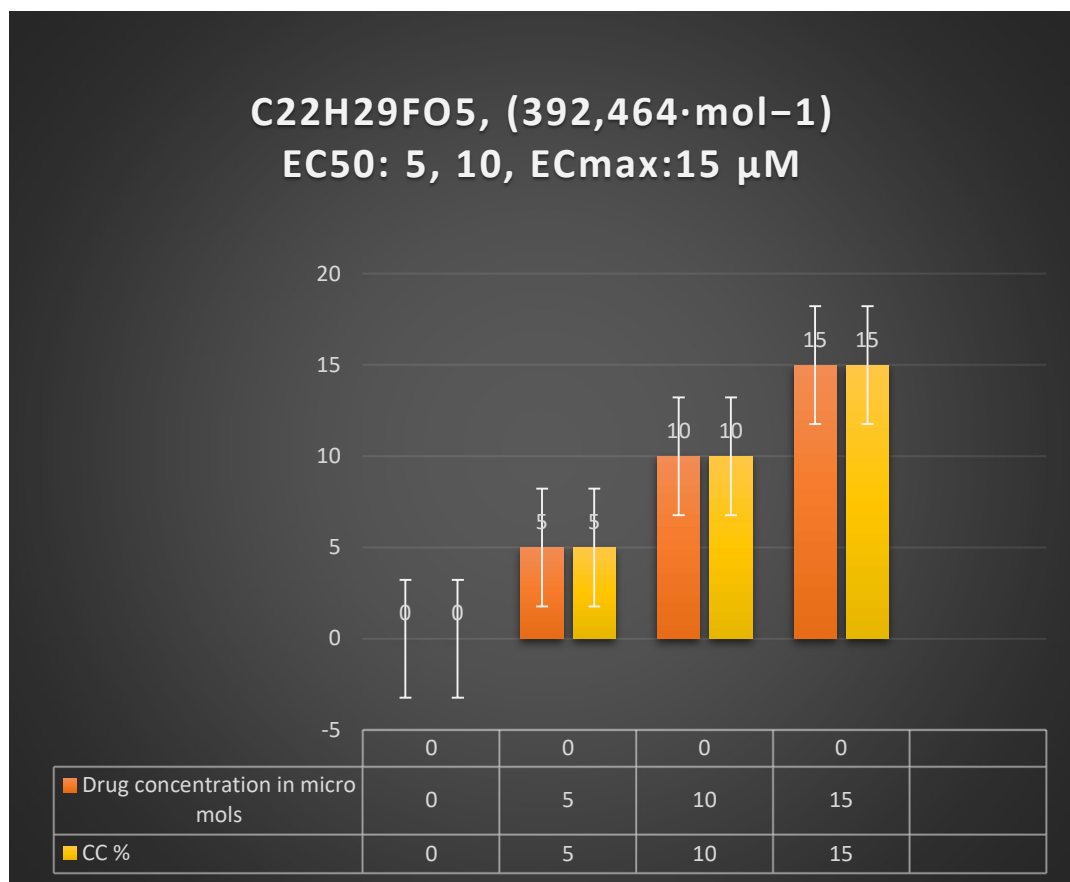


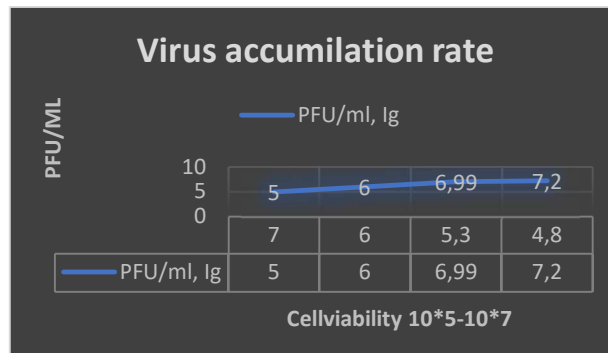
Figure 42 - The intact VeroE6 cells, seeded in 96-well plates, were inoculated with SARS-CoV-2 at a specific titter during a 24-hour infection phase, and then 10 μM Dexamethasone was added. The viral load was cytotoxicity high – MOI 2.

After 24 hours, the Vero cells had fused and exhibited an apparent cytopathic effect due to the progression of viral infection, as shown in Figure 40. Vero cells represent a robust testing model for viral inhibition assays due to their relatively high cell proliferation rates. Dexamethasone increases their growth potential and cell

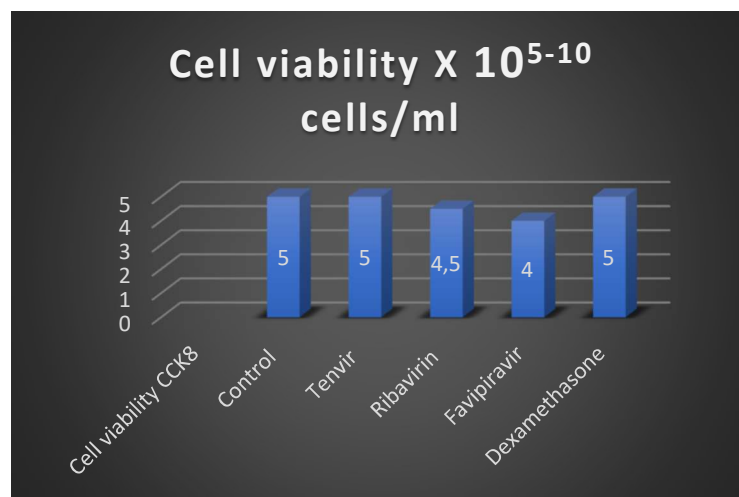
density. We seeded cells at a known density (e.g., 2×10^4 cells/cm²). To maintain log-phase growth, we must keep them at 5% CO₂ at 37 °C during all drug assay periods.

Viral PFU count comparison – the visual/direct antiviral effect of four drugs

The viruses were pre-incubated with each drug and then washed to remove the unbound drug before being infected into cell monolayers. This isolates the drug's effect on viral particles rather than host cells. Untreated virus (control) and cytotoxicity controls (drug + cells without virus) are included to ensure PFU reduction is not due to cell death.



A



B

Figure 43 – A. The virus accumulation dynamics in four replication orders on intact VeroE6 cells seeded in 96-well plates after inoculation with SARS-CoV-2 at a titer during a 24-hour infection phase, with treatments of 174 μ M Tenofovir (Tenvir), 205 μ M Ribavirin, 318 μ M Favipiravir, and 10 μ M Dexamethasone. The viral load was cytotoxicity high – MOI 02. B. Cell viability is directly proportional to viral inhibition; the highest cell viability was observed with Tenvir in CCK8 and MTT cell viability assays. n=3. Dexamethasone antiviral efficacy: 7.20 ± 0.04 ; Ribavirin antiviral efficacy: 6.40 ± 0.15 ; Tenofovir (TDF) antiviral efficacy: 5.03 ± 0.15 - reduction for two lg; Tenofovir (TAF) antiviral efficacy: 4.83 ± 0.15 reduction for two lg (once in China on the CCK8 Platform); Favipiravir antiviral efficacy: 6.99 ± 0.05 .

Cell viability decreased before the initiation of antiviral cell treatment due to cytopathic effect (CPE). Tenvir reduced virus accumulation by two lg. The antigenic test was sensitive at a concentration of 1×10^5 TCID₅₀/ml of viral particles.

Potency and efficacy of four studied drugs

In sharp contrast to Tenofovir and even ribavirin, favipiravir exhibits all three effective concentrations, namely EC_{10} , EC_{50} , and $EC_{max/90}$. Thus, we can say that favipiravir was expected to be the most potent drug, showing the least antiviral effect in the dissertation study, as indicated by the lowest PFU/ml and inhibition coefficient [91-98]. However, Favipiravir showed the worst drug- potency as well as efficacy. The full range of IC_{10-100} inhibition showed only pure TAF (Tenofovir) and TDF in tableted form, with IC_{100} . Ribavirin, however, showed an effective IC_{50} of only seven μM [114].

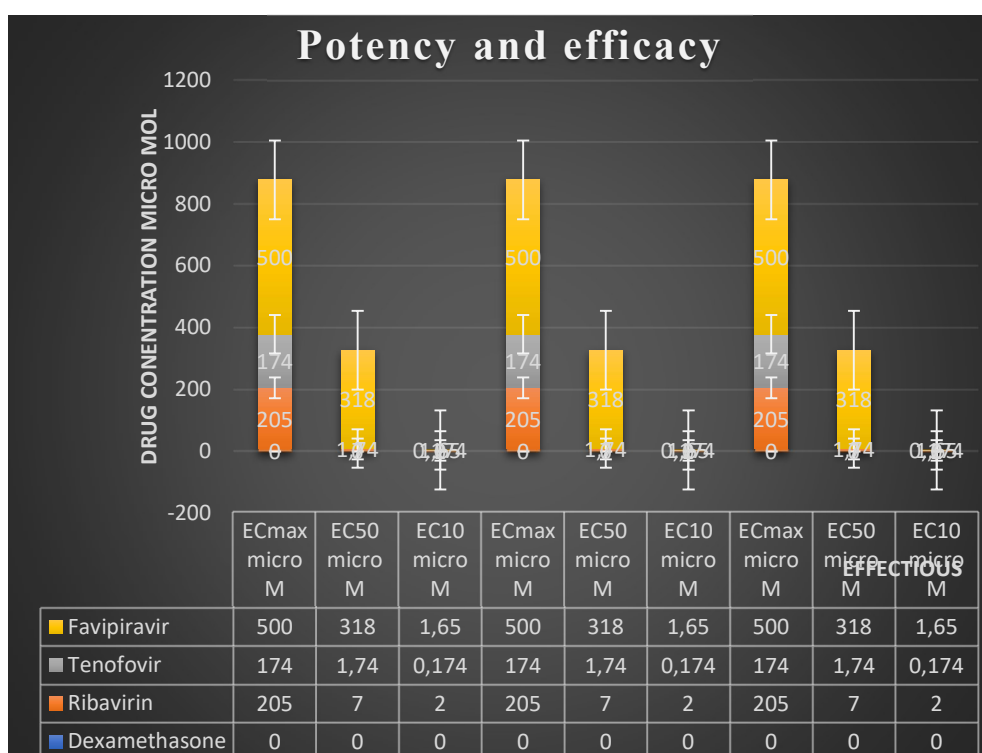


Figure 44 — Tenofovir is more effective in inhibition than Ribavirin and Favipiravir because it starts to work only at relatively high concentrations, whereas Ribavirin has an EC_{50} of 7 μM [114]. $n=3$. Key features: C_{10} =Favipiravir→1.65 μM , Ribavirin→2 μM and Tenvir→ 0.174 μM .

In conclusion, Favipiravir would have reached IC_{10} at 1,65 μM , but we detected only 37% viral inhibition at a relatively high prodrug concentration of Fabiflu, namely 318 μM . The IC_{100} of Favipiravir would be far beyond the acceptable cytotoxicity rates. The general conducted an antiviral drug assay, which showed effectiveness in terms of cell viability, supporting the inhibition of viral accumulation. Of course, not all cells survived; however, the cell prefiltration rate effectively substituted for the function of killer cells, and $EC_{max/90}$ maintained antiviral tendencies in the cell medium, as observed in both CCK8 and MTT solvents. In the case of CCK8, the components were water-soluble, whereas MTT required a small amount of organic solvent – phenol - to stabilise cell absorption.

3.7 The preclinical test of cytotoxic safe TAF and its antiviral properties in vivo on regular lab WT-Mice

Virus viability is confirmed via TCID₅₀ – count. The pH and temperature (improper solidification inhibits plaque formation) were checked, as were the count and overlay pH and temperature.

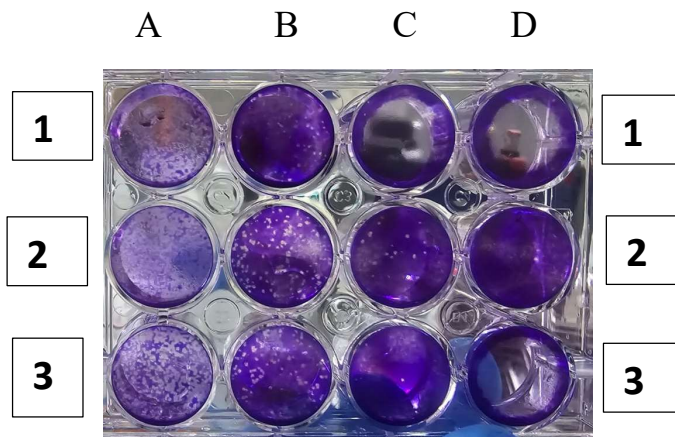


Figure 45 - Plaque assay on Vero E6 cells. Assessment of drugs' antiviral activity in murine upper airways (as a viral reservoir) against the SARS-CoV-2 Wuhan strain: A₁-MOI of 4, untreated control; A₂-MOI of 2+TAF 50 µg; A₃-MOI of 1+TAF 50 µg, 72-hour exposure. B₁-MOI of 1 untreated-control; B₂-MOI of 2+TAF 50µg; B₃-MOI of 3+TAF 50µg, 48hours exposure. C₁- MOI of 4 untreated-control; C₂- MOI of 4 MOI of 3+TAF 50µg; C₃- MOI of 2+TAF 50µg, 24hours exposure. D₁-MOI of 4 untreated controls; D₂-MOI of 2+TAF 50 µg; D₃-MOI of 2 untreated controls, with 12 hours of exposure in an incubator at 37 °C and 5% CO₂.

Tenofovir (TAF) had a significant effect on viral replication within the cells of the upper airways, and the viral titer was assessed using VeroE6 cells. Since Vero cells are permissive and susceptible to the SARS-CoV-2 virus, the plaque assay (Figure 46A) shows viral inhibition from 12 to 72 hours. TAF's prodrug design minimises off-target effects, enabling the evaluation of its safety in organs such as the kidneys and bones, which were historically affected by older analogs (e.g., TDF). Therapeutic index: Determines the dose range at which TAF is effective without causing harm, which is critical for human dosing strategies. The treatment involves infecting cells with the virus, overlaying them with a semi-solid medium, incubating them, staining, and counting the resulting plaques. The reduction in plaque number with TAF treatment indicates antiviral activity. In conclusion, Longer TAF exposure (e.g., 72h) correlated with more significant plaque reduction and lower viral load (Figure 45). Short exposures (12 hours) may show partial inhibition if TAF targets early replication steps, such as viral entry. The experiment provided a systematic evaluation of TAF's time-dependent antiviral efficacy, linking plaque reduction to viral load kinetics.

Antiviral Activity: Demonstrates TAF's ability to suppress viral replication in vivo, even in models using surrogate viruses (e.g., mouse-adapted HBV/HIV) or

humanised systems. WT mice may require adaptation (e.g., surrogate viruses, transgenic modifications) to study human-specific pathogens, such as HIV. Such mice are referred to as transgenic mice, allowing researchers to assess the efficacy of antiviral drugs before conducting further clinical trials.

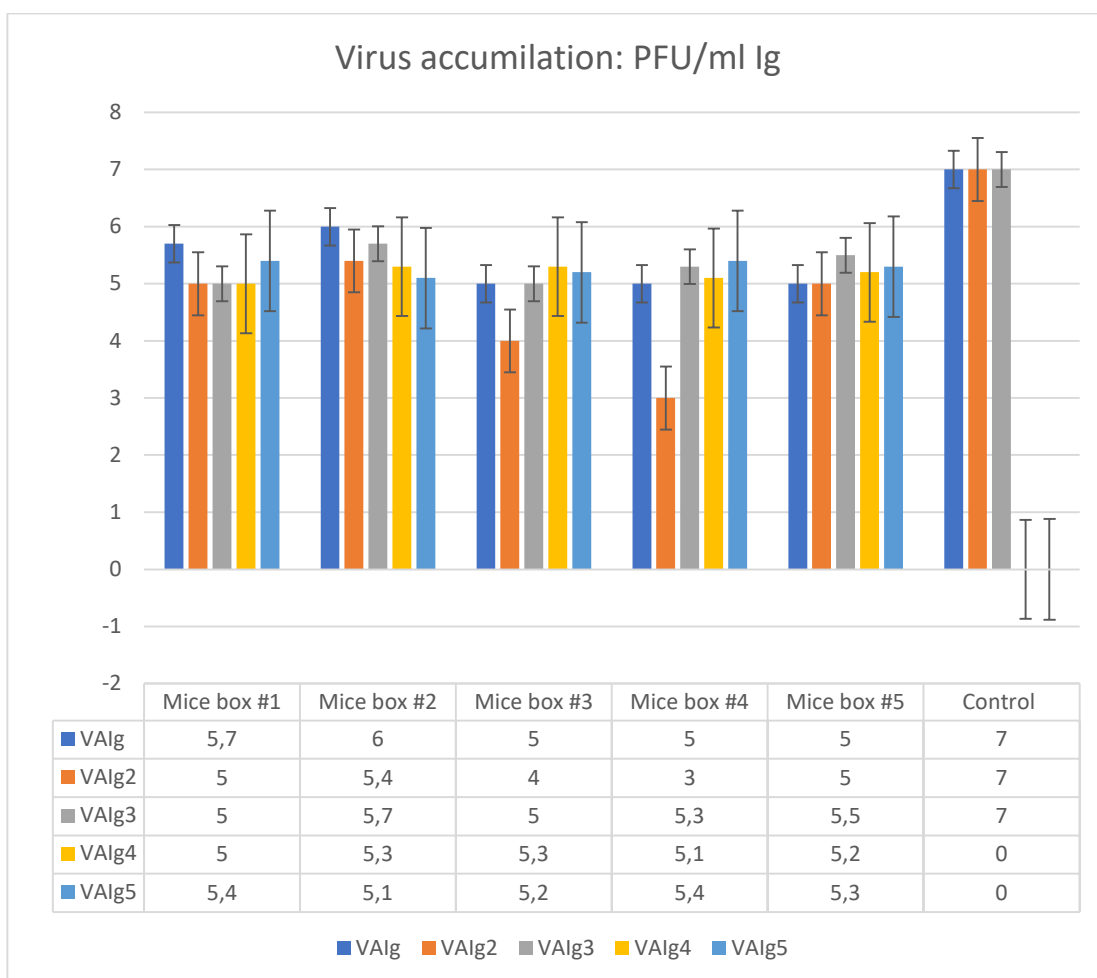


Figure 46 - Vero E6 cell culture virus accumulation suppression (24-72 hours of drug and virus exposure). The prodrug Tenvir-TAF (Tenofovir alafenamide) differs from Tenvir-TDF (tenofovir disoproxil fumarate). The plaque assay n=3. TAF has a lower concentration in tablet form – only 25mg, as per the data – with significant differences compared to the control ($p \leq 0.05$). The Wilcoxon test for related samples was used.

To conclude, despite species differences, safety and efficacy trends in mice often correlate with human outcomes, thereby de-risking clinical trials. Dose Optimization: Guides initial human dosing by identifying effective yet non-toxic levels in mice. Therefore, preclinical testing of TAF in wild-type (WT) mice provides a robust foundation for clinical development, striking a balance between safety, efficacy, and practicality while offering critical insights into its potential as a safer antiviral therapeutic. Even 50 $\mu\text{g/ml}$ of TAF demonstrated an antiviral effect on murine upper airway tissue.

3.8 Antivirals recommendation against SARS-COV 2 according to provided results on RdRP-inhibition activity in vitro

Some related in vivo tests on mice were conducted during the Chinese Exchange mobility program internship. Comparable conclusions were drawn regarding antiviral recommendations against SARS-CoV-2 based on the provided results of RdRP-inhibition activity in vitro. Since the inactive phase of COVID-19 typically lasts an average of 14 days, it is crucial to control the viral load, which significantly reduces the virus's ability to replicate. In addition, we have to take into consideration the side-effect potential of the antivirals, especially those that were initially designed for viral, either long-term or lethal infections like HIV, Ebola, and Hepatitis B and C. As this study demonstrated, Fabiflu (Favipiravir) has the lowest cellular toxicity impact and the shortest period of oral administration; however, it showed the weakest potential in inhibiting RdRP activity in vitro. Fabiflu or Favipiravir is the most specified drug against COVID-19 progression. Fabiflu is a medication for mildly to moderately infected adult individuals, helping patients recover. The starting dosage is 400mg daily, which can be increased to 1800mg twice on the first day of COVID-19 diagnosis, but not exceeding the recommended dosage (Appendix F). This medicine's most common side effects include increased blood uric acid levels, diarrhea, a decrease in the white blood cell count (specifically neutrophils), and elevated liver enzymes. To achieve a therapeutic effect, according to the manufacturer's instructions, Fabiflu is administered orally (by mouth), with a recommended dose of 1,800 mg twice on day 1, followed by 800 mg twice daily for up to 14 days. It means that the highest dose is needed to achieve the maximum effect of stopping the SARS-CoV-2 virus from multiplying. Doing so decreases viral load in the body. The producer claims a 100% positive clinical outcome if treatment is diagnosed on time under the supervision of a qualified medical professional. The most significant advantage of Fabiflu (Favipiravir) is its low side-effect potential, which allows for dosage allocation tailored to the individual needs of each patient and the progression of COVID-19. The maximum administration period is 14 days. However, we must still remember that to study the antiviral activity of a new drug, it is essential to determine whether rational activity can be uncoupled from the confounding effect of cellular toxicity. Cytotoxicity tests define the upper-limit drug concentration, which can be used in subsequent antiviral studies [90,93-94].

Tenvir (Figure 48), however, according to the manufacturers' prescription, must be used only once a day with 300mg Tenofovir. The maximum usage period is only 28 days; neither dosage nor period is included in any extensions. Nevertheless, Tenvir is the most effective antiviral drug in this study, with an optimal cytotoxicity concentration. Thus, even with a limited range of concentration and time scale, Tenvir is highly effective against SARS-COV 2 and can prevent COVID-19 from progressing to pneumonia or other health or life-threatening conditions. Tenvir could be considered a long-term treatment medicine because initially, it was designed to fight the chronic hepatitis B disease and primary HIV infection. The possible side effects of the fight against SARS-CoV-2 viral infection appear to be minimal, and on average, about seven days should be sufficient to bring COVID-19 under control with Tenvir as the primary

medication, under strict medical supervision. According to the instruction leaflet, Ribavirin (Figure 47) has the most potential for side effects. Still, it is capable of crippling the viral RNA as well as DNA-metabolism and is primarily prescribed against Hepatitis C viral infection with a combination with Interferon α . Ribavirin is the most aggressive purine-analogue medicine because, from a long-term perspective, it may cause Hemolytic anemia, an abnormal breakdown of red blood cells (RBCs), either in the blood vessels (intravascular hemolysis) or elsewhere in the human body (extravascular hemolysis). Ribavirin showed the lowest antiviral activity among the others in this study due to its optimal cytotoxic concentration, which could not induce RNA metabolic collapse. The instruction leaflet (Russian manufacturer) suggests administering Ribavirin 200mg every 8 hours initially and 400mg every 8 hours by the end of the week. This method is recommended to achieve the maximum concentration (Cmax) in blood plasma, which suppresses viral replication. In Figure 50, we can see that the maximum antiviral effectiveness of Favipiravir is achieved at 100 μ g, which is far above the cell survival threshold in vitro.

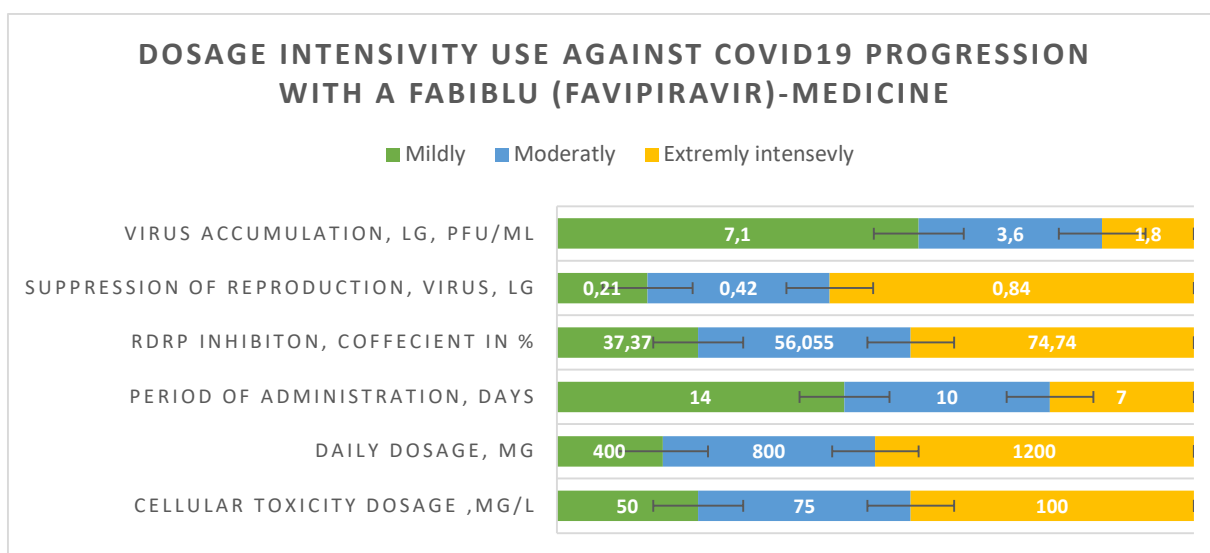


Figure 47 - The antiviral data of Favipiravir in the in vitro study and the clinical prescription to achieve viral multiplication activity in vivo—Fabiflu medicine dosage recommendation based on these in vitro studies and the manufacturer’s manual [Appendix F].

The green colour indicates the safest and lowest side-effect potential during oral administration. The blue colour indicates a moderate antiviral effect. Here, we can see not only the shorter period of drug usage but also relatively high antiviral effects, such as the RdRP inhibition coefficient and substantial viral reproduction suppression in decimal logarithm (lg) units, as well as Virus accumulation in lg PFU/ml. The yellow color shows the maximum antiviral effect manifested manually, as it could be seen as both the shortest and the most effective intensity with compromised Fabiflu side-effect potential. In our study, viral load accumulation began at a decimal logarithm (log) of 7. It was reduced by a decimal logarithm (log) of 5 with TDF and TAF isomers, which was relatively high, with at least 2 viral particles per cell (Figure 49).

DOSAGE INTENSIVITY USE AGAINST COVID19 PROGRESSION WITH A TENVIR (TENOFAVIR)-MEDICINE

PERIOD OF ADMINISTRATION, DAYS	28
CELLULAR TOXICITY DOSAGE, MG/ML	50
DAILY DOSAGE, MG	300
RDRP INHIBITION, COEFFICIENT, PERCENTAGE %	99,31
SUPPRESSION OF REPRODUCTION VIRUS, LG	2,17
VIRUS ACCUMULATION, LG, PFU/ML	5,03

Figure 48 - Tenvir’s (TDF) antiviral data from the in vitro study and the clinical prescription for achieving viral multiplying activity in vivo [Appendix F].

Tenvir demonstrated the highest antiviral potential; therefore, the manufacturer’s in vitro recommendations effectively mitigate usage risks both in vitro and in vivo, as shown in Figure 48.

DOSAGE INTENSIVITY USE AGAINST COVID19 PROGRESSION WITH A RIBAVERIN MEDICINE

PERIOD OF ADMINISTRATION, EVERY H	8
CELLULAR TOXICITY DOSAGE, MG/ML	50
DAILY DOSAGE, MG	600
RDRP INHIBITION, COEFFICIENT, PERCENTAGE %	80
SUPPRESSION OF REPRODUCTION VIRUS, LG	0,8
VIRUS ACCUMULATION, LG, PFU/ML	6,4

Figure 49 - Ribavirin’s antiviral data from an in vitro study and the clinical prescription for achieving viral multiplying activity in vivo [Appendix F].

Ribavirin remained quite effective, even in the presence of relatively high viral loads; however, its toxicity prevented us from achieving an IC50, as its CC was very sensitive. Its long history of use as a wide-spectrum antiviral agent demonstrates its

robust effectiveness, with significant cellular toxicity observed both in vitro and in vivo (Figure 49).

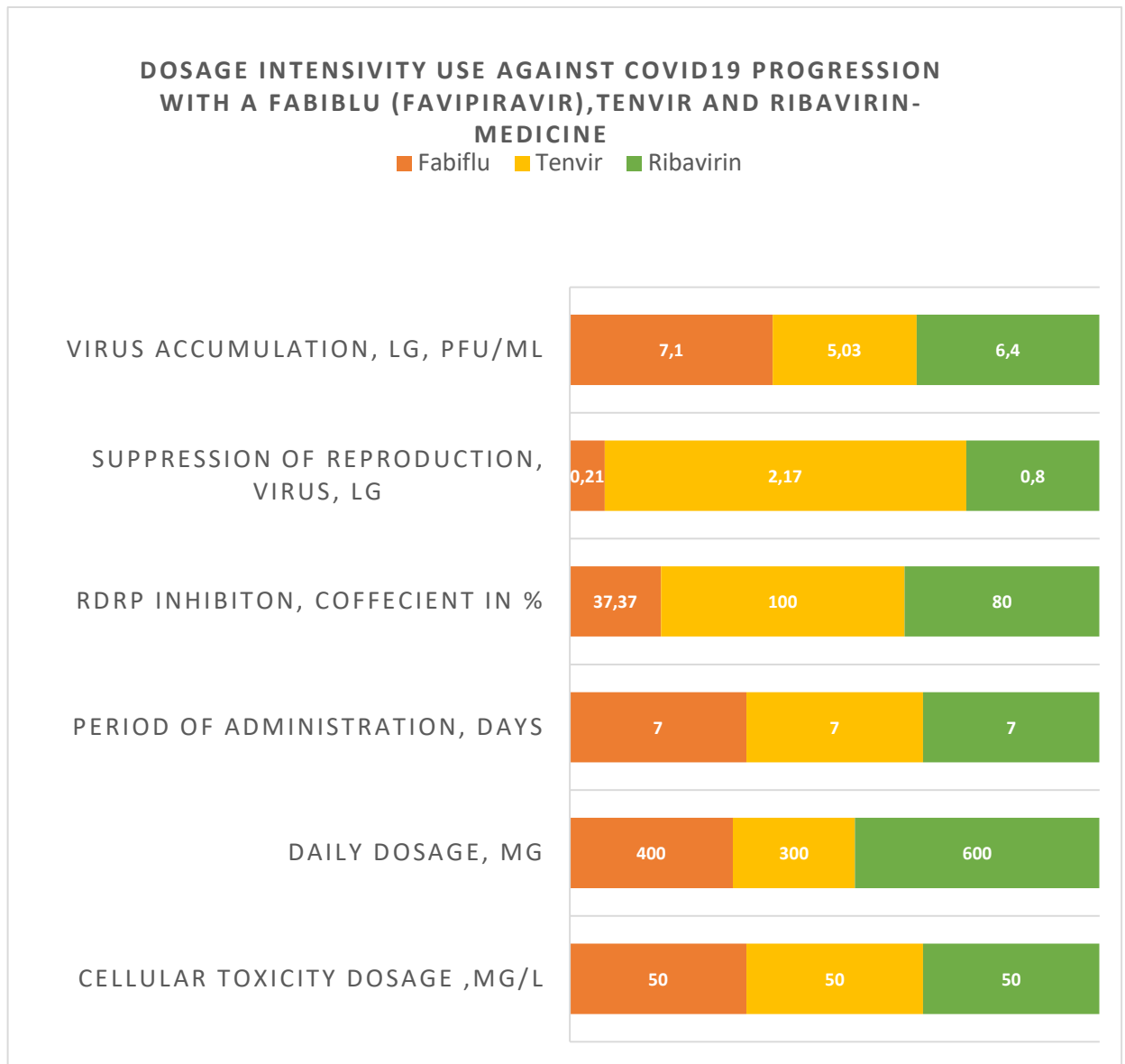


Figure 50 - Fabiflu drug dosage recommendations for all three antiviral drugs based on this in vitro study; the first leading indicator of our research is the safest drug concentration and the lowest possible side-effect potential during in vitro drug testing. In Figure 50, we can see the transparent effectiveness gradient with the drug concentrations in one tablet, where Fabiflu serves as a negative control for the antiviral inhibition assay, with only IC₃₇ at 50 µg. In contrast, Tenvir yields a positive result, achieving an IC₁₀₀ at the same drug concentration [Appendix F].

According to the Fabiflu inhibition assay information, the IC was 37. If 36.79% of cells do not become infected, what percentage will become infected? Based on probability calculations (not related to biology), at an MOI of 1, only about 63% of

cells are expected to become infected: $100\% - 36.79\% = 63\%$. However, we had MOI 2, which suggests that Favipiravir remains compelling enough to treat only mild SARS-CoV-2 infections.

Some chapter conclusions and some discussions were made towards antiviral efficacy study within dissertational work and research activity:

1. Favipiravir or T-705 did not meet any expectations as an effective anti-SARS-CoV2 drug, as it had shown many times before against Influenza A Favipiravir, an antiviral drug initially developed for the treatment of influenza, has been studied for its efficacy against SARS-CoV-2. Key inhibitory concentrations (IC) and related parameters from preclinical and clinical studies: EC_{50} (Half-Maximal Effective Concentration): In vitro studies report an EC_{50} of $61.88 \mu\text{M}$ against SARS-CoV-2, indicating moderate potency. This aligns with earlier findings for the Ebola virus ($EC_{50} \approx 67 \mu\text{M}$), suggesting that high doses are necessary for therapeutic effects. Safety margin: The cytotoxic concentration (CC_{50}) exceeds $400 \mu\text{M}$, yielding a selectivity index (SI) of >6.46 , reflecting a favourable safety profile at effective doses [111]. A study of 298 patients (149 per group) found that favipiravir reduced progression to severe disease, with an improvement of 83.2% compared to 69.1% on day 5 ($p < 0.001$) [112]. IC_{10} and IC_{100} : Specific IC_{10} or IC_{100} values are not explicitly reported in the studies. Efficacy in vivo depends on early administration and achieving plasma concentrations comparable to EC_{50} levels [113]. The IC_{50} was not achieved, as the IC_{10} ($1.65 \mu\text{M}$) was out of range for cell viability.
2. Tenofovir demonstrated maximum efficacy at optimal $CC\%$ levels in both isoforms, TDF and TAF. However, we could not detect its EC_{50} levels of TDF (approximately two μM), which confirms that this drug is nephrotoxic and that even the smallest amount is absorbed immediately without an antiviral effect; TAF results: $IC_{10} = 0.174 \mu\text{M}$, $IC_{50} = 1.74 \mu\text{M}$, and $IC_{100} = 174 \mu\text{M}$, respectively;
3. Dexamethasone exhibited optimal $CC\%$ levels at all IC_{10} , IC_{50} , and IC_{100} in vitro; however, it showed no antiviral activity or suppression of virus accumulation—0;
4. Ribavirin showed the most compromised results, with all IC_{10} , IC_{50} , and IC_{100} ranges correlating to relatively optimal $CC\%$ levels [114]. Even with lab stock in China, the true antiviral potency was not achieved: $IC_{10} = 2 \mu\text{M}$, $IC_{50} = 7 \mu\text{M}$. However, even at $205 \mu\text{M}$, inhibition of SARS-CoV-2 replication was only 90%. $IC_{90} = 205 \mu\text{M}$. The viral inhibition must be 100%;
5. The author could have achieved better results if the drugs had been combined, but this is a study from another research, and the cells presumably would not have survived under a dual drug toxicity load;
6. All drug inhibition assay results have been maintained for 24 hours only, as this passage is informative enough, and BSL3/4 lab time is limited;

7. The CCK8-kit viability test also lasted 24 hours due to informative enough data;
8. The MTT assay, however, lasted 5 days in China because the traditional pharmaceutical protocols suggest running 5 days of passages to provide detailed cell viability results;
9. In China, since pure and stock small concentrations of TAF were available, the IC₁₀, IC₅₀, and IC₁₀₀ values were determined, confirming that Tenofovir is a safe and potent anti-SARS-CoV-2 drug. The selectivity index (SI) is a quantitative measure used in various scientific fields to assess the specificity or preference of a process, compound, or system for a particular target over other targets. Its exact definition and calculation depend on the context. In drug development, the SI evaluates a compound's safety window by comparing its toxic and therapeutic effects. Formula:

$$SI = \frac{CC50}{EC50}(6)$$

For antiviral drugs, CC₅₀ (cytotoxic concentration to host cells) is divided by EC₅₀ (effective concentration against the virus). In mathematical formulas, a higher SI value indicates a safer drug; for example, an SI greater than 10 is often desirable. The Tenvir's selectivity index is SI₁₀ = 56, SI₅₀ = 5.2, and SI₁₀₀ = 0.48.

CONCLUSION

General results are positive, and according to a set of goals with all succeeded targets, including provisions that demonstrate a clear structure of this research, we can claim that the ‘Study the antiviral activity of drugs against the SARS-CoV-2 *virus in vitro*’ was informative. Tenvir (TDF/TAF): Tenvir (TDF/TAF) demonstrated the highest efficacy among the tested antivirals, effectively silencing SARS-CoV-2 replication by inhibiting NSP3 cleavage—a critical step that prevents the assembly of the viral RNA-dependent RNA polymerase (RdRP)—and potentially disrupting nucleoprotein (NP) synthesis. Remarkably, it maintained potency even at a high viral load (MOI 2), contrasting with the standard experimental MOI of 0.01. Ribavirin and Favipiravir: Ribavirin and Favipiravir exhibited lower efficacy at the tested concentrations. For instance, Ribavirin required 205 μM to inhibit SARS-CoV-2 *in vitro*, compared to the 100 μM dose effective against influenza in prior studies. These findings suggest that higher concentrations or combination therapies may be necessary to achieve viral clearance for SARS-CoV-2. Dexamethasone: Dexamethasone demonstrated no direct antiviral activity (as indicated in Tables 6 and 7) and induced mild cytotoxicity in Vero E6 cells at high doses. While it supports immune modulation in severe COVID-19 cases (e.g., reducing lung inflammation), its immunosuppressive risks make it unsuitable for early-stage treatment or immunocompromised patients. Hydroxychloroquine: Although hydroxychloroquine demonstrated activity in kidney cell cultures, it proved to be clinically ineffective. It fails to target lung-specific pathways involving TMPRSS2 and ACE2, which are crucial for SARS-CoV-2 entry into respiratory cells. Its misuse during the pandemic highlights the need for tissue-specific antiviral testing. Experimental Context: MOI 2 - The high viral load (MOI 2) was necessitated by laboratory constraints, such as limited viral stock volume (200 μL). While this elevated MOI risked rapid cell death, it underscored Tenofovir’s robust antiviral capability under stringent conditions. Cytotoxicity: Tenofovir displayed the safest profile at clinically relevant doses, whereas Ribavirin posed significant toxicity risks (e.g., hematological and organ damage). Favipiravir offered a balance between moderate antiviral efficacy and low cytotoxicity. Mechanistic Insights: RdRP Inhibition: The RNA-dependent RNA polymerase (RdRP), encoded by the conserved ORF1b gene, remains a stable antiviral target due to its proofreading activity, which limits mutation rates. Purine analogs like Tenofovir disrupt viral RNA synthesis through lethal mutagenesis. PCR Limitations: PCR diagnostics can detect non-infectious viral RNA fragments up to 21 days post-infection, potentially leading to false positives. Infectivity correlates with CT values: samples with CT values ≤ 35 indicate active transmissibility, while those with CT values ≥ 65 reflect non-infectious viral debris. Recommendations: Lung Cell Models - Antiviral efficacy should be validated in lung cell cultures to account for ACE2/TMPRSS2 expression, which is crucial for clinical relevance. Combination Therapies: Pairing agents like Ribavirin with Tenofovir could enhance efficacy and reduce the risk of resistance. Dose Optimization: Higher concentrations of Ribavirin and Favipiravir should be explored *in vitro*, with careful monitoring of toxicity. Tenofovir exhibits robust anti-SARS-CoV-2 activity against variants from Kazakhstan, but its clinical potential requires

validation in lung-specific models. Additionally, context-aware interpretation of PCR results (e.g., CT values) is essential to avoid misdiagnosis and optimise treatment strategies.

The main dissertational results and its scientific influence:

- ✓ 1) The whole genome of SARS-CoV-2/human/KAZ/B1.1/2021, Alpha variant strain was sequenced. The SARS-CoV-2/human/KAZ/B1.1/2021, also known as the Alpha variant strain, originated in Europe in 2021 and serves as the starting point of the phylogenetic tree. This branch has close relationships with European strains (Appendix A-C).
- ✓ 2) Mutations of SARS-CoV-2/human/KAZ/Britain/2021 and SARS-CoV-2/human/KAZ/B1.1/2021 strains compared to the reference sequence Wuhan-Hu-1 SARS-CoV-2. In my dissertation, only the ORF1b segment was relevant. It showed no significant mutations that could cause antiviral resistance in SARS-CoV-2/human/KAZ/B1.1/2021, the Alpha variant strain (Appendix D).
- ✓ 3) The cytotoxicity - safe concentration of Tenofovir was found to be - 50µg/ml or 174µM both for TDF and TAF (10nM is much safer than TDF's) – for IC₁₀₀. Furthermore, the evaluation of Tenofovir, Favipiravir, Ribavirin, and Dexamethasone using MTT and CCK8 cell viability assays in the context of SARS-CoV-2 infection provides critical insights into their potential antiviral efficacy and cytotoxicity. These assays, which measure mitochondrial activity (MTT) and cellular dehydrogenases (CCK8), provide a robust framework for quantifying the effects of drugs on cell viability and antiviral activity in vitro, particularly in models such as Vero E6 or other susceptible cell lines.
- ✓ 4) Tenvir (Tenofovir) is the most effective and potent antiviral drug among the three selected ones; however, it is not the safest. Accurate and proper usage can easily coupe the COVID-19 progression into mild and moderate illness stages. Tenvir (Tenofovir) is a potent antiviral drug among the four selected ones against SARS-CoV-2/human/KAZ/B1.1/2021, Alpha variant strain. Its cytopathic optimal viral load was found at MOI 2. The EC₅₀ in Tenvir's exposure (TDF) was not detected due to high cytotoxicity in renal Vero E6 cells; we obtained only an EC_{max}/IC_{max} at 50 µg/ml. The approximate estimation is 0.5 µg/ml or 1.74 µM of the EC₅₀ of tableted Tenvir (TDF).
- ✓ 5) The Inhibition coefficient IC₁₀ → IC₅₀ → IC₁₀₀ -Range was determined only in China, where the stock and pure TAF had an acceptable SI (selectivity index).
6) The preclinical test on WT mice confirmed TAF's Antiviral efficacy at a concentration of 50µg/ml.

Recommendations for specific use of results

The purine analogues Tenvir (tenofovir-TDF and TAF), Ribavirin, and Faviflu (Favipiravir) are effective against SARS-CoV-2/human/KAZ/B1.1/2021 Alpha Variant and are highly likely to be effective against any strain of concern of the SARS-Cov-2 virus. Therefore, they are recommended for clinical treatment against COVID-19 in mild and moderate stages of progression [Appendix F]. All four studied drugs

could treat COVID-19-infected patients, other pandemic-related outbreaks, and seasonal Influenza A and B-like infections within a proper antiviral time window. The methodological recommendations for optimal parameters of cytotoxicity tests could help conduct similar studies with other antiviral activity structures and combinations, as well as on different cell cultures, like respiratory tract tissue models, as suggested in the concluding part.

Assessment of the scientific level of the work performed

The scientific level of the provided work satisfies international research standards in this scientific field. The work used appropriate virological, biochemical, and molecular genetic methods. The antiviral effects on viral reproduction and its cytotoxicity range were researched. This study underscores the importance of integrating cytotoxicity and antiviral assays in early-stage drug screening. The combination of CCK-8 and MTT methodologies provides a robust framework for identifying safe and potent antiviral candidates, paving the way for advancing promising therapeutics into preclinical development.

REFERENCE

- 1 World Health Organization, - 2020. Coronavirus disease (COVID-19) weekly epidemiological update and weekly operational update. <https://www.who.int/emergencies/diseases/novel-coronavirus-2019/situation-reports>.
- 2 Jia Y, Shen G, Nguyen S, Zhang Y, Huang K-S, Ho H-Y, Hor W-S, Yang C-H, Bruning JB, Li C, Wang W-L. Analysis of the mutation dynamics of SARS-CoV-2 reveals the spread history and emergence of RBD mutant with lower ACE2 binding affinity// *BioRxiv*, - 2020. - Vol.3. - P. 2028-2038. <https://www.biorxiv.org/content/10.1101/2020.04.09.034942v2>.
- 3 Chiara M, Horner DS, Gissi C, Pesole G. Comparative genomics suggests limited variability and similar evolutionary patterns between major clades of SARS-CoV-2.// *BioRxiv*, - 2020. Vol.4. - P. 102-1035. <https://doi.org/10.1101/2020.03.30.016790>.
- 4 Lvan Dorp, Acman M, Richard D, Shaw LP, Ford CE, Ormond L, Owen CJ, Pang J, Tan CCS, Boshier FAT, Ortiz AT, Balloux F. Emergence of genomic diversity and recurrent mutations in SARS-CoV-2. // *Infect Genet Evol*, -2020. - Vol. 83.- P.104-111. <https://doi.org/10.1016/j.meegid.2020.104351>.
- 5 Walls AC, Park Y-J, Tortorici MA, Wall A, McGuire AT, Veerler D. Structure, function, and antigenicity of the SARS-CoV-2 spike glycoprotein. // *Cell*, -2020.- Vol.181.-P. 281–292. <https://doi.org/10.1016/j.cell.2020.02.058>.
- 6 Zhugunissov K, Zakarya K, Khairullin B, Orynbayev M, Abduraimov Y, Kassenov M, Sultankulova K, Kerimbayev A, Nurabayev S, Myrzakhmetova B, Nakhanov A, Nurpeisova A, Chervyakova O, Assanzhanova N, Burashev Y, Mambetaliev M, Azanbekova M, Kopeyev S, Kozhabergenov N, Issabek A, Tuyskanova M, Kutumbetov L. Development of the inactivated QazCovid-in vaccine: protective efficacy of the vaccine in Syrian hamsters. // *Front Microbiol*, - 2021.-Vol. 12.- P.720-727. <https://doi.org/10.3389/fmicb.2021.623171>.
- 7 Johns Hopkins University. COVID-19 data repository by the Center for Systems Science and Engineering (CSSE). //at Johns Hopkins University, - 2019. <https://github.com/CSSEGISandData/COVID-19>. Retrieved 15 October 2022.).
- 8 Gorbalenya, A.E. et al. The species severe acute respiratory syndrome-related coronavirus: classifying 2019-nCoV and naming it SARS-CoV-2. // *Nat. Microbiol*, - 2020. -Vol. 5.-P. 536–544. <https://www.nature.com/articles/s41564-020-0695-z>.
- 9 Lu, R. et al. Genomic characterization and epidemiology of 2019 novel coronavirus: implications for virus origins and receptor binding. // *Lancet*, -2020.-Vol. 395. - P. 565–574. [https://doi.org/10.1016/S0140-6736\(20\)30251-8](https://doi.org/10.1016/S0140-6736(20)30251-8).
- 10 Zhang YZ, Holmes EC. A Genomic Perspective on the Origin and Emergence of SARS-CoV-2. // *Cell*, -2020. -Vol. 16.- P. 223-227. <https://doi.org/10.1016/j.cell.2020.03.035>.

- 11 Zhang W, Cao S, Martin JL, Mueller JD, Mansky LM. Morphology and ultrastructure of retrovirus particles. // *AIMS Biophys*, - 2015. -Vol.2.-P. 343-369. <https://doi.org/10.3934/biophys.2015.3.343>.
- 12 Wyatt R, Sodroski J. The HIV-1 envelope glycoproteins: Fusogens, antigens, and immunogens. // *Science*, -1998. -Vol. 280.- P.1884-1888.
- 13 Wang, D. et al. Clinical characteristics of 138 hospitalized patients with 2019 novel coronavirus-infected pneumonia in Wuhan, China. // *JAMA*, - 2020.-Vol.323.-P. 1061–1069. <https://doi.org/10.1001/jama.2020.1585>.
- 14 Li, Q. et al. Early transmission dynamics in Wuhan, China, of novel coronavirus-infected pneumonia. // *N. Engl. J. Med*, -2020.-Vol. 382.- P. 1199–1207. <https://www.nejm.org/doi/full/10.1056/nejmoa2001316>.
- 15 Chan, J.F.W., et al. A familial cluster of pneumonia associated with the 2019 novel coronavirus indicating person-to-person transmission: a study of a family cluster. // *Lancet*, – 2020.-Vol. 395.- P. 514–523. [https://doi.org/10.1016/S0140-6736\(20\)30154-9](https://doi.org/10.1016/S0140-6736(20)30154-9).
- 16 Clinical management of COVID-19. // WHO, – 2022. -P. 35- 62.
- 17 Burashev Y., Khaidarov S., et al. Coding Complete Genome Sequence of the SARS-CoV-2 Virus Strain, Variant B.1.1, Sampled from Kazakhstan. // *Microbiology Resource Announcements*, - 2022.-Vol.12.-№12. – online: <https://journals.asm.org/doi/10.1128/mra.01114-22>.
- 18 Wu, F. et al. A new coronavirus associated with human respiratory disease in China. // *Nature*, - 2020. Vol.579. P. 265–269. <https://www.nature.com/articles/s41586-020-2008-3>.
- 19 Hoffmann, M. et al. SARS-CoV-2 cell entry depends on ACE2 and TMPRSS2 and is blocked by a clinically proven protease inhibitor. // *Cell*, - 2020. -Vol.181.-P. 271–280. <https://doi.org/10.1016%2Fj.cell.2020.02.052>.
- 20 Perlman, S. and Netland, J. Coronaviruses post-SARS: update on replication and pathogenesis. // *Nat. Rev. Microbiol*, -2009.-Vol. 7. - P. 439–450. <https://www.nature.com/articles/nrmicro2147>.
- 21 Snijder, E.J. et al. Ultrastructure and origin of membrane vesicles associated with the severe acute respiratory syndrome coronavirus replication complex. // *J. Virol*, -2006.-Vol. 80. - P.5927–5940.doi: [10.1128/JVI.02501-05](https://doi.org/10.1128/JVI.02501-05).
- 22 Wu, H.-Y. and Brian, D.A. Subgenomic messenger RNA amplification in coronaviruses. // *Proc. Natl. Acad. Sci. U. S. A*, -2010.-Vol. 107.- P.12257–12262. <https://doi.org/10.1073/pnas.1000378107>.
- 23 Shailendra K. Saxena and Sai V. Chitti. Molecular Biology and Pathogenesis of Retroviruses. // *Advances in Molecular Retrovirology*, – 2016. - Vol. 12.- P. 9-24. doi: 10.5772/62885.

- 24 Varmus H. Retroviruses. // Science, -1988.- Vol.240.- P.1427-1435.
- 25 Coffin JM. Structure and classification of retroviruses. // In: Levy, JA. The Retroviridae (First edition). New York: Plenum, - 1992. -ISBN 0-306-44074-1.- Vol.3, №3.- P. 20.
- 26 Rabson AB, Graves BJ. Synthesis and processing of viral RNA. In: Coffin JM, Hughes SH, Varmus HE, editors. // Retroviruses. Cold Spring Harbor (NY): Cold Spring Harbor Laboratory Press. -1997. - Vol.1.- P.223-236.
- 27 Bharat TA, Davey NE, Ulbrich P, Riches JD, de Marco A, Rumlova M, Sachse C, Ruml T, Briggs JA. Structure of the immature retroviral capsid at 8 Å resolution by cryoelectron microscopy. // Nature, – 2012. Vol. 487.-P. 385-389.
- 28 Clinical management of COVID-19 15th September 2022, WHO, - P.110.
- 29 Clinical management of COVID-19 15th September 2022, WHO, - P.113-115.
- 30 Marilyn J. Roossinck, Viren. // Springer, -2020. Vol.1, №2 -P. 28-32. <https://link.springer.com/book/10.1007/978-3-662-61684-0>.
- 31 Lu, R. et al. Genomic characterization and epidemiology of 2019 novel coronavirus: implications for virus origins and receptor binding. // Lancet, - 2020. - Vol. 395. - P. 565–574.
- 32 Zhang, Y.Z. and Holmes, E.C. A genomic perspective on the origin and emergence of SARS-CoV-2. // Cell, - 2020.-Vol. 181.-P. 223–227.
- 33 Roe M.K. et al., Targeting novel structural and functional features of coronavirus protease nsp5 (3CL^{pro}, M^{pro}) in the age of COVID-19 // Journal of General Virology, – 2021. Vol.102. – P. 123-139. <https://doi.org/10.1099/jgv.0.001558>.
- 34 Joshi S, Parkar J, Ansari A, Vora A, Talwar D and Tiwaskar M. Role of favipiravir in treating COVID-19. // Int J Infect Dis. – 2021. -Vol.102. -P. 501-508.
- 35 Delang L, Abdelnabi R, and Neyts J. Favipiravir as a potential countermeasure against neglected and emerging RNA viruses. // Antiviral Res, – 2018.- Vol. 153.- P. 85-94.
- 36 Wang M, Cao R, Zhang L, Yang X, Liu J and Xu M: Remdesivir and chloroquine effectively inhibit the recently emerged novel coronavirus (2019-nCoV) in-vitro. // Cell Res, - 2020. – Vol.30. - P. 269-71.
- 37 Graci JD, Cameron CE. Mechanisms of action of ribavirin against distinct viruses. // Rev Med Virol, – 2006. – Vol. 16. – P. 37-48.
- 38 Myung J.1., Kye-Hyung Kim. In vitro antiviral activity of ribavirin against severe fever with thrombocytopenia syndrome virus. // Korean J Intern Med,- 2017.- Vol. 32. - P.731–737.
- 39 Lee N, Hui D, Wu A, et al. A major outbreak of severe acute respiratory syndrome in Hong Kong. // N Engl J Med, -2003. Vol. 348, №2. – P.1986-1994.

- 40 Falzarano D, de Wit E, Martellaro C, Callison J, Munster VJ, Feldmann H. Inhibition of novel beta coronavirus replication by a combination of interferon-alpha2b and ribavirin. // *Sci Rep*, – 2013.- Vol.3, №1. P. 1686.
- 41 Koren G, King S, Knowles S, Phillips E. Ribavirin in treating SARS: A new trick for an old drug? // *CMAJ*. – 2003.- Vol.168, №3. - P. 1289-1292.
- 42 Balzarini, J.; Holy, A.; Jindrich, J.; Naesens, L.; Snoeck, R.; Schols, D.; De Clercq, E. Differential antiherpesvirus and antiretrovirus effects of the (S) and (R) enantiomers of acyclic nucleoside phosphonates: Potent and selective in vitro and in vivo antiretrovirus activities of (R)-9 (2phosphonomethoxypropyl)-2,6-diaminopurine. // *Antimicrob. Agents Chemother*, - 1993. -Vol. 37, №1. - P. 332–338.
- 43 Edited Tsai, C.-C.; Follis, K.E.; Sabo, A.; Beck, T.W.; Grant, R.F.; Bischofberger, N.; Benveniste, R.E.; Black, R. Prevention of SIV Infection in Macaques by (R)-9-(2-Phosphonylmethoxypropyl) adenine. // *Science*, – 1995. - Vol. 270, №5. – P. 1197–1199.
- 44 Elfiky, A.A. Ribavirin, Remdesivir, Sofosbuvir, Galidesivir, and Tenofovir against SARS-CoV-2 RNA dependent RNA polymerase (RdRp): A molecular docking study. // *Life Sci*, - 2020.- Vol. 253. - P. 117-192.
- 45 Edited Li, G.; Yue, T.; Zhang, P.; Gu, W.; Gao, L.-J.; Tan, L. Drug Discovery of Nucleos(t)ide Antiviral Agents: Dedicated to Prof. Dr. Erik De Clercq on Occasion of His 80th Birthday. // *Molecules*, – 2021. - Vol. 26.-P. 923.
- 46 Choy, K.-T.; Wong, A.Y.-L.; Kaewpreedee, P.; Sia, S.F.; Chen, D.; Hui, K.P.Y.; Chu, D.K.W.; Chan, M.C.W.; Cheung, P.P.-H.; Huang, X.; et al. Remdesivir, lopinavir, emetine, and homoharringtonine inhibit SARS-CoV-2 replication in vitro. // *Antivir. Res*, - 2020. - Vol. 178. – P. 104-107.
- 47 Rob W. Brooker; Zaal Kikvidze. Importance: an overlooked concept in plant interaction research. // *Journal of Ecology*, – 2008.- Vol. 96, №7. - P. 703–708. <https://doi.org/10.1111/j.1365-2745.2008.01373>.
- 48 Neubig, Richard R. "International Union of Pharmacology Committee on Receptor Nomenclature and Drug Classification. XXXVIII. Update on Terms and Symbols in Quantitative Pharmacology". // *Pharmacological Reviews*, – 2003. - Vol. 55, №6. - P. 597–606. doi:10.1124/pr.55.
- 49 Yousuke. A., et.al. Favipiravir (T-705), a broad-spectrum inhibitor of viral RNA polymerase. // *Proc. Jpn. Acad., Ser*, -2009.- Vol.3, №8.- P.232-239.
- 50 Perales, C., Gallego, I., de Ávila, A. I., Soria, M. E., Gregori, J., Quer, J., & Domingo, E. The increasing impact of lethal mutagenesis of viruses. // *Future Medicinal Chemistry*, - 2019.- Vol. 11. – P. 123-133.

- 51 Perales, C., Martín, V., & Domingo, E. Lethal mutagenesis of viruses. // *Current Opinion in Virology*, - 2011.-Vol. 1, № 9. - P. 419–422. doi: 10.1016/j.coviro.2011.09.001.
- 52 Crotty, S., & Andino, R. Implications of high RNA virus mutation rates: lethal mutagenesis and the antiviral drug ribavirin. // *Microbes and Infection*, -2002.- Vol. 4, №11. - P. 1301–1307. doi:10.1016/s1286-4579(02)00008-4.
- 53 Espy, N., Nagle, E., Pfeiffer, B., Garcia, K., Chitty, A. J., Wiley, M. Palacios, G. T-705 induces lethal mutagenesis in Ebola and Marburg populations in macaques. // *Antiviral Research*, -2019.-Vol.25.- P.123-152.
- 54 McDaniel, Y. Z., Patterson, S. E., & Mansky, L. M. Distinct dual antiviral mechanism that enhances hepatitis B virus mutagenesis and reduces viral DNA synthesis. // *Antiviral Research*. - 2019.-Vol. 25.-P.130-147.
- 55 Bull, J. J., Sanjuan, R., & Wilke, C. O. Theory of Lethal Mutagenesis for Viruses. // *Journal of Virology*, -2007.-Vol. 81, №2.- P. 2930–2939.
- 56 Xiaoying XuYuheng ChenXinyu LuWanlin ZhangWenxiu FangLuping YuanXiaoyan Wang. An update on inhibitors targeting RNA-dependent RNA polymerase for COVID-19 treatment: Promises and challenges. // *Biochemical pharmacology*. - 2022. -Vol. 205.- P.1236-1248.
- 57 Christian Powell, Christopher Chang, Stanley M. Naguwa, Gurtej Cheema, M. Eric Gershwin, Steroid-induced osteonecrosis: An analysis of steroid dosing risk. // *Autoimmunity Reviews*, - 2010. - Vol.33. - P.724-743.
- 58 Matthew K. SARS-associated coronavirus replication in cell lines. // *Emerg Infect Dis*. – 2006. - Vol. 12, №5. - P. 128-33. doi: 10.3201/eid1201.050496.
- 59 Arbeitskreis Blut, Untergruppe Bewertung Blutassoziierter Krankheitserreger. Influenza Virus. // *Transfus Med Hemother*, - 2009.-Vol.36.-P.32-39. doi: 10.1159/000197314.
- 60 Javanian, Mostafa Barary, Mohammad Ghebrehewet, Sam Koppolu, Veerendra Vasigala, Veneela Krishna Rekha Ebrahimpour, Soheil. A brief review of influenza virus infection // *Journal of Medical Virology*, – 2021. Vol.-93. P. 4638-4646. <https://doi.org/10.1002/jmv.26990>.
- 61 Peacock, Thomas P., Sheppard, Carol M., Staller, Ecco, Barclay, Wendy S., Host Determinants of Influenza RNA Synthesis// *Annual Review of Virology*,-2019.- Vol.6.-P. 215-233.<https://doi.org/10.1146/annurev-virology-092917-043339>.
- 62 N.M. Bouvier, P. Palese. The biology of influenza viruses // *Vaccine*, -2008.-Vol. 2, №7.- P. 49–53.
- 63 Palese P, Shaw ML. *Orthomyxoviridae*: the viruses and their replication. In: Knipe DM, Howley PM, editors. // *Fields virology*. Philadelphia: Lippincott Williams & Wilkins, - 2007.-Vol. 2, №3.-P.112-118.

- 64 Barbezange Cyril, Jones Louis, Blanc Hervé, Isakov Ofer, Celniker Gershon, Enouf Vincent, Shomron Noam, Vignuzzi Marco, van der Werf Sylvie. Seasonal Genetic Drift of Human Influenza A Virus Quasispecies Revealed by Deep Sequencing//Frontiers in Microbiology, -2018. -Vol. 9.-P. 1123-1137. doi: 10.3389/fmicb.2018.02596.www.frontiersin.org/journals/microbiology/articles/10.3389/fmicb.2018.02596.
- 65 Bedford, T., Riley, S., Barr, I. *et al.* Global circulation patterns of seasonal influenza viruses vary with antigenic drift. //Nature, -2015.-Vol. 523.-P.217–220 <https://doi.org/10.1038/nature14460>.
- 66 Bano I, Sharif M, Alam S. Genetic drift in the genome of SARS COV-2 and its global health concern. // J Med Virol. -2021.-Vol. 94.-P. 88 - 98. <https://doi.org/10.1002/jmv.27337>.
- 67 Walter Dörfer. Viren. // S. Fischer Verlag GmbH,- 2002.-Vol. 1, №3.-P. 70-72. ISBN 3-596-15369-7.
- 68 Wang, J., Wu, Y., Ma, C., Fiorin, G., Wang, J., Pinto, L. H., Lamb, R. A., Klein, M. L., & DeGrado, W. F. Structure and inhibition of the drug-resistant S31N mutant of the M2 ion channel of influenza A virus. //Proceedings of the National Academy of Sciences, - 2013.-Vol. 110.- P. 1315-1320. <https://doi.org/10.1073/pnas.1216526110>.
- 69 K. Martin, A. Helenius. Transport of incoming influenza virus nucleocapsids into the nucleus. // J. Virol. -1991.-Vol. 65.-P. 232–244.
- 70 Jiménez-Jiménez, F.J.; Alonso-Navarro, H.; García-Martín, E.; Agúndez, J.A.G. Anti-Inflammatory Effects of Amantadine and Memantine: Possible Therapeutics for the Treatment of Covid-19? // J. Pers. Med. – 2020.-Vol. 10. - P. 217-222. <https://doi.org/10.3390/jpm10040217>.
- 71 Richard Njunge. Rimantadine: A potential drug for COVID-19. // Authorea, - 2020. Online: doi:10.22541/au.158506001.13968819. <https://www.authorea.com/doi/full/10.22541/au.158506001.13968819>.
- 72 Gautam Kumar., Kakade Aditi Sakharam. Tackling Influenza A virus by M2 ion channel blockers: Latest progress and limitations. // European Journal of Medicinal Chemistry, – 2024. - Vol. 267. - P. 116-172. <https://doi.org/10.1016/j.ejmech.2024.116172>.
- 73 Smieszek, S.P.; Przychodzen, B.P.; Polymeropoulos, M.H. Amantadine disrupts lysosomal gene expression: A hypothesis for COVID-19 treatment. // Int. J. Antimicrob. Agents, - 2020.- Vol. 20.- P.104-106. <https://doi.org/10.1016/j.ijantimicag.2020.106004>.
- 74 Abreu, G.E.A.; Aguilar, M.E.H.; Covarrubias, D.H.; Durán, F.R. Amantadine as a drug to mitigate the effects of COVID-19. // Med. Hypotheses, -2020.-Vol.140.- P.109-115. <https://doi.org/10.1016/j.mehy.2020.109755>.
- 75 Zhou, Y.; Gammeltoft, K.A.; Galli, A.; Offersgaard, A.; Fahnøe, U.; Ramirez, S.; Bukh, J.; Gottwein, J.M. Efficacy of Ion-Channel Inhibitors Amantadine,

- Memantine and Rimantadine for the Treatment of SARS-CoV-2 In Vitro. // *Viruses*, – 2021.- Vol.13.-P. 2082-2089. <https://doi.org/10.3390/v13102082>.
- 76 Jones JC, Marathe BM, Lerner C, Kreis L, Gasser R, Pascua PNQ, Najera I, Govorkova E A. A Novel Endonuclease Inhibitor Exhibits Broad-Spectrum Anti-Influenza Virus Activity In Vitro. // *Antimicrob Agents Chemother*, -2016.-Vol. 60.-P. 5504-5514. <https://doi.org/10.1128/aac.00888-16>.
- 77 Yang T. Baloxavir Marboxil: The First Cap-Dependent Endonuclease Inhibitor for the Treatment of Influenza. // *Annals of Pharmacotherapy*, -2019.- Vol.53.- P.754-759. doi:[10.1177/1060028019826565](https://doi.org/10.1177/1060028019826565).
- 78 Jiajie Feng, et al. Discovery of a Macrocyclic Influenza Cap-Dependent Endonuclease Inhibitor // *J. Med. Chem*, -2024. -Vol.67.-P.2570–2583. <https://doi.org/10.1021/acs.jmedchem.3c01715>.
- 79 Yan Lou, Lin Liu, Hangping Yao, Xingjiang Hu, Junwei Su, Kaijin Xu, Rui Luo, Xi Yang, Lingjuan He, Xiaoyang Lu, Qingwei Zhao, Tingbo Liang, Yunqing Qiu, Clinical Outcomes and Plasma Concentrations of Baloxavir Marboxil and Favipiravir in COVID-19 Patients: An Exploratory Randomized, Controlled Trial // *European Journal of Pharmaceutical Sciences*, – 2021.- Vol. 157.- P. 1-7. <https://doi.org/10.1016/j.ejps.2020.105631>.
- 80 Dufasne F. Baloxavir Marboxil: An Original New Drug against Influenza. // *Pharmaceuticals (Basel)*, – 2021. - Vol.24. - P.28-32. <https://doi.org/10.3390/ph15010028>.
- 81 Yuan S., Wen L., Zhou J. Inhibitors of Influenza A Virus Polymerase. // *ACS Infect. Dis*, - 2018.- Vol.4.-P.218–223. <https://doi.org/10.1021/acsinfecdis.7b00265>.
- 82 Ju H., Zhang J., Huang B., Kang D., Huang B., Liu X., Zhan P. Inhibitors of Influenza Virus Polymerase Acidic (PA) Endonuclease: Contemporary Developments and Perspectives. // *J. Med. Chem*, - 2017.- Vol.60.-P.3533–3551. <https://doi.org/10.1021/acs.jmedchem.6b01227>.
- 83 Hayden, F.G., Shindo, N., Influenza virus polymerase inhibitors in clinical development. // *Curr Opin Infect Dis*, - 2019. -Vol. 32.- P.176–186. <https://doi.org/10.1097/>.
- 84 Parra-Rojas, C.; Nguyen, V.K.; Hernandez-Mejia, G.; Hernandez-Vargas, E.A. Neuraminidase Inhibitors in Influenza Treatment and Prevention–Is It Time to Call It a Day? // *Viruses*, – 2018.- Vol. 10.- P.454-467. <https://doi.org/10.3390/v10090454>.
- 85 Havasi A, Visan S, Cainap C, Cainap SS, Mihaila AA and Pop LA. Influenza A, Influenza B, and SARS-CoV-2 Similarities and Differences – A Focus on Diagnosis. // *Front. Microbiol*, -2022.-Vol. 13. – P. 908-925. doi: [10.3389/fmicb.2022.908525](https://doi.org/10.3389/fmicb.2022.908525). <https://www.frontiersin.org/journals/microbiology/articles/10.3389/fmicb.2022.908525/full>.

- 86 Dobson, J.; Whitley, R.J.; Pocock, S.; Monto, A.S. Oseltamivir treatment for influenza in adults: A meta-analysis of randomized controlled trials. // *Lancet*, - 2015.- Vol. 385.-P. 1729–1737.
- 87 McClellan, K.; Perry, C.M. Oseltamivir. // *Drugs*, - 2001.-Vol. 61.-P. 263–283.
- 88 Zendehtdel, Mohammad Bidkhor, Mohsen Ansari, Saeidreza Jamalimoghaddamsiyahkali, Azadeh Asoodeh. Efficacy of oseltamivir in the treatment of patients infected with Covid-19. // *Annals of Medicine and Surgery*, - 2022.- Vol.77.-P. 103-110. <https://doi.org/10.1016/j.amsu.2022.103679>.
- 89 de Oliveira Formiga, R., et al. Neuraminidase is a host-directed approach to regulate neutrophil responses in sepsis and COVID-19. // *British Journal of Pharmacology*, - 2023.-Vol. 180.-P. 14-18. <https://doi.org/10.1111/bph.16013>.
- 90 Huang, J.; Song, W.; Huang, H.; Sun, Q. Pharmacological Therapeutics Targeting RNA-Dependent RNA Polymerase, Proteinase and Spike Protein: From Mechanistic Studies to Clinical Trials for COVID-19. // *J. Clin. Med.*, - 2020.- Vol.9.- P.1131. <https://doi.org/10.3390/jcm9041131>.
- 91 Di Perri G. Tenofovir alafenamide (TAF) clinical pharmacology. // *Infez Med*, - 2021.-Vol 10.-P.378-385. doi: 10.53854/liim-2904-4. PMID: 35146360; PMCID: PMC8805468.
- 92 Furuta Y, Takahashi K, Kuno-Maekawa M et al. Mechanism of action of T-705 against influenza virus. // *Antimicrob Agents Chemother*, - 2005.-Vol. 49, №4.-P. 981–986.
- 93 R.B. MC Feedo, MPH, FACPM, FAAC COVID-19: Therapeutics and interventions currently under consideration. // *Disease-a-Month*, -2020/- Vol.66. - P.33-39.
- 94 James M. Sanders, PhD, PharmD; Marguerite L. Monogue, PharmD; Tomasz Z. Jodlowski, PharmD; James B. Cutrell, MD. Pharmacologic Treatments for Coronavirus Disease 2019 (COVID-19)// *Clinical Review & Education*, -2020 – Vol. 3. -P.1824-1836.
- 95 J. Grein, N. Ohmagari, D. Shin, G. Diaz, E. Asperges, A. Castagna, T. Feldt, G. Green, M.L. Green, F.-X. Lescure, E. Nicastrì, R. Oda, K. Yo, E. Quiros-Roldan, A. Studemeister, J. Redinski, S. Ahmed, J. Bennett, D. Chelliah, D. Chen, S. Chihara, S.H. Cohen, J. Cunningham, A. D’Arminio Monforte, S. Ismail, H. Kato, G. Lapadula, E. L’Her, T. Maeno, S. Majumder, M. Massari, M. Mora-Rillo, Y. Mutoh, D. Nguyen, E. Verweij, A. Zoufaly, A.O. Osinusi, A. DeZure, Y. Zhao, L. Zhong, A. Chokkalingam, E. Elboudwarej, L. Telep, L. Timbs, I. Henne, S. Sellers, H. Cao, S.K. Tan, L. Winterbourne, P. Desai, R. Mera, A. Gaggar, R.P. Myers, D.M. Brainard, R. Childs, and T. Flanigan. Compassionate Use of Remdesivir for Patients with Severe Covid-19. // *The New England journal of medicine*, -2021. - Vol. 2. -P. 2327-2336.

- 96 Warren TK, Jordan R, Lo MK, Ray AS, Mackman RL, Soloveva V, et al. Therapeutic efficacy of the small molecule GS-5734 against Ebola virus in rhesus monkeys. // *Nature*, - 2016.-Vol4. – P.531:381–5. doi:10.1038/nature17180.
- 97 Tchesnokov EP, Feng JY, Porter DP, Götte M. Mechanism of inhibition of Ebola virus RNA-dependent RNA polymerase by remdesivir. // *Viruses*, – 2019.- Vol.11.-P. 326-333. doi:10.3390/v1104032648.
- 98 Agostini ML, Andres E, Sims AC, Graham RL, Sheahan TP, Lu X, et al. Coronavirus susceptibility to the antiviral remdesivir (GS-5734) is mediated by the viral polymerase and the proofreading exoribonuclease. // *mBio*, - 2018.-Vol. 9-. P. 2018-2021. doi:10.1128/mBio.00221-18.
- 99 Хабриев Р.У. Руководство по экспериментальному (доклиническому) изучению новых фармакологических веществ/. Изд. -2-е.- М.: Медицина; 2005. – 127с.
- 100 Dr. Wu et al., aimed to identify Single-Domain Antibodies against SARS-CoV-2. Vero E6 cells was used in the evaluation of viral cytopathic effect (CPE)-based neutralization.CCK-8 was used to assess cell viability. // *Cell Host Microbe*, -2020. -Vol 1.-P.1-123. doi: 10.1016/j.chom.2020.04.023.
- 101 Barreto-Vieira DF, da Silva MAN, Garcia CC, Miranda MD, Matos ADR, Caetano BC, Resende PC, Motta FC, Siqueira MM, Girard-Dias W, Archanjo BS, Barth OM. Morphology and morphogenesis of SARS-CoV-2 in Vero-E6 cells. // *Mem Inst Oswaldo Cruz*. -2021.-Vol.2.-P.123-130. doi: 10.1590/0074-02760200443.
- 102 Kinoshita, H., Yamamoto, T., Kuroda, Y. *et al.* Improved efficacy of SARS-CoV-2 isolation from COVID-19 clinical specimens using VeroE6 cells overexpressing TMPRSS2 and human ACE2. // *Sci Rep*.-2024.-Vol.14.-P. 24-28. <https://doi.org/10.1038/s41598-024-75038-4>.
- 103 Pakorn Aiewsakun, Worakorn Phumphanjarphak, Natali Ludowyke, Priyo Budi Purwono, Suwimon Manopwisedjaroen, Chanya Srisaowakarn, Supanuch Ekronarongchai, Ampa Suksatu, Jirundon Yuvaniyama, Arunee Thitithanyanont, Systematic Exploration of SARS-CoV-2 Adaptation to Vero E6, Vero E6/TMPRSS2, and Calu-3 Cells // *Genome Biology and Evolution*. -2023.-Vol. 15.-P.323-235. <https://doi.org/10.1093/gbe/evad035>.
- 104 Tschulena U., et al. Mutation of a diacidic motif in SIV-PBj Nef impairs T-cell activation and enteropathic disease. // *Retrovirology*. -2011. -Vol.14.-P. 213-22.
- 105 <https://www.beckman.com/reagents/genomic/cleanup-and-size-selection/pcr/ampure-xp-protocol>.
- 106 <https://www.dojindo.com/EUROPE/products/CK04>.
- 107 American Type Culture Collection P.O. Box 1549 Manassas, VA 20108 USA www.atcc.org.

- 108 Sun SH, Chen Q, Gu HJ, Yang G, Wang YX, Huang XY, Liu SS, Zhang NN, Li XF, Xiong R, Guo Y, Deng YQ, Huang WJ, Liu Q, Liu QM, Shen YL, Zhou Y, Yang X, Zhao TY, Fan CF, Zhou YS, Qin CF, Wang YC. A Mouse Model of SARS-CoV-2 Infection and Pathogenesis. // *Cell Host Microbe*. – 2020.-Vol.8. -P. 124-133. doi: 10.1016/j.chom.2020.05.020.
- 109 Dinnon, K.H., Leist, S.R., Schäfer, A. *et al.* A mouse-adapted model of SARS-CoV-2 to test COVID-19 countermeasures. // *Nature*. -2020.-Vol. 586.- P. 560–566 <https://doi.org/10.1038/s41586-020-2708-8>.
- 110 Maria I. Zapata-Cardona, Lizdany Florez-Alvarez, Ariadna L. Guerra-Sandoval, Mateo Chvatal-Medina, Carlos M. Guerra-Almonacid, Jaime Hincapie-Garcia, Juan C. Hernandez, Maria T. Rugeles, Wildeman Zapata-Builes. In vitro and silico evaluation of antiretrovirals against SARS-CoV-2: A drug repurposing approach. // *AIMS Microbiology*. – 2023.-Vol. 9.- P. 20-40. doi: 10.3934/microbiol.2023002.
- 111 Joshi S, Parkar J, Ansari A, Vora A, Talwar D, Tiwaskar M, Patil S, Barkate H. Role of favipiravir in the treatment of COVID-19. // *Int J Infect Dis*.- 2021.- Vol. 102.-P. 501-508. doi: 10.1016/j.ijid.2020.10.069.
- 112 Siripongboonsitti, T., Muadchimkaew, M., Tawinprai, K. *et al.* Favipiravir treatment in non-severe COVID-19: promising results from multicenter propensity score-matched study (FAVICOV). // *Sci Rep*.- 2023.-Vol. 13.- P.148. <https://doi.org/10.1038/s41598-023-42195-x>.
- 113 Manuel Taboada. Effect of high versus low dose of dexamethasone on clinical worsening in patients hospitalised with moderate or severe COVID-19 pneumonia: an open-label, randomised clinical trial. // *JF - European Respiratory Journal*. -2022.-Vol.3-P.123-129. <https://doi.org/10.1183/13993003.02518-2021>.
- 114 Somovilla P, García-Crespo C, Martínez-González B, Soria ME, de Ávila AI, Gallego I, Mínguez P, Durán-Pastor A, Ferrer-Orta C, Salar-Vidal L, Esteban-Muñoz M, Zuñiga S, Sola I, Enjuanes L, Esteban J, Fernandez-Roblas R, Gadea I, Gómez J, Verdaguer N, Domingo E, Perales . Atypical Mutational Spectrum of SARS-CoV-2 Replicating in the Presence of Ribavirin. // *Antimicrob Agents Chemother*.-2023.-Vol. 67.-P.1315-22. <https://doi.org/10.1128/aac.01315-22>.
- 115 Khaidarov, S., Burashev, Y., Kozhabergenov, N., Usserbayev, B., Melisbek, A., Shirinbekov, M., Moldakaryzova, A., Beisenova, A., Mustafaeva, A., & Kydyrbaeva, A. Targeted in vitro- confirmation of the antiviral activity of Tenvir (Tenofovir) drug against the SARS-COV-2 virus variant B. in Kazakhstan and identifying NSP12 in the viral genome. // *Eurasian Journal of Applied Biotechnology*. - 2024.-Vol.2.-P. 49–60. <https://doi.org/10.11134/btp.2.2024.6>

APPENDIX A

Table 1– Parameters of sequencing primers; the entire SARS-CoV-2 / human / KAZ / B1.1/2021, Alpha variant strain genome ORF1ab and structure proteins (S, M, E and N-Proteins)

№	Orientation	Sequence (5'→3')	Begin	Stop	T	GC %	Product size(bp)
Pp 1	Forward	CTTCCCAGGTAACAAACCAAC	16	36	57.00	47.62	624
	Reverse	TTACGAAGAAGAACCTTGCG	639	620	56.11	45.00	
Pp 2	Forward	TTAGTGCACTCACGCAGTAT	111	130	56.97	45.00	732
	Reverse	GGCCACAGAAGTTGTTATCG	842	823	56.82	50.00	
Pp 3	Forward	GGTGTTACCCGTGAACTCAT	767	786	57.53	50.00	701
	Reverse	CCACCCTTACGAAGAATGGT	1467	1448	57.22	50.00	
Pp 4	Forward	TGAGCATAGTCTTGCCGAAT	1405	1424	57.01	45.00	672
	Reverse	CCACCTGTAATGTAGGCCAT	2076	2057	56.97	50.00	
Pp 5	Forward	TTTTCTCCCGCACTCTTGAA	1905	1924	57.37	45.00	739
	Reverse	ATTCGAGCAACATAAGCCC	2643	2624	56.48	45.00	

Pp 6	Forward	AAGCTCCATTGGTTGGTACA	2589	2608	57.03	45.00	674
	Reverse	TGTCTGATTGTCCTCACTGC	3262	3243	57.54	50.00	
Pp 7	Forward	TGAGTTCGCCTGTGTTGTGG	2872	2891	60.81	55.00	751
	Reverse	GCCGACAACATGAAGACAGT	3622	3603	58.49	50.00	
Pp 8	Forward	CAGTGGTTGTTAATGCAGCCAA	3429	3450	59.96	45.45	772
	Reverse	ATTCAGTAGTGCCACCAGCC	4200	4180	60.61	52.38	
Pp 9	Forward	TTTTGGTGCTGACCCTATACA	3724	3744	56.92	42.86	678
	Reverse	AGCATTTCTCGAAATTCCA	4401	4382	56.31	40.00	
Pp 10	Forward	TAGAGGAGGCAAAGACAGTG	4281	4300	56.57	50.00	629
	Reverse	ACCATCTAGGTGGAATGTGG	4909	4890	56.60	50.00	
Pp 11	Forward	AAACCATCTCACTTGCTGGT	4773	4792	57.34	45.00	750
	Reverse	TACACACCACGTTCAAGACT	5522	5503	56.74	45.00	
Pp 12	Forward	GGTGAAGCTGCTAACTTTTGT	5378	5398	57.01	42.86	661
	Reverse	AGCTTGCGTTTGGATATGGT	6038	6019	57.87	45.00	
Pp 13	Forward	ACGGTGCTTTACTTACAAAGTC	5811	5832	56.93	40.91	748
	Reverse	GCAGCCATTAGATCTGTGTG	6558	6539	56.59	50.00	
Pp 14	Forward	TGGATAATCTTGCCTGCGAA	6372	6391	57.29	45.00	748
	Reverse	GAACCAGTACAGTAGGTTGC	7119	7100	55.79	50.00	
Pp15	Forward	CCGCTGCTTTAGGTGTTTTA	7005	7024	56.35	45.00	687
	Reverse	GTAGTGACAAGTCTCTCGCA	7691	7672	57.01	50.00	
Pp 16	Forward	TGTGCATGTTGTAGACGGTT	7456	7475	57.75	45.00	741
	Reverse	GAATCAACAAACCCTTGCCG	8196	8177	57.94	50.00	

Pp 17	Forward	GTGCGGAAGTTGCAGTTAAA	8013	8032	57.23	45.00	703
	Reverse	GTGACACCACCATCAATAGC	8715	8696	56.50	50.00	
Pp 18	Forward	AAGATAGCACTTAAGGGTGGT	8534	8554	56.33	42.86	609
	Reverse	GCCATCCATGAGCACATAAC	9142	9123	56.93	50.00	
Pp 19	Forward	ACAAAGCTTGCCCATTGATT	8808	8827	56.47	40.00	620
	Reverse	AGCTACAATACCACCAGCTAC	9427	9407	57.18	47.62	
Pp 20	Forward	TTACCAGGAGTTTTCTGTGGT	9305	9325	56.77	42.86	733
	Reverse	TGATAGAGGTTTGTGGTGGT	10037	10018	56.06	45.00	
Pp 21	Forward	TGGATGGTTATGTTACACCT	9647	9667	56.91	42.86	704
	Reverse	GGTGTCTTAGGATTGGCTGT	10350	10331	57.21	50.00	
Pp 22	Forward	CCAAGACATGTGATCTGCAC	10169	10188	56.80	50.00	683
	Reverse	GCACACATATCTAAAACGGCA	10851	10831	56.97	42.86	
Pp 23	Forward	TTTAGCTTGGTTGTACGCTG	10666	10685	56.37	45.00	723
	Reverse	ACTCTCCTAGCACCATCATC	11388	11369	56.12	50.00	

Pp 6	Forward	AAGCTCCATTGGTTGGTACA	2589	2608	57.03	45.00	674
	Reverse	TGTCTGATTGTCCTCACTGC	3262	3243	57.54	50.00	
Pp 7	Forward	TGAGTTCGCCTGTGTTGTGG	2872	2891	60.81	55.00	751
	Reverse	GCCGACAACATGAAGACAGT	3622	3603	58.49	50.00	
Pp 8	Forward	CAGTGGTTGTTAATGCAGCCAA	3429	3450	59.96	45.45	772
	Reverse	ATTTCAAGTAGTCCACCAGCC	4200	4180	60.61	52.38	
Pp 9	Forward	TTTTGGTGCTGACCCTATACA	3724	3744	56.92	42.86	678
	Reverse	AGCATTTCTCGAAATTCCA	4401	4382	56.31	40.00	
Pp 10	Forward	TAGAGGAGGCAAAGACAGTG	4281	4300	56.57	50.00	629
	Reverse	ACCATCTAGGTGGAATGTGG	4909	4890	56.60	50.00	
Pp 11	Forward	AAACCATCTCACTTGCTGGT	4773	4792	57.34	45.00	750
	Reverse	TACACACCACGTTCAAGACT	5522	5503	56.74	45.00	
Pp 12	Forward	GGTGAAGCTGCTAACTTTTGT	5378	5398	57.01	42.86	661
	Reverse	AGCTTGCGTTTGGATATGGT	6038	6019	57.87	45.00	
Pp 13	Forward	ACGGTGCTTTACTTACAAAGTC	5811	5832	56.93	40.91	748
	Reverse	GCAGCCATTAGATCTGTGTG	6558	6539	56.59	50.00	
Pp 14	Forward	TGGATAATCTTGCCTGCGAA	6372	6391	57.29	45.00	748
	Reverse	GAACCAGTACAGTAGGTTGC	7119	7100	55.79	50.00	
Pp15	Forward	CCGCTGCTTTAGGTGTTTTA	7005	7024	56.35	45.00	687
	Reverse	GTAGTGACAAGTCTCTCGCA	7691	7672	57.01	50.00	
Pp 16	Forward	TGTGCATGTTGTAGACGGTT	7456	7475	57.75	45.00	741
	Reverse	GAATCAACAAACCCTTGCCG	8196	8177	57.94	50.00	
Pp 17	Forward	GTGCGGAAGTTGCAGTTAAA	8013	8032	57.23	45.00	703
	Reverse	GTGACACCACCATCAATAGC	8715	8696	56.50	50.00	
Pp 18	Forward	AAGATAGCACTTAAGGGTGGT	8534	8554	56.33	42.86	609

	Reverse	GCCATCCATGAGCACATAAC	9142	9123	56.93	50.00	
Pp 19	Forward	ACAAAGCTTGCCCATTGATT	8808	8827	56.47	40.00	620
	Reverse	AGCTACAATACCACCAGCTAC	9427	9407	57.18	47.62	
Pp 20	Forward	TTACCAGGAGTTTTCTGTGGT	9305	9325	56.77	42.86	733
	Reverse	TGATAGAGGTTTGTGGTGGT	10037	10018	56.06	45.00	
Pp 21	Forward	TGGATGGTTATGTTACACACCT	9647	9667	56.91	42.86	704
	Reverse	GGTGTCTTAGGATTGGCTGT	10350	10331	57.21	50.00	
Pp 22	Forward	CCAAGACATGTGATCTGCAC	10169	10188	56.80	50.00	683
	Reverse	GCACACATATCTAAAACGGCA	10851	10831	56.97	42.86	
Pp 23	Forward	TTTAGCTTGGTTGTACGCTG	10666	10685	56.37	45.00	723
	Reverse	ACTCTCCTAGCACCATCATC	11388	11369	56.12	50.00	

Pp 24	Forward	ATATGCCTGCTAGTTGGGTG	11226	11245	57.35	50.00	723
	Reverse	GTAAGTGGACACATTGAGCC	11948	11929	56.43	50.00	
Pp 25	Forward	AAATTGTTGGGTGTTGGTGG	11792	11811	57.00	45.00	647
	Reverse	GGAACACAACCATCTCTTGC	12438	12419	57.00	50.00	
Pp 26	Forward	AGCTTTTGCTACTGCTCAAG	12130	12149	56.35	45.00	670
	Reverse	ACCTCCCTTGTGTGTTGT	12799	12780	57.47	45.00	
Pp 27	Forward	AACAGCAGCCAAACTAATGG	12460	12479	56.60	45.00	722
	Reverse	GACCAGTACCAGTGTGTGTA	13181	13162	56.52	50.00	
Pp 28	Forward	TGGAACCACCTTGTAGGTTT	12891	12910	56.57	45.00	652
	Reverse	AGCCCTGTATACGACATCAG	13542	13523	56.52	50.00	
Pp 29	Forward	ACCCTGTGGGTTTTACTT	13341	13360	56.86	45.00	706
	Reverse	AACAATACCAGCATTTCGCA	14046	14027	56.32	40.00	
Pp 30	Forward	TACGCCAACTTAGGTGAACG	13963	13982	57.93	50.00	639
	Reverse	TAGATTACCAGAAGCAGCGT	14601	14582	56.36	45.00	
Pp 31	Forward	CCACTTCAGAGAGCTAGGTG	14478	14497	57.04	55.00	713
	Reverse	CTCTAGTGGCGGCTATTGAT	15190	15171	56.88	50.00	
Pp 32	Forward	CCAAGTCATCGTCAACAACC	14913	14932	57.03	50.00	644
	Reverse	CATTAACATTGGCCGTGACA	15556	15537	56.71	45.00	
Pp 33	Forward	GTGTTGTAGCTTGTACACC	15372	15391	56.96	50.00	659
	Reverse	TAGCTAAAGACACGAACCGT	16030	16011	56.62	45.00	
Pp 34	Forward	ATGTTGGACTGAGACTGACC	15834	15853	56.86	50.00	669
	Reverse	ACTTGTCCATTAGCACACAA	16502	16483	55.18	40.00	
Pp 35	Forward	TCCGTATGTTTGAATGCTC	16374	16393	56.80	45.00	712
	Reverse	TGGTCCCTGGAGTGTAGAAT	17085	17066	57.36	50.00	
Pp 36	Forward	TGGTAAACCTAGACCACCAC	16743	16762	56.47	50.00	750
	Reverse	GGTTCTAGTGTGCCCTTAGT	17492	17473	56.55	50.00	
Pp 37	Forward	TTGAGTGTGTCATGCCAG	17386	17405	56.55	45.00	658
	Reverse	CAGCTTGTAAGTTGCCACA	18043	18024	56.85	45.00	

Pp 38	Forward	TGTTGATTCATCACAGGGCT	17832	17851	57.11	45.00	632
	Reverse	GCGGTGGTTTAGCACTAACT	18463	18444	58.20	50.00	
Pp 39	Forward	AGGGGTGTCATGCTACTAGA	18314	18333	57.15	50.00	604
	Reverse	GTCCAGTCAACACGCTTAAC	18917	18898	57.06	50.00	
Pp 40	Forward	CTGCTTCAGACACTTATGCC	18695	18714	56.52	50.00	640
	Reverse	TCAAAAGCTGGTGTGTGGAA	19334	19315	57.86	45.00	
Pp 41	Forward	TCTATGATGCACAGCCTTGT	19088	19107	56.91	45.00	712
	Reverse	TTAGCCCAAAGCTCAAATGC	19799	19780	56.96	45.00	

Pp42	Forward	GTTGCAATTTAGGTGGTGCT	19466	19485	56.89	45.00	630
	Reverse	GTTTGGGACCTACAGATGGT	20095	20076	56.83	50.00	
Pp 43	Forward	AATTTGGGTGTGGACATTGC	19840	19859	57.16	45.00	643
	Reverse	ATGAACCTGTTTGCGCATC	20482	20464	56.90	47.37	
Pp 44	Forward	CCATCTGTAGGTCCCAAACA	20077	20096	56.83	50.00	600
	Reverse	TTGCCACGCTTGACTAGATT	20676	20657	57.53	45.00	
Pp 45	Forward	TCATAACAGATGCGCAAACA	20456	20475	56.06	40.00	711
	Reverse	TTATAGCCACGGAACCTCCA	21166	21147	58.13	50.00	
Pp 46	Forward	TGTTTTAAGACAGTGGTTGCC	20907	20927	56.93	42.86	738
	Reverse	ATGCAGGGGGTAATTGAGTT	21644	21625	56.77	45.00	
Pp 47	Forward	ACCACGCGAACAAATAGATG	21300	21319	56.53	45.00	622
	Reverse	ACAATAAGTAGGGACTGGGTC	21921	21901	56.43	47.62	
Pp 48	Forward	TACATGTCTCTGGGACCAATG	21765	21785	57.09	47.62	676
	Reverse	AGTGCACAGTCTACAGCATC	22440	22421	57.62	50.00	
Pp 49	Forward	TGCTGCAGCTTATTATGTGG	22345	22364	56.18	45.00	662
	Reverse	CATTACAAGGTGTGCTACCG	23006	22987	56.53	50.00	
Pp 50	Forward	TACAGGCTGCGTTATAGCTT	22849	22868	56.73	45.00	617
	Reverse	CACGCCAAGTAGGAGTAAGT	23465	23446	56.97	50.00	
Pp 51	Forward	ATGGTTTAACAGGCACAGGT	23193	23212	57.32	45.00	722
	Reverse	TTGTGCAAAAACCTTCTTGGGT	23914	23894	57.03	38.10	
Pp 52	Forward	CGTGCAGGCTGTTTAATAGG	23498	23517	56.89	50.00	729
	Reverse	AAAGGTCCAACCAGAAGTGA	24226	24207	56.58	45.00	
Pp 53	Forward	AAACCGTGCTTTAACTGGAA	23851	23870	55.79	40.00	721
	Reverse	ACTTTGAAGTCTGCCTGTGA	24571	24552	56.99	45.00	
Pp 54	Forward	CACTGTTAGCGGGTACAATC	24189	24208	56.25	50.00	665
	Reverse	TGAAACAAAGACACCTTCACG	24853	24833	56.97	42.86	
Pp 55	Forward	TGACTTATGTCCCTGCACAA	24756	24775	56.76	45.00	732
	Reverse	GTAGCGCGAACAAAATCTGA	25487	25468	56.85	45.00	
Pp 56	Forward	TGTGTCTGGTAACTGTGATGT	24925	24945	56.88	42.86	687
	Reverse	GAGTGCTAGTTGCCATCTCT	25611	25592	57.02	50.00	
Pp 57	Forward	CGATACCGATAACAAGCCTCA	25493	25512	56.92	50.00	655

	Reverse	GAACCGTCGATTGTGTGAAT	26147	26128	56.47	45.00	
Pp 58	Forward	GCCGTTCCAAAAACCCATTA	25790	25809	56.89	45.00	744
	Reverse	GAACCTGCCATGGCTAAAAT	26533	26514	56.35	45.00	
Pp 59	Forward	ACTACTAGCGTGCCTTTGTA	26200	26219	56.30	45.00	723
	Reverse	GAAGCGGTCTGGTCAGAATA	26922	26903	57.04	50.00	

Pp 60	Forward	GTGGCTCAGCTACTTCATTG	26795	26814	56.52	50.00	736
	Reverse	AATGGTGAATTGCCCTCGTA	27530	27511	57.20	45.00	
Pp 61	Forward	ACTCGCTACTTGTGAGCTTT	27426	27445	57.18	45.00	671
	Reverse	TTAGAACCAGCCTCATCCAC	28096	28077	56.92	50.00	
Pp 62	Forward	CTTGTCACGCCTAAACGAAC	27874	27893	57.43	50.00	655
	Reverse	GCCAATTTGGTCATCTGGAC	28528	28509	57.05	50.00	
Pp 63	Forward	ACCCCAAATCAGCGAAATG	28288	28307	56.96	45.00	728
	Reverse	TAGTGACAGTTTGGCCTTGT	29015	28996	56.98	45.00	
Pp 64	Forward	TCGTTCCATCACGTAGTC	28825	28844	56.80	50.00	641
	Reverse	CAGCAGGAAGAAGAGTCACA	29465	29446	57.17	50.00	
Pp 65	Forward	AATTTTGGGGACCAGGAACT	29126	29145	56.91	45.00	661
	Reverse	CAGCTCTCCCTAGCATTGTT	29786	29767	57.29	50.00	

Appendix B

The taxonomy of the SARS-CoV-2 strain human/KAZ/B 1.1/2021 the early SARS-COV2 lineage

Hierarchical Classification

- Realm: Riboviria
 - Kingdom: Orthornavirae
 - Phylum: Pisuviricota
 - Class: Pisoniviricetes
 - Order: Nidovirales
 - Family: Coronaviridae
 - Subfamily: Orthocoronavirinae
 - Genus: Betacoronavirus
 - Subgenus: Sarbecovirus
 - Species: *Severe acute respiratory syndrome-related coronavirus* (SARSr-CoV)
 - Virus: SARS-CoV-2 (the causative agent of COVID-19)
-

Strain Designation Breakdown

The strain name human/KAZ/B 1.1/2021; alpha variant provides additional contextual information:

Host: Human (*Homo sapiens*).

Country: Kazakhstan (ISO alpha-3 code: KAZ). -Alpha Variant

Lineage: This likely refers to B.1.1 (per Pango nomenclature, a sublineage of the broader B.1 lineage). The space ("B 1.1") may reflect a formatting inconsistency; standard Pango lineages use dots (e.g., B.1.1).

Collection Year: 2021. -Data collected and submitted

- Lineage Context: B.1.1 is an early SARS-CoV-2 lineage that gave rise to notable sublineage (e.g., B.1.1.7, the Alpha variant). However, this specific strain (B 1.1) may represent a localized or less-documented sublineage in Kazakhstan.
- Taxonomic Clarification: While the hierarchical classification (Realm to Species) is universal for SARS-CoV-2, strain names like this one are isolate identifiers, not part of formal taxonomy. They often include host, geographic origin, lineage, and collection date.

Cross-referencing with databases like GISAID or Pango may clarify its phylogenetic relationships for global tracking.

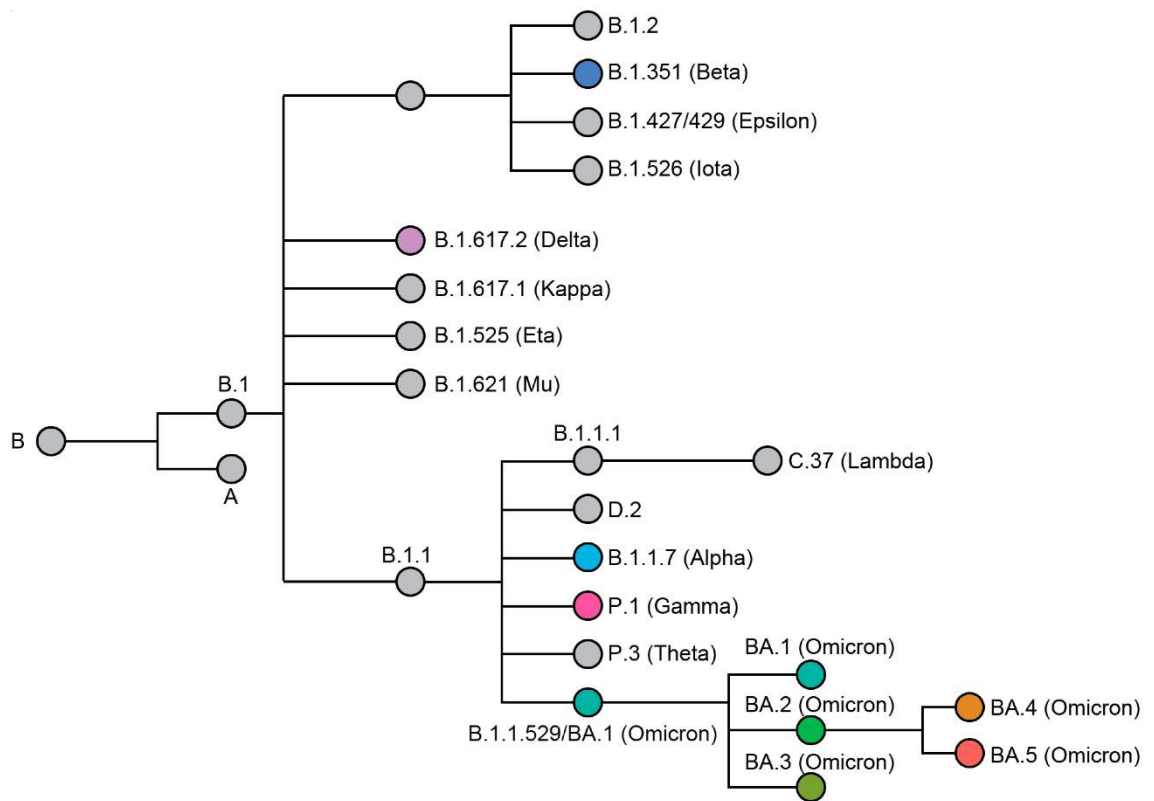
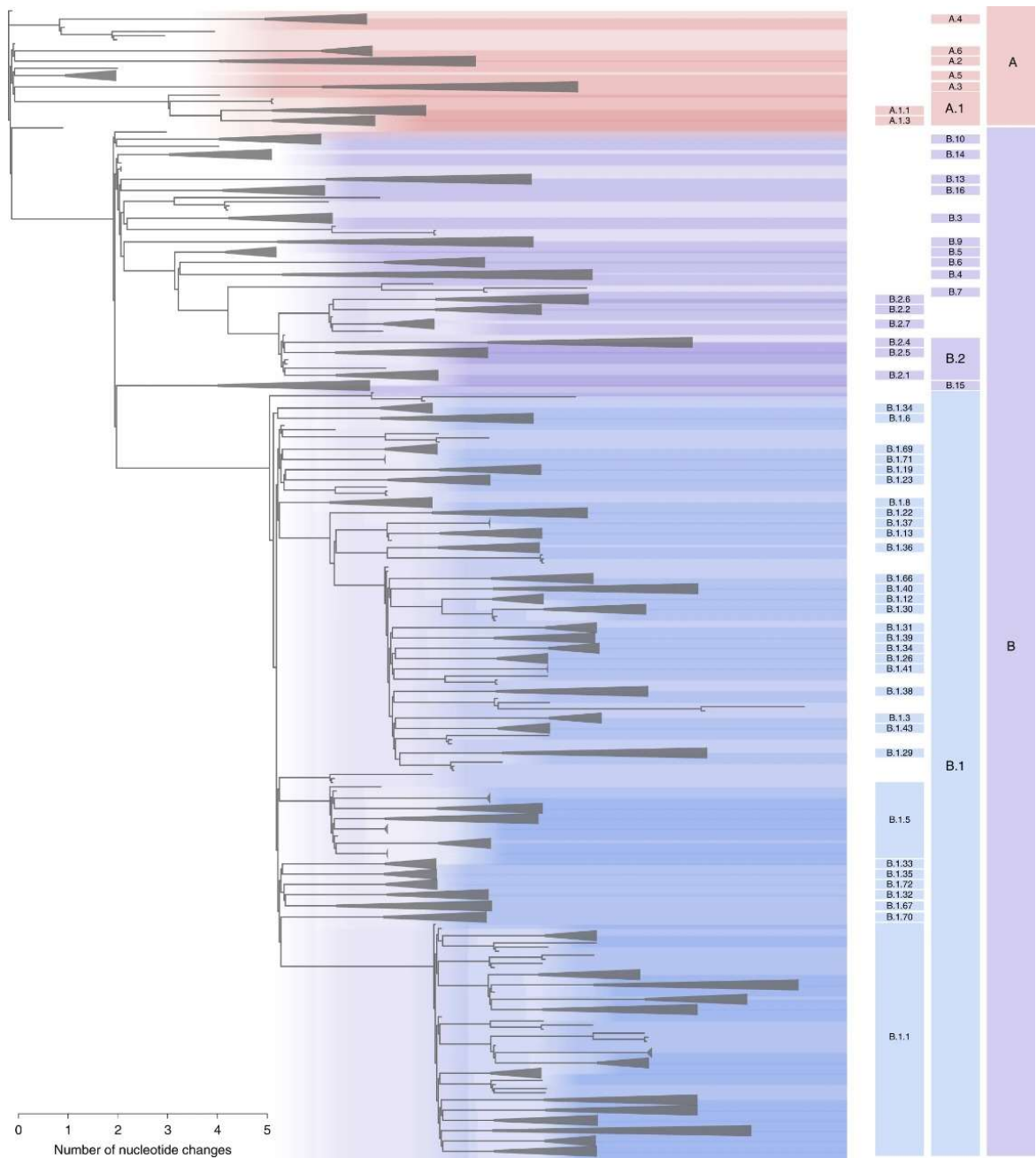


Figure 1- Phylogenetic relationship of named SARS-CoV-2 variants. Variants of concern (VOC) are represented by a colored node. The phylogenetic tree was adapted from data provided by NextStrain, CoVariants (i.e., covariants.org, <http://covariants.org> (accessed on 18 July 2022)), and Pangolin (i.e., cov-lineages.org, <http://cov-lineages.org>. Source: Wiegand, T.; Nemudryi, A.; Nemudraia, A.; McVey, A.; Little, A.; Taylor, D.N.; Walk, S.T.; Wiedenheft, B. The Rise and Fall of SARS-CoV-2 Variants and Ongoing Diversification of Omicron. *Viruses*. - 2022, -Vol.14.-P.20-29. <https://doi.org/10.3390/v14092009>

Lineage	Genomes	Date range	Comments
A	223	5 January-27 April 2020	The root of the pandemic lies in this lineage. Many Chinese sequences with global exports
A.1	1,116	20 February-25 March 2020	Primary outbreak in Washington State, USA
A.2	295	26 February-27 April 2020	European lineage
A.3	191	28 January-21 April 2020	USA lineage
A.5	118	23 February-26 April 2020	European lineage
B	1,713	24 December 2019-3 May 2020	The base of this lineage lies in China, with extensive global travel between multiple locations
B.1	7,438	24 January-10 May 2020	Comprises the large Italian outbreak; it now represents many European outbreaks, with travel within Europe and from Europe to the rest of the world
B.1.1	6,286	15 February-9 May 2020	Major European lineage; exports to the rest of the world from Europe
B.2	917	13 February-4 May 2020	With B.1, it comprises the large Italian outbreak
B.3	752	23 February-23 April 2020	UK lineage
B.4	258	18 January-14 April 2020	This is probably the primary Iranian outbreak

See <https://cov-lineages.org/> for full details of each lineage.

Figure 2 - Proposed nomenclature of early major lineages of SARS-CoV-2. B1.1. lineage was the closest to the SARS-CoV-2 strain/human/KAZ/B 1.1/2021, Alpha variant, due to European exports to the rest of the world. Source: Rambaut, A., Holmes, E.C., O'Toole, Á. *et al.* A dynamic nomenclature proposal for SARS-CoV-2 lineages to assist genomic epidemiology. *Nat Microbiol.* -2020.-Vol. 5.-P. 1403–1407. <https://doi.org/10.1038/s41564-020-0770-5>.



[Figure 2 - Maximum likelihood phylogeny of globally sampled sequences of SARS-CoV-2 downloaded from the GSAD database on 18 May 2020. Five representative genomes are included from each of the defined lineages. The most significant lineages represented by the proposed nomenclature system are highlighted with colored areas and labelled on the right. Triangles denote the remaining lineages defined by the nomenclature system. The scale bar represents the number of nucleotide changes within the coding region of the genome. Source: Rambaut, A., Holmes, E.C., O’Toole, Á. *et al.* A dynamic nomenclature proposal for SARS-CoV-2 lineages to assist genomic epidemiology. *Nat Microbiol.* -2020.-Vol. 5.-P. 1403–1407. <https://doi.org/10.1038/s41564-020-0770-5>.

Appendix C

The primary data of PCR tests (runs)

Table 1: The Quantitative Report, Information about the Test, and Quantitative Analysis Parameters.

The text name	Test 2021-03-29 (1)
Test begins	29.03.2021 10:24:30
Test ends	29.03.2021 12:10:50
Operator	Nurlan
Notes	none
Test run the version of	Rotor-Gene 1.8.17.5
Test signature	Test signature - correct.
Signal level Green	5,
Signal level Orange	5,
Signal level Red	5,
CT-value (Threshold)	0,05139
Exclude cycles till	1,000
Standard curve imported	None
Standard graph (1)	N/A
Standard graph (2)	N/A
Start normalization with a cycle (Cq)	11
Slope correction	None
Background Threshold (NTC)	0%
Response Efficiency Threshold	off
Normalization method	Dynamic background normalization

The samples were collected from patients with COVID-19 during the pandemic at the Scientific and Practical Center for Sanitary and Epidemiological Expertise and

Monitoring in Almaty. During Real-Time PCR identification, all samples showed a positive result, with a peak range of 17 to 30 cycles. Detection of SARS-COV-2 virus strains using real-time PCR and electron microscopy.

PCR identified the SARS-COV-2 virus from the samples received. The PCR conditions are presented in Tables 7 and 8.

Table 2 - Quantitative report, test information

The text name	Test 2021-03-29 (1)
Test begins	29.03.2021 10:24:30
Test ends	29.03.2021 12:10:50
Operator	Nurlan
Notes	None
The test was performed on the software version	Rotor-Gene 1.8.17.5
Test signature	Test signature -correct.
Signal level Green	5,
Signal level Orange	5,
Signal level Red	5,

Table 3- Quantitative analysis parameters

Ct-value (Threshold)	0,05139
Exclude cycles till	1,000
Standard curve imported	None
Standard graph (1)	N/A
Standard graph (2)	N/A
Start normalization with a cycle (Cq)	11
Slope correction	None
Background Threshold (NTC)	0%
Response Efficiency Threshold	off
Normalization method	Dynamic background normalization

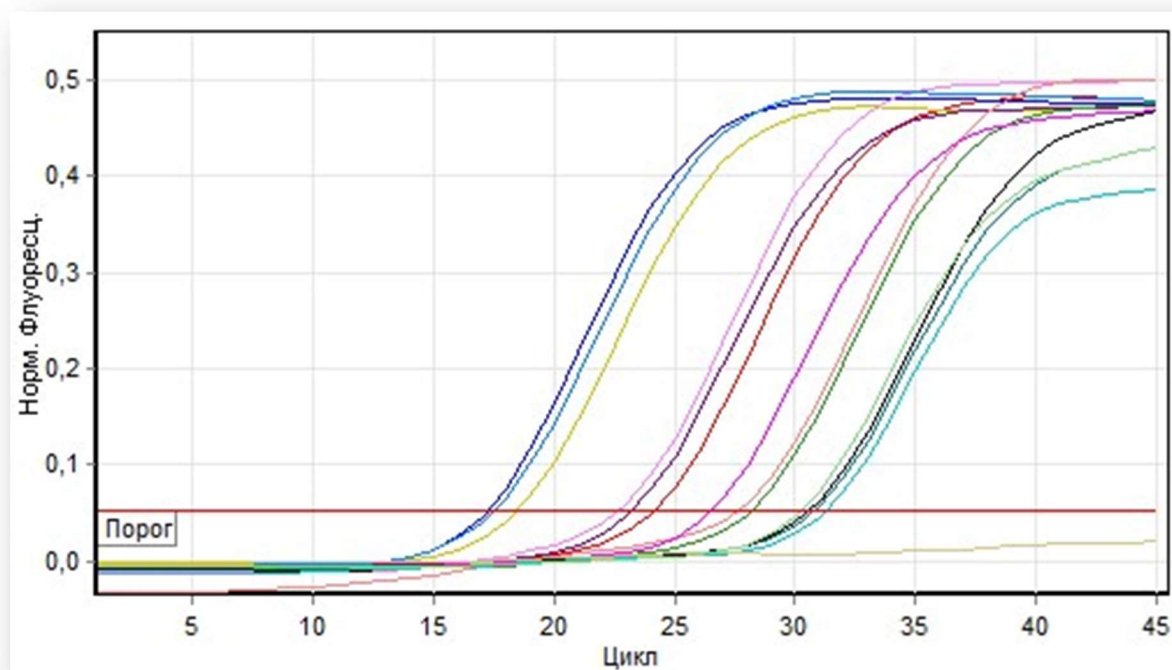
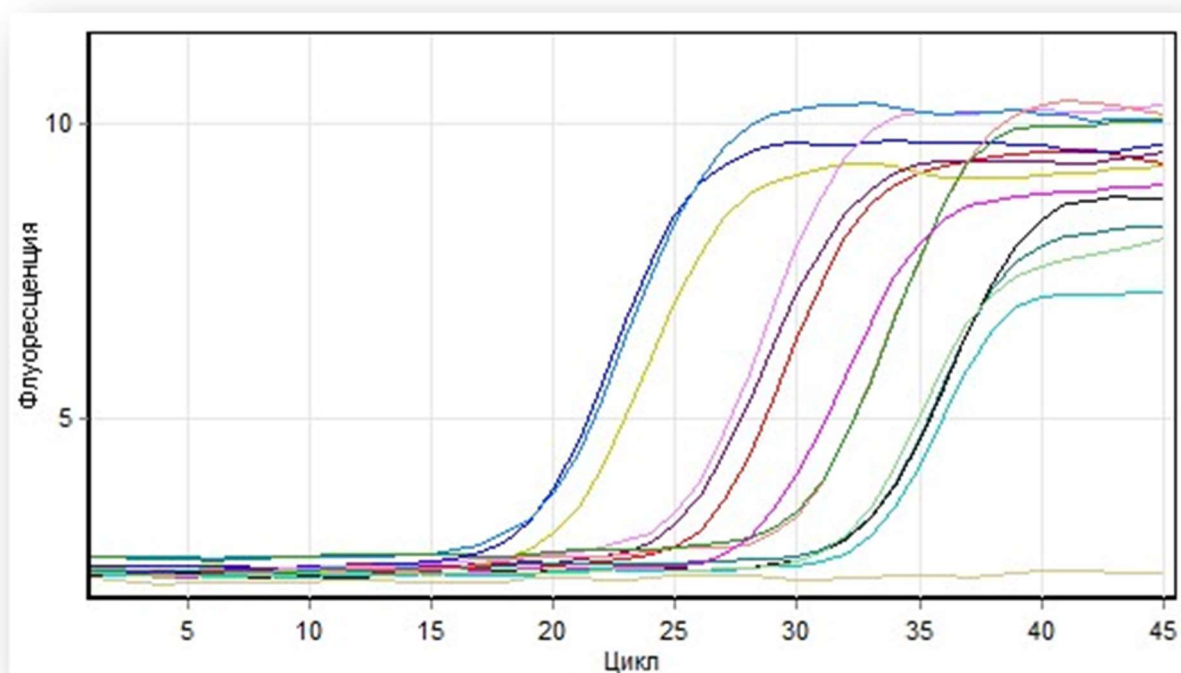


Figure 1- The initial data is the fluorescent signal Cycling A. Red and Quantitative data for Cycling A. Red. According to the peaks report, the following samples were taken for further proceedings with subsequent Ct (cycle threshold). Other samples above 25cycles and lower 20cycles were excluded [115].

*Note: Норм. Флуоресценц. -Normal fluorescence. Порог -Threshold. Цикл – Cycle

Appendix D

Mutations of SARS-COV2 -Kazakhstan's strains to Wuhan's original strain

Table 1 - Mutations of SARS-CoV-2/human/KAZ/Britain/2021 and SARS-CoV-2/human/KAZ/B1.1/2021 strains compared to the reference sequence Wuhan-Hu-1 SARS-CoV-2 (GenBank inventory number NC 045512.2) [17]

Gene	Gene product/region	Nucleotide position	Ref. base (NC 045512.2)	Sample base (OP684305.1; ON692539.1)	Protein alteration	Mutation type	Sample base	
5'UTR		106	C	T	106	Upstream	OP684305.1	
		241	C	T	241	Upstream	OP684305.1; ON692539.1	
ORF 1ab	Nsp 1	344	C	T	L27F	Non-synonymous	OP684305.1	
	Nsp 2	913	C	T	S36S	Synonymous	ON692539.1	
	Nsp 2	1688	A	C	L259L	Synonymous	ON692539.1	
	Nsp 2	2110	C	T	N435N	Synonymous	ON692539.1	
	Nsp 2	2530	A	G	E557E	Synonymous	OP684305.1	
	Nsp 3	3037	C	T	F106F	synonymous	OP684305.1; ON692539.1	
	Nsp 3	3267	C	T	T183I	Non-synonymous	ON692539.1	
	Nsp 3	4449	C	A	T577N	Non-synonymous	OP684305.1	
	Nsp 3	4455	C	T	A579V	Non-synonymous	OP684305.1	
	Nsp 3	4475	C	T	R586C	Non-synonymous	OP684305.1	
	Nsp 3	5388	C	A	A890D	Non-synonymous	ON692539.1	
	Nsp 3	5829	A	C	K1037T	Non-synonymous	OP684305.1	
	Nsp 3	5986	C	T	F1089F	Synonymous	ON692539.1	
	Nsp 3	6954	T	C	I1412T	Non-synonymous	ON692539.1	
	Nsp 3	7042	G	T	M1441I	Non-synonymous	ON692539.1	
	Nsp 4	9749	A	G	K399E	Non-synonymous	OP684305.1	
	Nsp 4	9867	T	G	L438R	Non-synonymous	OP684305.1	
	Nsp 5	10198	C	T	D48D	Synonymous	OP684305.1	
	Nsp 6	11195	C	T	L75F	Non-synonymous	ON692539.1	
	Nsp 6		11288	T	-	S106	deletion	OP684305.1; ON692539.1
			11289	C	-			OP684305.1; ON692539.1
			11290	T	-			OP684305.1; ON692539.1
			11291	G	-			OP684305.1; ON692539.1
			11292	G	-			OP684305.1; ON692539.1
			11293	T	-			OP684305.1; ON692539.1
			11294	T	-			OP684305.1; ON692539.1
			11295	T	-			OP684305.1; ON692539.1
		11296	T	-	OP684305.1; ON692539.1			

Gene	Gene product/region	Nucleotide position	Ref. base (NC 045512.2)	Sample base (OP684305.1; ON692539.1)	Protein alteration	Mutation type	Sample base
		14120	C	T			ON692539.1
		14408	C	T			OP684305.1; ON692539.1
		14676	C	T			ON692539.1
		15017	C	T			OP684305.1
		15279	C	T			ON692539.1
		16176	C	T			ON692539.1
		20405	C	T			ON692539.1
		20759	C	T			OP684305.1
		21080	A	G			OP684305.1
		21446	A	G			OP684305.1
		21215	A	G			ON692539.1
		21646	C	T			OP684305.1
		21648	C	T			OP684305.1
		21765	T	-			ON692539.1
		21766	A	-			ON692539.1
		21767	C	-			ON692539.1
		21768	A	-			ON692539.1
		21769	T	-			ON692539.1
		21770	G	-			ON692539.1
		21784	T	A			OP684305.1
		21789	C	T			OP684305.1
		21846	C	T			OP684305.1
		21991	T	-			ON692539.1
		21992	T	-			ON692539.1
		21993	A	-			ON692539.1
		23014	A	C			OP684305.1
		23063	A	T			ON692539.1
		23271	C	A			ON692539.1
		23403	A	G			OP684305.1; ON692539.1
		23520	C	T			OP684305.1
		23604	C	A			ON692539.1
		23709	C	T			ON692539.1
		23751	C	T			OP684305.1
		23997	C	T			OP684305.1
		24000	G	T			OP684305.1
		24506	T	G			ON692539.1
		24538	A	T			OP684305.1
		24914	G	C			ON692539.1
		25688	C	T			OP684305.1
		26110	C	T			OP684305.1
		25838	G	T			ON692539.1
		26895	C	T			OP684305.1
		27008	G	T			OP684305.1

ORF 6	ORF 6 protein	27281	G	A	W27*		ON692539.1
		27282	G	A			ON692539.1
		27285	T	A	NL28KF		ON692539.1
		27286	C	T			ON692539.1
ORF 7a	ORF7a protein	27389	C	T	3UTR		OP684305.1
		27630	C	T	A79A	Synonymous	OP684305.1
		27667	G	A	E92K	Non-synonymous	OP684305.1
		27739	C	T	L116F	Non-synonymous	OP684305.1
ORF 8	ORF8 protein	27972	C	T	W27*		ON692539.1
		28048	A	T	R52I	Non-synonymous	ON692539.1
		28095	A	T	K68*		ON692539.1
		28111	A	G	Y73C	Non-synonymous	ON692539.1
N	Nucleocapsid phosphoprotein	28280	G	C	D3L	Non-synonymous	ON692539.1
		28281	A	T			ON692539.1
		28282	T	A			ON692539.1
		28881	G	A	R203K	Non-synonymous	OP684305.1; ON692539.1
		28882	G	A	R203R	Synonymous	OP684305.1; ON692539.1
		28883	G	C	G204R	Non-synonymous	OP684305.1; ON692539.1
		28977	C	T	S235F	Non-synonymous	ON692539.1
		29436	A	T	K388I	Non-synonymous	OP684305.1
3'UTR		between 29733 and 29734	-	T	29733		OP684305.1
		between 29733 and 29734	-	A	29733		OP684305.1
		between 29755 and 29756	-	C	29755		OP684305.1
		between 29790 and 29791	-	T	29790		OP684305.1

The data presented in Table 1 show that the mutations of the studied strains have a total of 97 variations at the nucleotide level; among them, a total of 33 mutations were found in the SARS-CoV-2/human/KAZ/B1.1/2021 strain, and 35 mutations were found in the SARS-CoV-2/human/KAZ strain. /Britain/2021, and 7 mutations were detected in two strains (OP684305.1 and SARS-CoV-2/human/KAZ/Britain/2021). A deletion was detected in two studied strains at three different positions, which led to 18 single nucleotide deletions, of which nine single nucleotide deletions were common to both strains, six single nucleotide deletions were detected only in the SARS-CoV-2/human/KAZ/Britain/2021 strain, three single nucleotide deletions were Only the SARS-CoV-2/human/KAZ/B1.1/2021 strain was detected. Four single nucleotide insertions were identified in the SARS-CoV-2/human/KAZ/B1.1/2021 strain, which was not present in the reference strain. As can be seen from the table, 4.39 (41%) mutations were located in the ORF1ab genome region, 26 (27.3%) mutations were detected in the Spike protein, and 8 (8.4%) mutations were detected in gene N. Mutations in other regions of the virus, including 5UTR, ORF3a, M, ORF6, ORF7a, ORF8, and 3UTR were relatively 2 (,1%), 3 (3,15%), 1 (1%), 4 (4,2%), 4 (4,2%), 4 (4,2%) and 4 (4.2%), respectively [17].

APPENDIX E
MONOGRAPH
VIRUSES (SARS-COV2, INFLUENZA A, D) MODERN SCIENTIFIC
ASPECTS OF DIAGNOSIS AND TREATMENT

<p>МИНИСТЕРСТВО ЗДРАВООХРАНЕНИЯ РЕСПУБЛИКИ КАЗАХСТАН</p> <p>КАЗАХСКИЙ НАЦИОНАЛЬНЫЙ МЕДИЦИНСКИЙ УНИВЕРСИТЕТ ИМ.С.Д.АСФЕНДИЯРОВА</p> <p>С.Ж. Хайдаров, А.Ж. Молдакарывова Б. К. Нургалиева</p> <p>ВИРУСЫ (SARS-COV2, INFLUENZA A, D) СОВРЕМЕННЫЕ НАУЧНЫЕ АСПЕКТЫ ДИАГНОСТИКИ И ЛЕЧЕНИЯ</p> <p>МОНОГРАФИЯ</p> <p>Алматы - 2025</p>	<p>УДК: УДК: 616.99-07-08:578.834 ББК: 55.1 Х- 12</p> <p>Рецензенты:</p> <p>1. Битанова Э.Ж. - к.м.н., ассоциированный профессор, заведующий кафедрой общей иммунологии имени А.А. Шортанбаева, КазНМУ им.С.Д.Асфендиярова 2. Бурашев Е.Д. – PhD, заведующий лабораторией «Мониторинг инфекционных заболеваний» Научно-исследовательский институт проблем биологической безопасности, Гвардейск, Жамбылская область, Казахстан</p> <p>Авторы: Хайдаров С.Ж. - PhD, ассистент профессора кафедры молекулярной биологии и медицинской генетики КазНМУ им.С.Д.Асфендиярова Молдакарывова А.Ж. - к.б.н., заведующий кафедрой молекулярной биологии и медицинской генетики КазНМУ им.С.Д.Асфендиярова Нургалиева Б. К. - д.м.н., MSP, заведующий кафедрой профилактической и внутренних болезней КазНМУ им.С.Д.Асфендиярова</p> <p>Вирусы (SARS-CoV2, influenza A, D) современные научные аспекты диагностики и лечения Монография / Авторы: Хайдаров С.Ж., Молдакарывова А.Ж., Нургалиева Б.К. 2025 // Алматы: ООО Print+, 2025. - 352с.</p> <p>ISBN Представленная монография призвана расширить знания медицинских специалистов в области вирусологии. В работе проводится систематический анализ как традиционных, так и инновационных методов диагностики и лечения первичных вирусных инфекций. Ожидается, что данное исследование станет важным вкладом в развитие персонализированного подхода к ведению пациентов с первичными вирусными инфекциями, способствуя улучшению исходов лечения и повышению качества их жизни.</p> <p>УДК: УДК: 616.99-07-08:578.834 ББК: 55.1 Х- 12</p> <p>Утверждено и разрешено к изданию типографским способом РГП на ПХВ «Национальный научный центр развития здравоохранения имени Салидат Капрбековой» МЗ РК (№ от «___» 2025 года).</p> <p>© Хайдаров С.Ж., Молдакарывова А.Ж., Нургалиева Б.К. 2025</p>
--	--

APPENDIX F

DRUG BROCHURES

Favipiravir (pro-drug/active component)

Glenmark introduces higher strength (400 mg) of FabiFlu® to reduce pill burden of COVID-19 treatment

- *Glenmark is the first company in India to have received the regulator's approval for 400 mg dosage form*
- *Increased strength of FabiFlu® yet another milestone effort by Glenmark's in-house R&D*
- *Patients can now opt for a more relaxed dosage regimen when compared to 200 mg tablet and now need to take half the number of pills due to the introduction of 400 mg*
- *Glenmark remains the only company in India to successfully complete an randomized, controlled, open-labelled, multi-center Phase 3 clinical trial on Indian patients with mild to moderate Covid-19*

Mumbai, India; August 6, 2020: Glenmark Pharmaceuticals, a research-led, integrated global pharmaceutical company, today announced that it will introduce a 400 mg version of oral antiviral FabiFlu®, for the treatment of mild to moderate COVID-19 in India. The higher strength will improve patient compliance and experience, by effectively reducing the number of tablets that patients require per day.

A higher pill burden has been associated with lower adherence to therapy, the latter affecting viral suppression and overall treatment outcomes. Also reducing the pill burden has been a demand from doctors and patients to enable adherence. The 200 mg dosage of FabiFlu® required patients to take 18 tablets on Day 1 (nine in the morning and nine in the evening), followed by 8 tablets each day thereafter for a maximum of 14 days. With the new 400 mg version, patients will now have a more relaxed dosage regimen, with 9 tablets required on Day 1 (4.5 in the morning and 4.5 in the evening), and thereafter 2 tablets twice a day from Day 2 till end of the course.

Figure 1 – Fabiflu brochure, source: https://glenmark.b-cdn.net/gpl_pdfs/media/Glenmark-introduces-higher-strength-400-mg-of-FabiFlu.pdf

Tenofovir -TDF (pro-drug/active component)

DOSAGE AND ADMINISTRATION

Adults

For the treatment of HIV or chronic hepatitis B: The dose of TENOFOVIR (TDF) is 300 mg once daily taken orally without regard to food.

In the treatment of chronic hepatitis B, the optimal duration of treatment is unknown. TENOFOVIR may be discontinued if there is HBsAg loss or HBsAg seroconversion.

Adolescent Patients with HIV-1 Infection (12 Years of Age and Over)

Body weight ≥ 35 kg (≥ 77 lb): Take one 300 mg TENOFOVIR tablet once daily orally, without regard to food.

Dose Adjustment for Renal Impairment

Significantly increased drug exposures occurred when tenofovir disoproxil fumarate was administered to patients with moderate to severe renal impairment (see **ACTION AND CLINICAL PHARMACOLOGY, Renal Insufficiency**). Therefore, the dosing interval of TENOFOVIR should be adjusted in patients with baseline creatinine clearance < 50 mL/min using the recommendations in Table 15. These dosing interval recommendations are based on modeling of single-dose pharmacokinetic data in non-HIV and non-HBV infected subjects with varying degrees of renal impairment, including end-stage renal disease requiring hemodialysis. The safety and efficacy of these dosing interval adjustment recommendations have not been clinically evaluated in moderate to severe renal impairment, therefore, clinical response to treatment and renal function should be closely monitored in these patients.

No dose adjustment of TENOFOVIR tablets (300 mg) is necessary in patients with mild renal impairment (creatinine clearance 50–80 mL/min). Routine monitoring of calculated creatinine clearance, serum phosphorus, urine glucose and urine protein should be performed in patients with mild renal impairment (see **WARNINGS and PRECAUTIONS**).

Figure 2 – Tenvir (TDF) brochure, source: https://pdf.hres.ca/dpd_pm/00059975.PDF.

Ribavirin (pro-drug/active component)

"Pregnancy and breast-feeding")

- If you are a man and your female partner is of childbearing age (see section "Pregnancy and breast-feeding").
- If you have a heart problem. In this case you will need to be monitored carefully. A heart recording (ECG or electrocardiogram) is recommended prior to and during treatment.
- If you develop a heart problem along with intense fatigue. This may be due to anaemia caused by Ribavirin.
- If you have ever had anaemia (the risk of developing anaemia is higher in women compared to men, in general).
- If you have a problem with your kidneys. Ribavirin treatment may need to be decreased.
- If you have had an organ transplant (such as liver or kidney) or have one planned in the near future.
- If you develop symptoms of an allergic reaction such as difficulty in breathing, wheezing, sudden swelling of the skin and mucous membranes, itching or rashes. Ribavirin treatment must be stopped immediately and you should seek medical help immediately.
- If you have ever had depression or develop symptoms associated with depression (e.g. feelings of sadness, dejection, etc) while on treatment with Ribavirin (see section 4).
- If you are an adult who has or had a history of substance abuse (e.g. alcohol or drugs).
- If you are under the age of 18. The efficacy and safety of Ribavirin in combination with peginterferon alfa-2a or interferon alfa-2a have not been sufficiently evaluated in patients under the age of 18 years.
- If you are co-infected with HIV and are being treated with any anti-HIV medicinal products.
- If you have been withdrawn from previous therapy for hepatitis C because of anaemia or low blood count.

Before treatment with Ribavirin, kidney function must be tested in all patients. Your doctor must also test your blood before starting treatment with Ribavirin. The blood tests should be repeated after 2 and 4 weeks of treatment, and thereafter as frequently as your doctor thinks is necessary.

Ribavirin contains Sodium
This medicine contains less than 1 mmol sodium (23 mg) per film-coated tablet, that is to say essentially 'sodium free'.

3. How to take Ribavirin

Always take this medicine exactly as your doctor has told you. Check with your doctor or pharmacist if you are not sure. Your doctor will decide the correct dose for you depending on your body weight, and type of virus and the medicine you take in combination with Ribavirin.

The recommended dose ranges between 800mg to 1400mg/day depending on the other medicines you are using in combination with Ribavirin.

For 200 mg:

- 800 mg/day: Take 2 Ribavirin 200 mg tablets in the morning and 2 tablets in the evening
- 1000 mg/day: Take 2 Ribavirin 200 mg tablets in the morning and 3 tablets in the evening
- 1200 mg/day: Take 3 Ribavirin 200 mg tablets in the morning and 3 tablets in the evening
- 1400mg/day: Take 3 Ribavirin 200mg tablets in the morning and 4 tablets in the evening

For 400 mg:

The recommended dose ranges between 800 mg to 1400 mg/day depending on the other medicines you are using in combination with Ribavirin.

- 800 mg/day: Take 1 Ribavirin 400 mg tablet in the morning and 1 tablet in the evening
- 1000 mg/day: Patients are advised to take Ribavirin 200 mg tablets
- 1200 mg/day: Patients are advised to take Ribavirin 200 mg tablets
- 1400 mg/day: Patients are advised to take Ribavirin 200 mg tablets

In the case of combination therapy with other medicines please follow the dosing regimen recommended by your doctor and refer also to the package leaflets of the other medicines.

Swallow the tablets whole and take the tablets with food.

As ribavirin is teratogenic (may cause abnormalities in the

Figure 3 –Ribavirin brochure, source: <https://www.medicines.org.uk/emc/files/pil.7108.pdf>

Dexamethasone (pro-drug/active component)

Corticosteroids may pass into breast milk. A risk to the new-borns/infants cannot be excluded. A decision on whether to continue/discontinue breast feeding or to continue/ discontinue therapy with dexamethasone should be made taking into account the benefit of breast feeding to the child and the benefit of dexamethasone therapy to the woman.

Driving and using machines

Do not drive, use any tools or machines or carry out any hazardous tasks if you experience side effects, such as confusion, hallucinations, dizziness, tiredness, sleepiness, fainting or blurred vision.

Dexamethasone Tablet contains lactose

If you have been told by your doctor that you have an intolerance to some sugars, contact your doctor before taking this medicine.

3. How to take Dexamethasone Tablet

Always take this medicine exactly as your doctor or pharmacist has told you. Check with your doctor or pharmacist if you are not sure.

Dexamethasone is in the form of tablets 1 mg and 4 mg. The tablet can be divided into equal halves.

Dexamethasone is given in usual doses of 0.5 to 10 mg daily, depending on the disease being treated. In more severe disease conditions doses above 10 mg per day may be required. The dose should be titrated to the individual patient response and disease severity. In order to minimize side effects, the lowest effective possible dose should be used.

Figure 4 –Dexamethasone brochure, source: <https://www.medicines.org.uk/emc/files/pil.10720.pdf>